Etude des processus écophysiologiques caractérisant la distribution du carbone entre les sources et les puits au sein de la charpentière du pommier. Eléments pour un modèle fonction-structure

Emna Bairam

UNIVERSITE
BRETAGNE
LOIRE

AGRO
CAMPUS
OUEST

Emna BAIRAM • 27 mars 2017

Thèse AGROCAMPUS OUEST
sous le label de l'Université Bretagne Loire
pour obtenir le grade de
DOCTEUR D'AGROCAMPUS OUEST
Spécialité Biologie et Agronomie

ÉCOLE DOCTORALE • Végétal, Environnement, Nutrition, Agroalimentaire, Mer (VENAM)

LABORATOIRE D'ACCUEIL • UMR 1345 INRA - Agrocampus Ouest - Université d'Angers Institut de Recherche en Horticulture et Semences (IRHS)

Étude des processus écophysiologiques caractérisant la distribution du carbone entre les sources et les puits au sein de la charpentière du pommier. Éléments pour un modèle fonction-structure

Soulaiman SAKR
Professeur, Agrocampus Ouest / *président*

Winfried KURTH
Professeur, Université de Göttingen / *rapporteur*

Paul-Henry COURNÈDE
Professeur, École Centrale Paris / *rapporteur*

Pierre-Eric LAURI
Ingénieur de recherche, INRA Montpellier / *examinateur*

Evelyne COSTES
Directrice de recherche, INRA Montpellier / *examinatrice*

Gerhard BUCK-SORLIN
Professeur, Agrocampus Ouest / *directeur de thèse*

Mickaël DELAIRE
Maître de conférences, Agrocampus Ouest / *co-encadrant de thèse*

N° ordre :2017-12
N° série : C129

Thèse AGROCAMPUS OUEST

Sous le label de l'Université de Bretagne Loire

Pour obtenir le grade de

DOCTEUR D'AGROCAMPUS OUEST

Spécialité : Biologie et Agronomie

Ecole Doctorale : Végétal, Environnement, Nutrition, Agroalimentaire, Mer (VENAM)

Laboratoire d'accueil : Unité Mixte de Recherche 1345, Institut de Recherche en Horticulture et Semences (Institut National de la Recherche Agronomique-Agrocampus Ouest-Université d'Angers), Angers, France

Emna BAIRAM

Étude des processus écophysiologiques caractérisant la distribution du carbone entre les sources et les puits au sein de la charpentière du pommier. Éléments pour un modèle fonction-structure

Soutenue le 27/03/2017

Composition du Jury

Pr. Winfried KURTH
Université de Göttingen, Department Ecoinformatics, Biometrics and Forest Growth – Rapporteur
Pr. Paul-Henry COURNEDE
Ecole Centrale Paris, Mathématiques et Informatique pour la Complexité et les Systèmes – Rapporteur

Dr. Pierre-Eric LAURI
INRA Montpellier, UMR System Campus Montpellier SupAgro – Examinateur
Dr. Evelyne COSTES
INRA Montpellier, UMR Amélioration génétique et adaptation des plantes méditerranéennes et tropicales – Examinateur
Pr. Soulaiman SAKR
Agrocampus-Ouest Angers, Sciences du Végétal pour l'Agriculture et l'Horticulture – Examinateur

Pr. Gerhard BUCK-SORLIN
Agrocampus-Ouest Angers, Sciences du Végétal pour l'Agriculture et l'Horticulture – Directeur et Encadrant de thèse
Dr. Mickaël DELAIRE
Agrocampus-Ouest Angers, Sciences du Végétal pour l'Agriculture et l'Horticulture – co-Encadrant de thèse

Remerciements

Pour commencer, je remercie Gerhard et Mickaël pour avoir encadré et orienté cette thèse. Je vous suis reconnaissante pour votre investissement, votre soutien et vos conseils à travers les différentes étapes de son élaboration. Sans votre participation et votre implication, notamment au cours de la dernière ligne droite qui a été plus que chargée, cette thèse ne serait pas ce qu'elle est aujourd'hui. Gerhard, tous nos échanges aussi bien professionnels qu'humains ont constitué pour moi un enrichissement considérable au cours de ces années. Je te remercie pour chaque conversation au cours de laquelle mes réflexions prenaient forme, toutes ces idées qui émergeaient au cours de nos réunions, d'avoir cru en moi et de m'avoir laissé la liberté d'orienter le travail vers certaines directions quand moi-même je n'y croyais qu'à moitié, et aussi pour avoir appuyé et enrichi chaque étape de ce travail. Ta passion pour ce que tu entreprends et ton sens humain qui surgissait à travers chaque échange ont fait de cette thèse un parcours agréable même dans ses moments les plus durs. Mickaël, avec ta discrétion, tu as toujours géré tous les travaux avec un calme et une bonne humeur impressionnants et tes réflexions, nos échanges sur la physiologie des pommes m'ont été plus que précieux. Je salue également le fait que tu n'aies jamais hésité à contribuer aux tâches les plus complexes comme les plus encombrantes. L'humilité dont tu fais preuve tous les jours malgré la richesse scientifique que tu détiens est tout à ton honneur.

Christian, je te remercie également pour toutes les manips qu'on a réalisées ensemble sur le verger ou au laboratoire, les mesures interminables sous la pluie et le beau temps, les discussions intéressantes qu'on a souvent eues en observant une branche ou un bourgeon et les fois où on s'est arrêtés crayon en main et pied à coulisse en attente pour que tu me fasses remarquer tous ces détails subtils sur l'embranchement, la croissance des pommes, la fascinante différence entre les variétés ou les caractères morphologiques de tel ou tel organe. Plusieurs de ces idées ont germé et toutes ont contribué à la réalisation de ce travail. Ta connaissance des vergers de pommiers mieux que quiconque et tes observations judicieuses ont été un point fort au cours de cette thèse.

Je tiens aussi à remercier tous les autres membres de l'équipe et en particulier, Pascale pour toutes les réflexions qu'on a eues au sujet des processus écophysiologiques ; ta contribution au cours des réunions autour de l'avancement de la thèse et la pertinence de tes observations ont été une aide considérable au cours de ces trois années, et bien que nos échanges au quotidien aient été brefs, ils ont toujours été agréables, laissant transparaître les qualités humaines dont tu es riche. Je remercie également Sylvain, Mathilde, Isadora, Julienne, Magalie ainsi qu'Antoine pour avoir contribué à la réalisation de ce travail et pour avoir été là les jours où les manips au labo ou sur le terrain se sont faites rudes.

Je remercie Winfried KURTH et Paul-Henry COURNÈDE pour avoir accepté la charge d'être rapporteurs et aussi Pierre-Eric LAURI, Evelyne COSTES et Soulaiman SAKR pour celle d'être examinateurs. Je leur suis reconnaissante à tous d'avoir accepté d'évaluer ce travail.

J'aimerais remercier Michel GÉNARD, Evelyne COSTES, Adelin BARBACCI, Mathilde ORSEL et Sabine DEMOTES pour avoir constitué aux cours de ces trois années mon comité de suivi de thèse. Vos conseils et la justesse de vos évaluations ont précieusement aiguillé cette thèse.

Je remercie également les membres de l'équipe FruitQual et ceux de l'IRHS qui m'ont accueillie et soutenue au cours de ces années de thèse. Ça a été un plaisir d'échanger avec vous tous au cours des

réunions, quelques cafés ou dans les laboratoires. En particulier, je remercie François LAURENS et Mathilde BRIARD qui ont fait que j'aie le temps nécessaire pour finaliser ce travail.

Je remercie tout particulièrement Gilles HUNAULT pour ses conseils et ses explications en statistiques. Je lui suis vraiment reconnaissante pour sa disponibilité, sa réactivité et son tempérament si agréable.

Je remercie Anita qui a toujours été là pour gérer les petits et les gros pépins administratifs. Au-delà de ça, Anita, tu as été une belle rencontre pour moi. Nos conversations, ta bienveillance et ta présence m'ont été très chères. Merci pour toutes tes petites pensées, les gâteaux, les coordonnées pour les cours de piano, les mails de rappel quand j'avais la tête ailleurs et ton soutien si subtil dans tellement d'autres choses. Tu feras indéniablement partie des personnes qui m'ont marquée au cours de mon parcours.

J'aimerais également remercier les membres du service informatique pour avoir été là et d'avoir réagi si promptement à chaque fois que j'ai eu besoin d'eux. François et Olivier, je vous suis reconnaissante pour avoir réglé ces petits soucis d'écrans, de souris, de logiciels qui sans vous auraient fait de ma vie un enfer.

Je remercie également Michel, Bruno, Benoît et Malika pour nos petits échanges et les conversations qu'on a pu avoir.

J'en arrive à mon noyau dur : Camille, Florent, Morgan, Eric, Ferréol, Gaëtan, Gaelle, Aurélie, Quentin et Christelle. Je me félicite d'avoir fait votre connaissance et d'avoir évolué au cours de ces trois années au sein de votre aura. Vous faites partie de ces personnes dont on se félicite d'en croiser quelques-unes au cours de sa vie et vous, vous avez bombardé la mienne en même temps ou presque.

Camille, avec nos caractères 'sauvages', il nous a fallu un peu de temps pour nous apprivoiser l'une l'autre mais une fois que la glace a été brisée, j'ai découvert en toi une petite merveille. Grâce à toi, mêmes les moments les plus sombres ont été lumineux. En écrivant ces lignes, j'ai une foule de souvenirs qui se bousculent : les D'Lices Pub, les expéditions en boulangerie cinq minutes après qu'on ait décidé de faire attention, les fous rires et les larmes, les textos sans fin, les notes sur le tableau, la virée à Venise et j'en passe. Je te remercie d'avoir été là pour moi ces dernières années, d'avoir gardé les loups à chaque fois que j'en ai eu besoin, d'avoir pensé aux Paris-Brest aux bons moments, de m'avoir poussée à courir, moi qui détestais ça, encouragée à arrêter de fumer, aidée à m'organiser, boostée et tellement encore. Si on devait avoir une étoile pour veiller sur nous, sans l'ombre d'un doute, tu auras été la mienne.

Florent, merci pour ton caractère si agréable, toutes les fois où tu t'es allié à moi contre Camille et toutes celles où tu contrais nos vannes avec un sourire serein, ta patience quand je m'oubliais à battre la mesure, mais aussi toutes ces réparties que tu nous sortais aux moments où l'on s'y attendait le moins. Le calme et la bonne humeur qui émanent de toi ont clairement imprégné le "bureau des thésards" pendant ces longues journées de travail.

Morgan, tu es été mon allié pour les pauses dans le froid et sous la pluie. Je te remercie d'avoir été là pour moi à chaque fois que j'en ai eu besoin et même les fois où je ne le demandais pas, tu m'as apporté ton soutien. Outre ton intégrité et ta gentillesse, j'admire ta rigueur au travail, ta capacité à te donner les moyens pour réaliser ce que tu entreprends. Je ne sais pas si je te l'ai déjà dit mais, pour moi, tu es un exemple.

Gaëlle, tu incarnes la douceur et le calme. Tu sais mettre les gens à l'aise en toute discrétion. Avec toi, on n'a pas besoin de se ressembler pour s'apprécier. Je te remercie pour toutes ces choses qu'on a partagées, d'avoir été là dans les moments les plus gais comme les plus difficiles, de m'avoir apporté ton soutien dans tant de situations. A travers cette finesse qui t'est propre, tu as toujours su être authentique dans tes relations et tes sentiments. Et moi, j'ai eu la chance de croiser ton chemin.

Ferréol, tu es pour moi un ami remarquable. Nos discussions pour refaire le monde, nos convergences, nos divergences, feront à jamais partie des échanges les plus intéressants que j'ai pu avoir. Tu as toujours été là quand j'ai eu besoin de toi, au cours des déménagements et pour le changement des bougies et parfois pour des activités plus ludiques comme les coloriages ou les virées en tracteur. Merci de faire partie de ma vie.

Gaëtan, les mots me manquent pour qualifier tout ce que tu m'as apporté. Je te suis reconnaissante pour ton soutien et ta patience au cours de ces derniers mois, tu as rendu mon quotidien tellement plus simple et plus agréable. Derrière ta modestie, se cache un scientifique rigoureux et un homme doté d'une gentillesse démesurée. Merci d'avoir été à mes côtés aussi bien pour surmonter les épreuves professionnelles que personnelles, pour ta bienveillance et ta disponibilité. A tes côtés, j'ai appris tellement de choses sur la gastronomie alsacienne, les ours maléfiques du Canada et surtout comment reconnaître une vraie étoile ;)

Aurélie, qu'est-ce que ça a été bon de te connaître. Je ne sais pas quel pouvoir tu as à déclencher des fous-rires dès qu'on entre dans un périmètre de deux mètres autour de toi. Tu es une personne avec qui on se sent tout de suite à l'aise. Nos conversations, nos soirées, nos Monday, tes Pichey, et combien d'autres délires ! Tu es un vrai bout-en train. Et t'avoir autour est un bonheur.

Eric, avec toi, j'ai partagé tellement de délires ! Rien qu'à y penser, j'en ai le sourire aux lèvres. Ton air désinvolte, ta façon cash de dire les choses, ta volonté à vouloir profiter de la vie, à être positif, à vouloir flinguer les murder parties avant leur commencement font tout le charme de ta personne. Merci pour avoir été présent même après ton départ, pour avoir été là à chaque fois que tu pouvais, à m'avoir toujours encouragée et soutenue dans tout ce que j'entreprenais. Tu es un ami véritable, et pourtant t'es tellement breton ! :p

Quentin, merci à toi pour ne jamais avoir rechigné à descendre une table en chaîne massif six étages sans ascenseur, pour m'avoir coachée dans des sports où on peut saigner du nez, les barbecues à l'étang, les bons plans de voitures, les travaux à la maison. Tu es tellement prévenant et agréable, une personne sur laquelle on peut compter. Je te remercie de ta bienveillance constante durant ces années.

Camille (ou Kmi !), merci à toi pour tous nos échanges, les restos du midi, nos discussions pour refaire le monde, nos avis qui convergent et ceux qui divergent, tes pensées régulières, toutes les fois où tu m'as apporté ton soutien et tes encouragements. C'est bon de te compter parmi mes amis.

Claude et Adrien, je suis heureuse que vous soyez arrivés à temps pour que je croise votre chemin ! Claude, tu as apporté cette petite touche fêtarde dont on avait tous tellement besoin. Je t'ai connu à travers ta bonne humeur, ton humour, la facilité que tu as à prendre la vie telle qu'elle vient et à en profiter à fond, improviser des barbecues à la dernière minute, frapper aux portes comme un malade, faire semblant de faire des pompes et prétendre que c'est les autres qui te déconcentrent. J'espère sincèrement qu'on aura l'occasion de se recroiser ! Adrien, je t'aurais apprécié malgré ton second degré qui dépasse le vingtième degré et les blagues qui se travestissent en pics. Cependant, j'ai passé

de super moments en ta compagnie et j'ai beaucoup apprécié nos échanges au cours de ces derniers mois. J'espère vraiment que tu mèneras à bien ce que tu entreprends ! ;)

Je remercie également Mylène, Virginie, Coline, Laura et Aurélie. Merci pour toutes les fois où vous avez été là, pour les moments super qu'on a passés ensemble, les repas, les soirées, les cinés, les virées, les laser-games, les guinguettes. C'était super de vous avoir au cours de ces années.

Je voudrais aussi remercier toutes les personnes que j'ai pu côtoyer à Agrocampus pour la bonne ambiance dont ils sont responsables. Je remercie particulièrement Marie-Pierre, Vanessa, Valérie, Lolly, Bruno, Emanuel, Laurent, Mathilde, Annie, Sébastien, Jocelyne, Denis, Daniel et Sylvie.

Je dédie une pensée particulière à mes parents Lilia et Ridha. Vous m'avez soutenue de bout en bout et vous avez toujours cru en moi. Ma Lily, savoir que je peux compter sur toi est un vrai socle pour moi, ta force et ta douceur m'ont accompagnée au cours de toutes les étapes de ma vie et m'accompagneront toujours. Papa, tu es pour moi un modèle de sérieux, de réussite et d'intégrité à la fois, je te remercie de ton amour et ta confiance. Je vous dois à tous les deux tout ce que j'ai pu accomplir, et ce travail en fait partie.

Je remercie également Touta, Emir, Ness et Tijani. Malgré la distance, vous avez toujours été là pour moi et votre aide, conseils et présence m'ont été et me sont toujours chers.

Ma délicate Sara et mon doux Sélim, mes petits et pourtant si grands amours, malgré votre jeune âge, vous m'avez toujours soutenue avec tellement de maturité. Sachez que vous avez été le moteur principal dans tout ce que j'ai entrepris. Je ne vous remercierai jamais assez de votre patience, votre amour inconditionnel, votre douceur et votre esprit vif. Toutes vos qualités font ma fierté et j'espère que j'arriverai à vous rendre ne serait-ce que le millième du bonheur que vous me procurez jour après jour. Vous êtes mon cocon le plus douillet et c'est à vous deux que je dédie ce travail.

On m'a dit un jour que la thèse changeait la vie des doctorants. Ce que j'en sais, c'est qu'elle a changé la mienne. Merci à vous tous qui de près ou de loin y avez contribué.

Sommaire

INTRODUCTION GÉNÉRALE

"If an apple blossom or a ripe apple could tell its own story, it would be, still more than its own, the story of the sunshine that smiled upon it, of the winds that whispered to it, of the birds that sang around it, of the storms that visited it, and of the motherly tree that held it and fed it until its petals *were unfolded and its form developed."*

Lucy Larcom

1. CONTEXTE DE LA THESE

Le pommier, Malus domestica Borkh, est une espèce d'arbres fruitiers de la famille des Rosacées. Avec une production mondiale d'environ 80 millions de tonnes en 2014 (FAO), la pomme occupe la troisième place en termes de production de fruits, après celles des agrumes et des bananes. La production européenne moyenne calculée sur la base de 5 ans de 2010 à 2014 est d'environ 12 millions de tonnes (FranceAgrimer, 2016) et la France se positionne comme 7ème producteur mondial et 3ème producteur européen avec 1,6 millions de tonnes et une superficie totale de production de près de 36 mille hectares en 2015. Sur la période 2010-2015, on observe une forte oscillation du rendement de production qui peut être attribuée aux conditions climatiques comme les dégâts dus au gel, les précipitations, des périodes de températures basses au moment de la floraison ou de périodes de fortes chaleurs à l'approche de la récolte (FranceAgrimer, 2016). Le maintien du rendement constitue un enjeu économique fort pour les producteurs français afin de pouvoir se démarquer des autres pays où les coûts de production sont souvent moins élevés. Au-delà du rendement, le maintien voire l'amélioration de la qualité des produits doit également permettre à la filière pomme française de maintenir sa position commerciale à l'échelle internationale dans un contexte de plus en plus concurrentiel.

La qualité de la pomme, et plus globalement celle des fruits, dépend d'une multitude de facteurs qui peuvent être endogènes ou exogènes et qui interagissent entre eux. Les facteurs exogènes comportent les pratiques culturales (taille, éclaircissage), l'environnement (radiation lumineuse, température de l'air et du sol, taux de dioxyde de carbone dans l'air, apport en eau et en minéraux…), l'impact des pathogènes. Les facteurs endogènes, eux, sont de 2 types : d'ordre génétique lié au cultivar ou au génotype indépendamment du milieu ; et d'ordre éco-physiologique lié aux compétitions trophiques – notamment pour le carbone – pouvant exister au sein de l'arbre à différents niveaux d'échelle. Ainsi, une meilleure compréhension du fonctionnement de l'arbre fruitier en relation avec son milieu est primordiale afin d'assurer une bonne gestion des cultures, faire face aux différentes contraintes environnementales et proposer des techniques culturales adéquates.

L'alimentation des fruits en carbone constitue l'un des paramètres principaux dans la détermination de la qualité de la pomme. Depuis sa production ou sa remobilisation depuis les organes sources (feuilles et tissus de réserves), le carbone est transporté jusqu'aux organes puits (les fruits, notamment) où il s'accumule et participe à leurs croissances. Une meilleure compréhension du transport et de la répartition du carbone dans le cadre de ces relations sources/puits au cours du

développement du fruit devrait permettre de mieux comprendre voire de prédire la qualité du fruit à la récolte. La répartition du carbone entre les différents organes puits au sein d'un arbre fruitier dépend à la fois de la répartition spatiale des sources et des puits et de la capacité des puits à attirer le carbone pour leurs croissances. Le transport du carbone au sein de l'arbre fruitier est donc un processus complexe dont l'étude nécessite à la fois une prise en compte des composantes structurales liées à l'architecture de l'arbre et fonctionnelles liées aux relations sources/puits et au transport des assimilats. Chez le pommier, cette complexité est accentuée notamment par la diversité des types de pousses végétatives (longues, courtes, préformées ou sylleptiques), l'âge du bois porteur et la composition des unités fructifères. Toutefois sa compréhension constitue un enjeu majeur afin de mieux maîtriser in fine la croissance des fruits et leur qualité.

C'est dans ce contexte que s'inscrivent une partie des activités de recherche de l'équipe QualiPom (Qualité des Pomoïdées) de l'UMR IRHS (Institut de Recherche en Horticulture et Semences) qui vise l'étude et la modélisation des processus écophysiologiques impliqués dans la croissance et l'élaboration de la qualité de la pomme. Pour cela, l'équipe a fait le choix de ne pas aborder l'échelle globale de l'arbre mais de se restreindre à la branche fruitière de premier ordre appelée « charpentière » qui constitue la composante principale de l'architecture du pommier. L'un des objectifs de l'équipe est donc le développement d'un modèle de type FSPM (Functional-Structural Plant Modelling) à l'échelle de la charpentière du pommier permettant de simuler la croissance et la qualité des pommes par une prise en compte du transport de l'eau et la production, le transport et la répartition des assimilats à l'échelle de la charpentière. Le travail de thèse présenté ici constitue une première étape dans l'élaboration de ce modèle.

2. ETAT DE L'ART

L'étude du transport et de la répartition des assimilats se base sur la compréhension des mécanismes physiologiques permettant de véhiculer les glucides photosynthétisés au niveau des feuilles matures vers les autres organes de la plante. De façon schématique, le transport des glucides se fait entre les organes sources qui fournissent les glucides et les organes puits qui vont les recevoir. Le transport dépend d'une multitude de facteurs à savoir le stade de développement des organes, la distance séparant les organes, la vascularisation, la force de puits des organes ainsi que le pool de carbone disponible. L'architecture de l'arbre constitue la structure physique qui va impacter l'ensemble de ces processus. D'abord, la surface foliaire ainsi que l'insertion, la superposition,

l'orientation et l'exposition des feuilles sont des facteurs déterminants de la capacité photosynthétique et donc de la production de carbone. Par ailleurs, la topologie et le port des arbres en relation avec les distances entre les sources et les puits peuvent aussi influencer le transport. Enfin, l'architecture vasculaire, correspondant au réseau interne de transport, constitue un facteur important dans le contrôle de la distribution des assimilats carbonés. En 1968, Aristid Lindenmayer (Lindenmayer 1968a, b) introduisit un formalisme mathématique constituant des règles de réécriture en parallèle appliqué à une chaine de symboles. Ce formalisme, désormais connu sous la désignation « Lindenmayer-systems » ou "L-systems", a été relayé par des informaticiens et infographistes et a ensuite évolué en méthodologie permettant la simulation de la dynamique de l'architecture des végétaux. La combinaison de cette méthodologie avec une autre approche de modélisation – celle des modèles basés sur les processus (« process-based models » ou « crop models ») – a mené à une nouvelle approche en modélisation qui a pour but de faire le lien entre l'architecture d'une part et les processus physiologiques contrôlant le développement, la croissance et la fructification du végétal d'autre part et ce, à différentes échelles spatiales et temporelles. Ces modèles sont désignés par le terme "Functional-Structural Plant Models" (FSPMs) (Vos et al. 2010, Buck-Sorlin 2013).

2.1. Production et répartition des assimilats à l'échelle de la branche fruitière chez le pommier

Une partie de ce paragraphe reprend une mini-review réalisé*e par l'équipe et publiée dans* la revue Frontiers in Plant Science (Fanwoua et al., 2014).

2.1.1. L'architecture et structures fructifères chez le pommier

La notion d'architecture a été officiellement introduite par Hallé et Oldeman (1970) qui ont établi des modèles architecturaux de classification des arbres en se basant sur la morphologie et les ramifications selon les espèces. L'architecture – à savoir l'organisation dynamique de ses composantes et leur distribution spatiale – joue un rôle essentiel dans l'interception de la lumière disponible dans l'environnement de la plante. En effet, cette dernière déploie son appareil végétatif dans l'espace afin d'optimiser l'interception du rayonnement qui lui parvient. Cependant, les angles d'incidence des rayonnements directs varient en permanence en fonction de la trajectoire solaire. L'environnement lumineux d'une plante est également modifié par le rayonnement diffus provenant de différentes parties de l'hémisphère du ciel et est perturbée par la végétation voisine (Fourcaud et al, 2008). L'architecture de la plante est aussi modifiée à travers l'attribution des assimilats qui détermine les différents taux de croissance des organes. En même temps, la plante est soumise à des

contraintes mécaniques externes, telles que les forces de gravité ou le vent, et doit adapter sa forme et développer des structures de soutien. Afin d'adapter leur forme à l'environnement en constante évolution, et en réponse à la concurrence des plantes voisines, les plantes développent progressivement leur architecture en fonction des activités sources-puits et des facteurs endogènes. Dans le contexte des plantes cultivées, les producteurs modifient consciemment l'architecture des plantes (par exemple par la taille) afin d'optimiser la production et la qualité de la biomasse. Les sélectionneurs choisissent également de nouvelles variétés possédant les traits morphologiques souhaités. La structure en 3 D de la plante est alors un facteur clé pour l'intégration et la compréhension des relations entre les fonctions des différents organes au niveau de la plante entière (Fourcaud et a1, 2008).

L'architecture de l'arbre est donc importante dans l'étude du transport puisqu'elle constitue la structure porteuse des différents flux et signaux qui contrôlent le fonctionnement et le développement des différents organes des plantes (Godin et Sinoquet, 2005). Chez le pommier, la charpentière, qui désigne la branche de premier ordre, constitue la composante structurale principale de l'architecture de l'arbre.

Il existe néanmoins une variabilité architecturale entre les différents cultivars du pommier. Lespinasse et Delort (1986) ont proposé une classification des architectures du pommier selon l'angle d'insertion des branches sur le tronc, la distribution des branches, la distribution des fruits sur les branches et le type de rameaux porteurs des fruits. Ainsi les différents cultivars de pommiers ont été classés en 4 groupes (Figure 1) ; cette classification ayant ensuite été modifiée par Lespinasse (Lespinasse, 1992) suite à l'apparition de variétés colonnaires :

* Le type I : Ce type est colonnaire dans le sens où il est caractérisé par un axe principal unique ne portant que des rameaux courts sur lesquels se trouvent les structures "spur" de fructification.
* Le type II: C'est aussi un type "spur". L'arbre a tendance à être basitone avec des angles d'insertion ouverts. Les ramifications fruitières se situent sur des branches âgées proches du centre de l'arbre.
* Le type III : C'est un type à forte ramification, avec une certaine dominance apicale. Il est caractérisé par une fructification en position terminale ou en position latérale pour les rameaux longs.

* Le type IV : Ce type regroupe les cultivars caractérisés par une ramification acrotone au port retombant. Les points de fructification se situent majoritairement en position terminale sur rameaux de 1 an.

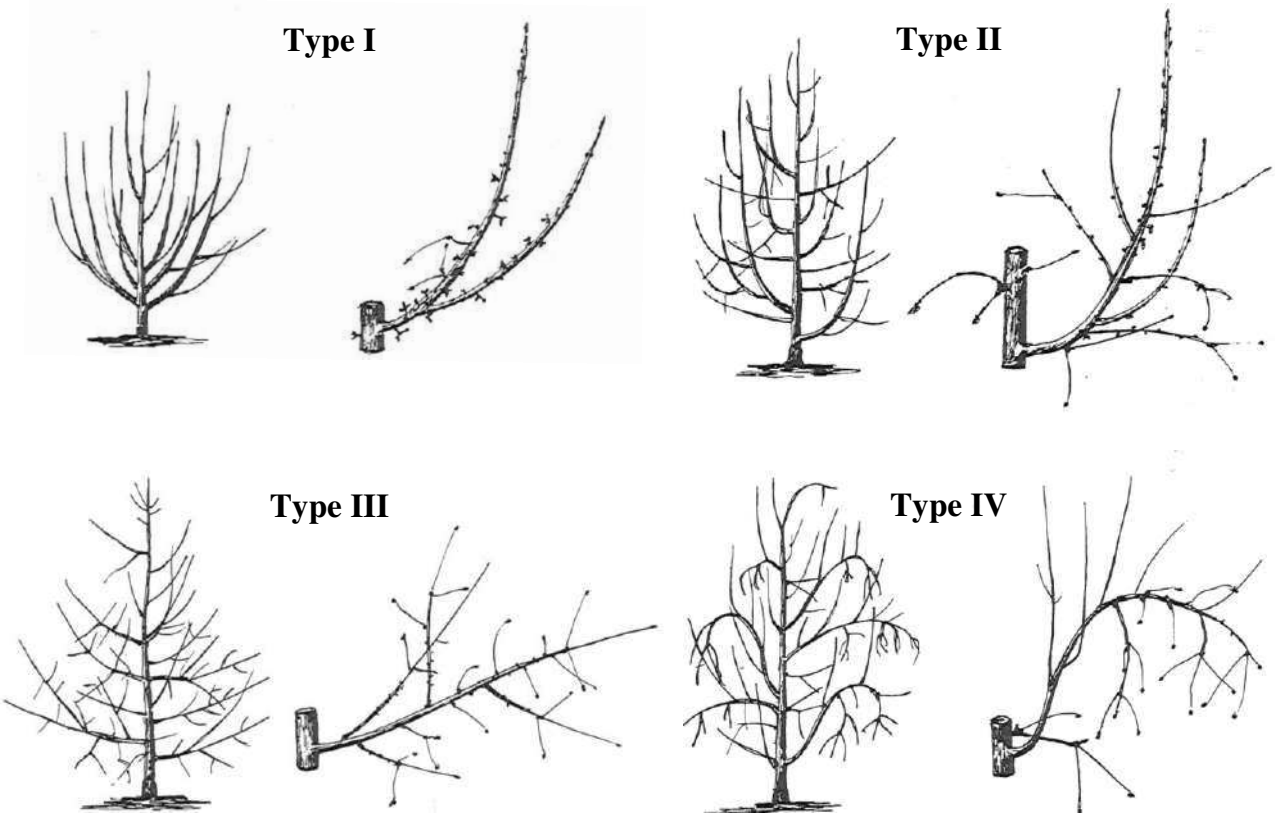

Figure 1. Les différents types architecturaux chez le pommier (d'après Lespinasse, 1980)

Au sein de chaque charpentière, sont retrouvés tous les organes aériens du pommier qu'ils soient végétatifs ou fructifères, sources ou puits. L'architecture des arbres est définie par l'organisation de ses sous-structures qui résulte de l'activité des méristèmes (Costes et al., 2006). En effet, le méristème se trouve au sein du bourgeon auquel il a donné naissance et tous les tissus formés chez le végétal résultent d'une activité méristématique. Le pommier est une espèce à feuilles caduques dont les bourgeons entrent en dormance sous l'effet des températures basses et du raccourcissement des jours (Lauri et al., 1996). La dormance est un processus nécessaire à la survie, le développement et l'architecture de la plante. Très souvent, la levée de la dormance engendre une augmentation de la division cellulaire et des changements dans le développement. (Horvath et al., 2003). Au printemps, en fonction du génotype et des conditions environnementales, une partie des bourgeons vont reprendre leur activité physiologique. Chez le pommier, on distingue 2 types de

bourgeons : les bourgeons végétatifs et les bourgeons florifères qualifiés de « mixtes ». Ainsi, les bourgeons végétatifs donnent naissance aux pousses végétatives annuelles composées d'une succession de phytomères, chaque phytomère étant constitué d'un nœud, d'un entre-nœud, d'une feuille et d'un méristème axillaire (Room et al., 1994 ; Seleznyova et al., 2003). Les pousses végétatives peuvent être soit longues, soit courtes selon les conditions environnementales et leurs positions sur la charpentière (Costes et al., 2006 ; Stéphan et al., 2007). Les bourgeons « mixtes », eux, se développent en une pousse très courte appelée bourse portant une rosette de feuilles préformées, correspondant aux primordia foliaires contenus initialement dans le bourgeon, surmontée d'une inflorescence de 5 à 7 fleurs en corymbe. Dès la floraison, à l'aisselle d'une ou plusieurs feuilles de rosette se développent une ou plusieurs pousses végétatives appelées pousses de bourse à partir de méristèmes axillaires (Costes et al., 2006). Les premières feuilles qui se trouvent à la base de la pousse de bourse sont généralement préformées alors que celles qui vont se développer par la suite sont néoformées. L'ensemble, composé de la rosette de feuilles, de la bourse, de la (ou des) pousse(s) de bourse et du corymbe, est qualifié de « spur » (Figure 2) qui peut être considéré comme une unité fonctionnelle.

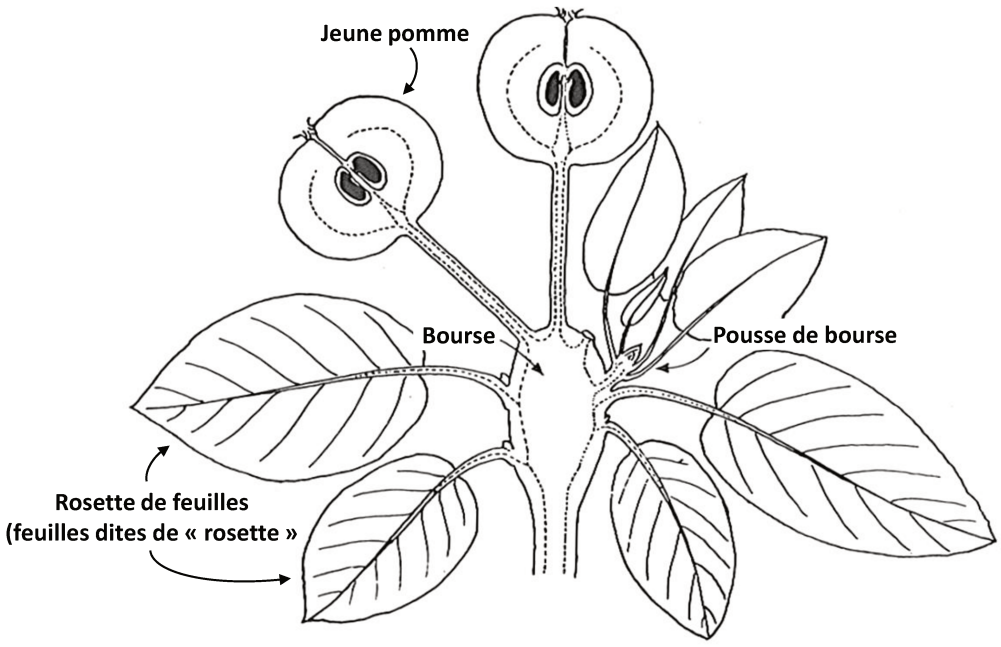

Figure 2. Dessin du « spur » du pommier (adapté de Luckwill, 1970)

La charpentière est donc formée de l'ensemble des pousses qui se sont développées chaque année à partir des bourgeons végétatifs ou mixtes. Le nombre d'organes sources et d'organes puits ainsi que

leur répartition sur la charpentière varient en fonction des génotypes, mais aussi d'une charpentière à une autre sur un même arbre.

2.1.2. Les organes sources et puits

Tout organe qui peut exporter les sucres à un moment de son développement peut être considéré comme une source de carbone et tout organe qui va recevoir les sucres à un moment de son développement est considéré comme un puits et ce durant cette phase. Au cours de leurs développements, les différents organes constitutifs de la charpentière peuvent être soit d'abord puits puis sources pour le carbone (cas des feuilles) ou rester puits (cas des fruits) ou bien encore d'abord sources puis puits (cas des organes de réserves). Ainsi, les jeunes feuilles sont des puits puisqu'elles sont hétérotrophes étant donné qu'elles ont besoin, dans les premières phases de leur développement, d'importer le carbone d'autres organes sources tandis que les feuilles matures sont des sources puisqu'elles sont autotrophes et qu'elles produisent même des glucides en excès qui seront transportés vers les organes puits. Les feuilles matures sont ainsi la principale source de glucides chez les plantes. Les jeunes feuilles commencent à être autotrophes peu de temps après qu'elles se soient étalées et la transition hétérotrophie/autotrophie se fait progressivement de la base vers la partie apicale de la feuille (Turgeon, 1989). De la même manière, le fruit, connu pour être un puits important pour le carbone, est également capable de produire par lui-même du carbone au cours des phases très précoces de son développement même si cette production reste, a priori, trop faible pour satisfaire sa demande. Clijsters (1969) a ainsi pu mettre en évidence une activité photosynthétique non négligeable au niveau de la peau des jeunes pommes qui décroît au cours du développement du fruit en lien avec une réduction de la teneur en chlorophylle de la peau.

Ainsi, le transport du carbone pour une même structure architecturale peut se comporter différemment en fonction du stade de développement et l'âge des organes sources et puits. Son étude nécessite donc la prise en compte à la fois des composantes architecturale et temporelle.

2.1.2.1. Sources et production de carbone

La production de carbone est assurée par la photosynthèse qui est souvent exprimée comme la résultante de la structure de la feuille (forme, surface et orientation) et l'effet de l'interception lumineuse (Mierowska et al., 2002 ; Li et Lakso, 2004). La position et l'orientation de la feuille influencent son exposition à la lumière, et donc le taux de photosynthèse. Ainsi, les feuilles situées aux extrémités des branches, et donc plus exposées à la lumière, ont un taux de photosynthèse plus important que celles en situations plus ombragées (Li et Lakso, 2004). De la même manière, la

position des pousses végétatives les unes par rapport aux autres et leur densité au sein de la canopée impactent donc la production de carbone de l'arbre (Lakso et Grappadelli, 1992 ; Wünsche et Lakso, 2000a ; Li et Lakso, 2004). La maîtrise du développement végétatif est donc déterminante pour permettre une production de carbone satisfaisante en lien avec la charge en fruits. Par ailleurs, il a été montré que le rendement en fruits est davantage corrélé à l'interception lumineuse par les feuilles du spur qu'à celles des pousses végétatives (Wünsche et Lakso, 2000a), ce qui implique une conduite des arbres maximisant l'exposition lumineuse des spurs (Figure 3). On pourrait ainsi penser que les feuilles du spur sont les plus impliquées dans l'apport du carbone aux fruits et qu'en maximisant l'interception lumineuse des feuilles des pousses végétatives, on induit une réduction du rendement par le biais d'un fort ombrage des sites fructifères.

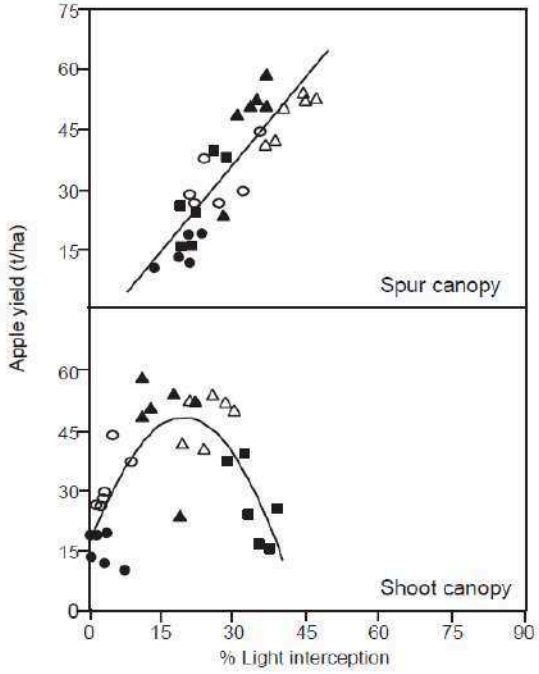

Figure 3. Relation entre le rendement en fruits et le pourcentage d'interception lumineuse au niveau de l'ensemble des feuilles, soit des spurs soit des pousses végétatives, pour différents systèmes de production de pommier (d'après Wünsche et Lakso, 2000a).

La variabilité dans le taux de photosynthèse des feuilles est également dépendante de leurs morphologies (taille, forme) qui varient selon la taille de pousse. Ainsi, la taille des feuilles est plus importante sur les pousses longues que sur les pousses courtes. En effet, une étude menée par Lauri et Kelner (2001) sur deux cultivars de pommiers a montré que, bien que le nombre de feuilles portées par l'ensemble des pousses courtes sur la branche est beaucoup plus important que celui des feuilles portées par l'ensemble des pousses longues, la surface totale des feuilles de pousses longues est la

plus élevée au sein de la branche. Au sein du spur, la taille des feuilles préformées (feuilles de rosette essentiellement) est déterminée l'année précédente, par le niveau d'éclairement du rameau portant le spur. Ainsi, les spurs portés par des rameaux ombragés l'année précédente donne des feuilles plus petites avec un taux de photosynthèse plus faible que celles de spurs portés par des rameaux ayant été en pleine lumière (Tustin et al., 1992). Les caractéristiques morphologiques ou la capacité photosynthétique des feuilles sont également différentes selon que le spur porte ou non des fruits (Schechter et al., 1992) et la charge en fruits (Palmer et al., 1997). Ainsi, l'activité photosynthétique des feuilles est plus faible lorsque le niveau de charge en fruits, et donc la demande en carbone, est faible et serait liée à la réduction de la conductance stomatique due à une augmentation de la teneur en amidon des feuilles (Palmer, 1992 ; Blanke, 1997 ; Wünsche et al., 2005). De la même manière, une incision annulaire ou girdling (suppression d'une portion d'écorce pour limiter l'exportation de carbone) à la base d'une pousse végétative conduit à une diminution de la photosynthèse des feuilles de la pousse (Cheng et al., 2008 ; Fan et al., 2010). Les techniques culturales telles que la taille des arbres ou l'éclaircissage des fruits impactent donc la photosynthèse des feuilles en agissant sur leur exposition à la lumière (Mierowska et al., 2002 ; Li et Lakso, 2004) ou la variation du ratio sources-puits (Blanke, 1997 ; Cheng et al., 2008). D'autres techniques telles que la courbure (ou arcure) des branches – qui chez certains cultivars de pommiers permet de favoriser la floraison (Lauri et Lespinasse, 2001 ; Han et al., 2007) – peut aussi induire une augmentation de l'épaisseur des feuilles, la conductance des stomates et le taux de photosynthèse (Ming-Yu et al., 2008).

Outre les feuilles matures, qui peuvent être considérées comme les principales sources de carbone, les réserves carbonées composées d'amidon et de sucres solubles et qui peuvent représenter jusqu'à 30% de la matière sèche du pommier (Oliveira et Priestley, 1988), constituent également une source de carbone remobilisable au printemps. Toutefois, l'alimentation des fruits par le carbone remobilisé reste très limitée puisqu'il a été montré que la remobilisation des réserves carbonées au printemps décline très vite dès le stade floraison (Hansen, 1971 ; Hansen et Grauslund, 1973).

2.1.2.2. Fruits (puits) et croissance

Au sein de la branche fruitière du pommier, les fruits constituent les principaux puits pour le carbone. Toutefois, d'autres organes ou tissus sont également des puits pour le carbone, notamment les tissus de stockage tels que l'écorce, ou bien encore les pousses et rameaux pour leurs croissances primaires et secondaires. Dans ce cas précis, à l'échelle du spur, la bourse subit au cours du développement végétatif, une croissance en diamètre qui peut être relativement forte chez certaines

variétés telles que ‘Rome Beauty’ (observations personnelles). Les variétés acrotones présentant des bourses de grande taille ont tendance à réguler naturellement leur production d’une année à l’autre tandis que les variétés basitones caractérisées par des bourses plus petites sont beaucoup plus sujettes à l’alternance (Lespinasse et Delort, 1993). Par ailleurs, sur la base des travaux conduits sur le poirier (Zaïdi et al., 1993), on peut supposer qu’elle pourrait permettre l’accumulation de réserves carbonées utilisables l’année suivante mais également jouer un rôle mécanique grâce à l’accumulation de tissus de soutien afin d’éviter qu’elle ne casse sous le poids des fruits en croissance. Néanmoins, peu d’études ont été faites sur le rôle de la bourse et son rôle précis mériterait toutefois d’être élucidé.

a) Les phases de développement de la pomme

La pomme est un « faux fruit » ou piridion résultant du développement de l’ovaire et du réceptacle floral fusionné avec la base des pièces du périanthe et de l’androcée. A maturité le fruit comprend alors 3 zones : une zone interne appelée endocarpe qui est composé des loges carpellaires contenant les pépins et correspondant au développement de l’ovaire ; une zone charnue ou parenchyme cortical ou cortex appelée mésocarpe et correspondant majoritairement au développement du réceptacle floral ; une zone externe appelée épicarpe correspondant à la peau de la pomme composée de l’épiderme et d’une couche de cuticule.

En conditions optimales, l’évolution de la croissance du fruit (en poids frais ou en diamètre) suit une courbe sigmoïde caractéristique pour laquelle on peut distinguer 3 phases de développement (Figure 4). La première phase correspondant à la phase de division cellulaire qui suit la fécondation et au cours de laquelle le nombre de cellules du cortex augmente fortement grâce à une activité mitotique intense qui perdure pendant 3 à 5 semaines. Durant cette première phase, le poids et le diamètre du fruit évoluent peu. La phase de division cellulaire est déterminante pour la taille finale de la pomme puisqu’il a été montré que le poids à la récolte de la pomme était fortement corrélé au nombre de cellules corticales (Goffinet et al, 1995). La deuxième phase correspond à la phase de grossissement du fruit au cours de laquelle on observe une forte activité d’expansion cellulaire avec une nette réduction de l’activité mitotique. Cette phase d’expansion cellulaire s’accompagne également d’une évolution des méats cellulaires en véritables espaces intercellulaires dont le volume peut représenter jusqu’à 25-30% du volume total du parenchyme cortical (Herremans et al., 2015). Enfin, la troisième et dernière phase correspondant à la phase de maturation de la pomme qui se caractérise par un fort ralentissement de la croissance du fruit et par de nombreuses modifications physiologiques et biochimiques permettant au fruit d’acquérir l’aptitude à mûrir. Cette dernière phase

se termine par la phase de mûrissement, qui chez la pomme est de type climactérique et s'accompagne donc d'une forte activité respiratoire et de production d'éthylène, et conduit à rendre le fruit consommable. En production, la récolte des pommes est souvent réalisée avant cette phase de mûrissement afin de pouvoir ensuite stocker les fruits durant de longues périodes.

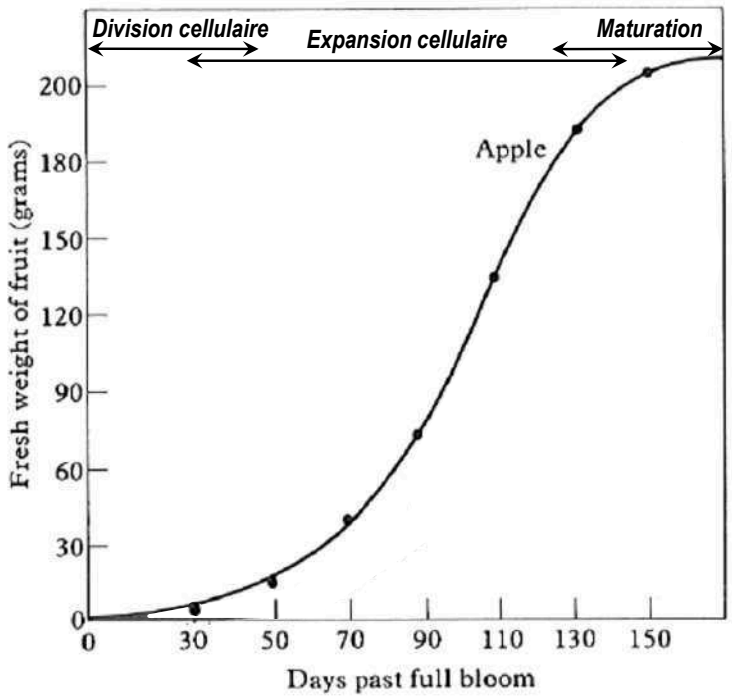

Figure 4. Courbe de croissance typique d'une pomme selon une sigmoïde permettant de distinguer les trois phases de de son développement (modifié depuis Westwood, 1978)

b) Alimentation hydrique de la pomme

Contrairement à d'autres fruits comme la pêche, l'alimentation xylémienne en eau du fruit n'est pas pilotée par son activité transpiratoire. En effet, du fait notamment d'une cuticule qui s'épaissit rapidement (Miller, 1982), l'activité transpiratoire de la pomme diminue très rapidement au cours de son développement (Jones et Higgs, 1982). Des travaux conduits par Lang (1990) et Lang et Volz (1998) ont permis de montrer que l'alimentation en eau du fruit était étroitement liée à la surface des feuilles du spur grâce un processus faisant intervenir des variations jours/nuits de potentiels hydriques entre les feuilles et les fruits conduisant à un efflux d'eau le jour et un influx la nuit avec un bilan net positif. Ces variations jours/nuits permettraient également l'alimentation en calcium du fruit. Ce processus reste toutefois limité dans le temps car progressivement, avec le développement du parenchyme cortical, les vaisseaux de xylème du fruit deviennent non fonctionnels

(Dražeta et al., 2004) et l'entrée d'eau dans le fruit ne peut alors être assurée que par le flux phloémien.

c) Alimentation en carbone et force de puits du fruit

La pomme est alimentée en carbone grâce au sorbitol et au saccharose qui sont les deux principales formes de transport chez le pommier (Teo et al., 2006). Une fois dans la pomme, le sorbitol est converti en fructose via la sorbitol déshydrogénase et le saccharose en partie en glucose et fructose via l'action d'invertases et de la sucrose synthase (Figure 5). Une partie du glucose est ensuite polymérisée en amidon qui s'accumule dans les plastes. Au cours de la phase d'expansion cellulaire, la pomme accumule donc majoritairement du fructose, du saccharose et de l'amidon. Lors de la phase de maturation, l'amidon est progressivement dépolymérisé conduisant à une forte augmentation de la concentration en glucose. Cette dépolymérisation de l'amidon est d'ailleurs utilisée comme indicateur pour le déclanchement de la récolte. A la récolte, les sucres de la pomme sont ainsi composés majoritairement de fructose, de glucose et de saccharose (Berüter, 2004).

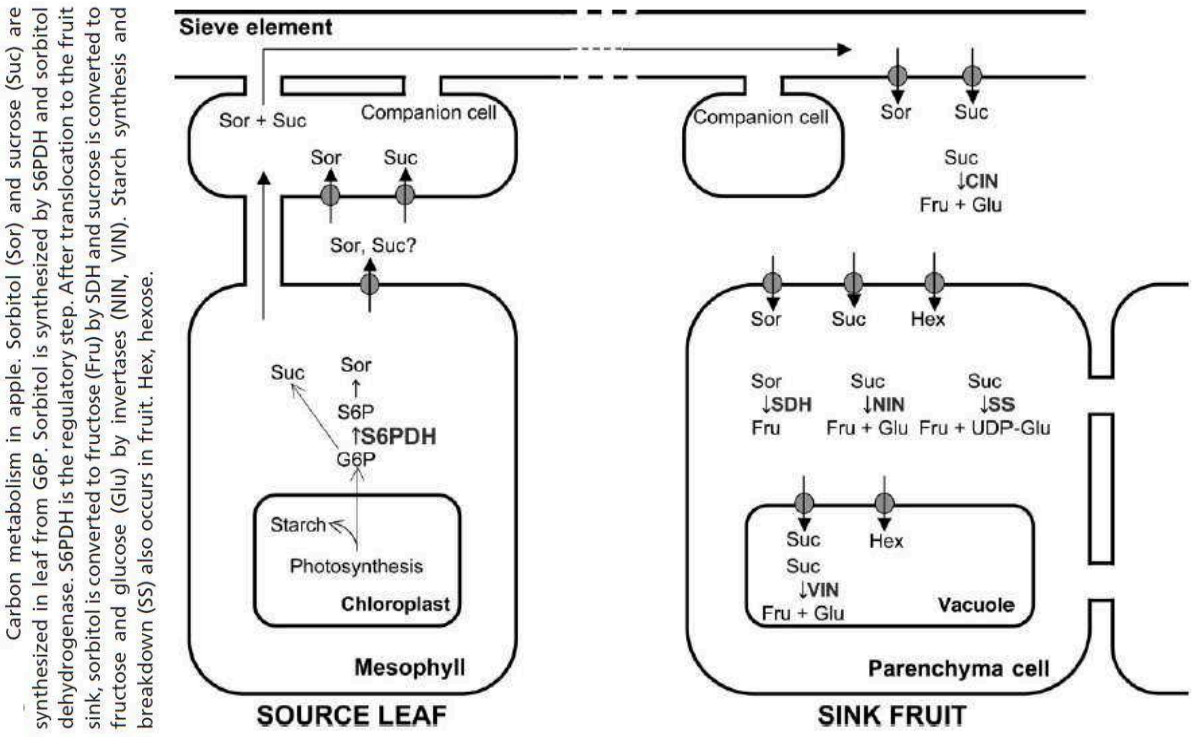

Figure 5. Métabolisme et transport du carbone entre la feuille (sources) et le fruit (puits) chez le pommier (d'après Teo et al., 2006)

L'alimentation en carbone de la pomme au cours de son développement est pilotée par sa force de puits qui peut être définie comme sa capacité à attirer les assimilats (Ho, 1988). La force de puits d'un organe peut être calculée, selon Warren-Wilson (1972), comme étant le produit entre la taille de l'organe – qui peut être présenté par un nombre de cellules – et son activité puits – qui est définie comme étant l'activité métabolique pilotant la demande en carbone de l'organe puits. Chez la pomme, comme indiqué plus haut, le nombre de cellules étant déterminé très précocement, cela laisse supposer que la force de puits du fruit est en partie déterminée dès la fin de la phase de division cellulaire. Concernant l'activité puits, les travaux conduits par Archbold (1992, 1999) semblent indiquer qu'elle pourrait être déterminée par l'activité de la sorbitol déshydrogénase. Par approximation et en conditions non limitantes, la force de puits d'un fruit peut être assimilée à sa vitesse de croissance absolue (absolute growth rate), l'activité puits à sa vitesse de croissance relative (relative growth rate) par rapport à son poids initial (Marcelis, 1996).

2.1.3. Transport et répartition des assimilats

Beaucoup de travaux conduits sur différentes espèces fruitières, et en particulier le pommier, tendent à montrer que le transport et la répartition des assimilats seraient pilotés d'une part par la distance sources/puits (les sources alimentant les puits les plus proches) (Bruchou et Génard, 1999) et d'autre part la force de puits des organes puits (Gucchi et al., 1995, Zhang et al., 2005). La répartition des assimilats entre les sources et les puits évolue donc au cours de leurs développements et peut donc être considérée à deux niveaux d'échelle au cours du temps.

2.1.3.1. Au stade précoce *: l'échelle «* spur »

Au début de la saison, la croissance des pousses et des fruits a lieu simultanément sur la branche fruitière ce qui conduit à une forte compétition entre les puits végétatifs et fructifères. Dans les deux premières semaines après la floraison, les jeunes fruits de chaque spur sont presque entièrement alimentés par les feuilles de la rosette (Tustin et al., 1992). Pendant cette période les assimilats produits par les pousses de bourse et les pousses végétatives sont exportés vers leurs extrémités afin d'alimenter les jeunes feuilles encore hétérotrophes pour le carbone et qui exercent une force de puits plus importante que celle des fleurs ou des jeunes fruits (Tustin et al., 1992 ; Grappadelli et al., 1994). Cela peut même conduire au sein du spur à ce qu'une partie du carbone produit par les feuilles de rosette serve à alimenter la pousse de bourse en croissance (Tustin et al., 1992). Grappadelli et al. (1994) ont estimé ainsi que les jeunes feuilles de pommier sont des puits prioritaires jusqu'à ce qu'elles atteignent la moitié ou le tiers de leur taille adulte et ce n'est que trois à

cinq semaines après la floraison, que 50% du carbone fixé par les feuilles de la pousse de bourse sont exportés vers le fruit (Tustin et al., 1992). La pousse de bourse ne commence à exporter le maximum de sa production de carbone que lorsqu'elle atteint environ 10 feuilles bien étalées et exposées à la lumière (Grappadelli et al., 1994). Les fruits portés par des spurs avec des pousses de bourse courtes sont donc plus rapidement alimentés en carbone par ces pousses que ceux portés par des spurs avec de longues pousses de bourse.

La compétition trophique intra-spur qui s'exerce au stade précoce entre le fruit et le développement de la pousse de bourse est accentuée par celle existant entre les fruits du même spur. En effet, au cours de leurs développements les fruits d'un même spur entrent en compétition pour le carbone avec en général le fruit central ou « king fruit » dominant les fruits latéraux ce qui peut même conduire plus tard à une abscission des fruits latéraux (Bangerth et al., 2000). La floraison au sein du corymbe étant centrifuge (la fleur centrale s'épanouissant la première), cette différence de taille entre le « king fruit » et les fruits latéraux s'explique par une fécondation plus précoce pour la fleur centrale et donc un développement plus précoce du fruit central qui exerce alors une force de puits plus importante.

Toutefois, dans la situation d'une faible vigueur végétative du spur (petites feuilles de rosette et/ou pousse de bourse très courte) ou ratio feuilles/fruits intra-spur faible, les fruits peuvent également être alimentés en carbone à partir de spurs non fructifères et d'autres spurs fructifères vigoureux plus distants. (Grappadelli et al., 1994).

Les compétitions trophiques qui s'opèrent précocement au sein du spur (pousse/fruit et fruit/fruit) s'avèrent déterminantes pour la taille finale du fruit à la récolte puisqu'elles sont susceptibles de pénaliser la phase de division cellulaire du fruit qui est associée à une forte respiration et donc une forte demande en carbone.

2.1.3.2. Stades plus avancés *: l'échelle «* branche fruitière »

A des stades plus avancés, une quantité croissante d'assimilats produits par les feuilles des pousses végétatives est exportée vers les fruits et les autres parties de la branche (Wünsche et Lakso, 2000a). La mise en place de cet export est toutefois retardée si les pousses sont en situation ombragée (Grappadelli et al., 1994). Pour une feuille donnée, l'export en dehors de la pousse qui la porte dépend de sa position sur la pousse et du stade de développement de la pousse : les feuilles positionnées à la base exportent plus de 80% de leurs assimilats en dehors de la pousse alors que celles situées en zone apicale exportent seulement 20% (Hansen, 1967a). La présence de fruits sur la

branche influence aussi le schéma de distribution des assimilats. Quand le fruit grossit, sa force de puits grandissante, il devient capable d'importer des assimilats de sources éloignées (Hansen 1967b). Hansen (1969) a ainsi montré que le ratio feuilles/fruits à différents points de la branche influence la direction et la quantité de flux de carbone dans la branche. Il a observé que des spurs avec un faible ratio feuilles/fruits importent davantage de carbone à partir des pousses végétatives ou des spurs sans fruits. Les travaux conduits par Black et a1. (2000) semblent également indiquer que cette importation de carbone à partir de pousses végétatives éloignées permet de compenser les compétitions trophiques pouvant s'exprimer entre des spurs proches les uns des autres. Ces observations suggèrent une certaine remise en cause de l'importance de la distance dans la répartition des assimilats entre les sources et les puits. Déjà, Hansen (1969) avait observé que l'importation du carbone « extra-spur » était plus élevée pour les fruits proches des sources dans seulement 61% des cas étudiés. Dans la plupart des autres cas, l'importation du carbone la plus élevée était enregistrée sur le deuxième fruit le plus proche de la source et dans des cas plus rares sur le troisième et le quatrième fruit plus proche (Figure 6). De tels schémas d'allocation, pas directement reliés au facteur distance, pourraient être associés à l'architecture vasculaire de la branche.

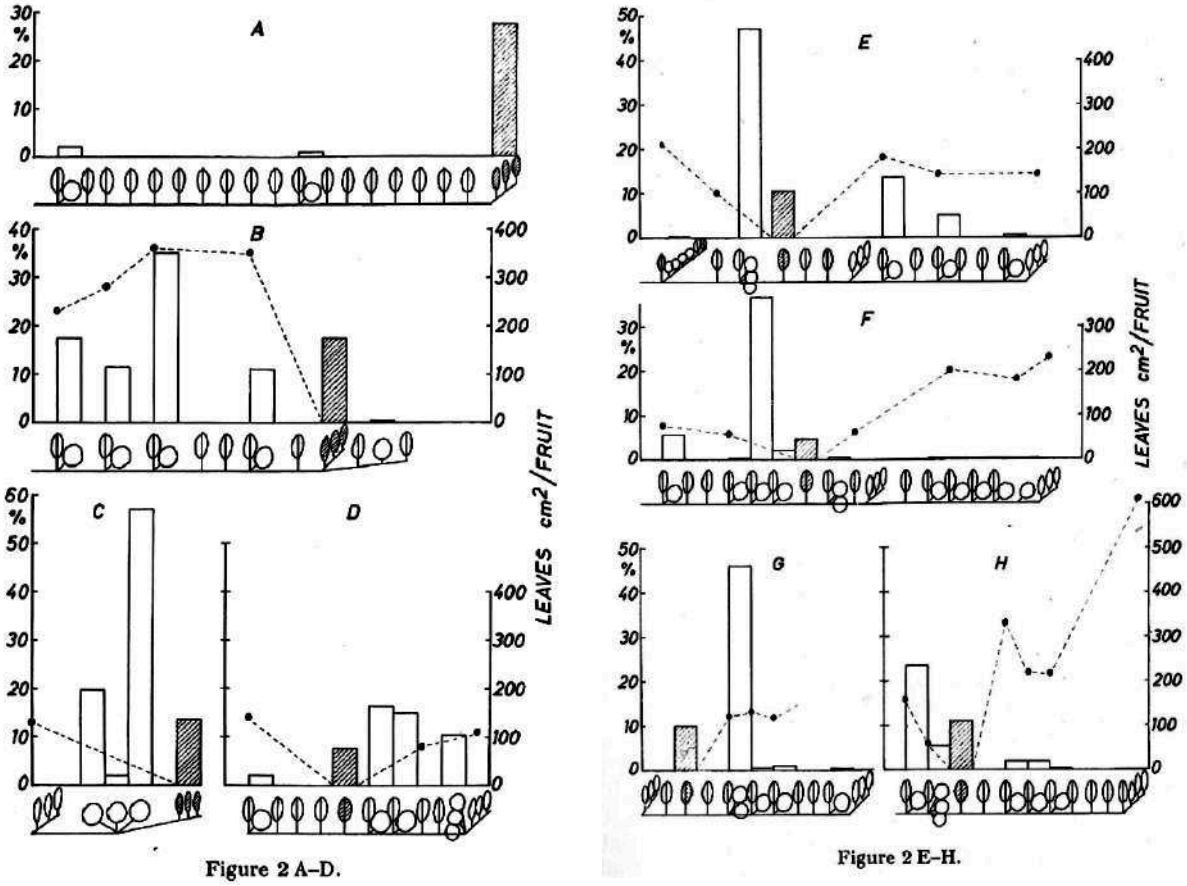

Figure 2 A–D.

Figure 2 E–H.

Figure 2. ***Translocation to fruits from extension shoots*** **(A–B–C)** ***or from spurs without fruits*** **(D–H). Activity in fruits and in exposed leaves (columns) on branch sections, given in per cent of total ^{14}C taken up immediately following exposure. = leaf bearing spur, = fruit, = extension shoot. Apex of branch to the right. Exposed parts hatched. Only the sequence and number of spurs are shown, not their actual mutual distance. The points drawn indicate the leaf/fruit ratios (cm²/fruit) calculated from cm² leaves and number of fruits taken from exposed leaves (not included) up to and including the spur above which the point is placed.**

Figure 6. Résultats de travaux conduits par Hansen (1969) mettant en évidence que la distance sources – puits ne peut pas expliquer à elle seule la translocation de ^{14}C depuis les feuilles sources (en hachuré) et les puits (en blanc).

2.1.3.3. Le rôle du système vasculaire

A l'architecture de la charpentière est associée celle du système vasculaire. Le système vasculaire est composé de deux types de tissus dont le développement se fait généralement en même temps : le xylème à travers lequel circulent l'eau et les sels minéraux et le phloème permettant le transport des composés organiques (Aloni, 1987 ; Niu et al., 2011). Le système vasculaire est à l'origine de la connexion des organes sources spécifiques à différents puits, et par conséquent détermine les voies principales pour la distribution des assimilats dans la branche. Bien que la proximité des puits des organes sources soit importante dans leur importation de carbone, des exemples où des feuilles exportaient des assimilats vers des puits plus éloignés ont été notés sur le

pommier et sur d'autres espèces (Hansen, 1969 ; Barlow, 1979 ; Antognozzi et al., 1991). Plusieurs auteurs ont émis l'hypothèse que ces observations pourraient être liées à l'existence de connexions vasculaires privilégiées entre la feuille source et le puits éloigné (Hansen, 1969 ; Minchin et al., 1997). En effet, certains vaisseaux émergeant des feuilles peuvent s'étendre sur plusieurs nœuds et avoir des connexions avec des organes éloignés (Watson et Casper, 1984 ; Dengler, 2006). Des études histologiques ont montré que les connexions vasculaires sont étroitement liées à la phyllotaxie de la plante (Barlow, 1979 ; Orians et al., 2005 ; Dengler, 2006). La phyllotaxie est représentée par une fraction dans laquelle le numérateur et le dénominateur se rapportent respectivement au nombre de tours autour de l'axe de la plante et le nombre de feuilles se situant entre deux feuilles superposées (Watson et Casper, 1984). Chez le pommier, la phyllotaxie est de 2/5 ou de 3/8 (Costes et al., 2006) et les feuilles alignées verticalement appartiennent à la même orthostiche (Watson et Casper, 1984). Les feuilles appartenant à des orthostiches adjacentes pourraient être connectées les unes aux autres, mais les connexions vasculaires les plus directes se trouvent entre les feuilles de la même orthostiche (Barlow, 1979 ; Watson et Casper, 1984). Par conséquent, le flux des assimilats dans la même orthostiche devrait rencontrer moins de résistance qu'entre des orthostiches adjacentes (Orians et al., 2005). Barlow (1979) a ainsi suivi, grâce à du carbone marqué, l'acheminement du carbone produit dans une feuille à la base d'un rameau végétatif de pommier et de prunier et en a déduit que le carbone était exporté majoritairement depuis la feuille source vers des feuilles successives appartenant à la même orthostiche (Figure 7).

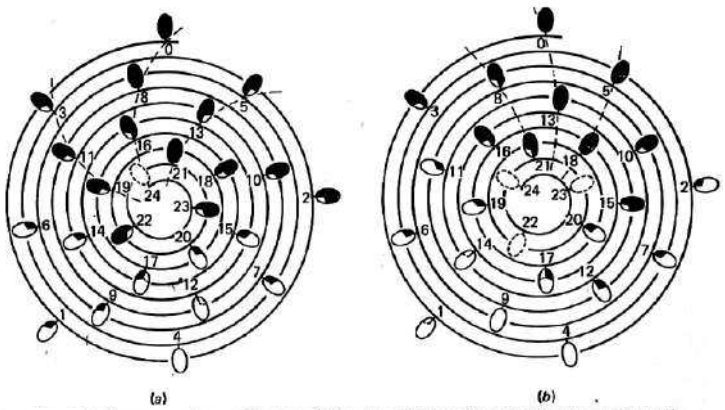

(a) (b)

Leaf arrangement round the stem of (a) apple, with leaves inserted at the average observed angle of 136·7°, and (b) plum, angle 137·8°. The source leaf is marked 0, and successive leaves upward are numbered 1–24. The distribution patterns agree reasonably well with a 'vascular phyllotaxis' of (a) 3/8 and (b) 5/13; the dashed lines indicate three of the sets of leaves which are assumed to have the most direct vascular connexions. In most cases only the dominant pattern found in each leaf is shown, but in certain leaves a less frequent pattern is indicated by broken lines. Data were not available for leaves 24 in (a) and 22–24 in (b) – their positions are indicated by the broken outlines.

Figure 7. Mise en évidence de l'importance de la phyllotaxie chez la pousse végétative du pommier et du prunier dans le transport du carbone entre sources et puits (d'après Barlow, 1979)

Par extrapolation à la branche, il existerait alors une connexion privilégiée entre les sources et les puits fructifères qui pourrait alors remettre en cause la distance entre les sources et les puits comme facteur prioritaire dans la répartition des assimilats, participerait à la compétition entre les puits pour l'importation des assimilats (Orians et al., 2005) et pourrait également affecter la tolérance de l'arbre aux stresses environnementaux selon Zanne et al. (2006). En effet, la modification de l'architecture vasculaire en réponse à des changements dans le développement de la plante – stress ou techniques culturales – pourrait ainsi altérer les voies majeures pour la distribution des assimilats. Le débourrement des bourgeons et la naissance de nouveaux organes sont accompagnés par un établissement de nouvelles connexions vasculaires (Aloni, 1987). Le développement des tissus vasculaires est lié aux dynamiques du transport des auxines qui sont produites par les jeunes organes en croissance et transportées de façon basipétale (Aloni, 1987 ; Lucas et al., 2013). Dans la pomme, la différenciation du système vasculaire dans le pédicelle commence avant la floraison et se termine 3 à 4 semaines après et avant le stade du grossissement rapide du fruit (Dražeta et al., 2004). De petits vaisseaux de faible conductivité se développent avant la floraison, alors que les larges vaisseaux à haute conductivité sont formés après (Lang et Ryan, 1994 ; Dražeta et al., 2004). Chez d'autres espèces d'arbres, l'augmentation de l'importation du carbone par le fruit en réponse à l'incision annulaire a été associée à l'augmentation de la surface vasculaire dans le pédicelle du fruit (Antognozzi et al., 1991 ; Bustan et al., 1995). Sané et al. (2012) ont émis l'hypothèse que l'augmentation de l'importation des assimilats par le fruit dans l'inflorescence du pommier pourrait être corrélée avec une augmentation de la vascularisation de la bourse.

2.2. La modélisation comme outil pour l'arboriculture fruitière

Un modèle est la représentation, souvent sous forme algorithmique sur un ordinateur, d'une partie de la réalité, et d'habitude, d'un système que l'on veut étudier. Les modèles sont utilisés pour abstraire, décrire, simuler, extrapoler et enfin comprendre la fonction des systèmes complexes, comme par exemple les plantes. Les modèles n'intègrent pas tous les processus impliqués dans le système que l'on cherche à modéliser et nécessitent donc une sélection qui doit être raisonnée afin d'obtenir une représentation simplifiée du système qui toutefois est réaliste, compréhensible et utilisable (Figure 8).

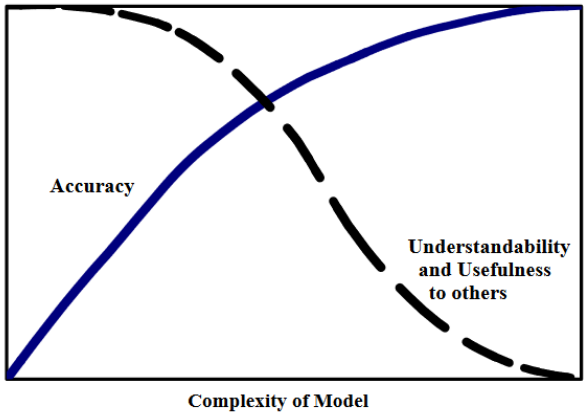

Fig. 1 General diagram indicating that as models increase in complexity from the most simple (e.g. single driving factor), the accuracy of predictions may increase, but the understandability of all the interactions and regulation of the model decreases. Finding an appropriate balance is a challenge with all models, but especially with crop models in natural environments.

Figure 8. Schéma de Goldschmidt et Lakso (2005) illustrant le fait que plus un modèle augmente en complexité plus il devient pertinent, mais qu'il perd en parallèle en compréhensibilité et ainsi en utilité pour les praticiens. Le défi serait donc de construire un modèle qui soit à la fois pertinent et suffisamment compréhensible.

Cette sélection est souvent guidée d'une part par les disciplines (agronomie, agriculture et horticulture, biologie, écologie, foresterie, paysage, infographie et informatique, mathématiques et langues formelles) des individus ou des groupes qui développent ce type d'approche pour les plantes, et d'autre part par l'utilisation qui en est faite. En général, ces différentes utilisations peuvent être classées, de manière non exclusive, en trois groupes, selon les objectifs visés. Le premier groupe correspond aux modèles avec un intérêt purement scientifique qui sont développés par des chercheurs pour des chercheurs. Ils servent notamment à mieux comprendre un processus (eco-)physiologique en lien ou pas avec la structure de la plante, et ne sont généralement pas appliqués ni applicables en pratique par des non-scientifiques par manque d'interfaces. Le deuxième groupe comprend les modèles servant à visualiser les plantes, pour des raisons pédagogiques (enseignement en biologie) ou bien commerciales (visualisation infographique de paysages/plantes individuels). Ce groupe de modèles ne considère souvent que la structure et la morphologie car ce qui compte, dans ce cas, c'est l'apparence réaliste de la plante. Enfin, le troisième groupe correspond aux modèles utilisés comme outils d'aide à la décision (OAD). Cette classification n'est bien sûr pas exclusive car un bon nombre de modèles peuvent émarger dans deux voire les trois groupes.

Au-delà de cette classification basée sur les objectifs assignés au modèle, les modèles peuvent être classés, notamment en écophysiologie végétale, selon qu'ils ne prennent en compte que

les processus (Process-Based Models) ou bien qu'ils intègrent en plus et en interaction l'architecture de la plante (Functional-Structural Plant Models).

2.2.1. La modélisation basée sur les processus (Process-Based Models ou PBM)

Les premiers modèles qui ont décrit des aspects de croissance et de développement des pommiers étaient du type « Process-Based Models », donc sans prise en considération de l'architecture de l'arbre ou de ses branches. Alan Lakso (Johnson et Lakso, 1986 a et b ; Lakso et Johnson, 1989 ; Lakso et al., 1995, 1999, 2000) peut être qualifié de pionnier dans ce domaine. La plupart de ses modèles simulent d'une manière simplifiée l'accumulation de la matière sèche au sein de l'arbre, avec un pas journalier, et donc en prenant en considération des processus intégrés plutôt que des taux instantanés (par heure, minute ou seconde), ceci éliminant la complexité de changement en rayonnement journalier. L'intégral journalier de la photosynthèse est calculé par une approche basée sur l'efficacité d'utilisation du rayonnement (radiation use efficiency), prenant en compte le taux maximal de la photosynthèse, l'efficacité photochimique, l'intégrale du rayonnement journalier, la longueur du jour, le coefficient d'extinction du couvert ainsi que l'index de la surface foliaire (ou la fraction de la lumière interceptée disponible). Puis, dans ce type de modèle, le développement de la surface foliaire est basé sur le cumul des degrés-jours, un taux constant de production de feuilles par degré-jour, avec le nombre de pousses et la fraction des pousses en état de croissance en même temps. La respiration est contrôlée par la température. Tandis que la respiration du bois et des feuilles dépend des surfaces, celle du fruit dépend de son poids.

Une autre approche, correspond au modèle QualiTree (Lescourret et al., 2011 ; Mirás-Avalos et al., 2011, 2013a et b ; Figure 9). C'est un modèle de croissance de pêcher centré sur les rameaux mixtes et les fruits. Il intègre des modèles à plusieurs échelles : des tissus (notamment pour les fruits) à l'arbre tout entier. Son exécution s'étend de l'apparition des fruits à la récolte. Il permet de simuler des techniques culturales comme l'éclaircissage et la taille en vert. Son prédécesseur, le modèle de Lescourret et al. (1998), décrit un système isolé comprenant les éléments pousses et fruits qui simule l'assimilation journalière du carbone et son allocation vers les puits. Le système simulé est divisé en trois compartiments : les fruits, la tige d'un an, et les pousses feuillées récentes. Dans ce modèle, la croissance des organes puits est contrôlée par un réservoir de carbone comprenant la quantité journalière de carbone produit par les feuilles ainsi que celle mobilisée des réserves si la demande des organes puits dépasse la quantité produite par la photosynthèse.

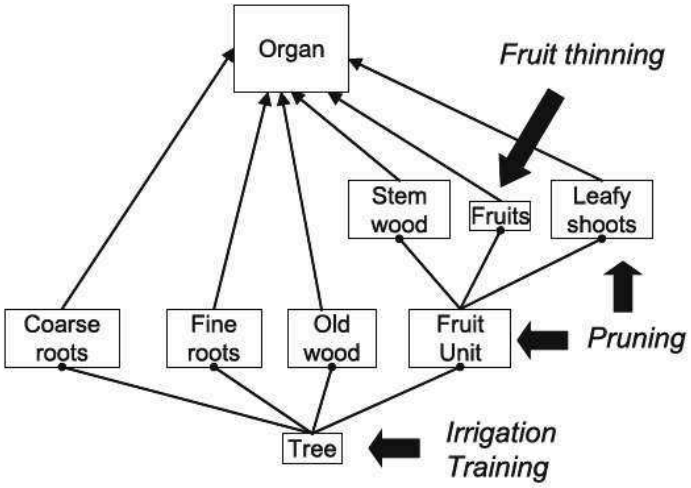

Fig. 1 Structure of QualiTree according to the UML language. *Boxes* are classes, and *lines* are relationships between classes, dealing either with generalisations (*arrows* Stem wood is an organ) or with composition (*black circles* Tree is composed of coarse roots, fine roots, etc.). Cultivation practices and their targets are indicated

Figure 9. Schéma objet-orienté du modèle QualiTree (Lescourret et al. 2011), illustrant les relations entre les différentes classes (compartiments) ainsi que les pratiques de gestion prises en considération par le modèle.

Le sous-modèle décrivant la photosynthèse inclut une rétroaction inhibitoire baissant le taux d'assimilation en fonction des réserves foliaires en amidon et le modèle est capable d'apprécier l'effet de l'extinction luminaire causée par les feuilles. Finalement, l'assimilation du carbone par les fruits est prise en considération, offrant ainsi la possibilité de couplage de ce modèle avec les modèles du type Fruit Virtuel (Fishman et Génard, 1998 ; Lechaudel et al., 2005 ; Génard et al. 2007 ; Etienne et al., 2013 ; Nordey et al., 2014 ; Figure 10). Ces modèles ont pour objectif de simuler, pour différentes espèces fruitières (pêcher, manguier, bananier…), d'une manière générique, les processus écophysiologiques au sein du fruit et dans son entourage immédiat (pétiole du fruit), qui mènent à la mise en place des composantes moléculaires contribuant à la qualité du fruit : le(s) sucre(s), l'amidon, l(es) acide(s) et l'eau, mais aussi la couleur ; et leur dynamique au cours de la maturation du fruit, de la nouaison à la récolte. Les processus modélisés sont la photosynthèse foliaire, la demande du fruit en assimilats, la respiration du fruit, le stockage et la remobilisation des assimilats des réserves dans la feuille et tige.

Figure 1. Schematic representation of the relationships between sub-models as considered in the virtual fruit.
The sub-models simulate carbon balance of a fruit-bearing stem, sugar and citric acid metabolism within the fruit, fruit water balance, skin conductance and microcracking, fruit respiration and ethylene metabolism. The inputs to the model (red) are weather data, stem water potential, and the state of the system at the beginning of the simulation (number of leafy shoots and fruits, initial values of fruit mass, leaf area, sugar and acid concentrations). The outputs (blue) are flesh and stone mass, sugar and acid content, skin microcracking, and emission of gases.

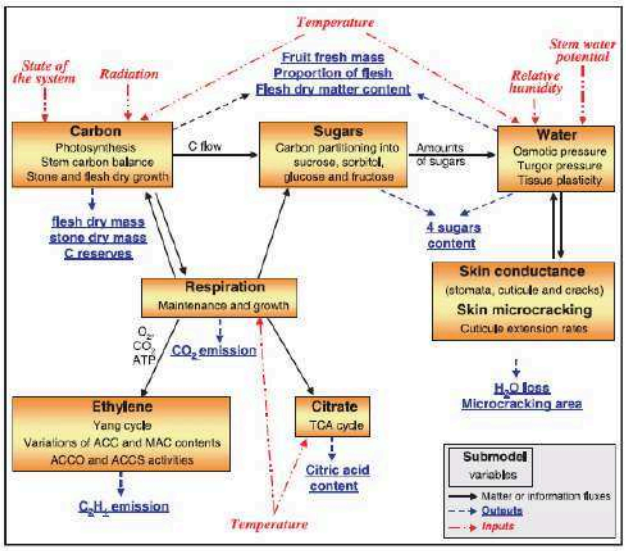

Figure 10. Schéma illustrant le principe des modèles de la même classe que Fruit Virtuel (Génard et al., 2010)

2.2.2. La modélisation structuro-fonctionnelle (Functional-structural plant models ou FSPM)

*2.2.2.1. Importance de la prise en compte de l'archit*ecture pour le pommier

Contrairement à certaines espèces fruitières comme le pêcher où le mode de conduite et de taille des arbres conduit à simplifier l'architecture à un ensemble de rameaux longs portant les fruits et les pousses végétatives en position axillaire, chez le pommier les opérations de taille ne conduisent pas à réduire la complexité existante. Cette complexité s'exprime au travers des différents types architecturaux (cf. partie 2.1.1.) déterminés par différentes longueurs de pousses végétatives (Costes, 2003, Seleznyova et al., 2003) et de bois porteur (pousses courtes : lambourdes, médianes : brindilles couronnées et longues : rameaux longs). Chez le pommier, la prise en compte de l'architecture s'avère donc être une nécessité pour la modélisation.

2.2.2.2. Principe de la modélisation FSPM

La modélisation nommée « Modélisation structuro-fonctionnelle des plantes », qui est mieux connue par son nom Anglais « Functional-Structural Plant Modelling » avec l'acronyme FSPM, a été définie par Vos et al. (2010) de la manière suivante : « Functional-structural plant models, FSPMs or virtual plant models are the terms used to refer to models explicitly describing the development over time of the 3D architecture or structure of plants as governed by physiological processes which, in *turn, are driven by environmental factors".* Buck-Sorlin (2013) a légèrement modifié et élargi cette

définition en précisant que FSPM (Figure 11) représente une approche visant à décrire une plante par la création d'un modèle informatique (le plus souvent objet-orienté) de sa structure et par une sélection des processus physiologiques et biophysiques, et ceci à différents niveaux d'échelle : organe, plante (individu), couvert (population) ou peuplement (un petit groupement des plantes en rangs et lignes), et dans lequel les processus sont modulés par l'environnement de chaque organe qualifié de « phylloclimate » selon Chelle (2005).

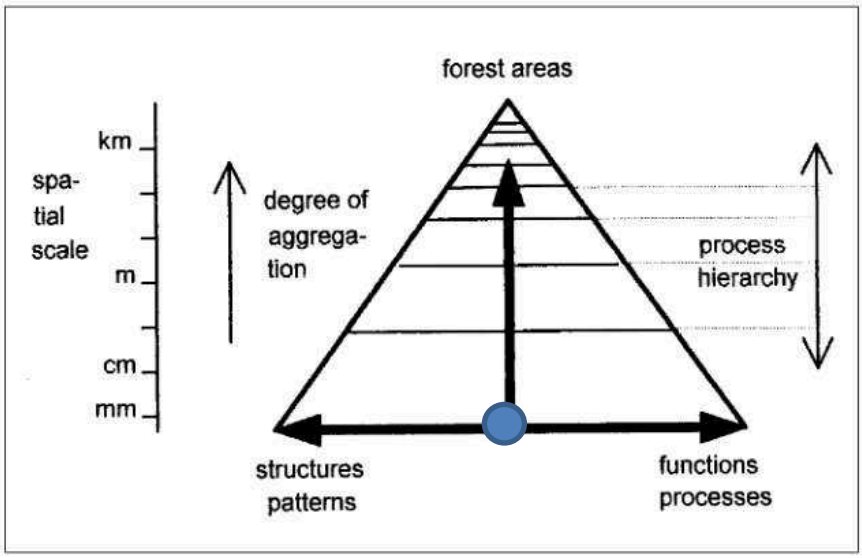

Figure 11. Schéma représentant, sous forme d'un triangle, un panorama des modèles de plantes en fonction du degré d'intégration ou agrégation. La position des FSPM est le point bleu à la base du triangle, à l'échelle individuelle, et entre les deux côtés basals du triangle qui, eux, représentent les modèles purement structurels ou purement fonctionnels (d'après Kurth 1994, modifié).

La structure comprend la topologie explicitée (connexion entre organes) ainsi que la géométrie (orientation, inclination, et forme) des organes et de la plante. A l'échelle de l'individu, cette organisation constitue l'architecture de la plante. Un FSPM peut prendre en considération le changement dans le temps d'un organe par rapport à sa structure et ainsi simuler la croissance, l'extension, ou bien encore les processus de ramification d'une plante donnée. Cette classe de FSPM est qualifiée de « dynamique » par opposition au FSPM « statique » pour lequel la structure reste inchangée dans le temps et est donc non simulée et constitue alors une entrée du modèle pour analyser l'hétérogénéité des processus physiologiques simulés en lien avec la structure. C'est cette prise en compte de la géométrie et topologie des éléments structurels qui distinguent les FSPM de leurs prédécesseurs, les modèles basés sur des processus (en Anglais crop models ou encore Process-Based Models) (Buck-Sorlin, 2013).

Les processus physiologiques et physiques habituellement pris en compte comprennent les fonctions essentielles ou « primaires », basiques et caractéristiques, telles que la photosynthèse et la croissance (accumulation de la biomasse ainsi que l'extension d'un organe en longueur, en diamètre ou en surface) dépendant des facteurs environnementaux tels que la température, le rayonnement photosynthétiquement actif (PAR), la concentration en CO_2 de l'air, ou encore l'humidité relative de l'air. Ces processus (ou fonctions) sont normalement implémentés à l'échelle de l'organe et requièrent un paramétrage à partir de données environnementales avec une résolution spatiale et temporelle assez fines.

Une caractéristique clé des FSPM est l'existence des rétroactions entre structure et certaines fonctions. Ainsi, une structure donnée (statique ou le résultat de l'application des règles de croissance) peut moduler la sortie locale d'un processus : par exemple, l'auto-ombrage des feuilles peut engendrer localement une diminution de la lumière interceptée et donc de la photosynthèse ; d'un autre côté, toutes les structures sont construites et entretenues par des processus : par exemple la croissance des structures est assurée en partie par les assimilats issus de la photosynthèse (Buck-Sorlin, 2013).

2.2.2.2. Applications aux plantes et espèces fruitières

Les études qui ont utilisé des FSPM sont nombreuses : citons, à titre d'exemple, les premiers modèles appliqués aux arbres développés par les pionniers et protagonistes de FSPM : le modèle LIGNUM par Sievänen et al. (2000) ; ou le modèle de l'épicéa par Kurth (1994), un des premiers exemples d'application des grammaires sensitives de croissance – nommées « sensitives » car équipées de capteurs virtuels simulant la perception de la lumière ou des obstacles – (Figure 12). Ce formalisme des « sensitive growth grammars » était réalisé dans la continuité des L-systèmes évoqués plus haut (Lindenmayer 1968a, b).

Les premières implémentations dans le domaine agronomique ont été réalisées par Fournier et Andrieu (1999) et Fournier et al. (2003) pour les céréales (respectivement les modèles ADEL-maize et ADEL-wheat), suivies par des modèles sur l'orge (Buck-Sorlin et al. 2008), le riz (Luquet et al. 2006 ; Xu et al. 2011) et les plantes ornementales comme le rosier (Buck-Sorlin et al. 2011 ; Figure 13). Concernant les espèces fruitières, on peut citer les modèles développés pour la vigne (Pallas et al. 2009), le kiwi (Cieslak et al. 2011a, b), le palmier (Pallas et al. 2013), le pêcher (L-Peach: Allen et al. 2005 ; Lopez et al. 2008, Smith et al. 2008) et enfin le pommier (MAppleT: Costes et al. 2008, da Silva et al. 2014).

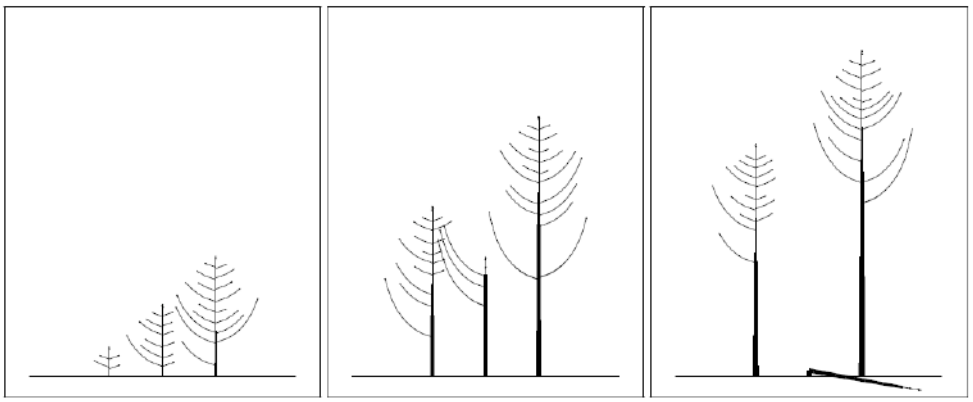

Fig. 9: Competition for light in a simple 2D tree stand, consisting of 3 uneven-aged trees, produced by GROGRA from the sensitive growth grammar *light2d.ssy* (see Table 3).
The steps 12, 25 and 31 are shown.

Figure 12. Exemple d'un modèle utilisant « the sensitive growth grammars » pour simuler la compétition pour la lumière dans un petit groupement d'arbres (Kurth 1998).

Figure 13. Exemple pour un FSPM d'une plante ornementale, avec interaction avec la structure : rosier à fleurs-coupées (Buck-Sorlin, 2009, non publié).

Chez le pommier, le modèle MAppleT (Costes et al. 2008, da Silva et al. 2014) est dédié à la simulation de l'architecture de jeunes pommiers en combinant la topologie et la géométrie dans une seule simulation de manière à ce que l'architecture du pommier devienne un trait émergent des interactions entre les processus des croissances primaire et secondaire des pousses. Plus récemment, Pallas et al. (2016), en reprenant le modèle MAppleT et le couplant avec QualiTree (Figure 14), ont cherché à adapter QualiTree au pommier afin de pouvoir simuler des traits décrivant la croissance des différents organes ainsi que leurs variabilités intra-arbre. Dans cette approche, MAppleT a été utilisé pour générer des architectures correspondant au cultivar 'Fuji' en intégrant la variabilité intra- et inter-individuelle. Ces architectures étaient ensuite importées dans QualiTree pour simuler la croissance des pousses et des fruits pendant un cycle de développement. QualiTree a été modifié afin de prendre en considération le polymorphisme au niveau des pousses du pommier. Les résultats montrent que l'approche combinant MAppleT et QualiTree est appropriée pour la simulation des traits de croissance et d'architecture à l'échelle de l'arbre (surface foliaire totale, nombre et types de pousses, poids de fruits à la récolte).

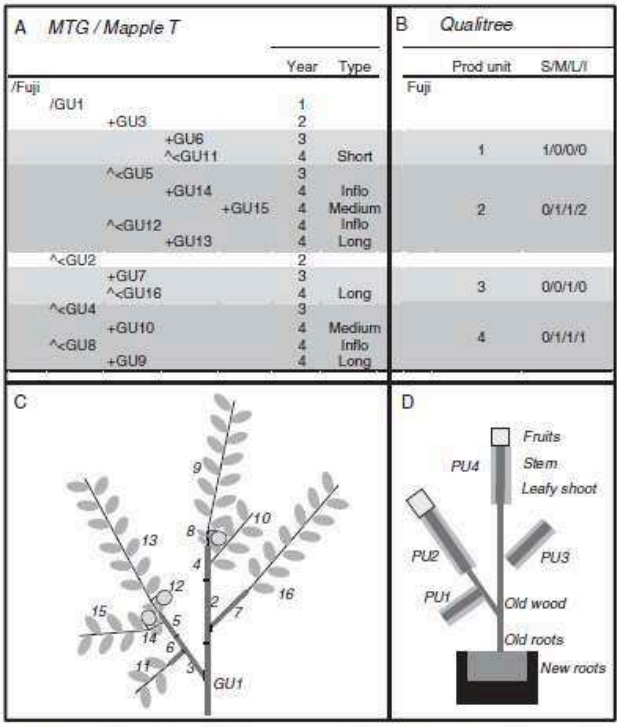

FIG. 1. Schematic representation of the procedure used to convert multiscale tree graphs (MTGs) generated by MappleT into QualiTree architecture in a simplified example. (A) MTG generated by MappleT and represented at the growth unit (GU) scale. (B) Conversion of the MTG into QualiTree architecture described at the production unit scale. S, M, L and I refer to short, medium, long and inflorescence GUs, respectively. (C) Schematic representation of the plant in MappleT. (D) Schematic representation of the plant in QualiTree. The numbers in C refer to the GU label.

Figure 14. Représentation schématique de la procédure utilisée pour convertir les graphes multi-échelles des arbres (MTG) générés par MAppleT en architecture lisible par QualiTree (Pallas et al., 2016)

Il est à citer que le modèle GreenLab tel que présenté par De Reffye et al. (2009) se positionne comme un hybride de PBM et de FSPM puisque les principes sur la base desquels il est construit appartiennent pour une partie aux PBM et pour l'autre aux FSPM. En effet, GreenLab a en commun avec les PBM : le fait que la biomasse émane d'un réservoir commun et est directement liée à l'index de surface foliaire et l'efficience d'utilisation de la lumière ; la production de la biomasse et sa distribution constituent deux processus indépendants ; la répartition de la biomasse se fait entre les organes en compétition vis-à-vis du réservoir commun. Par contre, GreenLab a en commun avec les FSPM d'autres principes : les organes sont hiérarchisés selon leur âge physiologique ; la quantification de l'organogénèse ; la géométrie et la topologie de la plante (représentations en 3D) ; la possibilité d'intégrer le comportement stochastique (Kang et al., 2008a). Par ailleurs, ce modèle est capable de simuler la dynamique de modification de l'architecture et les phases d'apparition et de croissance des organes en fonction des conditions environnementales (Mathieu, 2006). Grâce à sa construction, GreenLab a l'avantage de pouvoir être adapté à une multitude d'espèces végétales – le maïs (Guo et al., 2006 ; Ma et al., 2006) ; le concombre (Mathieu et al., 2007) ; le blé (Kang et al., 2008b) ; l'eucalyptus (Diao et al.,2012) – ainsi qu'à un couvert végétal composé de différentes plantes par exemple pour la compétition pour la lumière (Cournède et al., 2008).

2.2.2.3. Acquisitions des données et leurs utilisations

Le point commun de tous les modèles de type FSPM est qu'ils requièrent un nombre important de paramètres dont souvent un nombre considérable de paramètres « cachés ». Ces derniers désignent les paramètres qui ne sont pas du tout évidents à cerner ou prédire au cours de la mise en place des processus inclus dans le modèle ; ou s'ils sont identifiés, dont les valeurs ne sont pas mesurables (du moins facilement) ; ou encore dont les mesures mènent à la destruction de la structure et donc l'impossibilité d'acquérir des mesures dynamiques sur une même structure. De plus, la rigueur des analyses statistiques requiert un nombre suffisamment important de mesures d'une même variable, couplées avec les mesures d'autres variables dépendantes. Un réseau de corrélations des variables peut donner une trame pour la structuration du futur modèle, dans le sens où il permettrait de donner une indication sur quels processus clés seraient à inclure dans le modèle. Pour paramétrer un modèle, il est donc possible de mesurer les paramètres en question expérimentalement ou bien les estimer indirectement à partir de données expérimentales faites sur d'autres variables. Dans le cas échéant, certains paramètres peuvent être récupérés à partir de la bibliographie. Toutefois, cette dernière alternative implique une perte d'informations autour du contexte d'acquisition des données

qui lui est rarement bien documenté dans les publications. En d'autres termes, le contrôle du degré de justesse des corrélations est diminué et le modèle s'en retrouve pénalisé par de plus grandes simplifications. Idéalement, il serait donc favorable de mesurer le maximum de variables d'état d'un système végétal et ensuite explorer les réseaux de corrélations afin de détecter et mieux cerner les processus indépendants de ceux qui sont fortement en lien avec d'autres. Une telle approche est routinière dans le domaine de la génomique ou transcriptomique, en absence totale des connaissances sur la structuration des régulations des processus.

2.3 Objectifs de la thèse

Les objectifs de la thèse s'inscrivent dans l'objectif plus global de l'équipe ; celui d'élaborer un modèle FSPM à l'échelle de la charpentière du pommier afin de simuler le transport du carbone et prédire la croissance et la qualité des fruits. Pour ce modèle, il a été décidé de ne pas simuler l'architecture (donc la « structure ») mais de l'utiliser comme une variable d'entrée du modèle. Concernant la partie « fonctionnelle » du modèle, trois processus seront simulés : la production de carbone par les feuilles, le transport et la répartition du carbone produit et enfin la croissance et la qualité du fruit.

Dans ce contexte, les objectifs de la thèse visent (i) d'une part, pour la partie « structure », à proposer un modèle simple basé sur des relations allométriques et utilisant quelques variables faciles à acquérir afin de pouvoir reconstruire l'architecture initiale d'une branche donnée (ii) et d'autre part, pour la partie « fonctionnelle », à mieux cerner les rôles des différents organes sources et puits et la répartition du carbone comme indicateur de la qualité du fruit en considérant deux niveaux d'échelle : le spur et la branche fruitière. L'ensemble du travail de thèse est basée sur deux campagnes expérimentales menées en 2014 et 2015 chez 3 variétés de pommes : 'Ariane', 'Fuji' et 'Rome Beauty' choisies pour leurs morphologies contrastées. Les expérimentations ont consisté en une manipulation des ratios entre les sources et les puits en effectuant des effeuillages et des suppressions des fruits, à différents stades de développement et en ciblant différents types de pousse. Des analyses statistiques, utilisant notamment les réseaux de corrélation, ont été conduites avec l'espoir de pouvoir voir « émerger » des mécanismes d'allocation du carbone et proposer des premiers éléments de paramétrage du modèle. Il aurait en plus été souhaité, dans le cadre de la thèse, de paramétrer et calibrer globalement le modèle, mais en considérant la charge liée à l'acquisition de la base de

données et celle accordée à l'analyse statistique des données écophysiologiques et leur interprétation, il a été décidé de n'inclure qu'une petite partie de ce modèle (chapitre 3).

L'ensemble du manuscrit est composé de 3 chapitres construits comme des articles scientifiques à soumettre ou déjà publiés dans des revues internationales à comité de lecture (cf chapitre 2) et d'une discussion générale :

Le chapitre 1 est dédié à une étude expérimentale, conduite en 2014 à l'échelle du spur, qui visait à démontrer l'effet d'effeuillages précoces des deux différents types de pousses au sein du spur (rosette et pousse de bourse) sur la qualité des fruits, en analysant finement les corrélations entre les variables caractérisant les organes sources et puits. Le questionnement scientifique dans cette première étude était tripartite : Quel est le rôle des feuilles de rosette et des feuilles de la pousse de bourse ? Quel est le rôle de la bourse du pommier ? Et finalement quelle est l'influence du spur sur les relations sources/puits et la bourse ? Ce questionnement nous a amené à élaborer quatre hypothèses : H1 : L'apport en carbone avant la nouaison est déterminant pour la division cellulaire ; H2. Le spur est autonome à des stades précoces ; H3. A des stades précoces, ce sont les feuilles de rosette qui alimentent l'inflorescence ; H4. Il y a des différences de comportement entre les trois variétés choisies dans cette étude dues à leurs différences architecturales.

Le chapitre 2 présente de nouveaux modèles qui permettent la reconstruction de l'architecture initiale d'une branche comme entrée dans un modèle structuro-fonctionnel du pommier, avec une emphase sur la prédiction de la surface foliaire à l'échelle de la pousse ainsi que la forme et la surface de chaque feuille, utilisant des relations allométriques entre les variables décrivant l'architecture des pousses. Les modèles ont été calibrés et testés utilisant deux jeux de données, un pour la paramétrisation et la calibration, l'autre pour la validation. Ainsi il a été prouvé que les modèles sont suffisamment robustes pour la prédiction de la surface foliaire des trois cultivars étudiés dont la morphologie des feuilles et des pousses est différente.

Le chapitre 3 s'inscrit dans la continuité du chapitre 1. Etant donné les résultats de la campagne expérimentale de 2014 qui n'étaient pas entièrement aptes à expliquer la dynamique d'allocation du carbone vers les fruits, l'expérimentation de 2015 avait pour principal objectif d'élargir l'analyse des relations sources/puits à l'échelle de la branche fruitière. Pour cela, comme pour le chapitre 1, une manipulation du ratio sources/puits mais à l'échelle de la branche a été réalisée, en utilisant des charpentières et des sous-charpentières extrêmement simplifiées par rapport à leur structure initiale. En outre, ce dispositif nous a également permis de tester un premier modèle FSPM de production de carbone et de croissance des fruits pour une branche du cultivar 'Fuji' en

simulant l'interception lumière et la photosynthèse potentielle à partir des structures reconstituées selon le modèle allométrique présenté dans le chapitre 2.

En dernier, l'ensemble des résultats obtenus sont discutés et des perspectives à court et moyen termes sont proposées pour le développement du FSPM.

Chapitre 1

Impact of Defoliation on Growth and Development of Spur Organs in Apple

Ce chapitre a été rédigé en Anglais afin d'être envoyé à une revue internationale à comité de lecture.

Abstract Chez le pommier, les rameaux et tiges, qui jouent à la fois le rôle de structures vasculaires et de supports, constituent l'architecture de l'arbre reliant les sources et les puits. A l'échelle de la branche fruitière et pour une année donnée, en plus du bois porteur (rameaux mis en place les années précédentes), on peut distinguer 2 types de structures : les pousses végétatives issues du développement de bourgeons végétatifs et les spurs issus du développement de bourgeons floraux (qualifiés de « mixtes » chez le pommier). Le spur est composé d'une bourse, des feuilles de rosette, d'une ou deux pousse(s) de bourse et de l'infrutescence. Dans des travaux antérieurs, il a été mis en évidence le rôle crucial des sources proches de fruits (à l'échelle du spur) sur la croissance et la taille finale du fruit à la récolte laissant ainsi supposer qu'il existe de fortes corrélations de croissance entre les différents organes constitutifs du spur. Afin de mieux élucider le rôle joué par ces sources dans le développement précoce du fruit et l'importance des relations de croissance entre les organes du spur, nous avons conduit des expériences impliquant une défoliation précoce (au moment de la floraison ou deux semaines plus tard) partielle ou totale du spur (suppression de la pousse de bourse et/ou des feuilles de rosette). Un nombre important de variables morphologiques relatives aux différents organes du spur ont été mesurées pour 3 différents cultivars avec des architectures contrastées : 'Ariane', 'Fuji', et 'Rome Beauty'. Des analyses par réseaux de corrélations nous ont permis de mettre en évidence une forte indépendance entre les caractéristiques des organes reproducteurs (fruits et pépins) et végétatifs (feuilles et bourse) avec toutefois une certaine modulation en fonction des cultivars. Nos travaux ont également permis de montrer un effet différent selon les cultivars selon la suppression précoce des feuilles de rosette et/ou de la pousse de bourse mettant en évidence l'importance relative de ces deux types de sources pour le développement précoce des fruits. L'ensemble des données acquises constituent en plus un jeu de données utilisable pour paramétrer un modèle structuro-fonctionnel à l'échelle de la branche fruitière du pommier.

Impact of defoliation on growth and development of spur organs in apple

Emna Baïram, Mickaël Delaire, Christian LeMorvan, Gerhard Buck-Sorlin

Unité Mixte de Recherche 1345, Institut de Recherche en Horticulture et Semences (INRA-Agrocampus Ouest-Université d'Angers), Angers, France

Keywords: Malus x domestica Borkh., apple, spur, sugar transport, allometry, defoliation.

Abstract

In apple, stems that function as vascular and support structures, and that constitute the architecture of a first-order fruit-bearing branch (FBB) connect sources and sinks. At the branch scale, vegetative shoot and flowering spur make up the FBB, while at the scale of the spur, rosette, bourse, bourse shoot and fruit are the constituting organs. In order to elucidate the role of early local carbon sources for fruit growth, we carried out experiments involving early defoliation (around the time of full bloom FB and two weeks afterwards: FB2) of the two types of spur leaves (bourse shoots or rosettes, or both). A large number of traits characteristic for the spur organs (fresh and dry weights, organ dimensions) was measured on three different cultivars ('Ariane', 'Fuji', and 'Rome Beauty') that exhibited contrasting spur and branch architecture. We used detailed networks to map and visualize the correlations among spur traits. Generally, reproductive (fruit and pips) traits turned out to be largely independent from vegetative (leaf and stem) spur characteristics, but this was moderated by a clear cultivar effect. Defoliation only had a drastic effect when it was total and applied early (at FB), else its effects were rather subtle and exhibited interaction with the cultivar. The extensive correlated data set obtained in the present study will be used to parameterize a functional-structural plant model of the apple branch, which subsequently could be used as a scientific tool to integrate knowledge in apple ecophysiology

1. Introduction

In apple, the distribution of assimilates changes during the development of the fruit and the vegetative structures. Sugar redistribution starts with the transport of assimilated carbon, in the form of sorbitol or sucrose, from source organs to the different sink organs (Teo et a1., 2006.). Sources and sinks are connected via internodes, which function as vascular and support structures, and which

constitute the architecture of the first-order fruit bearing or carrier branch. Such a branch (Figure 1) essentially consists of three types of shoots: vegetative shoots, bourses, and bourse shoots.

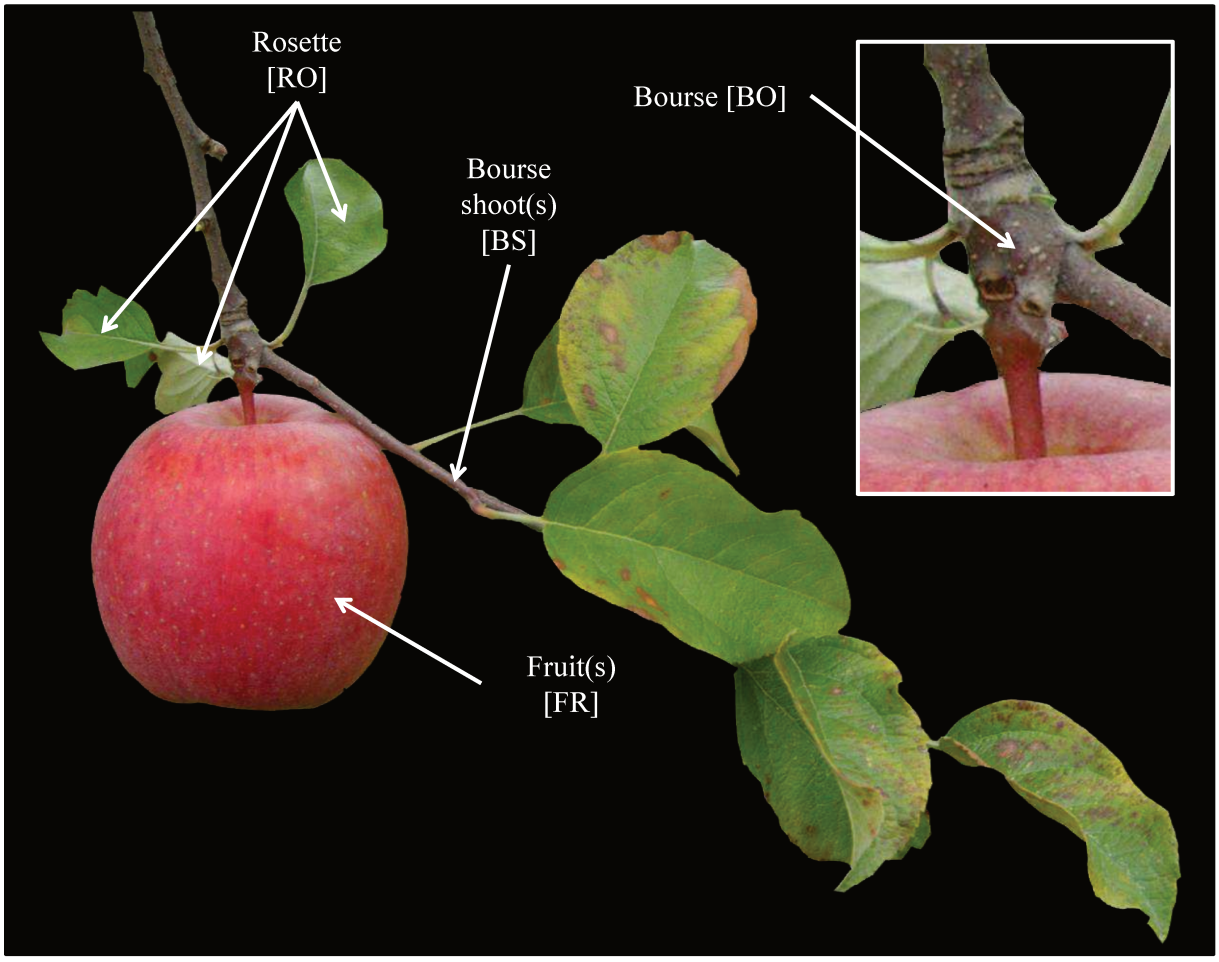

Figure 1. Representation of the different organs on a spur: Fruit(s) (FR), bourse (BO), rosette (RO) and bourse shoot(s) (BS) (E. Bairam, 2014)

While a vegetative shoot is a regular short or long shoot with an intact terminal bud that will grow out into a shoot in the following season, a bourse is a short shoot formed from a mixed bud, with a rosette of preformed leaves and a terminal inflorescence bearing one to six flowers, and in the axil of rosette leaves, one or two sylleptic shoots (bourse shoots), that function as a relay to continue the axis after the terminal bud is used up by the formation of the terminal inflorescence. The product of one mixed bud (bourse, bourse shoot(s), and inflorescence) is also referred to as a "spur" (Fanwoua et al., 2014). The influence of this branch architecture on the distribution of assimilates is complex and far from being well elucidated. Experiments in which the movement of radioactively labelled carbon into the different organs has been followed up give some indications as to the role branch architecture

plays on assimilate redistribution (Hansen, 1967; Tustin et al., 1992; Grappadelli et al., 1994, Poirier-Pocovi et al., unpubl.). These studies showed that the developmental state of the sources and sinks as well as their position on the branch exert an influence on assimilate distribution. Accordingly, two types of hierarchical scales must be taken into account: the temporal scale linked to the developmental state of the sources and sinks; and the spatial scale, thereby considering the scale « spur » and the scale « fruit-bearing branch ». During early growth in spring, after the breaking of the mixed buds, growth of vegetative structures and fruits takes place simultaneously on the fruit-bearing branch of apple, thereby leading to a strong competition between vegetative (internodes and young leaves) and generative sinks (fruits). In the first two weeks after flowering, the young fruits of each spur are almost exclusively fed by the rosette leaves (Tustin et al., 1992). During this period the assimilates produced by bourse shoots and vegetative shoots are being exported to their respective shoot tips in order to feed the young leaves (Tustin et al., 1992; Grappadelli et al., 1994). Shoot-tips and young leaves have a higher sink strength than flowers and young fruits. This can even lead to a situation where part of the carbon produced by the rosette leaves will nourish the developing bourse shoot (Tustin et al., 1992). Grappadelli et al. (1994) thus reckon that the young apple leaves are primary sinks up to the state where they have reached a third to half of their adult size. Johnson and Lakso (1986) have shown that, at the spur scale, assimilate export from bourse shoots will only take place after a certain development of the bourse shoot. Until three to five weeks after flowering, up to 80% and 50% of the sugars produced by rosette and bourse shoot leaves, respectively, are exported to the fruit (Tustin et al., 1992; Wünsche and Lakso, 2000). The onset of fruit growth can also depend on the import of sugars from non-fruiting spurs and other vigorous fruit-bearing spurs (Grappadelli et al., 1994). Provision of sugars at an early developmental stage is crucial for the cell division phase of the fruit, which is known for its strong effect on the sink strength of the fruit as well as on final fruit size (Goffinet et al., 1995 ; Wünsche and Lakso, 2000). Moreover, fruit development depends on pollination and number of seeds is correlated to fruit size (Murneek and Schowengerdt, 1935; Einset, 1939, Drazeta et al., 1999). Under these conditions, one can assume that strong correlations exist in terms of growth, among the different organs that make up the spur, specifically with respect to the strength of the carbon sources and sinks. With respect to the sinks, none of the studies cited above have taken into account the bourse, which is the stem that bears the fruits and the vegetative structures of the spur. There is some evidence that the bourse also constitutes a carbon sink, notably when it comes to reserve formation in autumn, as has been shown for pear (Zaïdi et al., 1993), given its strong growth in diameter during fruit development. Depending on the cultivar, size of the fruit,

the bourse, the rosette leaves, as well as the vigor of the bourse shoot may vary strongly (personal observation). This, in turn, may have consequences on source-sink relations at the heart of the spur, namely during the early phase of fruit development where the carbon allocated to fruits essentially is provided by the rosette leaves, while competing with the developing bourse shoot, as outlined above. In such a situation, a reduction of carbon source before or during the cell division phase of the fruit might thus have repercussions on the growth dynamics and on final fruit size, with developmental differences among the cultivars. Thus, the removal or pruning of a vigorous bourse shoot might favor the cell division phase, in contrast to the removal of rosette leaves, which might be unfavorable for cell division. The objectives of the present study were thus (1) to investigate the potential correlations in terms of growth, existing among the different organs of the same spur, as can be assumed from previous studies, yet with the difference that we take here into account the bourse; and (2) to study the effect of altering carbon sources inside the spur on fruit and bourse growth, using an experimental setup involving the early removal of rosette or bourse shoot leaves, or both. In order to study the impact of the "dimension" of the spur, the entire study was carried out on two apple cultivars that exhibit strongly contrasting spur morphology: 'Ariane', which is characterized by rather short bourse shoots, small bourses and equally small rosette leaves; and 'Rome Beauty', which possesses long bourse shoots, large bourses and equally large rosette leaves. The study was completed by some results obtained from 'Fuji', a cultivar with spurs that are intermediate in size. The experimental results obtained in this study and a follow-up study will be used in a multi-scaled FSPM of the apple fruit-bearing branch (Bairam et a1., in preparation, chapter 3).

2. Material and Methods

2.1. Plant material and experimental design

All experiments were performed on apple trees planted in 2008 in an experimental orchard at the INRA experimental unit in Beaucouzé, France. The cultivars selected for this experiment were 'Ariane', 'Fuji' and 'Rome Beauty' (in the following abbreviated as AR, FU, and RB, respectively). The experiments were conducted in 2014 for the three cultivars and completed in 2015 (FU only). 'Ariane' is a modern cultivar that was developed by INRA Angers, by crossing a hybrid of 'Florina' x 'Prima' with pollen from 'Golden Delicious', and released in the year 2000, as a scab-resistant cultivar. The 'Fuji' cultivar is a hybrid developed by growers at Tohoku Research Station in Fujisaki,

Aomori, Japan, in the late 1930s, and has been commercialized since 1962. The origin of this cultivar are two American apple cultivars: ‘Red Delicious’ and ‘old Virginia Ralls Genet’. Finally, ‘Rome Beauty’ is an old American cultivar, which originated from a single seedling found in a nursery in Rome Township, Lawrence County, Ohio, US, in 1815. The experimental orchard consists of three rows of 96 trees each, or 72 blocks of four trees, arranged regularly (including three other cultivars).
The experiment conducted in 2014 aimed at studying the impact of removing bourse shoot (BS) leaves, rosette (RO) leaves, or both of them, at full bloom and two weeks after full bloom, on fruit quality, bourse, bourse shoot and rosette morphological traits. Some days before full bloom of each cultivar, 409, 380 and 100 spurs were labelled on AR, RB and FU trees, respectively. Defoliations consisted in (1) removing the rosette leaves: ‘modality RO’, (2) removing the bourse shoot: ‘modality OP’, (3) removing both the rosette leaves and the bourse shoot: ‘modality OO’ and (4) a control modality without any defoliation: ‘modality RP’. In order to avoid the braking of the shoot supporting the spur, the spurs were not isolated by girdling from the rest of the branch. The defoliations were carried out at full bloom (FB) and two weeks after FB (FB2). FB, in 2014, occurred on April 10, April 14 and April 22 for AR, FU and RB, respectively. At each of FB and FB2, four spurs per branch were defoliated according to the four modalities. For AR, 16 additional branches were selected to test only the modalities RP, RO and OP both at FB and FB2. Therefore, the number of samples depended on cultivars (Table 1).

Table1. Number of spur samples for each defoliation treatment (RP, RO, OP and OO) applied at both defoliation times (FB and FB2) and for each cultivar

	Cultivar					
	'Ariane'		'Fuji'		'Rome Beauty'	
Modality	FB	FB2	FB	FB2	FB	FB2
RP	72	60	20	20	60	50
RO	60	48	10	10	50	40
OP	60	48	10	10	50	40
OO	44	36	10	10	50	40

The position of each treatment on the branch was selected randomly using R. Thinning each spur to one fruit (king fruit) was done on May 27, May 28, and June 5, 2014, for AR, FU and RB, respectively. At the time of FB and FB2, 10 to 12 control spurs (i.e. the RP modality), were collected for each cultivar. Then, for AR and RB, spurs of each modality were destructively sampled. On the

one hand, this was done at four times for the FB treatment, i.e. nine to twelve spurs harvested four, eight and twelve weeks after FB, followed by 18 to 24 spurs at time of fruit harvest. On the other hand, shoots were sampled at three times for the FB2 treatment, i.e. nine to twelve spurs collected six and fourteen weeks after FB, as well as 18 to 24 spurs at harvest (Figure 2). Due to the low number of spurs available in the 'Fuji' cultivar in 2014, ten spurs for each modality and each treatment date were collected at the time of fruit harvest only. Leaves of the rosette and bourse shoots removed at FB and FB2 for setting up the modalities were collected and dried, and then the total leaf dry weight of each rosette and bourse shoot was measured. The spurs intended to be collected at each sampling date were selected randomly at the start of the experiment.

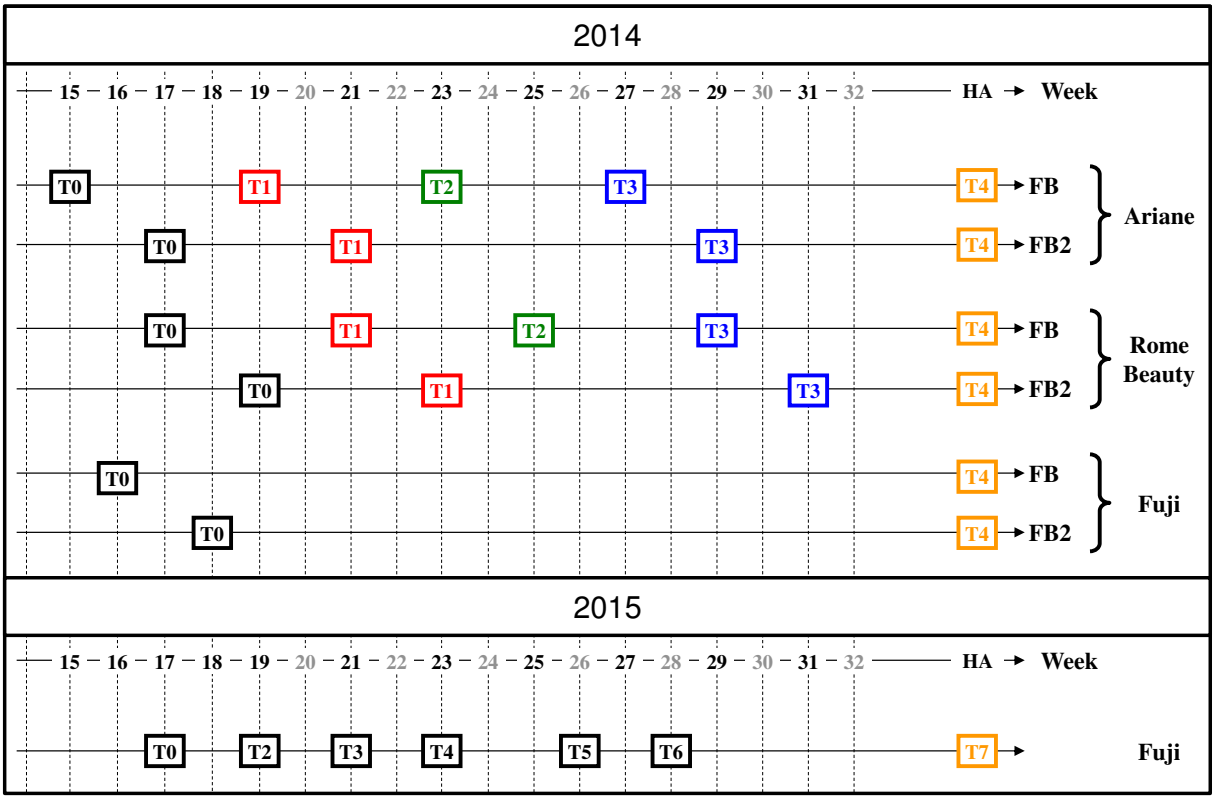

Figure 2. Schedule of the sampling dates for 'Ariane' (AR), 'Fuji' (FU) and 'Rome Beauty' (RB) in 2014 and 2015, respectively. In 2014, defoliations were carried out at full bloom (FB) and two weeks after full bloom (FB2) while no defoliations were applied in 2015. T0 refers to the sampling carried out on the day the treatments were set up in 2014 and to the day of full bloom of FU in 2015. Ti refers to the i^{th} sampling per genotype and type of defoliation date. HA refers to harvest date.

Number of dropped fruits was also recorded. Morphological measurements of fruits (diameter, fresh and dry weight) including pips at harvest (number, fresh and dry weight of full and empty ones) and

peduncles (fresh and dry weight), of bourses (diameter, height, fresh and dry weight), rosettes (number of leaves, total leaves dry weight), and bourse shoots (length, number of leaves, leaf dry weight, stem dry weight) were carried out at each sampling date. For fruits collected, a flesh sample of each fruit was taken, weighed and freeze-dried. The total dry weight of each fruit was approximately estimated by extrapolation (Rule of Three) using the total fresh weight of the fruit, the fresh weight and the dry weight of the flesh sample. Moreover, for each sampling date, all leaves of the rosette of 9 to 12 sampled spurs of each of RP and RO modalities, as well as all the leaves of the bourse shoot of 9 to 12 samples of each of RP and OP modalities were scanned. A flatbed scanner (HP Scanjet G4010) with a resolution of 150 dpi was used for this and resulting images were saved in Portable Network Graphics (png) format. Assuming that leaf shape is elliptical (Freeman and Bolas, 1956), leaf blade area, length and width were measured using ImageJ 1.48v software and the leaf ranks recorded. Total leaf area of each rosette and bourse shoot were calculated as the sum of its individual leaf areas. Moreover, at harvest, the numbers of full and empty pips were recorded and their total fresh and dry weight measured for each fruit.

During the second experiment conducted in 2015, 16 FU spurs were collected at 7 different phenological stages (FB, FB+2, FB+4, FB+6, FB+9, FB+11 weeks, respectively, and at fruit harvest) in order to complete the morphological measurements of intermediate stages that were missing in the 2014 samples of FU. In 2015, full bloom in FU was recorded on April 20. The same variables as in 2014 were recorded plus the ranks of rosette leaves; however, no defoliation treatments were applied, and spurs were considered for leaf area scans and measurements of morphological traits mentioned above for 2014. In 2015, 30 further fruits of each cultivar were collected at harvest. Their diameter, height, circumference, volume, fresh and dry weight were measured. All fruits collected in 2015 were cut, and dried during 6 days at 60°C in a ventilated oven (type HORO 900 V/RS, Dr. Hofmann GmbH, Stuttgart, Germany). Treatments of leaf area involved both 2014 samples and 2015 FU samples. The number of samples depended on cultivar and type of shoot (Table 2).

Table 2. Number of bourse shoots and associated leaves and number of spurs and associated rosette leaves used for leaf area treatment for each cultivar.

	Bourse shoot		Rosette	
Cultivar	Number of shoots	Number of leaves	Number of spurs	Number of leaves
'Ariane'	154	1053	174	701
'Fuji'	99	708	129	522
'Rome Beauty'	114	972	134	778

2.2. Developmental time

Developmental time was first measured using growing degree hours [(1) GDH, base temperature T_b=7°C (Anderson and Richardson, 1982)], calculated using hourly air temperatures (°C) obtained from the Beaucouzé weather station (47° 28' N, 0° 37' W, 50 m a.s.l.) accessible via the INRA Climatik platform, https://intranet.inra.fr/climatik_v2/ :

$$GDH_i = \sum_{h=1}^{24}(HT_h - T_b) \quad (1)$$

Here, HT_h is replaced by T_b if $HT_h < T_b$; HT_h is the hourly air temperature at hour h; and GDH_i are the growing degree hours on day i. Cumulated GDD (GDD_{cum}) for each sampling day were calculated using equation 2. GDD_{cum} calculation starts at full bloom.

$$GDD_{cum} = \sum_{i=FB}^{D} \frac{GDH_i}{24} \quad (2)$$

where FB is day of full bloom and D is the number of days since FB.

2.3. Correlations between morphological traits inside the spur

Correlations between all available quantitative variables representing morphological traits of the organs making up the spur were first established in order to visualize them using the qgraph package in R. These visual networks were created based on correlations between variables established using the Pearson method. Only correlations above 0.5 were represented in order not to overcrowd the graphs with arrows. This package visualizes traits as shaded circles and correlations as straight lines between traits, whose line widths vary with the degree of correlation (i.e., heaviest lines represent the highest correlations). In this preliminary analysis we distinguished the following traits: of the bourse (BO) [diameter (Dia), height (H) measured from the base to the top, fresh weight (FW), dry weight (DW) and volume (V)] of the bourse shoot (BS) [number of bourse shoots having developed on the spur (NBS), length of the bourse (Len), number of leaves (nL), total leaf area (TLA), dry weight of the stem (DWS), dry weight of the leaves (DWL) and total dry weight of both stem and leaves (TDW)]; of the rosette (RO) [nL, TLA and DW]; and of the fruit (FR) [Dia, FW, DW, V, fresh weight of the peduncle (FWP) and dry weight of the peduncle (DWP)]. Even though the pips (PI) are a part the fruit, their traits were plotted using a separate category in order to distinguish the relations that the pips have with the other traits of the fruit. This was done especially because several variables were collected for pips: number of full pips (nF), number of empty pips (nE), fresh weight of full pips (FWF), fresh weight of empty pips (FEW), dry weight of full pips (DWF) and dry weight of

empty pips (DWE). Finally, the GDD were integrated in the networks to show which variables were correlated to developmental time.

Firstly, a general network pooling all treatments, all developmental stages and the three cultivars was established in order to evaluate globally the correlation between morphological traits inside the spur of apple. Then for each cultivar, a specific network with all developmental stages and treatments was constructed in order to compare the three cultivars. Lastly, in order to see if the correlations between organs inside the spur show a different pattern at the very early stages (i.e. before the treatments were applied), a final set of networks was generated for samples collected at FB and FB2 for each cultivar. Based on the interpretation of the former networks, we selected the most interesting numerical variables and analyzed them, using the GGally and ggplot2 packages of R. The output included (i) the distribution of the size of samples among each variable, (ii) the pattern of distribution of each selected variable as a function of the other ones and (iii) the correlations calculated using the Pearson model. Therefore, we selected three BS variables: total leaf area (TLA_{BS}), stem dry weight (DW_{BS_St}) and leaf dry weight (DW_{BS_L}); two rosette (RO) variables: total leaf area (TLA_{RO}) and leaf dry weight (DW_{RO_L}); five fruit (FR) variables: diameter (Dia_{FC}), fresh weight (FW_{FC}), dry weight (DW_{FC}), volume (V_{FC}) and peduncle fresh weight (FW_{FC_Pd}); and 5 bourse (BO) variables: diameter (Dia_{BO}), height (H_{BO}), fresh weight (FW_{BO}), dry weight (DW_{BO}) and volume (V_{BO}). Finally, the mean dry weight of the principal organs (i.e. FR, BO, BS and RO) was plotted as a function of developmental time for AR, FU and RB, respectively. The purpose of this exercise was to visualize the accumulation dynamics of dry matter for each organ in order to compare them with each other and among cultivars.

Secondly, networks for each treatment were generated for each cultivar in order to evaluate the effect of each defoliation treatment on correlation networks within a cultivar.

2.4. Impact of defoliation treatments on fruit and bourse

2.4.1. Control of the treatment effect on spur leaves development and pips number

Firstly, in order to be sure that defoliation treatment did not have any modifying effect on the further development of the remaining bourse shoot or rosette leaves (namely under the RO and OP treatments) that might have limited the impact of the defoliation treatment on fruit and bourse growth, their TLA were compared to those obtained in the control spur (RP treatment) throughout all development stages and for each cultivar. Furthermore, for total leaf area of the rosette and the

bourse shoot, and for AR and RB, tests (ANOVA, Kruskal-Wallis) were conducted on 2014 data in order to establish the phenological stage of development (expressed in GDD) since full bloom from which onwards each shoot type for each cultivar was fully developed in terms of number of leaves and total leaf area. For FU, ANOVA and Kruskal-Wallis analysis were carried out on 2015 and 2014 pooled data to compare total leaf area and number of leaves (rosettes and bourse shoots) as a function of developmental stage (expressed in GDD) in order to establish the sampling stages at which the spur shoots were fully developed. Secondly, the potential effect of the defoliation treatment on pollination that could have had an indirect effect on fruit growth was tested by comparing the number of full pips (N_{PI}) per fruit for each defoliation treatment at harvest.

2.4.2. Impact on fruit drop

In order to provide an overall test for analyzing fruit drop as a function of developmental time from FB to harvest, Cox proportional hazards regression models as part of the survival package of R were used. In doing so, a Cox regression model was fitted in order to compare the differences among cultivars with respect to fruit drop, while another one was used for comparing the differences among cultivars in the control only. Then, for each cultivar, and pooling FB and FB2 data, a one-way proportional hazards Cox model was used in order to compare the impact of type of defoliation on fruit drop. Afterwards, a two-way proportional hazards Cox model was used in order to compare the impact of treatments (type of defoliation x time of defoliation) on fruit drop. In the models established, the log hazard ratio varied as a function of the natural logarithm of developmental time. Differences between cultivars or treatments were confirmed if the p-value was smaller than 0.05. For each cultivar, the probability of fruit drop was estimated for each treatment with comparison to fruits of the control modality (RP) and the time of defoliation FB. Moreover, fruit drop was graphically represented for each cultivar and each treatment using adjustment survival plots using the Kaplan-Meier method in the survival package of R. Survival in this study refers to the number of fruits that did not drop. The impacts of treatments were interpreted using odds ratios as the latter approximate how much more likely the outcome will occur in a given category relative to a reference category (Hosmer and Lemeshow 1989).

2.4.3. Impact on fruit and bourse growth

Because of the high correlation coefficients established between the variables referring to traits within the same organ, two variables were used for both bourse and fruit for the analysis of the impact of treatments: total fresh weight (FW_{FR}) and flesh dry matter concentration ($\%DW_{FR}/FW_{FR}$)

in the case of the fruit and total fresh and dry weight (FW_{BO} and DW_{BO}) in the case of the bourse. First, groups combining both defoliation treatments and times of defoliation were defined and comparisons made between them for variables cited above. However, the samples were collected at intervals of two weeks between FB and FB2 treatments and therefore, the corresponding samples were not collected at the same dates during intermediate stages between FB and harvest. So far, the impact of time of defoliation could not be compared during intermediate developmental stages until harvest. Therefore, a one-way ANOVA or Kruskal-Wallis test – depending on an assessment of the normality of distribution of residuals – served to check if the time of defoliation (FB and FB2) had a different impact. This was done only for spurs collected at harvest for each cultivar. Then a second analysis was carried out for each developmental stage (expressed in growing degree-days, GDD) and for each cultivar in order to analyze the impact of defoliation treatments on the same variables as above considering spurs defoliated at FB and FB2 separately. The main aim of these analyses was to study the difference between defoliation treatments and time of defoliation at each developmental stage on fruit and bourse growth for each cultivar. Lastly, a one-way ANOVA was conducted considering both defoliation times together in order to test the impact of defoliation treatments at harvest whatever the time of application. In all statistical analyses involving comparisons between treatments, normality of the residuals was checked using Shapiro-Wilk test before conducting ANOVA. This said, ANOVA is robust even when the normality hypothesis is violated, if sample size of each group is at least 25 (Feir-Walsh and Toothaker, 1974; Schmider et al., 2010). We therefore used ANOVA also in cases where normality of residuals was not given if the number of samples per group was above 30. However, in those latter cases, a graphic observation of the distribution of residuals and a Kruskall Wallis test were used in order to check the coherence of results. When studying groups containing less than 30 samples and exhibiting a non-normal distribution of residuals, Kruskall Wallis test was automatically applied. Models were run with R (version 0.98.1062.0) and the model significance was evaluated based on $P<0.05$.

3. Results

3.1 Correlations between morphological traits inside the spur

Observations of all the networks and correlation patterns established allowed distinguishing two main groups in all cultivars (Figures 3, 4, 6-8). The first group comprised most bourse shoot and bourse variables whereas the second one involved fruit and phenological time variables. The rosette variables were generally in a separate group with some exceptions.

3.1.1. All treatments taken together

The general network of the correlations among morphological variables of samples collected at different developmental stages of the three cultivars and involving all the treatments (Figure 3A) showed that the morphological traits of the bourse, the bourse shoot and the rosette were highly correlated whereas they were very poorly correlated with fruit traits. In this general network, fruit diameter was also correlated with the fresh weight of the full pips but not with their total number. The fresh and dry weights of empty pips were correlated – which was not surprising; however, they were not correlated with the rest of the variables. Fruit diameter, fresh and dry weights were also correlated with GDD. However, except for the diameter and the volume of the bourse, the other variables of the bourse, the bourse shoot and the rosette were not correlated with developmental time of the spur from FB to harvest. The number of bourse shoots – which are either one or two – did not seem to be correlated with any of the other variables. When looking at the same correlations as above, for each cultivar (Figure 3 B-D), some differences were distinguishable. In RB, fruit fresh and dry weight seemed to be more correlated with bourse dry weight than in AR and FU. In AR and RB, the fresh weight of the peduncle was correlated with the other traits of the fruit, whereas for FU this particular variable did not seem to be much correlated with the other ones. In AR, the dry weight of the peduncle was much more correlated with the fruit variables than it was the case in FU. However, this latter variable was also correlated with the bourse traits and in AR even with bourse shoot traits. Moreover, the traits of the empty pips generally were not correlated with the other variables except in FU in which they were negatively correlated with the traits of full pips. In RB, traits of full pips were only correlated with each other, not with other traits, whereas in FU, fresh weight of empty pips was positively correlated with the rosette traits. At very early stages, the correlations among all variables were higher (Figure 4). However, once more, cultivar differences became apparent: FW and DW of

the fruit were not very correlated to the other variables in AR and FU, whereas in RB these variables were strongly correlated with bourse dry weight (Figure 4) as seen before in the network established for all developmental stages (Figure 3).

The matrix of correlations (Figure 5) confirmed that the strongest correlations were found among variables inside the same organ. Indeed, we observed linear patterns linking TLA and DW for BS and RO, respectively, for each of the three cultivars. We also observed linear patterns between FW and DW inside FR and BO, respectively. Finally, we observed linear patterns between FW, DW and V of the fruit. However, the volume exhibited a pattern that seemed to follow a power equation as a function of both FW and DW. The graphs indicate that the pattern was also cultivar-dependent. We observed a similar pattern inside the bourse: both FW and DW were correlated with Dia and H.

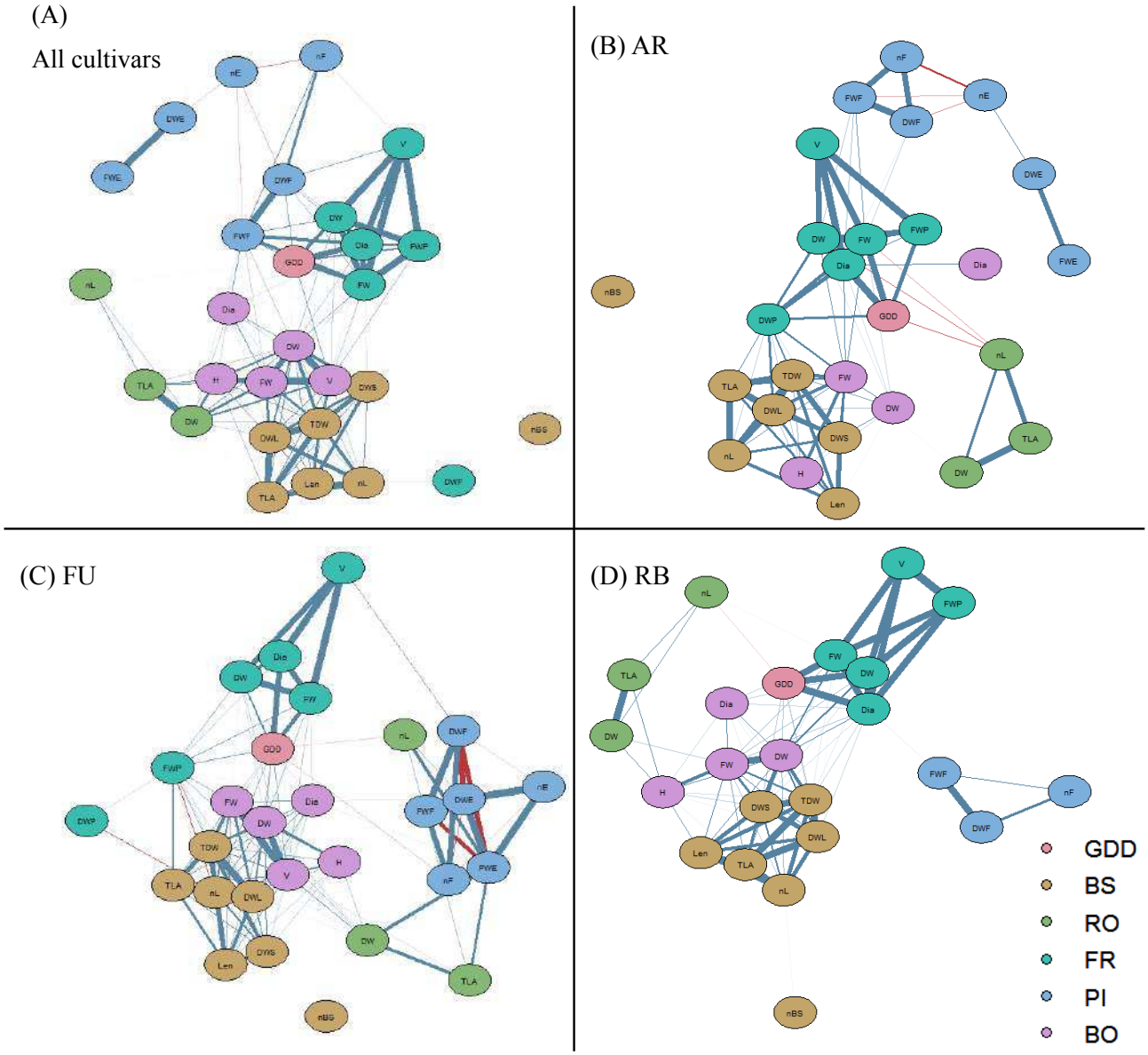

Figure 3. Correlations between variables inside the apple spur for all treatments and all cultivars pooled (A), and each cultivar [‘Ariane’ (AR), ‘Fuji’ (FU) and ‘Rome Beauty’ (RB)] separately (B-D, respectively). Variables were joined by a line when the correlation coefficient was at least 0.5 (blue line: positive correlation; red line: negative correlation), and line width increased with an increasing coefficient. GDD: Growing degree-days; organs: BS: bourse shoot; RO: rosette; FR: fruit; PI: pips; BO: bourse. Variables: nBS: number of bourse shoots; nL: number of leaves (BS, RO); TLA: total leaf area (BS, RO); Len: length; DWS: dry weight of the stem; DWL: dry weight of the leaves; TDW: total dry weight; DW: dry weight (RO, FR, BO); Dia: diameter (FR, BO); FW: fresh weight (FR, BO), V: Volume (FR, BO); FWP: fresh weight of peduncle; DWP: dry weight of peduncle; nF: number of full pips; nE: number of empty pips; FWF: fresh weight of full pips; FWE: fresh weight of empty pips; DWF: dry weight of full pips; DWE: dry weight of empty pips; H: height.

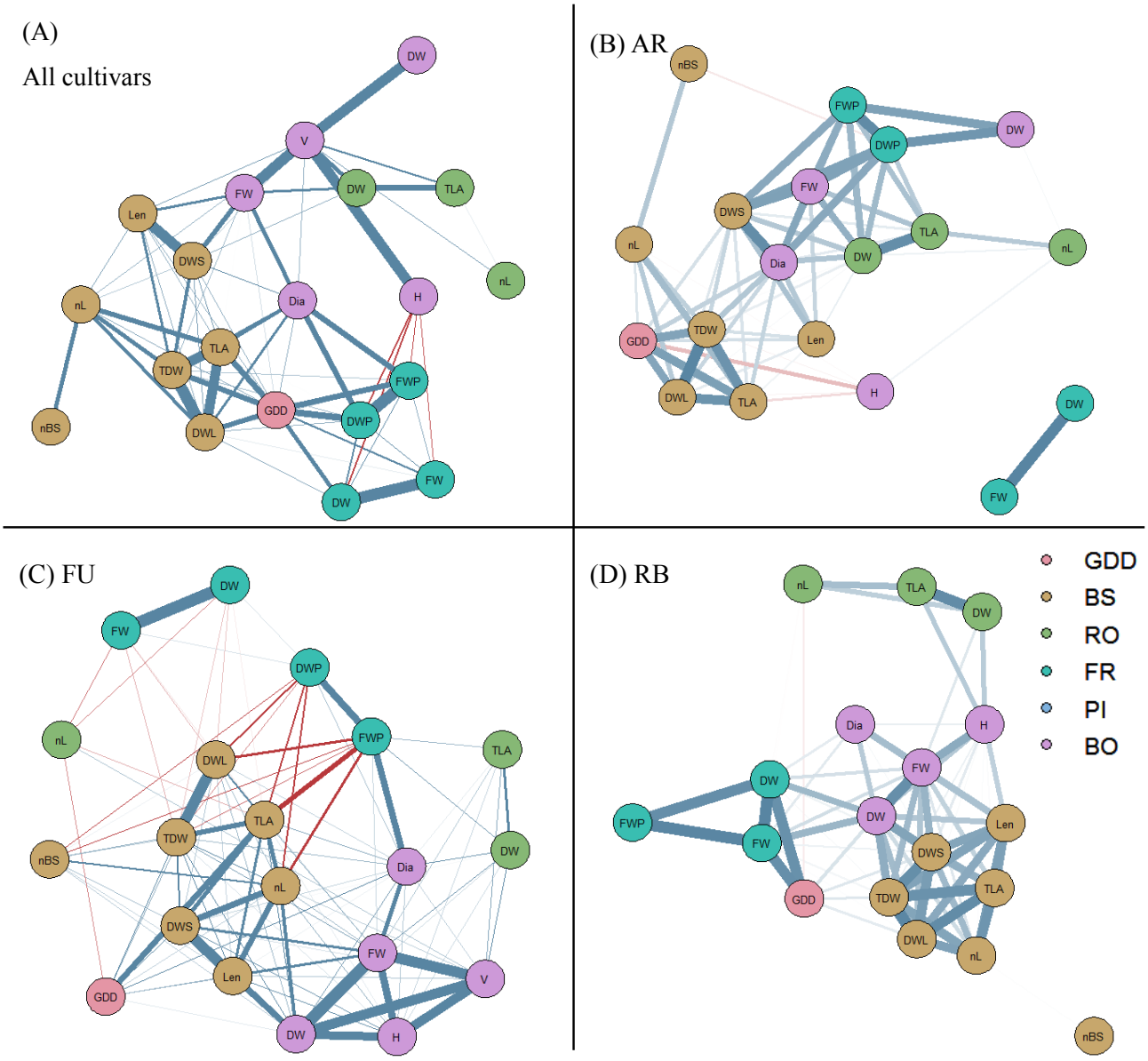

Figure 4. Correlations between variables inside the apple spur before the defoliation treatments for all cultivars pooled (A), and each cultivar separately ['Ariane' (AR), 'Fuji' (FU) and 'Rome Beauty' (RB)] separately (B-D, respectively). GDD: Growing Degree-days; organs: BS: bourse shoot; RO: rosette; FR: fruit; BO: bourse. Variables: nBS: number of bourse shoots; nL: number of leaves (BS, RO); TLA: total leaf area (BS, RO); Len: length; DWS: dry weight of the stem; DWL: dry weight of the leaves; TDW: total dry weight; DW: dry weight (RO, FR, BO); Dia: diameter (FR, BO); FW: fresh weight (FR, BO), V: Volume (FR, BO); FWPd: fresh weight of peduncle; DWPd: dry weight of peduncle; H: height. For further information, see legend of Fig. 3

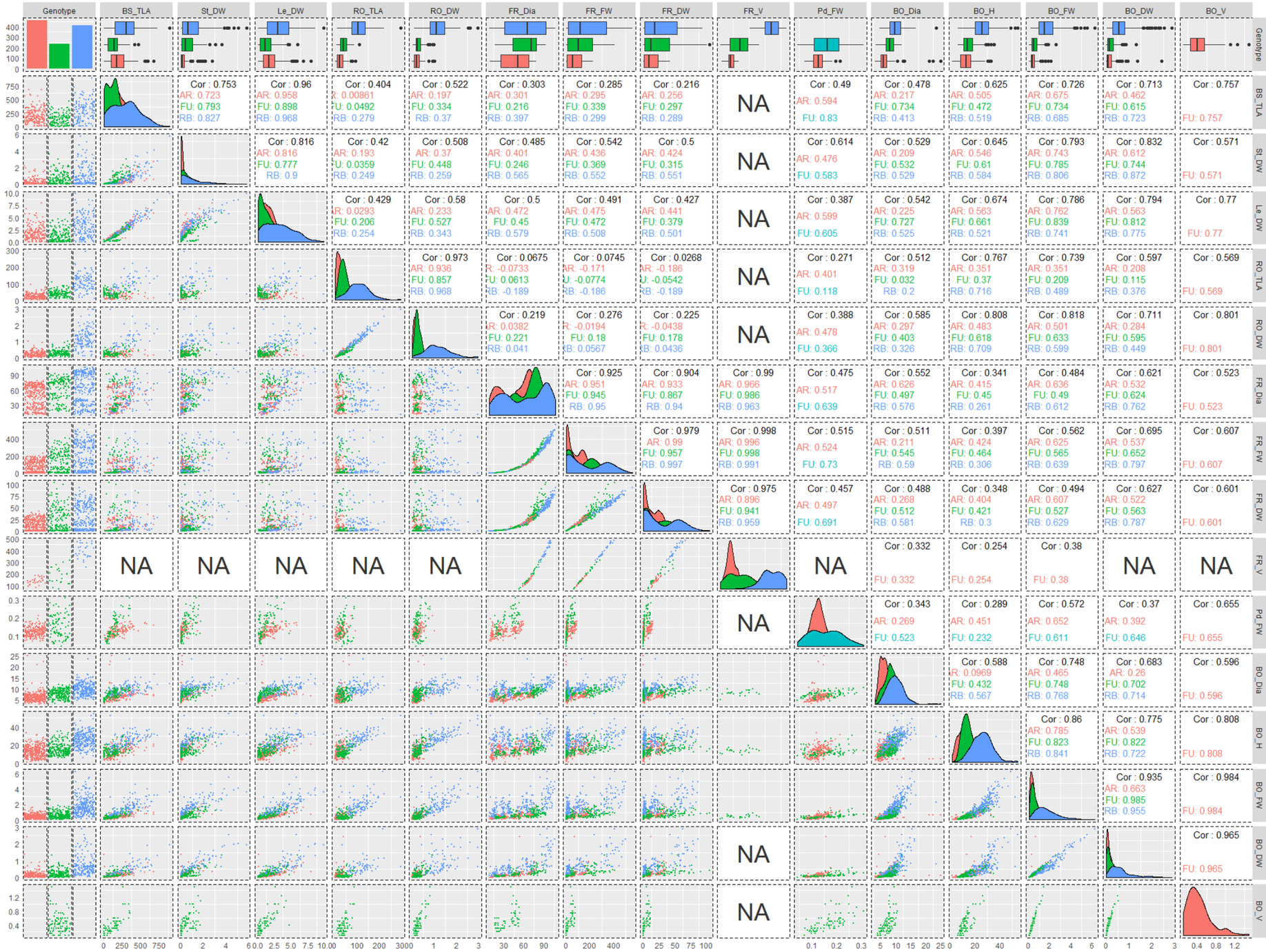

Figure 5. Pearson's correlation matrix for 15 traits of apple organs (bourse shoot BS, rosette RO, fruit FR) of three cultivars ('Ariane' AR, red; 'Fuji' FU, green; and 'Rome Beauty' RB, blue): BS_TLA: total leaf area of bourse shoots, St_DW: stem dry weight; Le_DW: leaf dry weight; RO_TLA: total leaf area of the rosette; RO_DW: rosette dry weight; FR_Dia: fruit diameter; FR_FW: fruit fresh weight; FR_DW: fruit dry weight; FR_V: fruit volume; Pd_FW: peduncle fresh weight; BO_Dia: bourse diameter; BO_H: bourse height; BO_FW: bourse fresh weight; BO_DW: bourse dry weight; BO_V: bourse volume. Point clouds of relations are indicated below the diagonal while correlation coefficients for the three cultivars are indicated above the diagonal of the matrix. On the diagonal the distribution of the traits for the three cultivars can be seen while in the first row box plots of each trait are depicted.

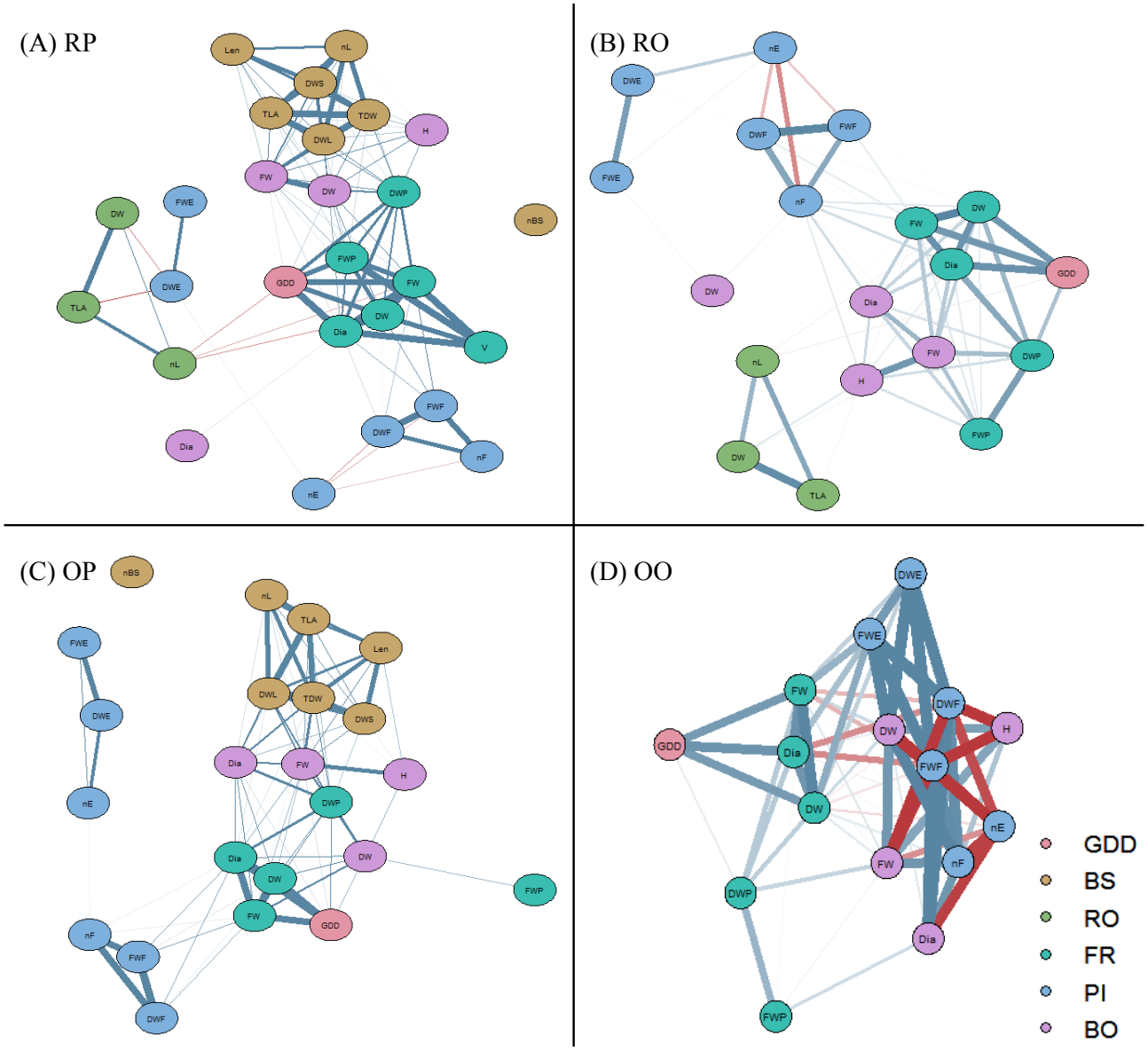

Figure 6. Correlations between variables inside the apple spur in 'Ariane' for both defoliation dates pooled (FB and FB2) and for each defoliation treatment (RP: control, RO: removal of bourse shoot leaves, OP: removal of rosette leaves and OO: removal of both bourse shoot and rosette leaves). GDD: Growing degree days; organs: BS: bourse shoot; RO: rosette; FR: fruit; PI: pips; BO: bourse. Variables: nBS: number of bourse shoots; nL: number of leaves (BS, RO); TLA: total leaf area (BS, RO); Len: length; DWS: dry weight of the stem; DWL: dry weight of the leaves; TDW: total dry weight; DW: dry weight (RO, FR, BO); Dia: diameter (FR, BO); FW: fresh weight (FR, BO), V: Volume (FR, BO); FWPd: fresh weight of peduncle; DWPd: dry weight of peduncle; nF: number of full pips; nE: number of empty pips; FWF: fresh weight of full pips; FWE: fresh weight of empty pips; DWF: dry weight of full pips; DWE: dry weight of empty pips; H: height. For further explanations, see legend of Fig. 3.

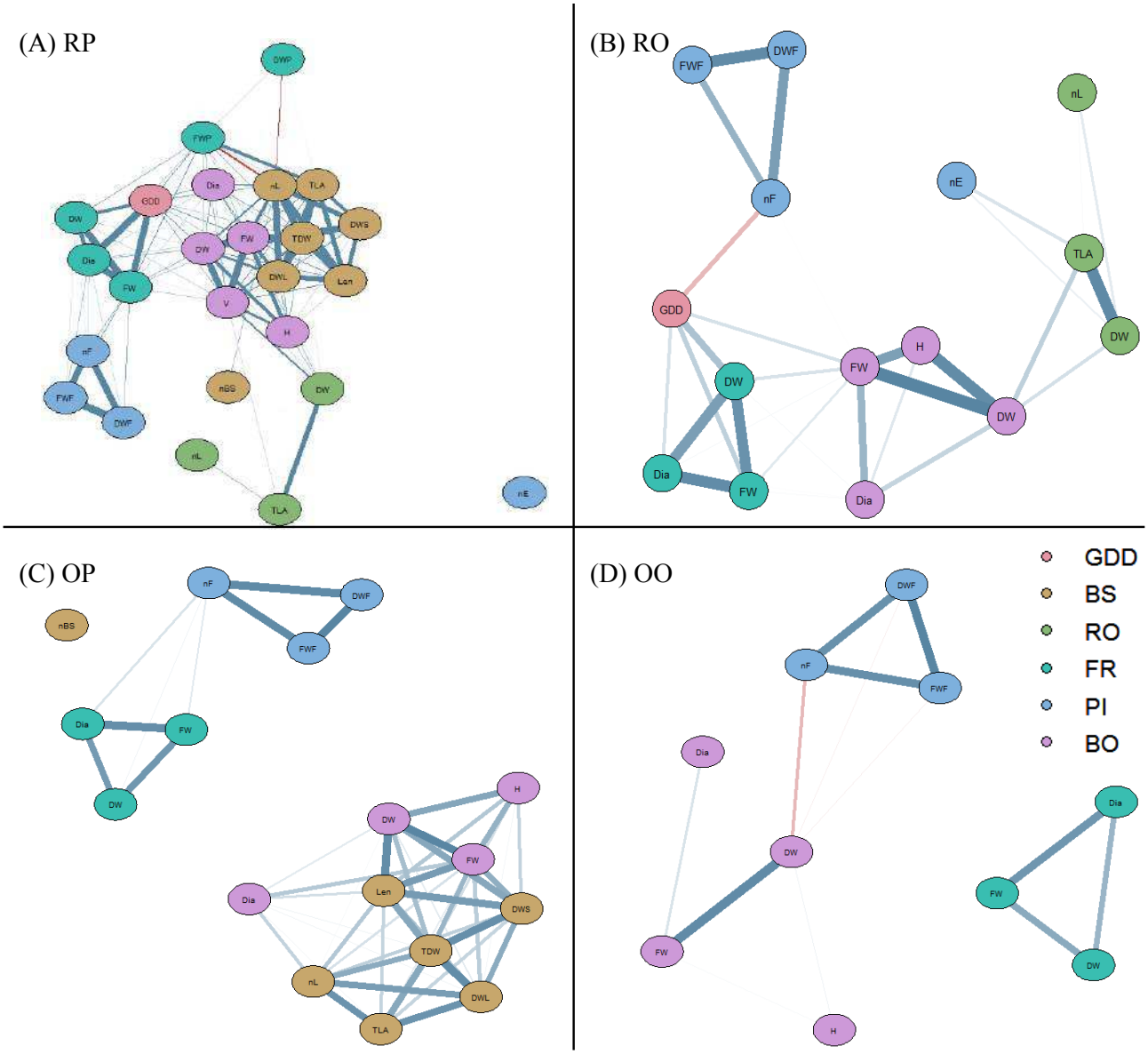

Figure 7. Correlations between variables inside the apple spur in 'Fuji' for both defoliation dates pooled (FB and FB2) and for each defoliation treatment (RP: control, RO: removal of bourse shoot leaves, OP: removal of rosette leaves and OO: removal of both bourse shoot and rosette leaves). GDD: Growing degree days; organs: BS: bourse shoot; RO: rosette; FR: fruit; PI: pips; BO: bourse. Variables: nBS: number of bourse shoots; nL: number of leaves (BS, RO); TLA: total leaf area (BS, RO); Len: length; DWS: dry weight of the stem; DWL: dry weight of the leaves; TDW: total dry weight; DW: dry weight (RO, FR, BO); Dia: diameter (FR, BO); FW: fresh weight (FR, BO), V: Volume (FR, BO); FWPd: fresh weight of peduncle; DWPd: dry weight of peduncle; nF: number of full pips; nE: number of empty pips; FWF: fresh weight of full pips; FWE: fresh weight of empty pips; DWF: dry weight of full pips; DWE: dry weight of empty pips; H: height. For further explanations, see legend of Fig. 3.

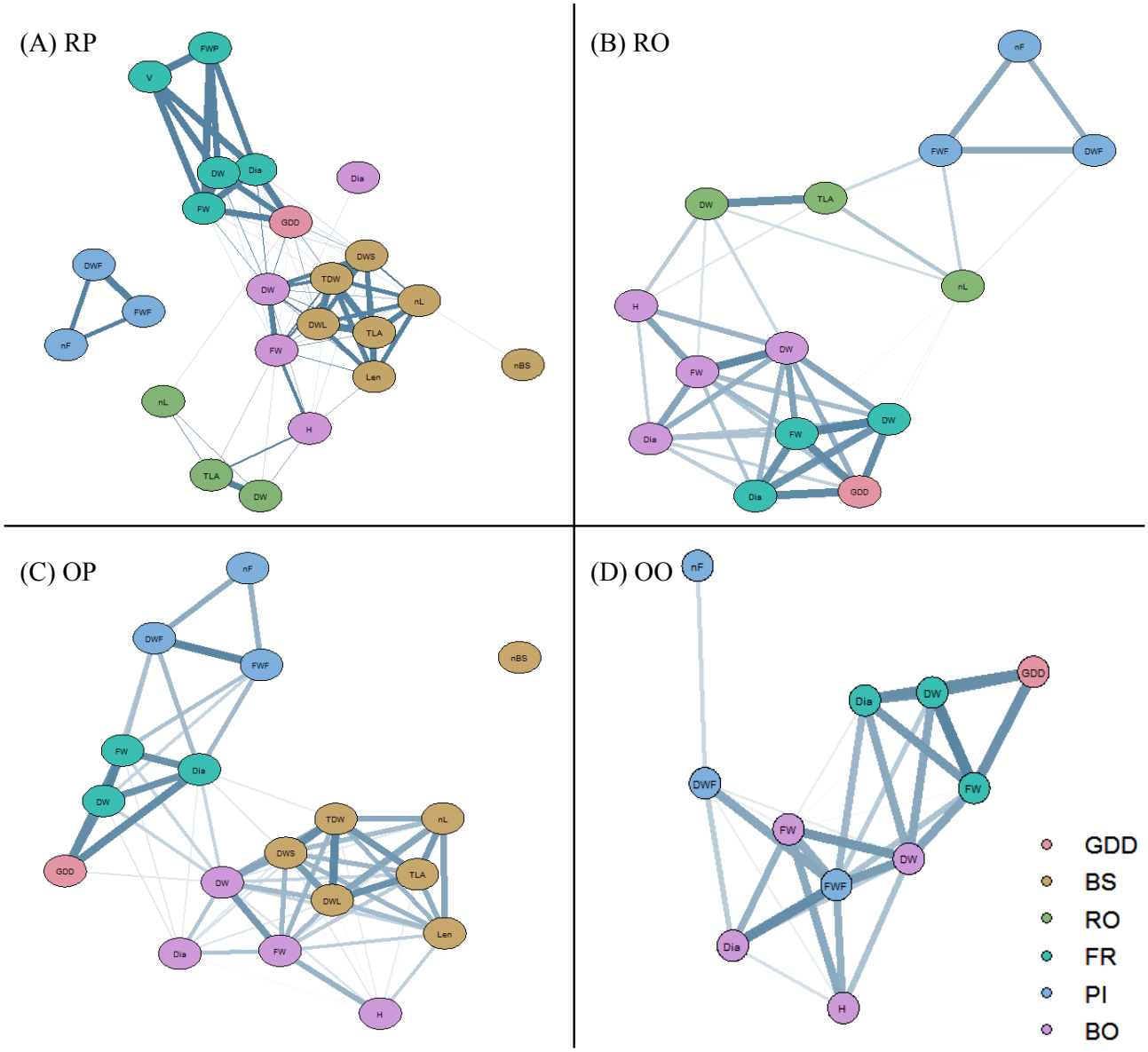

Figure 8. Correlations between variables inside the apple spur in 'Rome Beauty' for both defoliation dates pooled (FB and FB2) and for each defoliation treatment (RP: control, RO: removal of bourse shoot leaves, OP: removal of rosette leaves and OO: removal of both bourse shoot and rosette leaves). GDD: Growing degree days; organs: BS: bourse shoot; RO: rosette; FR: fruit; PI: pips; BO: bourse. Variables: nBS: number of bourse shoots; nL: number of leaves (BS, RO); TLA: total leaf area (BS, RO); Len: length; DWS: dry weight of the stem; DWL: dry weight of the leaves; TDW: total dry weight; DW: dry weight (RO, FR, BO); Dia: diameter (FR, BO); FW: fresh weight (FR, BO), V: Volume (FR, BO); FWPd: fresh weight of peduncle; DWPd: dry weight of peduncle; nF: number of full pips; nE: number of empty pips; FWF: fresh weight of full pips; FWE: fresh weight of empty pips; DWF: dry weight of full pips; DWE: dry weight of empty pips; H: height. For further explanations, see legend of Fig. 3.

3.1.2. Effect of defoliation treatments on correlation networks

As a response to the removal of BS leaves (RO modality), in AR and RB (Figures 6 and 8), the bourse and the fruit traits seemed to be strongly correlated, whereas the correlation was still smaller in FU (Figure 7). In response to the removal of rosette leaves (OP modality), fruit and bourse traits seemed to be more correlated in AR and RB (Figures 6 and 8) whereas no correlation was observed for FU (Figure 7). However, these correlations in AR and RB were still smaller than those observed in the RO modality, and this was especially the case in RB (Figures 6 and 8). Under the OO treatment (removal of both bourse shoot and rosette leaves) low or no correlations between fruit and bourse variables were observed in AR and in particular FU (Figures 6 and 7), respectively, whereas in RB strong correlations emerged, especially between bourse dry weight and fruit fresh and dry weight (Figure 8).

3.2. Treatment impacts

3.2.1. Control of treatment effects on spur leaves development and pips number

No significant influence of the defoliation treatments on the one hand, and the timing of defoliation (FB and FB2) on the other hand, on the total leaf area of bourse shoot and rosette leaves was found (data not shown). However, a significant difference in TLA for rosette leaves was observed between cultivars with high, intermediate and low value for RB (108 cm^2), FU (42 cm^2) and AR (25 cm^2), respectively; and a higher value for bourse shoot leaves in RB (382 cm^2) compared to AR (214 cm^2) and FU (206 cm^2) at harvest. For each cultivar, TLA of the bourse shoot increased throughout early developmental stages of the spur and bourse shoots were fully developed at 201, 275 and 345 GDD for FU, RB and AR respectively (data not shown). We assumed that rosettes were fully developed at full bloom, as the mean total leaf areas for the three cultivars were the highest at the earliest sampling dates. However, even if a significant difference was found between groups of rosettes sampled at different phenological stages for a same cultivar (certainly due to natural variability among spurs), still the means were not correlated with phenological sampling dates. In fact, the only group truly apart in terms of rosette total leaf area and number of leaves for the three cultivars, respectively, was the one collected at harvest. This result is explained by the high number of rosette leaves that had dropped at harvest especially in AR and RB.

Concerning the number of full pips, no significant difference between defoliation treatments was observed whatever the defoliation time except for the OO treatment applied at full bloom which induced a decrease in the number of full pips in both AR and FU (Figure 9).

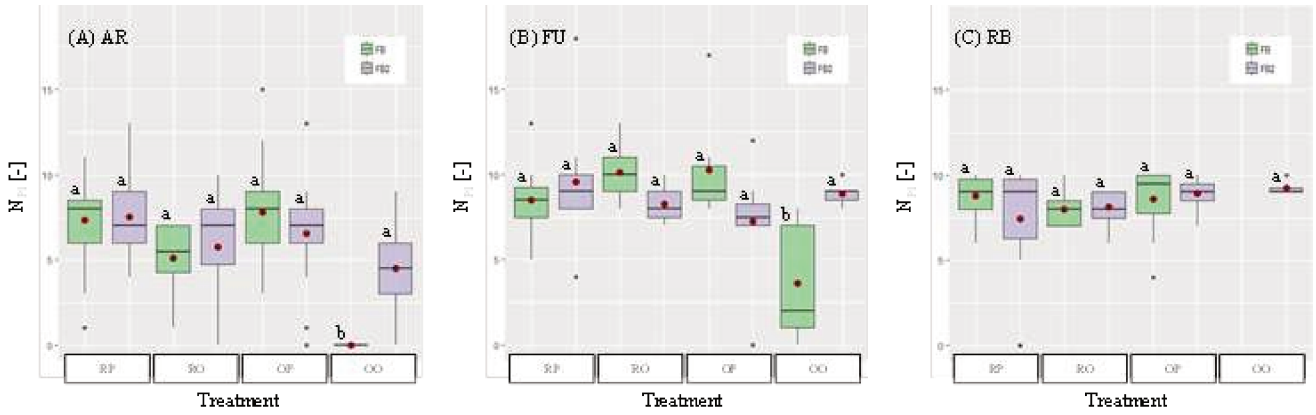

Figure 9. Boxplots of number of full pips (N_{PI}) as a function of treatment in 'Ariane' (AR), 'Fuji' (FU) and 'Rome Beauty' (RB), and mean values for each treatment (●). FB treatment (defoliation) applied at full bloom; FB2: treatment (defoliation) applied two weeks after full bloom; RP: control treatment; OP: defoliation of rosette leaves; RO: defoliation of bourse shoot leaves; OO: defoliation of all spur leaves (rosette and bourse shoot). Data within each cultivar with the same letter are considered to be non-significantly different according to one-way ANOVA results ($P<0.05$).

3.2.2. Fruit drop

In AR, 90 fruits among 314 (22%) dropped before harvest. In FU, this rate was 20 fruits of 80 (25%) whereas in RB, 99 fruits of 261 (28%) were shed before harvest (data not shown). The Cox regression model fitted in order to compare the differences in fruit drop among cultivars because of defoliations showed that there was no significant difference between FU and RB. However, AR showed a significant difference to both FU and RB ($P < 2.10^{-16}$ and $P = 1.11 \times 10^{-13}$, respectively). The probability of fruit drop in FU and RB from FB to harvest was, respectively, 3.65 and 6.54 times higher than in AR. Moreover, even if FU and RB did not show a significant difference in fruit drop, still the probability of fruit drop was 1.79 times higher in FU than in RB as a response to defoliation (data not shown). However, if we consider only the RP modality (control), there was no difference between cultivars with respect to fruit drop and most fruits were retained on the spur until harvest. The two-way proportional hazards Cox models built for AR, FU and RB (Table 3), show that for the three cultivars there was no significant difference between the two times of defoliation (FB, FB2) among all modalities of defoliation. However, even if in FU there was no difference between defoliation treatments with respect to fruit drop, in the two other cultivars, the modality OO exhibited a significant difference with respect to the control modality (RP). Indeed, removing all the leaves on the spur raised the probability of fruit drop 74.8 and 32.9 times in AR and RB, respectively, against a factor of 6.4 in FU. Moreover, in AR, the RO modality had a significant impact on fruit drop

compared to the RP modality and the probability of fruit drop was 27 times higher when removing the bourse shoot compared to the control. In RB, both RO and OP were significantly different from RP in fruit drop and the p-values and probabilities of fruit drop compared to the control were quite similar for both modalities. Indeed, under both RO and OP, the probability of fruit drop was around 5.3 times higher than under the control.

The representation for each cultivar and each treatment using adjustment survival plots with the Kaplan-Meier method in the survival package on R (Figure 10) confirmed the above results. Indeed, it was observed that the control modalities (RP) at both FB and FB2 were those in which the probability of fruit drop was the lowest of the three cultivars. Furthermore, in the modality OO probability of fruit drop was the highest. However, even if there was no significant difference between the times of applying the treatments (FB vs FB2), Table 3 and Figure 10 show that the probability of fruit drop was higher in almost all cases when treatments were applied at FB. Only one exception was observed: in RB, the probability of fruit drop was higher in the control of FB2 than in the control of FB (Figure 10) but this difference was not significant. In AR and FU the probability of fruit drop in the control was the same for FB and FB2. Figure 10 also shows that in the OO modality the probability of fruit drop was higher at early developmental stages than in other treatments. Just after OO, the RO modality was the one that exhibited the highest probability of fruit drop and the fruits dropped earlier than in OP and RP.

Table 3. Results of the impact of defoliation treatments compared to the control (RP), with both defoliation dates (FB and FB2) pooled or separated, on fruit drop using Cox two-way regression models in AR, FU and RB cultivars. Treatments: RO, bourse shoot leaves removed; OP: rosette leaves removed; OO: bourse shoot and rosette leaves removed. *, ** and *** for P-value < 0.05, 0.01 and 0.005, respectively.

Cultivar	Defoliation time	Treatment	coef	exp(coef)	P(>|z|)	
'Ariane'	Both dates	OO	4.3149	74.8033	2.36e-05	***
		OP	1.8747	6.5186	0.0826	.
		RO	3.2969	27.0298	0.0013	**
	FB2 compared to FB	All treatments	-0.0103	0.9898	0.9942	
		OO	-0.6539	0.5201	0.6511	
		OP	-0.1846	0.8315	0.9045	
		RO	-0.7499	0.4724	0.6083	
'Fuji'	Both dates	OO	1.8500	6.3570	0.0915	.
		OP	1.2110	3.3580	0.2941	
		RO	0.7480	2.1130	0.5414	
	FB2 compared to FB	All treatments	-2.76e-15	1.0000	1.0000	
		OO	-0.6381	0.5283	0.6885	
		OP	-0.4635	0.6291	0.7830	
		RO	-0.4635	1.5900	0.7830	
'Rome Beauty'	Both dates	OO	3.4923	32.8610	1.82e-06	***
		OP	1.6760	5.3439	0.0321	*
		RO	1.6750	5.3389	0.0322	*
	FB2 compared to FB	All treatments	0.4198	1.5217	0.6456	
		OO	-1.2228	0.2944	0.2021	
		OP	-0.1703	0.8434	0.8671	
		RO	-1.2705	0.2807	0.2451	

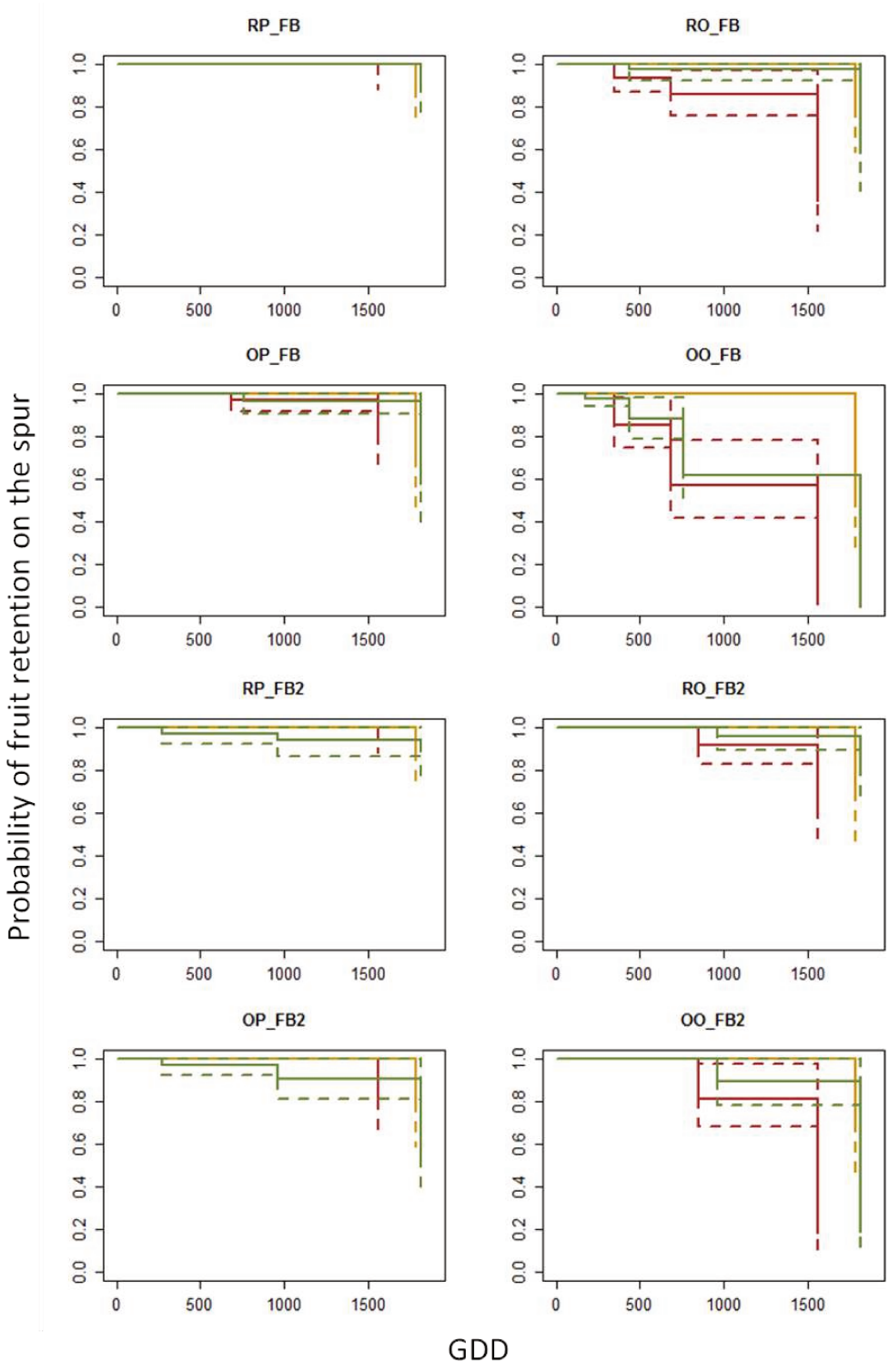

Figure 10. Adjustment survival plots showing the probability of fruit drop from FB to harvest for AR (—), FU (—) and RB (—) for each treatment. FB treatment (defoliation) at full bloom; FB2: treatment (defoliation) two weeks after full bloom; RP: control treatment; OP: defoliation of rosette leaves; RO: defoliation of bourse shoot leaves; OO: defoliation of all spur leaves (rosette and bourse shoot). Dotted lines represent the confidence interval at 5%.

3.2.3. Fruit fresh weight and flesh dry matter concentration

Considering both defoliation times together, the OO treatment tended to reduce FW_{FR} in AR at harvest, yielding a significant difference compared to the control (RP) (Table 4). This difference seemed to be due to the OO treatment being applied at FB, which induced a significant decrease in FW_{FR} compared to other treatments (Figure 11). In FU, we were able to observe a similar trend in the OO treatment; however, the decrease in FW_{FR} at harvest was not significant compared to the control (Table 4). Contrary to AR and FU, in RB, the OO treatment did not induce any strong and significant effect on FW_{FR} at harvest (Table 4). On the other hand, in FU and RB, the RO treatment tended to increase FW_{FR} with only a significant effect compared to the control in RB (Table 4), especially when the RO treatment was applied at FB2 (Figure 11). For the OP treatment, no significant effect was noticed at harvest except for RB with the lowest values obtained for FW_{FR}, which were significantly different from those obtained under the RO treatment (Figure 11, Table 4). For all cultivars, defoliation treatments did not induce any significant change in flesh dry matter concentration (Table 4, Figure 11), which was significantly different among cultivars at harvest with higher value for FU, AR and RB, respectively.

Table 4. Impact of defoliation treatments at harvest considering both defoliation times together (FB and FB2) on fruit fresh weight (FW_{FR}) and flesh dry matter concentration (DW_{FR}/FW_{FR}) in 'Ariane', 'Fuji' and 'Rome Beauty' (means (SE)). Data within each cultivar with the same letter are considered to be not significantly different based on one-way ANOVA results ($P<0.05$).

Cultivar	Treatment	FW_{FR} (g)			DW_{FR}/FW_{FR} (%)		
'Ariane'	RP	140.6	(4.3)	a	18.7	(0.2)	a
	RO	137.7	(8.1)	ab	18.6	(0.3)	a
	OP	145.0	(5.0)	a	18.8	(0.5)	a
	OO	97.7	(16.7)	b	18.3	(0.2)	a
'Fuji'	RP	259.8	(16.9)	ab	21.6	(1.0)	a
	RO	282.3	(16.8)	a	20.6	(0.8)	a
	OP	237.1	(18.7)	ab	20.0	(0.7)	a
	OO	206.2	(11.5)	b	22.0	(1.2)	a
'Rome Beauty'	RP	350.5	(12.1)	a	16.7	(0.1)	a
	RO	406.8	(11.6)	b	16.0	(0.2)	a
	OP	317.8	(12.4)	a	16.5	(0.2)	a
	OO	335.8	(44.6)	ab	17.0	(0.2)	a

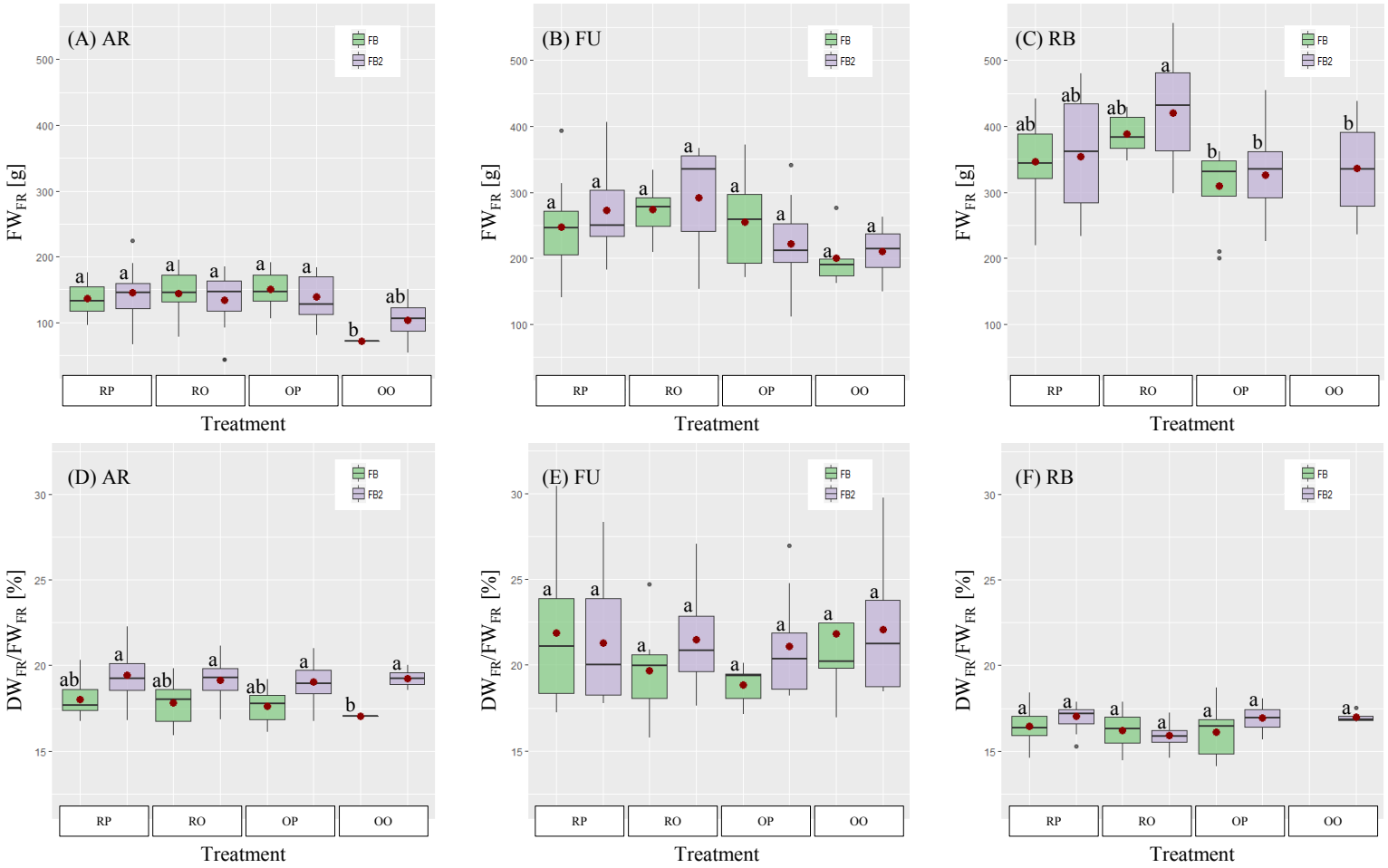

Figure 11. Boxplots of fresh weight and flesh dry weight content of the fruit [FW_{FR} (g) and DW_{FR}/FW_{FR} (%)] as a function of treatments for 'Ariane' (AR), 'Fuji' (FU) and 'Rome Beauty' (RB) and mean values for each treatment (●). FB treatment (defoliation) at full bloom; FB2: treatment (defoliation) two weeks after full bloom; RP: control treatment; OP: defoliation of rosette leaves; RO: defoliation of bourse shoot leaves; OO: defoliation of all spur leaves (rosette and bourse shoot). Within the same cultivar, treatments with the same letter are considered to be non-significantly different according to one-way ANOVA results ($P<0.05$).

Table 5. Impact of defoliation treatments applied at full bloom (FB) or two weeks later (FB2) on fruit fresh weight (FW_{FR}) at each developmental stage expressed in growing degree-days (GDD) since FB, in 'Ariane', 'Fuji' and 'Rome Beauty' (means (SE)). For each development stage, data within each genotype with the same letter are considered to be non-significantly different according to a one-way ANOVA test ($P<0.05$).

		Defoliation time							
		FB				FB2			
		Defoliation treatment							
Cultivar	Development stage	RP	RO	OP	OO	RP	RO	OP	OO
'Ariane'	GDD138	1.3 (0.2) a	1.2 (0.1) a	1.4 (0.1) a	1.1 (0.2) a	-	-	-	-
	GDD247	-	-	-	-	6.4 (0.5) a	5.2 (0.4) a	6.2 (0.4) a	3.1 (0.5) b
	GDD345	13.4 (0.9) a	11.8 (1.2) a	15.2 (0.9) a	6.8 (2.0) b	-	-	-	-
	GDD681	45.5 (1.7) a	44.4 (2.1) a	44.7 (2.3) a	46.5 / a	-	-	-	-
	GDD849	-	-	-	-	73.2 (3.6) a	56.8 (6.8) a	68.7 (4.6) a	57.6 (11.9) a
	GDD1559	136.2 (4.8) a	144.3 (12.1) a	151.2 (5.8) a	72.1 / b	145.0 (7.3) a	133.5 (10.9) a	138.8 (8.1) a	104.1 (20.0) a
'Fuji'	GDD1786	247.2 (24.8) a	273.4 (14.9) a	254.4 (28.3) a	200.5 (20.1) a	272.3 (23.7) a	292.3 (33.0) a	222.1 (25.5) a	210.3 (14.7) a
'Rome Beauty'	GDD174	3.2 (0.4) a	3.1 (0.3) a	2.5 (0.4) a	1.5 (0.2) b	-	-	-	-
	GDD276	-	-	-	-	13.1 (0.9) a	12.3 (0.8) ab	10.6 (1.7) ab	8.2 (1.5) b
	GDD435	28.8 (1.2) a	24.9 (0.9) bc	24.6 (1.6) b	19.7 (2.7) c	-	-	-	-
	GDD760	95.9 (6.5) ab	106.5 (6.8) a	82.9 (7.6) b	88.7 / ab	-	-	-	-
	GDD963	-	-	-	-	145.0 (8.6) a	140.8 (6.5) a	123.5 (9.1) ab	107.0 (9.0) b
	GDD1816	346.8 (14.3) b	389.1 (8.1) a	310.2 (15.7) b	-	354.2 (20.1) a	420.9 (19.4) a	326.1 (20.1) a	335.8 (44.7) a

Analyzing the impact of defoliation during all developmental stages and modalities for FB and FB2 separately on fruit fresh weight (Table 5) showed that, in AR, only the treatment OO showed an effect with a decrease in FW_{FR} values which was only significantly different from other treatments at harvest when applied at FB (Figure 11). Significant differences under the OO treatment were also observed at an early stage (GDD345 for FB and GDD247 for FB2). However, in this case, the results could be explained by the fact that the sampled fruits were small and were perhaps ready to drop at this stage, since for the following sampling dates until harvest no significant differences were observed. In FU, even if not significant, the OO treatment tended to reduce FW_{FR} at harvest while RO increased it and this irrespective of the time of defoliation, compared to the control (Figure 11). This trend effect of OO and RO treatments was also observed in RB but only during early and late developmental stages, respectively, and could be explained for OO by the same hypothesis exposed before for AR (Table 5). Even if FW_{FR} under RO treatment in RB was higher at harvest when treatment was applied at FB2, a significant difference to other modalities of defoliation was only observed at early defoliation (FB, Table 5). Contrary to AR and FU, in RB, OP treatment induced a decrease in FW_{FR} throughout all developmental stages especially when applied at FB which led to a significant difference compared to control (RP) before harvest and to RO treatment at harvest (Table 4). Concerning flesh dry matter concentration, no significant difference was observed between defoliation treatments throughout all developmental stages excepted for AR at an early stage when the treatment was applied at FB2 and for RB under RO treatment applied at FB2 (Table 6). In this latter case, a significant reduction in flesh dry matter concentration was associated with a higher fruit fresh weight (Table 5). Even if there was a non-significant difference in fruit fresh weight (FW_{FR} and DW_{FR}) at harvest between both defoliation times (i.e. FB and FB2) for each treatment (data not shown), the kinetics of fruit growth expressed as FW_{FR} as a function of GDD (Figure 12) tended to be different for the two times of defoliation. This was notably the case in both AR and RB when subject to the defoliation modality RO. In fact, fresh biomass accumulation seemed to start earlier when the bourse shoot was removed at FB compared to FB2. In RB, all modalities tended to have lower mean FW_{FR} at harvest when defoliation was carried out early (at FB), whereas, in AR, mean FW_{FR} tended to be higher under both RO and OP treatments when defoliations were carried out at FB. In AR, the OO modality seemed to reduce FW_{FR} at harvest compared to the other modalities independent of the time of defoliation (FB and FB2), while in RB FW_{FR} at harvest was only reduced when defoliation was applied at FB, compared to the other modalities.

Table 6. Impact of defoliation treatments applied at full bloom (FB) or two weeks later (FB2) on fruit flesh dry weight content [(DW_{FR}/ FW_{FR}, %) at each developmental stage expressed in growing degree-days (GDD) in 'Ariane', 'Fuji' and 'Rome Beauty' (means (SE)). For each developmental stage, data within each cultivar with the same letter are considered to be non-significantly different according to a one-way ANOVA test ($P<0.05$).

		Defoliation time															
		FB								FB2							
		Defoliation treatment															
Cultivar	Development stage	RP			RO			OP			OO			RP			
'Ariane'	GDD138	12.9	(0.2)	a	12.9	(0.2)	a	12.4	(0.1)	a	12.8	(0.2)	a	-			
	GDD247	-			-			-			-			11.5	(0.2)	bc	
	GDD345	11.7	(0.1)	a	11.8	(0.2)	a	11.3	(0.2)	a	11.8	(0.2)	a	-			
	GDD681	15.9	(0.4)	a	16.0	(0.2)	a	16.3	(0.2)	a	15.5	/	a	-			
	GDD849	-			-			-			-			16.7	(0.2)	a	
	GDD1559	18.0	(0.2)	a	17.8	(0.4)	a	17.6	(0.2)	a	17.0	/	a	19.4	(0.3)	a	
'Fuji'	GDD1786	21.9	(1.6)	a	19.7	(1.1)	a	18.8	(0.4)	a	21.8	(2.1)	a	21.3	(1.3)	a	
'Rome Beauty'	GDD174	12.6	(0.2)	a	12.7	(0.3)	a	12.4	(0.3)	a	12.9	(0.2)	a	-			
	GDD276	-			-			-						11.4	(0.2)	a	
	GDD435	13.9	(0.2)	a	13.2	(0.3)	a	13.8	(0.2)	a	13.3	(0.3)	a	-			
	GDD760	15.1	(0.2)	a	14.7	(0.3)	a	15.2	(0.2)	a	14.5	/	a	-			
	GDD963	-			-			-			-			15.7	(0.2)	a	
	GDD1816	16.4	(0.2)	a	16.2	(0.3)	a	16.1	(0.4)	a	-			17.0	(0.2)	a	

		RO			OP			OO									
Cultivar	Development stage																
'Ariane'	GDD138	-			-			-									
	GDD247	11.8	(0.1)	b	11.2	(0.2)	c	12.6	(0.1)	a							
	GDD345	-			-			-									
	GDD681	-			-			-									
	GDD849	16.9	(0.3)	a	16.8	(0.2)	a	16.8	(0.4)	a							
	GDD1559	19.1	(0.3)	a	19.0	(0.3)	a	19.3	(0.3)	a							
'Fuji'	GDD1786	21.5	(1.2)	a	21.1	(1.1)	a	22.1	(1.6)	a							
'Rome Beauty'	GDD174	-			-			-									
	GDD276	11.3	(0.2)	a	11.5	(0.2)	a	11.7	(0.3)	a							
	GDD435	-			-			-									
	GDD760	-			-			-									
	GDD963	15.3	(0.2)	a	15.9	(0.3)	a	15.8	(0.3)	a							
	GDD1816	15.9	(0.2)	b	16.9	(0.2)	a	17.0	(0.2)	a							

3.2.4. Bourse fresh and dry weight

As observed for fruit, the difference between both defoliation times (i.e. FB and FB2) for bourse fresh and dry weight at harvest was not significant (data not shown). However, some differences due to defoliation treatment modalities and/or time of application could be noticed at harvest. The effect of the OO treatment on bourse fresh and dry weight for both defoliation times together was the same as that observed for fruit in AR and FU, with values being lower than the control at harvest, especially for early defoliation (at FB, Table 7, Figure 13). In RB, contrary to what was observed for fruit, the OO treatment induced a significant decrease in FW_{BO} and DW_{BO} compared to the control at harvest (Table 7). The RO treatment induced an increase in bourse weight only for RB, this increase was significant for FW_{BO} (Table 7) and especially when the treatment was applied late (at FB2, Figure 13) as observed for fruit under this treatment. As seen before in fruit, the effect of the OP treatment on the bourse was only observed in RB, with significantly lower values of FW_{BO} compared to the control for the RO treatment at harvest (Table 7, Figure 13).

Table 7. Impact of defoliation treatments at harvest considering both defoliation times together (FB and FB2) on bourse fresh (FW_{BO}) and dry (DW_{BO}) weight in 'Ariane', 'Fuji' and 'Rome Beauty' (means (SE)). Data within each cultivar with the same letter are considered to be non-significantly different according to one-way ANOVA results ($P<0.05$).

Cultivar	Treatment	Bourse FW (g)			Bourse DW (g)		
'Ariane'	RP	0.69	(0.09)	a	0.33	(0.06)	a
	RO	0.59	(0.07)	a	0.26	(0.03)	ab
	OP	0.67	(0.07)	a	0.39	(0.08)	a
	OO	0.24	(0.06)	b	0.07	(0.02)	b
'Fuji'	RP	0.95	(0.07)	a	0.41	(0.04)	a
	RO	0.92	(0.09)	a	0.40	(0.06)	a
	OP	0.87	(0.08)	a	0.38	(0.04)	a
	OO	0.69	(0.08)	a	0.29	(0.03)	a
'Rome Beauty'	RP	2.83	(0.27)	a	1.47	(0.14)	a
	RO	3.77	(0.29)	b	1.79	(0.18)	a
	OP	1.85	(0.22)	c	0.89	(0.15)	b
	OO	1.57	(0.19)	c	0.61	(0.09)	b

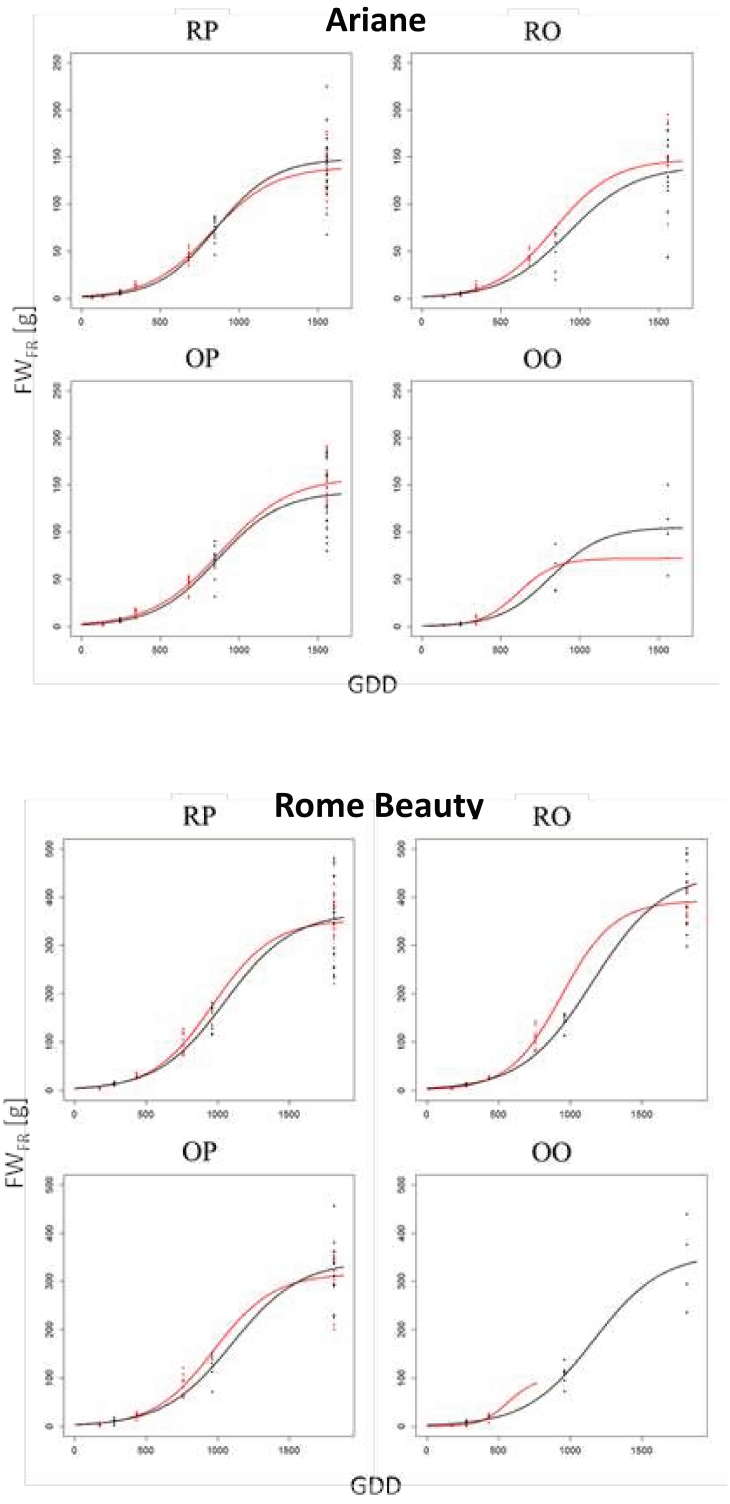

Figure 12. Modelling fresh weight of the fruit (FW_{FR}) as a function of GDD in 'Ariane' and 'Rome Beauty' as a response to 4 modalities (RP, RO, OP and OO) and two times [FB (—) and FB2 (—)] of defoliation. Data modelled using the nls function in R.

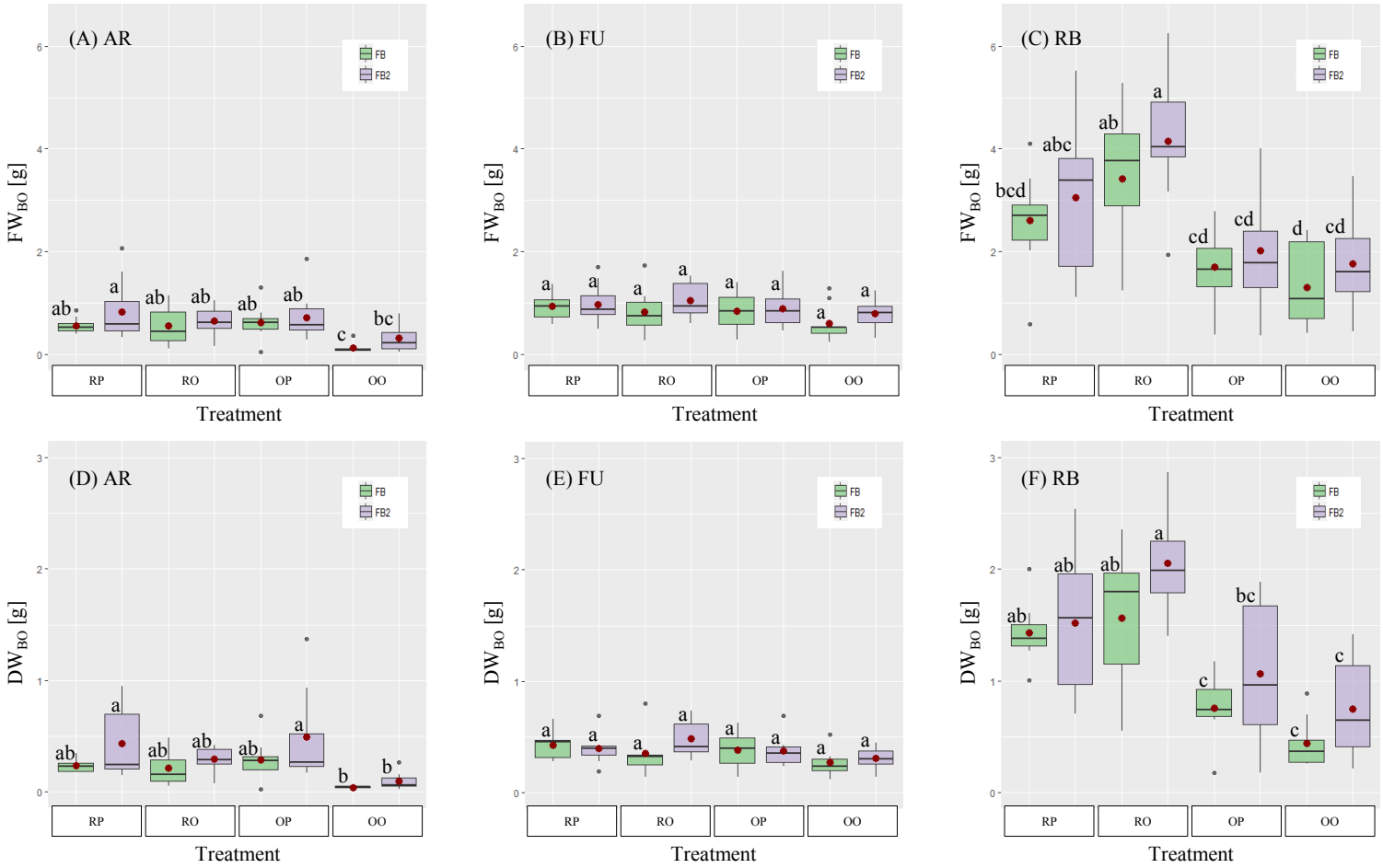

Figure 13. Boxplots of fresh (FW_{BO}) and dry (DW_{BO}) weight of the bourse as a function of defoliation treatment for 'Ariane' (AR), 'Fuji' (FU) and 'Rome Beauty' (RB) and mean values for each treatment (●). FB treatment (defoliation) applied at full bloom; FB2: treatment (defoliation) applied two weeks after full bloom; RP: control treatment; OP: defoliation of rosette leaves; RO: defoliation of bourse shoot leaves; OO: defoliation of all spur leaves (rosette and bourse shoot). Within the same cultivar, treatments with the same letter are considered to be non-significantly different according to one-way ANOVA results ($P<0.05$).

Table 8. Impact of defoliation treatments applied at full bloom (FB) or two weeks later (FB2) on bourse fresh weight (FW_{BO}) at each developmental stage expressed in growing degree-days (GDD) after FB in 'Ariane', 'Fuji' and 'Rome Beauty' (means (SE)). Data within each cultivar with the same letter are considered to be non-significantly different according to a one-way ANOVA test ($P<0.05$).

		Defoliation time															
		FB								FB2							
		Defoliation treatment															
Cultivar	Development stages	RP			RO			OP			OO			RP			
'Ariane'	GDD138	0.23	(0.06)	a	0.23	(0.04)	a	0.20	(0.04)	a	0.17	(0.04)	a	-			-
	GDD247	-			-			-			-			0.39	(0.04)	a	0.38	(0.05)	a	0.34	(0.04)	a	0.32	(0.06)	a
	GDD345	0.42	(0.06)	a	0.25	(0.02)	bc	0.36	(0.06)	ab	0.22	(0.05)	c	-			-
	GDD681	0.54	(0.08)	a	0.42	(0.09)	a	0.51	(0.08)	a	0.19	(0.04)	b	-			-
	GDD849	-			-			-			-			0.79	(0.09)	a	0.53	(0.09)	b	0.56	(0.06)	ab	0.30	(0.11)	c
	GDD1559	0.55	(0.05)	a	0.55	(0.12)	a	0.62	(0.09)	a	0.13	(0.05)	b	0.83	(0.16)	a	0.64	(0.08)	a	0.72	(0.13)	a	0.32	(0.09)	b
'Fuji'	GDD1786	0.93	(0.09)	a	0.82	(0.14)	ab	0.84	(0.12)	ab	0.61	(0.12)	b	0.97	(0.13)	a	1.05	(0.13)	a	0.90	(0.12)	a	0.79	(0.10)	a
'Rome Beauty'	GDD174	1.51	(0.28)	a	1.10	(0.19)	a	0.95	(0.20)	a	0.78	(0.13)	a	-			-
	GDD276	-			-			-			-			1.23	(0.12)	a	1.77	(0.25)	a	1.35	(0.2)	a	1.35	(0.29)	a
	GDD435	1.49	(0.25)	a	1.34	(0.2)	a	1.21	(0.18)	a	1.12	(0.19)	a	-			-
	GDD760	2.22	(0.3)	a	2.21	(0.26)	a	1.63	(0.18)	ab	0.93	(0.25)	b	-			-
	GDD963	-			-			-			-			1.99	(0.31)	a	1.88	(0.21)	a	1.60	(0.19)	a	1.15	(0.24)	a
	GDD1816	2.60	(0.3)	a	3.42	(0.42)	a	1.70	(0.24)	b	1.30	(0.27)	b	3.06	(0.47)	b	4.16	(0.41)	a	2.02	(0.39)	b	1.77	(0.28)	b

Table 9. Impact of defoliation treatments applied at full bloom (FB) or two weeks later (FB2) on bourse dry weight (DW_{BO}) at each developmental stage expressed in growing degree-days (GDD) after FB in Ariane, Fuji and Rome Beauty (means (SE)). Data within each cultivar with the same letter are considered to be non-significantly different according to a one-way ANOVA test ($P<0.05$).

		Defoliation time															
		FB								FB2							
		Defoliation treatment															
Cultivar	Development stage	RP			RO			OP			OO			RP			RO			OP			OO		
'Ariane'	GDD138	0.04	(0.01)	ab	0.05	(0.02)	a	0.04	(0.01)	ab	0.03	(0.01)	b	-			-			-			-		
	GDD247	-			-			-			-			0.11	(0.02)	a	0.11	(0.02)	a	0.09	(0.02)	a	0.10	(0.03)	a
	GDD345	0.14	(0.02)	a	0.09	(0.01)	b	0.09	(0.02)	b	0.05	(0.02)	b	-			-			-			-		
	GDD681	0.19	(0.03)	a	0.14	(0.03)	a	0.18	(0.03)	a	0.06	(0.02)	b	-			-			-			-		
	GDD849	-			-			-			-			0.29	(0.05)	a	0.44	(0.26)	a	0.22	(0.03)	a	0.06	(0.02)	b
	GDD1559	0.24	(0.02)	a	0.21	(0.07)	a	0.29	(0.06)	a	0.04	(0.01)	b	0.43	(0.11)	a	0.29	(0.04)	a	0.49	(0.14)	a	0.10	(0.03)	b
'Fuji'	GDD1786	0.42	(0.06)	a	0.35	(0.08)	ab	0.38	(0.07)	ab	0.27	(0.06)	b	0.40	(0.06)	a	0.48	(0.09)	a	0.38	(0.06)	a	0.30	(0.05)	a
'Rome Beauty'	GDD174	0.38	(0.09)	a	0.28	(0.06)	ab	0.26	(0.06)	ab	0.14	(0.04)	b	-			-			-			-		
	GDD276	-			-			-			-			0.36	(0.04)	a	0.53	(0.09)	a	0.39	(0.1)	a	0.30	(0.07)	a
	GDD435	0.62	(0.09)	a	0.50	(0.07)	ab	0.40	(0.07)	ab	0.31	(0.06)	b	-			-			-			-		
	GDD760	0.81	(0.13)	a	0.70	(0.05)	a	0.54	(0.06)	ab	0.32	(0.11)	b	-			-			-			-		
	GDD963	-			-			-			-			0.86	(0.13)	a	0.73	(0.11)	ab	0.62	(0.11)	ab	0.36	(0.10)	b
	GDD1816	1.43	(0.12)	a	1.56	(0.27)	a	0.76	(0.13)	b	0.44	(0.09)	b	1.52	(0.26)	ab	2.05	(0.21)	a	1.06	(0.29)	bc	0.75	(0.14)	c

The impact of defoliation during all developmental stages and modalities for FB and FB2 separately on FW_{BO} and DW_{BO} (Tables 8 and 9) gave almost the same trends as for fruits with a decreased value under the OO treatments for AR and FU but also, contrary to fruits, for RB, especially when the OO treatment was applied at FB. However, in RB, bourses sampled at harvest in response to an early OO treatment (at FB) did no longer bear any fruit. As seen before for fruits, in FU and RB, the RO treatment did not induce any significant changes in bourse fresh or dry weight; however, an increase in means was observed under this treatment especially when the treatment was applied at FB2 in RB and only for this defoliation date in FU. Contrary to AR and FU and similarly to the fruit, in RB, the OP treatment induced a decrease in bourse fresh and dry weight throughout all development stages especially when applied at FB which led to a significant difference compared to the control (RP) and RO treatment at harvest (Tables 8 and 9).

4. Discussion

4.1 Correlations between morphological traits inside the spur

In the present study, fruit variables, independent of the cultivar and in particular those linked to fruit growth (fresh and dry matter) seemed to be globally only weakly correlated to variables of other spur organs, particularly source organs with respect to carbon (rosette and bourse shoot). Moreover, the absence of a strong correlation was equally obvious in early developmental stages of the spur. This seems to suggest that in this study fruit growth ultimately depended only very little on sources within the spur, even during early developmental stages, which is in contradiction to earlier studies (Wünsche and Lakso, 2000). Denne (1963) studied how fruit development (rate and duration of growth, cell division, and cell expansion) in three apple cultivars (‘Cox’, ‘Daugherty’ and ‘Sturmer’) was affected by within-tree factors. The study found that fruit size at harvest was related to the position of the fruit on the spur, seed number, spur size, number of fruits set on the spur, and date of flowering. This is in contrast to our findings, which showed no or only very weak correlations among fruit, pip, and bourse traits, though within the same organ variables were strongly correlated. It is nevertheless difficult to conclude on this issue as the analysis of source-sink relations in our study is solely based on a “morphological” analysis. Indeed, it would have been good to integrate more “physiological” or “functional” variables such as the photosynthetic capacity of leaves, which is known to evolve with leaf age (Lieth and Pasian, 1990) and sink strength of fruit within the spur

(Poirier-Pocovi et al., unpublished). Early removal of rosette or bourse shoot leaves, i.e. during full bloom also did not lead to a marked modification of correlations between fruit growth and leaves left on the spur. This seems to suggest that the carbon necessary for fruit growth could come from sources outside the spur as has already been shown by (Grappadelli et al., 1994), in a situation where spurs are not very vigorous as in the present study, due to the removal of part of the leaves. The only modifications observed as a consequence of defoliation were the stronger correlations between bourse dry matter and fruit fresh or dry weight, but this effect was only marked in 'Ariane' and above all, 'Rome Beauty', particularly when the bourse shoot had been removed. In 'Rome Beauty' this correlation was even more important in the absence of all spur leaves (OO treatment), and we were able to observe that under this defoliation condition as well as for the three cultivars fruit drop, even when occurring rather late, systematically lead to a necrosis or atrophy of the bourse. The strong correlation of growth between the bourse and the fruit could be explained by a stronger vascularization of the bourse in order to facilitate nourishing the growing fruit in the absence of nearby sources, even more so when the bourse shoot, which is usually a strong carbon supplier for the fruit during full development of the latter (Abbot, 1960), has been removed. In such a situation, the bourse could even be a stronger source for carbon reserves as suggested by its higher fresh and dry weight associated with bigger fruit at harvest in the cultivar 'Rome Beauty', following the removal of the bourse shoot. This increase in bourse weight could be induced by an increase in photosynthetic capacity of rosette leaves which could increase carbon accumulation in the bourse. Incidentally, it would be interesting to know if under these conditions the carbon reserves invested in this way could not be immediately usable for the developing fruit, given the weak availability of carbon sources within the spur. All this remains hypothetical but could be tested by a histological and biochemical analysis of the developing bourse during fruit development, thereby comparing the three cultivars as well as the different defoliation treatments.

In any case, our results tended to show that it is difficult to explain fruit growth when only the spur scale is taken into consideration. Consequently, considering the next higher scale, that of the fruit-bearing branch, could be more suitable. For such a scale, given the complexity of the fruit bearing branch a functional-structural plant modelling (FSPM) approach (Buck-Sorlin, 2013) could be an appropriate tool to integrate existing botanical and ecophysiological knowledge and to test the plausibility of hypotheses. Such an approach has several advantages: first, it can simulate and visualize transport processes that are normally invisible or very difficult to be demonstrated experimentally, under outdoor conditions and at the organ or branch scale. Second, it can help to quantify certain hidden model parameters that are impossible to measure. An excellent example of

the application of the FSPM approach to apple is MAppleT (Costes et al., 2008; Da Silva et al., 2014): this model is dedicated to simulating the architecture of young apple trees by combining topology and geometry in a single simulation. This is done in a way that the architecture of an apple tree becomes an emergent feature arising from process interactions, concerning primary and secondary shoot growth as well as fruit growth.

4.2 Impact of defoliation treatments on fruit growth

In this study we wanted to test the influence of early defoliation (removal of rosette or bourse shoot leaves) at two development stages: at full bloom and two weeks after, on fruit quality traits. Our results showed that the main significant effect of the defoliation treatments on fruit was observed only when the treatment was applied very early at full bloom compared to FB2. Also, defoliation could not be attributed, except for the treatment involving the removal of all spur leaves, to a modification in pollination as the seed number was nearly the same at harvest no matter what defoliation treatment was applied at full bloom. However, after full bloom, fruitlet development can vary in time, due to a number of internal and external factors (pollination rate, time between pollination and fertilization, fertilization rate, early growth rate of fruitlets) so that at least at FB2 fruitlets in our study might have exhibited a higher heterogeneity in development (Denne 1960; Smith 1950). In our study, this becomes apparent, for example, by the higher variability in fruit fresh weight at harvest when defoliation was applied at FB2 (see table 5) compared to FB. The timing of defoliation will theoretically have an impact on fruit development, but as seen in this study other factors (such as the overall source-sink ratio, the ability of sinks to draw sources, and the capacity of leaves to compensate for defoliation by upregulating assimilation rate (Bairam et al., chapter 3) will tend to dilute this effect.

The main result was that in our study, defoliation did not have a marked effect on fruit growth, except for the total defoliation treatment in ‘Ariane’ and ‘Fuji’ and both rosette and bourse shoot removal treatments in ‘Rome Beauty’. Rather, defoliation tended to have an effect on fruit survival rate, with severe defoliation (OO modality), particularly when applied at full bloom, decreasing the overall survival rate of fruits, as a consequence of lower carbon availability for the fruit. This also led to a significant reduction in size for the remaining fruits until harvest. In addition to a reduction in carbon availability for fruits, total leaf removal could also strongly reduce fruit water influx (Lang and Volz, 1998). Lang (1990) has demonstrated that water influx into the apple fruit is strongly correlated with spur leaf area thus inducing an increase in fruit drop and a reduction in fruit size.

Bourse shoot removal also induced an increase in fruit drop yet different in terms of intensity according to the cultivar, which could be explained by branch architecture. Thus, 'Ariane' reacted most severely to bourse shoot removal with respect to fruit drop compared to 'Rome Beauty'. In 'Ariane', rosette leaves are generally rather inconspicuous with respect to the bourse shoots, contrary to 'Rome Beauty'. At a first glance, removal of bourse shoot in 'Rome Beauty' should thus have less severe consequences than in 'Ariane'. This is because in 'Ariane' rosette leaves might not exclusively supply the carbon needed for fruit growth, which is mainly supplied at an early developmental stage by rosette leaves as demonstrated by Tustin et al. (1992), and therefore could induce severe fruit drop. On the other hand, the higher effect of rosette leaf removal on fruit drop in 'Rome Beauty' compared to 'Ariane' could be explained by a higher sink strength during early development of the bourse shoot in 'Rome Beauty', where the young bourse shoot could thus compete with the young fruit for carbon resources. This hypothesis is in accordance with our results that have shown that bourse shoot vigor was higher in 'Rome Beauty' than in 'Ariane', with higher values for bourse shoot leaf area achieved more quickly in 'Rome Beauty' than in 'Ariane'. Furthermore, the hypothesized higher competition for carbon allocation during early development between fruit and bourse shoot growth in 'Rome Beauty' could also have an impact on the fruit cell division stage, which in turn could explain the difference in fruit size at harvest of the remaining fruits. Actually, any reduction in carbon availability during the fruit cell division stage could reduce cell number inside the fruit, which is known to be very determinant for fruit sink strength and therefore fruit size at harvest (Goffinet et al., 1995). This hypothesis could explain why, under the early bourse shoot removal treatment in 'Rome Beauty', fruit weight was significantly higher compared to results obtained when only rosette leaves were removed. However, this result supposes that during the later fruit cell expansion stage, and under a treatment involving the removal of the bourse shoot, fruit could import carbon from rosette leaves and certainly, as exposed before, outside the spur as the consequence of its strong sink strength. In the particular case of 'Fuji', the absence of a particular defoliation effect on fruit drop or fruit growth could be explained by global fruit load on the tree: the latter was very low in this cultivar in 2014, which could have led to a situation where fruits subject to a defoliation treatment imported carbon, at least during the early development stage, from other parts of the branch or tree which could in turn have reduced the impact of carbon shortage.

Our results confirmed the importance of the early development stage of a fruit on its growth and final size at harvest. They furthermore pointed out the rule of competition between fruit and bourse shoot growth within the spur just after full bloom, which could have had an impact on fruit sink strength

and subsequently fruit size at harvest when growth is largely sink-driven (sufficient carbon availability). However, our results are not as pronounced as we had originally expected, and we therefore suppose that carbon used during fruit cell division could also be allocated from outside the spur. This hypothesis could explain differences obtained between 'Ariane' and 'Rome Beauty'. In fact, in 'Rome Beauty', due to its type IV architecture (Lespinasse and Delort, 1984) a spur and a vegetative shoot are separated by a rather long distance, in contrast to 'Ariane' (type III). This restricts, in 'Rome Beauty', the possibility for fruits to import carbon from outside the spur at least at the beginning of cell division because of its low sink strength at this stage, again in contrast to 'Ariane'. One way to validate this hypothesis of the importance of carbon outside the spur for fruit growth could be to isolate each spur by removing a ring of phloem and bark at their base (i.e. applying a girdling treatment). In this case, however, it could become difficult to conclude as to what the real net impact of the defoliation treatments on fruit size at harvest was, given the fact that under any defoliation treatment the fruit in any case requires, a priori, carbon from outside the spur for its growth.

5. Conclusions and Perspectives

The aim of the present study was to increase the knowledge about the complex relations that exist between sources and sinks within the spur of apple. The system was perturbed using removal of leaves from different shoot types within the spur at early phenological stages and a large number of traits measured, thereby creating a huge correlative dataset that was visualized using correlation networks. The analysis of these networks as well as the direct comparison of traits subject to different defoliation treatments yielded a number of new insights into the processes involved in assimilate allocation to fruits that were partly in contradiction with the literature. Most notably, fruit development appeared to be relatively unrelated to source characteristics within the spur, hinting at the possibility that fruits, once established, will be able to draw sources from outside their own spur. In order to further elucidate this hypothesis, we designed in a follow-up study (chapter 3), an experimental system that included entire, simplified fruit-bearing branches consisting of several spurs and vegetative shoots, whose architecture was described in its entirety.

6. Conflict of Interest

The authors declare that the research was conducted in the absence of any commercial or financial relationships that could be construed as a potential conflict of interest.

7. Author Contributions

EB, MD and GBS conceived and designed the work; EB, MD and CLM collected the experimental data. EB, MD and GBS analyzed and interpreted the data; EB conducted the programming in R; EB, MD and GBS wrote the paper; all authors approved the final version.

8. Funding

The doctoral thesis of EB was funded by a strategic bourse of the Région Pays de la Loire, France, convention no. 2011-12596. All financial help is duly acknowledged.

9. Acknowledgments

Mathilde Orsel-Baldwin, Isadora Rubin, Sylvain Hanteville, Julienne Fanwoua and Antoine Roche helped with measurements in the field and the laboratory. Michael Henke developed the initial ImageJ script for the automatic measurement of leaf surfaces from scanned images. Antoine Roche scanned leaves and saved images for leaf area analysis. The staff of the experimental unit at Beaucouzé provided day-to-day maintenance of the orchard. All help is gratefully acknowledged.

Chapitre 2

Models for Predicting the Architecture of Different Shoot Types in Apple

Ce chapitre a été publié dans la revue Frontiers in Plant Sciences, section Plant Biophysics and Modelling en janvier 2017:

Baïram, E., Delaire, M., Le Morvan, C. and Buck-Sorlin, G. (2017). Models for Predicting the Architecture of Different Shoot Types in Apple. Front. Plant Sci., 8:65

Abstract Chez le pommier, la charpentière (branche de premier ordre, portant des fruits) d'un arbre est caractérisée par une architecture comprenant trois types de pousses : bourse (portant la rosette), pousse de bourse, et pousse végétative. Son architecture globale ainsi que celle de chaque pousse détermine donc la distribution des organes sources (feuilles) et puits (fruits) et pourrait avoir une influence sur la quantité de carbone alloué aux fruits. La connaissance de l'architecture – en particulier de la position et la surface des feuilles – est nécessaire pour quantifier la production de carbone mais son acquisition est souvent complexe. Afin de reconstruire cette architecture initiale de manière simplifiée, des modèles utilisant peu de variables faciles à mesurer ont été établis sur la base de relations allométriques. Ces modèles ont été élaborés pour trois cultivars aux architectures contrastées : 'Fuji', 'Ariane', et 'Rome Beauty'. L'ensemble du travail effectué a permis de modéliser et ainsi reconstituer la surface foliaire totale ainsi que la surface foliaire individuelle pour chaque feuille de chaque type de pousse et pour chaque cultivar à partir de seulement deux variables d'entrée facilement mesurables : le nombre total des feuilles par pousse, et la longueur de la feuille la plus grande par pousse. Ces modèles pourront ensuite être utilisées pour la reconstruction de la structure de branche fruitière prise comme variable d'entrée dans le cadre du développement du modèle structuro-fonctionnel.

frontiers in Plant Science

ORIGINAL RESEARCH
published: 01 February 2017
doi: 10.3389/fpls.2017.00065

Models for Predicting the Architecture of Different Shoot Types in Apple

*Emna Baïram *, Mickaël Delaire, Christian Le Morvan and Gerhard Buck-Sorlin **

Unité Mixte de Recherche 1345, Institut de Recherche en Horticulture et Semences (Institut National de la Recherche Agronomique-Agrocampus Ouest-Université d'Angers), Angers, France

In apple, the first-order branch of a tree has a characteristic architecture constituting three shoot types: bourses (rosettes), bourse shoots, and vegetative shoots. Its overall architecture as well as that of each shoot thus determines the distribution of sources (leaves) and sinks (fruits) and could have an influence on the amount of sugar allocated to fruits. Knowledge of architecture, in particular the position and area of leaves helps to quantify source strength. In order to reconstruct this initial architecture, rules equipped with allometric relations could be used: these allow predicting model parameters that are difficult to measure from simple traits that can be determined easily, non-destructively and directly in the orchard. Once such allometric relations are established they can be used routinely to recreate initial structures. Models based on allometric relations have been established in this study in order to predict the leaf areas of the three different shoot types of three apple cultivars with different branch architectures: "Fuji," "Ariane," and "Rome Beauty." The allometric relations derived from experimental data allowed us to model the total shoot leaf area as well as the individual leaf area for each leaf rank, for each shoot type and each genotype. This was achieved using two easily measurable input variables: total leaf number per shoot and the length of the biggest leaf on the shoot. The models were tested using a different data set, and they were able to accurately predict leaf area of all shoot types and genotypes. Additional focus on internode lengths on spurs contributed to refine the models.

Keywords: ***Malus x domestica*** **Borkh., apple, leaf surface, shoot architecture, allometry, modeling, apple branch**

OPEN ACCESS

Edited by:
Alexander Bucksch,
University of Georgia, USA

Reviewed by:
David Ford,
University of Washington, USA
Guillaume Lobet,
Forschungszentrum Jülich, Germany

****Correspondence:***
Emna Baïram
emna.bairam@gmail.com
Gerhard Buck-Sorlin
gerhard.buck-sorlin@agrocampus-ouest.fr

Specialty section:
This article was submitted to Plant Biophysics and Modeling, a section of the journal Frontiers in Plant Science

Received: *27 September 2016*
Accepted: *12 January 2017*
Published: *01 February 2017*

Citation:
Baïram E, Delaire M, Le Morvan C and Buck-Sorlin G (2017) Models for Predicting the Architecture of Different Shoot Types in Apple. Front. Plant Sci. 8:65. doi: 10.3389/fpls.2017.00065

INTRODUCTION

The study of plant architecture is a discipline that attempts to understand and explain plant form and structure and the processes underlying its formation (Barthélémy, 1991). Vascular plants have developed different architectures as part of their genetic blueprint and in response to a changing environment (Sussex and Kerk, 2001). The size, shape and spatial orientation of plant organs are, therefore, not pure coincidence but the result of a morphogenetic program which is carried out by a whole range of physiological processes. Therefore, "reading" the architecture could be a starting point for a better understanding of this underlying program. Of these architectural traits, leaf area has a particular impact on fruit quality as it is directly involved in several physiological processes such as light interception and photosynthesis (Björkman and Demmig-Adams, 1995; Štampar et al., 1999).

Studies on the influence of tree architecture on physiological functioning can be conducted in several ways: Two suitable tools are ecophysiological experimentation and functional-structural plant modeling (FSPM) (Vos et al., 2010; Buck-Sorlin, 2013): Ecophysiological experiments aim at changing the microenvironment of a selected plant and its organs and even at pushing it to an extreme limit, in order to obtain knowledge about the growth and developmental potential in a certain parameter space. FSPM aims at the integration of the dynamics of known physiological processes with information about the topology and geometry of organs (plant architecture) using mainly rule-based mathematical modeling (Buck-Sorlin, 2013).

In order to represent initial architecture there are several methods at hand and it is worthwhile to invest some time in developing a work flow to obtain "good" plant architecture with reduced effort. Casella and Sinoquet (2003) name several approaches: (1) describe architecture as a collection of individual 3-D geometric shapes; (2) model 3D architecture of a population of plants using stochastic, fractal or Lindenmayer-system (Lindenmayer, 1968a,b) methods or (3) describe architecture using a 3D digitizing method. All these methods have their advantages and disadvantages (for a review see Prusinkiewicz, 1998): The first method is suitable for the representation of the context of a detailed tree model, but too coarse for the modeling of leaf photosynthesis. The second one, despite being relatively quickly put into place, can still turn out to be too inaccurate for the description of leaf-scale photosynthesis since due to the stochastic method of architecture construction the reproducibility of a given real architecture is difficult. Apart from that, this method requires extensive calibration with measured data sets. The third method, though the most accurate one, is unsuitable for logistic reasons in the orchard: in the absence of a socket an electricity generator needs to be used, and there might be interference with the steel wires used for fixing the drip irrigation system, quite apart from the fact that digitizing is a tedious task and the structure to be digitized is often too complex to be acquired in 1 day.

Yet another, alternative approach is to use allometric relations between traits at the organ and intermediate (shoot, branch) scales: The principle is to obtain faithful models for the prediction of traits that are difficult to measure or that involve destruction of the organ, e.g., leaf area, by traits that are more readily measured (e.g., leaf blade length) or easily and non-destructively scored in the orchard (leaf number, rank, order). Once such allometric relations are established they can be used routinely to recreate initial structures. As with all indirect measures they need to be well tested as they bear the risk of cumulative error.

In apple two types of buds are distinguished: the mixed and the vegetative bud. The mixed bud, independent of its position on the shoot (apical or lateral), contains primordia of vegetative and reproductive organs and will develop into a spur. Thus the spur consists of a short shoot called "bourse" on which the primordia of preformed leaves will extend, as well as one or two sylleptic shoots called "bourse shoots" and the inflorescence (Fanwoua et al., 2014). The vegetative bud develops into a vegetative shoot. In temperate species, short axes are composed of preformed organs only whereas long axes are composed of both preformed and neoformed organs successively (Costes et al., 2014); therefore, branch architecture is essentially determined by the developmental fate of these two bud types (**Figure 1**).

In this study we decided to concentrate on the prediction of leaf area: of all the traits contributing to branch architecture (leaf area, leaf blade and petiole orientation in space), it is the one that is most easily determined (as will be shown below) and yet very influential for light interception (Falster and Westoby, 2003). It was shown for apple that leaf area was the second most influential trait for light interception, after internode length (Da Silva et al., 2014). The distribution of leaves on the shoot and their size distribution clearly have an influence on light interception and leaf photosynthesis at the branch scale (Massonnet et al., 2008).

Any good model should be minimal in terms of number of input variables and the time invested in measurements but also efficient in simulating the output variable of interest. Therefore, the main aim of this study was to find models predicting the area of leaves of the three main shoot types of apple: bourse shoot (BS), rosette (RO) and vegetative shoot (VS), and this as a function of other traits on the same shoot that were either easy to score (total leaf number per shoot) or relatively quickly measured (length of the longest leaf of a given shoot). A secondary aim was to model the position of leaves on the shoot (length of the internodes) as a function of simple measured traits (length of the shoot). Such leaf area distributions can then serve to reconstruct the architecture of an apple branch used as an input for a functional-structural plant model of the first-order branch of apple, with emphasis on sugar transport (Bairam et al., unpubl.).

MATERIALS AND METHODS

Plant Material and Experiments

All experiments were performed on apple trees planted in 2008 in an experimental orchard at the INRA experimental unit in Beaucouzé, France. The cultivars selected for this experiment were "Ariane," "Fuji," and "Rome Beauty" (in the following abbreviated as AR, FU, and RB, respectively). The main purpose of this study was to develop an allometric model for the prediction of the distribution of individual leaf areas along a certain shoot type, as well as of the total leaf area for a given shoot, namely the bearing spurs and vegetative shoots as they are the most cumbersome to be measured in the orchard. The models presented here were developed to take into account the impact of the genotype (G, with values AR, FU, and RB, see above) and the type of the shoot (*j*, which has the value "BS" for the bourse shoot, "RO" for the rosette and "VS" for the vegetative shoot). Shoots of each type were collected, and the leaves were scanned using a flatbed scanner (HP Scanjet G4010) with a resolution of 150 dpi and saved in portable network graphics (png) format. Leaf blade area, length and width were measured using ImageJ 1.48v software, assuming that leaf shape is elliptical (Freeman and Bolas, 1956). Total leaf area on each shoot was calculated as the sum of its individual leaves.

The models predicting individual/total leaf area use allometric relations between easily recorded input variables such as the length of the ellipse of the biggest leaf on the shoot (L_{max}), the

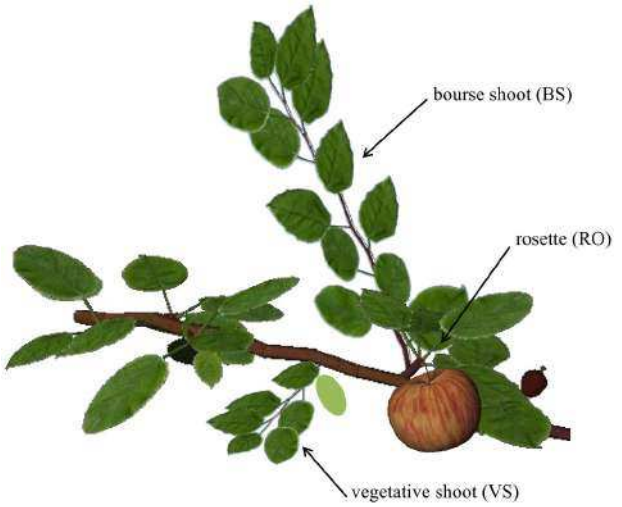

FIGURE 1 | Representation of the three shoot types on the first-order branch of apple. RO, rosette; BS, bourse shoot; and VS, vegetative shoot. Figure produced using the GroIMP platform (Hemmerling et al., 2008).

number of leaves (*nl*) and the acropetal leaf rank (*R*). These models were built using different parameters and each of them was estimated using regression models. For rosettes and bourse shoots, enough data was available to be split into training and testing sets: the first data set was used for the estimation of the parameters and the second one for the testing of the model (Snee, 1977; Montgomery et al., 2015). Therefore, models were parameterized, calibrated and tested. For vegetative shoots, a simple model was built as there was not enough data for testing it.

Modeling the Leaf Area of Bourse Shoots and Rosettes

Data used in this study consisted of a first data set from an experiment conducted in 2014 and a second, complementary data set collected in 2015 (Bairam et al., unpublished). The variables describing architectural traits of bourse shoots and rosettes [shoot length, number of leaves, leaf individual surface, leaf length, leaf width, and leaf rank (the latter only for bourse shoots)] extracted from the two sets were used for modeling total shoot leaf area and individual leaf area distribution along the stem. In the 2014 experiment, spurs of AR and RB were collected at eight different developmental stages from full bloom to harvest, and spurs of FU were collected at full bloom, 2 weeks after full bloom and at harvest. The experiment conducted in 2014 aimed at studying the impact of removing bourse shoot leaves, rosette leaves or both of them at full bloom and 2 weeks after full bloom, on fruit quality, bourse shoot and rosette (bourse) morphological traits. To develop an allometric model for the prediction of final leaf area, we needed a sufficiently large data set. However, the data set available in this study (2014 experiment, Bairam et al., unpublished) already included three defoliation treatments. In order to enlarge the database for the parameterization of our model beyond the control data, we checked whether the defoliation treatments had a significant impact on the following variables used in the model: total leaf area and number of leaves of bourse shoot and rosette, respectively. The statistical tests were carried out separately, on each genotype for each sampling date and each type of shoot. Results (ANOVA, Kruskal-Wallis) showed that there was no significant influence of the defoliation treatments (Bairam et al., unpublished). This allowed us to pool the data available for these variables, involving all defoliation treatments, and to use them in the model. 174, 49, and 134 rosettes of AR, FU and RB, respectively, as well as 336, 80, and 280 bourse shoots of AR, FU and RB, respectively, were retained from the 2014 experiment. Afterwards, for AR and RB, tests (ANOVA, Kruskal-Wallis) were conducted on 2014 data in order to establish the phenological stage of development expressed in growing degree days (GDD) since FB from which onwards each type of shoot for each genotype was fully developed in terms of number of leaves and total leaf area. This developmental time was first measured using growing degree hours [GDH, base temperature $T_b = 7°C$ (Anderson and Richardson, 1982)] calculated using hourly air temperatures (°C) obtained from the weather station of Beaucouzé (47° 28′ N, 0° 37′ W, 50 m a.s.l.) and accessed from the INRA Climatik platform, https://intranet.inra.fr/climatik_v2/:

$$GDH_i = \sum_{h=1}^{24} (HT_h - T_b) \quad (1)$$

Here, HT_h is replaced by T_b if $HT_h < T_b$; HT_h is the hourly air temperature at hour h; and GDH_i are the growing degree hours on day i. Cumulated GDD (GDD_{cum}) for each sampling day were calculated using Equation 2. The starting point of GDD_{cum} is full bloom (FB) which, in 2014, occurred for AR on April 10th, for FU on April 14th and for RB on April 22nd while in 2015, full bloom occurred for FU on April 20th.

$$GDD_{cum} = \sum_{i=FB}^{D} \frac{GDH_i}{24} \quad (2)$$

where *FB* is day of full bloom and *D* is the number of days since *FB*.

During the second experiment conducted in 2015, the same variables as in 2014 were recorded plus the ranks of rosette leaves; however, based on the results of the 2014 experiment no defoliation treatments were applied and only spurs of FU at different phenological stages (FB, FB+2, FB+4, FB+6, FB+9 weeks) were considered. For FU, ANOVA and Kruskal-Wallis analysis were carried out on 2015 and 2014 data to compare total leaf area and number of leaves (rosettes and bourse shoots) as a function of developmental stages (expressed in GDD) in order to establish the sampling stages at which the spur shoots were fully developed. Therefore, fully developed bourse shoots and rosette shoots, respectively, were pooled for each genotype. All shoots of the same type and the same genotype considered to be fully developed in terms of total leaf area and numbers of leaves were used in this study for building the allometric models. Total leaf areas and numbers of leaves of bourse shoots of AR, FU, and RB, were fully developed at 345, 201, and 275 GDD, respectively. Groups of bourse shoots of each genotype were selected from these physiological ages

onwards, until harvest. Rosette shoots were assumed to be fully developed at full bloom as the mean total leaf areas for the three genotypes were the highest at the earliest sampled spurs. However, even if a significant difference was found between groups of rosettes sampled at different phenological stages for a same genotype, still the means are not correlated with phenological sampling dates and the only group really apart in terms of rosette total leaf area and number of leaves for the three genotypes, respectively, was the one collected at harvest (Bairam et al., unpublished). Therefore, only rosettes collected before harvest were retained for the rest of the study. Only selected spurs were used for the rest of this study and data selected for each genotype and each shoot type was split randomly into a training set (2/3 of data) and a testing set (the remaining 1/3 of data) for setting up the models. The procedure to build the models for predicting bourse shoot and rosette individual leaf area is summarized in **Figure 2**. In the following, the steps followed for building the models described in the flow chart are explained.

The variation of individual leaf areas of 153, 97, and 112 bourse shoots, respectively, of AR, FU, and RB, as a function of leaf rank is shown in (**Figures 3A–C**), and of 80 rosettes of FU considered to be fully grown shoots in (**Figure 3D**). Based on these observations, it was assumed that leaf size follows a rank-specific pattern typical for both bourse shoots and rosettes. In this study, we aimed to establish the pattern and parameterize it for each genotype and each type of shoot. However, the total leaf area of the shoot which can be calculated by integrating the sum of the areas of individual leaves of each rank seemed to be correlated with the number of leaves per shoot and the area of the biggest leaf (**Figure 3**). Furthermore, if this hypothesis would prove to be true, the result would confirm the existence of an allometric relation between the total leaf area on the one hand and the number of leaves and individual leaf area on the other.

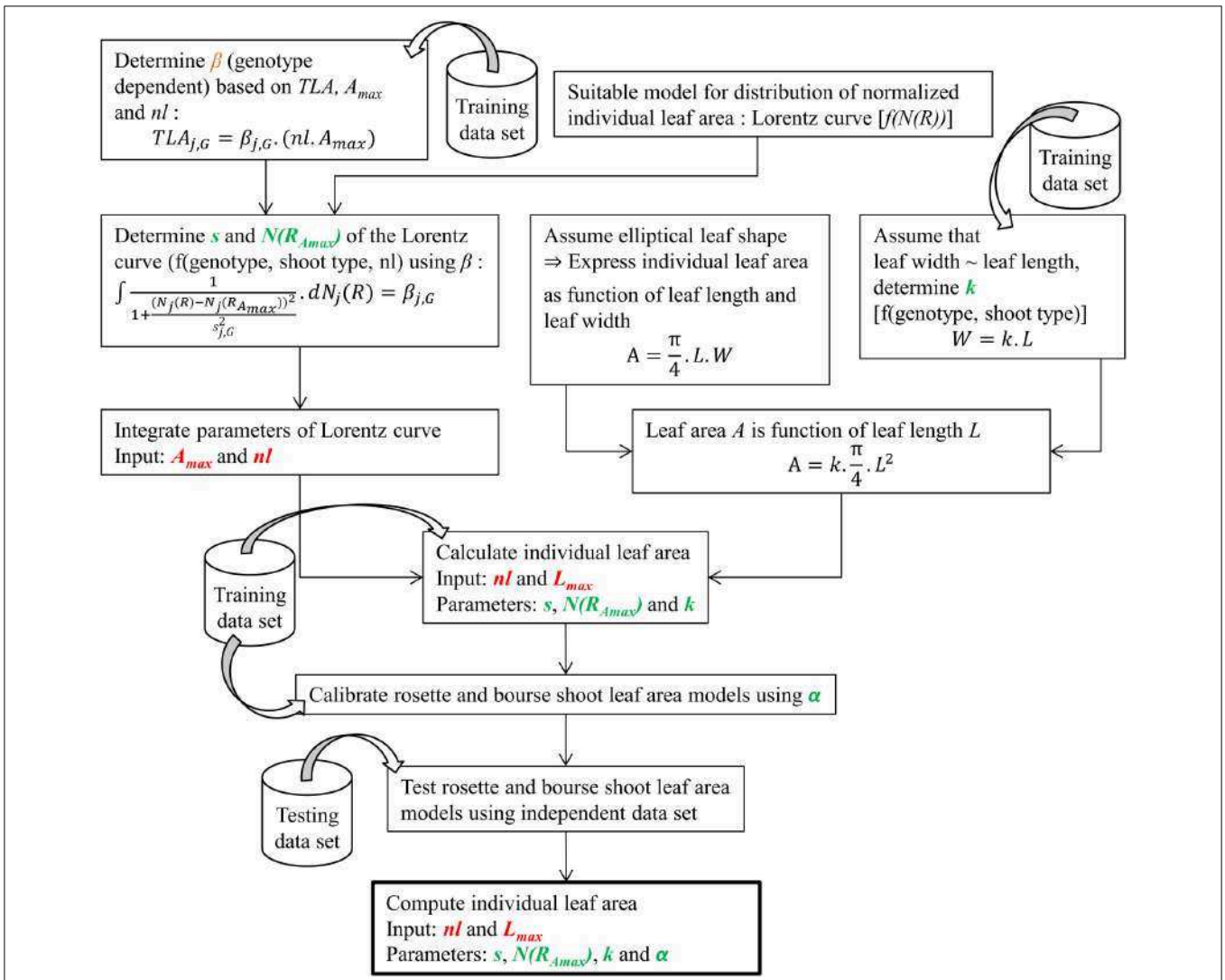

FIGURE 2 | Diagram summarizing the steps involved in modeling bourse shoot and rosette individual leaf area (for further explanations see text and equations).

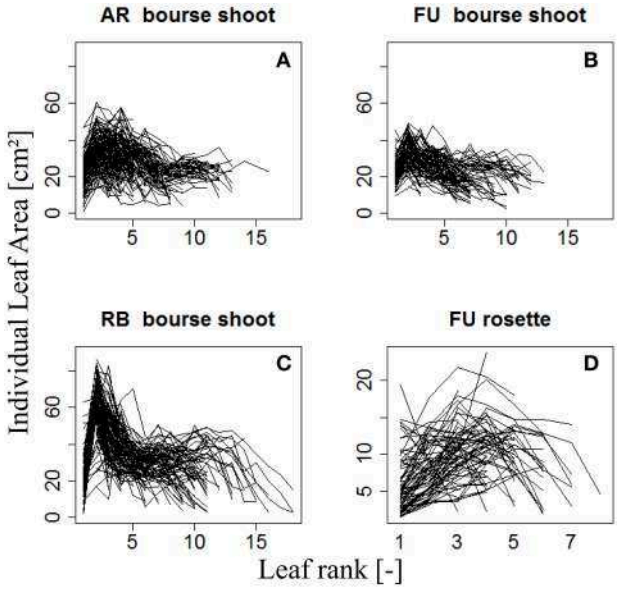

FIGURE 3 | Distribution of individual leaf area as a function of leaf rank of AR, FU, and RB bourse shoots (*N* = 153, 97, and 112, respectively) (A–C) and of FU rosettes (*N* = 80) **(D)**. Each line joins the individual leaf areas of a single shoot.

Moreover, if individual leaf areas follow a stable pattern along the shoot, this would mean that only one of these areas would be necessary as an input to the model, and that then the biggest leaf area would be an appropriate variable. Therefore, the assumption made and expressed in (Equation 3) implies that total leaf area (*TLA*) of the shoot is somehow related to the area of the biggest leaf (A_{max}) and the number of leaves (*nl*).

$$TLA_{j,G} = \beta_{j,G}.(nl.A_{max}) \quad (3)$$

ANOVA and Kruskal-Wallis tests were carried out on the selected data set in order to check if there is a significant difference of the parameter $\beta_{j,G}$ among genotypes for a same shoot type. Groups of samples showing no significant difference were pooled and the training setestablished before were used in order to fix $\beta_{j,G}$ using linear regressions between the variable *TLA* and the variable $nl.A_{max}$.

Therefore, total leaf area of a shoot can be estimated by two variables: the area of the biggest leaf on the shoot (A_{max}) and the number of leaves (*nl*) it bears. Thus, we made the assumption that the normalized individual leaf area [$N(A_R)$, expressed as the ratio of the individual leaf area by the biggest leaf area on the shoot (Equation 4a)] is a function of the normalized leaf rank [*N(R)*], calculated as the ratio of the rank of the leaf divided by the number of leaves on the shoot (Equation 4b). However, we could observe that in bourse shoots, the leaf with the biggest area was by far the most often the second one (**Table 1**). Hence, in order to adjust a maximum of the curves describing $N(A_R)$ as a function of *N(R)*, the normalized rank for bourse shoots was calculated by dividing [the rank (*R)* minus 2] by the number of leaves (Equation 4c). Indeed, subtracting two from the rank of the biggest leaf (2) will result in a normalized rank which is always zero and will lead to a very good alignment of the curves. Besides, with this method, the entire curve is just shifted to the left without being stretched or compressed.

TABLE 1 | Distribution of the leaves with the biggest area on bourse shoots with respect to their rank for AR, FU, and RB genotypes.

Genotype	Rank					
	1	2	3	4	5	6
AR	0.65%	50.00%	26.62%	15.58%	5.84%	1.30%
FU	8.08%	68.69%	14.14%	3.57%	0.89%	_
RB	_	87.50%	8.04%	3.57%	0.89%	_

$$N(A_R) = \frac{A_R}{A_{max}} \quad (4a)$$

$$N_{RO}(R) = \frac{R}{nl} \quad (4b)$$

$$N_{BS}(R) = \frac{R-2}{nl} \quad (4c)$$

The models were established from predicting the normalized area of each leaf $N(A_R)$ as a function of the normalized leaf rank $N_j(R)$ by using the area of the biggest (in terms of leaf area) leaf (A_{max}) on each shoot as a predictor of the other leaf areas. This hypothesis is expressed by Equation (5).

$$N(A_R) = f_{j,G}(N_j(R)) \quad (5)$$

For each type of shoot and each genotype, we looked for a function $f_{j,G}$ that models the normalized area of each leaf on the shoot as a function of its normalized rank. $N(A_R)$ was plotted as a function of $N_j(R)$, giving a certain pattern (**Figure 4**). We then tried to find a model that best described this relationship: a bilinear (broken stick) model and a Lorentz function. The first model requires five parameters while the second one only needs three. The Lorentz function has been successfully used by other workers (Buck-Sorlin, 2002; Evers et al., 2005, 2007; Gu et al., 2014) to predict leaf length in cereals and cotton. In this study, this function was chosen to model leaf areas of bourse shoots and rosettes.

$$f_{j,G}(x) = \frac{M}{1 + \frac{(x-x_0)^2}{s^2}} \; ; \; j\epsilon\{BS; RO\} \quad (6)$$

The maximum is reached for $x = x_0$, with *M* being the maximum value. *s* defines the slope of the curve of the function $f_{j,G}$. For both bourse shoots and rosettes, $f_{j,G}$ *(x)* corresponds to the normalized leaf area and *x* to the normalized leaf rank. x_0 is the normalized rank of the leaf with highest area on the shoot [$N_j(R_{Amax})$]. Consequently, the maximum of the function has the value of the normalized biggest area, i.e., $M = 1$ (Equation 7).

$$f_{j,G}(N_j(R)) = N(A_R) = \frac{1}{1 + \frac{(N_j(R) - N_{j,G}(R_{Amax}))^2}{s^2_{j,G}}} ; j\epsilon\{BS; RO\} \quad (7)$$

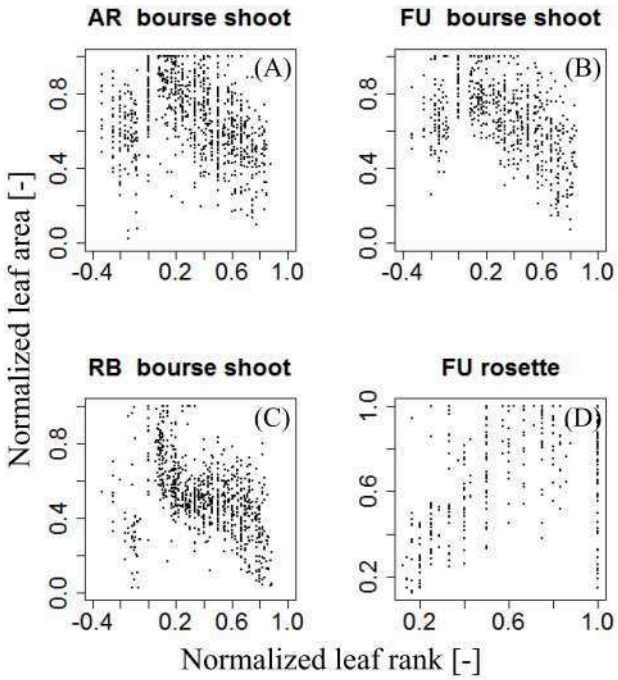

FIGURE 4 | Distribution of individual normalized leaf area plotted against normalized leaf rank of AR, FU, and RB bourse shoots (*N* = 153, 97, and 112) (A–C) and FU rosettes (*N* = 80) **(D)**.

After normalization for each type of shoot, Equations 7a and 7b are obtained:

$$f_{BS,G}(N_{BS}(R)) = N(A_R) = \frac{1}{1 + \frac{(N_{BS}(R))^2}{s^2_{BS,G}}} \quad (7a)$$

$$f_{RO,G}(N_{RO}(R)) = N(A_R) = \frac{1}{1 + \frac{(N_{RO}(R) - N_{RO,G}(R_{A_{max}}))^2}{s^2_{RO,G}}} \quad (7b)$$

Therefore, based on the fact that (i) the total leaf area ($TLA_{j,G}$) of a shoot of type "j" is the sum of the individual areas A_R of leaves and (ii) its value depends on the pattern described by Equations 7a and 7b, the models (Equation 3) were derived as follows:

$$\begin{aligned} TLA_{j,G} &= \beta_{j,G}.(nl.A_{max}) \\ \sum_{R=1}^{nl} A_R &= \beta_{j,G}.(nl.A_{max}) \\ \sum_{R=1}^{nl} \frac{A_R}{A_{max}}.\frac{1}{nl} &= \beta_{j,G} \\ \sum_{R=1}^{nl} \frac{N(A_R)}{nl} &= \beta_{j,G} \\ \int f_{j,G}(N_j(R)).dN_j(R) &= \beta_{j,G} \end{aligned}$$

$$\begin{cases} \int_{\frac{-2}{nl}}^{\frac{nl-2}{nl}} \frac{1}{1 + \frac{(N_{BS}(R))^2}{s^2_{BS,G}}}.dN_{BS}(R) = \beta_{BS,G} \\ \int_0^1 \frac{1}{1 + \frac{(N_j(R) - N_{RO,G}(R_{A_{max}}))^2}{s^2_{RO,FU}}}.dN_{RO}(R) = \beta_{RO,G} \end{cases}$$

$$\begin{cases} [s_{BS,G}.\text{atan}(\frac{N_{BS}(R)}{s_{BS,G}})]_{\frac{-2}{nl}}^{\frac{nl-2}{nl}} = \beta_{BS,G} & (8a) \\ [s_{RO,G}.\text{atan}(\frac{N_{RO}(R) - N_{RO,G}(R_{A_{max}})}{s_{RO,G}})]_0^1 = \beta_{RO,G} & (8b) \end{cases}$$

When solving Equation 8a used for the bourse shoot leaf area model, the only parameter to fix was $s_{BS,G}$ and its different values were calculated as a function of the value of $\beta_{BS,G}$ (which is unique for a same genotype and shoot type) and *nl* (from 1 to 18). Equation 8b used for parameterizing the rosette leaf area model does not take into account the number of leaves and it was solved using only $\beta_{RO,G}$. However, in this second equation two parameters of the model [$s_{RO,G}$ and $N_{RO,G}(R_{Amax})$] had to be fixed. Both equations 8a and 8b were solved using the solver functionality of Microsoft Excel software (Microsoft, Redmond, WA, USA).

Starting from Equation 7, the model is expressed as:

$$\begin{aligned} N(A_R) &= \frac{1}{1 + \frac{(N_j(R) - N_j(R_{A_{max}}))^2}{s^2_{j,G}}} \; ; \; j\epsilon\{BS; RO\} \\ A_R &= \frac{A_{max}}{1 + \frac{(N_j(R) - N_j(R_{A_{max}}))^2}{s^2_{j,G}}} \; ; \; j\epsilon\{BS; RO\} \quad (9) \\ A_R &= \frac{A_{max}}{1 + \frac{(R - R_{A_{max}})^2}{\frac{nl^2}{s^2_{j,G}}}} \; ; \; j\epsilon\{BS; RO\} \\ A_R &= \frac{A_{max}}{1 + \frac{(R - R_{A_{max}})^2}{nl^2 \cdot s^2_{j,G}}} \; ; j\epsilon\{BS; RO\} \quad (10) \end{aligned}$$

By fixing the latter parameters, it was possible to calculate the normalized area of each leaf, using only the number of leaves on the shoot and the area of its biggest leaf. However, as the leaf area is not easily measurable non-destructively, further allometric relations are required for predicting leaf areas using variables that are more easily accessible. Leaf length and width seem to be the most obvious candidates for modeling the leaf area as we consider the leaf blade to be elliptical (Equation 11). Observations of leaves indicate that the length/width ratio is constant for a same genotype and shoot type (Equation 12). Assuming this is confirmed, only the variable "length of the leaf" (L) could be retained for calculating the individual leaf area. This assumption is stated as follows: (i) the ratio between the length (L) and the width (W) of a leaf is a constant parameter ($k_{j,G}$) for the same shoot type (j) and the same genotype (G) and (ii) apple leaves have the shape of an ellipse (Freeman and Bolas, 1956). These two hypotheses are captured by Equations 11 and 12.

$$A = \pi \frac{L.W}{4} \quad (11)$$

$$\frac{W}{L} = k_{j,G} \quad (12)$$

The Shape of an ellipse is defined by its eccentricity e, i.e., the ratio between the distance from the center to a focus and the distance between that focus to a vortex (Equation 13a). Therefore, $k_{j,G}$ can be expressed as a function of $e_{j,G}$ (Equation 13b). If $e_{j,G}$ is proven

to be invariant for a same genotype and a same type of shoot, it could be used in the model as the constant for leaves on shoots of type j and of cultivar G; $0 < k_{G,j} \leq 1$

$$e_{j,G} = \frac{\sqrt{L^2 - W^2}}{L} \quad (13a)$$

$$k_{j,G} = \sqrt{1 - e_{j,G}^2} \quad (13b)$$

Therefore, $e_{j,G}$ was calculated for each leaf used in this study using Equation 13a, as it is an indicator of the shape of the ellipse defined by the leaf. Then, a first test was done in order to check if there is a significant difference in $e_{j,G}$ among the leaves of different ranks in a shoot within the same cultivar for each type of shoot. A second test was conducted to verify if there is a significant difference of $e_{j,G}$ among the three genotypes for each type of shoot. Moreover, even if the leaf shape is genotype dependent, the environment can influence it during the last stages of leaf development (Tsukaya, 2004). Therefore, a test was done in order to check if there is a significant difference of $e_{j,G}$ between 2014 ($N = 323$ and $N = 159$, for bourse shoots and rosettes, respectively) and 2015 ($N = 385$ and $N = 363$, for bourse shoots and rosettes, respectively) leaves of FU. Leaf data with no significant difference in e were pooled and the training set of the bearing spurs was used to fix $k_{j,G}$ using a linear model.

Combining Equations (11) and (12), the following relation (14) is obtained:

$$A = \frac{\pi}{4}.k_{j,G}.L^2 \quad (14)$$

By combining Equation (10) and Equation (14), equation (15) is obtained.

$$A_R = \frac{\frac{\pi}{4}.k_{j,G}.L_{max}^2}{1 + \frac{(R - R_{A_{max}})^2}{nl^2.s_{j,G}^2}}; j\epsilon\{BS; RO\} \quad (15)$$

In this way, L_{max} (the length of the biggest leaf on the shoot) and nl are the only two required input variables.

Using the models established we calculated individual leaf area and total leaf area on a shoot as the sum of the calculated individual leaf areas on the training set. Comparisons were made using the linear model between measured and calculated total leaf areas on each type of shoot and each genotype separately. Then, calibrations were made using a parameter $\alpha_{j,G}$ referring to the slope of the axis defined by measured total leaf area on a shoot ($TLA_{j,G}$) as a function of calculated total leaf area on a shoot ($CTLA_{j,G}$) of the training set. $\alpha_{j,G}$ was calculated for each type of shoot and each genotype separately.

The final model calculating individual leaf area is:

$$A_R = \alpha_{BS,G} \frac{\frac{\pi}{4}.k_{BS,G}.L_{max}^2}{1 + \frac{(R-2)^2}{nl^2.s_{BS,G}^2}} \quad (16a)$$

$$A_R = \alpha_{RO,G} \frac{\frac{\pi}{4}.k_{RO,G}.L_{max}^2}{1 + \frac{(R - nl.N_{RO,G}(R_{A_{max}}))^2}{nl^2.s_{RO,G}^2}} \quad (16b)$$

The testing set was then used for calculating individual and total leaf areas. Using the testing data set, comparisons were made between measured and calculated data (i) for each established parameter, (ii) for individual leaf area and (iii) total leaf area on each shoot of each genotype using the linear model. P-values and coefficients of determination R^2 were calculated in order to analyze and interpret the significance and the goodness of fit of the models. For rosettes, as the ranks of leaves on the bourse were not recorded in the 2014 experiment, comparisons between measured and calculated values of individual area were done only on data from 2015.

Modeling the Leaf Area of Vegetative Shoots

For modeling the leaf area of vegetative shoots, 20 vegetative shoots each of AR and FU were collected on July 3rd, 2015 when they were considered to be fully developed, then scanned and analyzed as described for bourse shoots and rosettes. Total leaf area on each vegetative shoot was calculated as the sum of areas of individual leaves. Leaf ranks on each shoot were recorded, and lengths and dry weights of the shoots and the leaves measured. The variation of individual leaf areas of the 20 vegetative shoots of AR and FU as a function of leaf rank is shown in (**Figures 5A,B**): leaf area increases with rank for both genotypes. However, the pattern is heterogeneous when based on absolute leaf length measurements and ranks. We therefore normalized both leaf areas (Equation 4a) and ranks (Equation 4b). On visual inspection, the distribution of $N(A_R)$ as a function of $N(R)$ on vegetative shoots of both genotypes (**Figures 5C,D**) seems to describe a linear pattern (Equation 17). We made the assumption that A_R is proportional to the square of leaf length ${L_R}^2$ as for bourse shoots and rosettes (Equation 14). Eccentricity ($e_{VS,G}$) of the ellipse was calculated for each leaf and comparison tests were made between the two genotypes, then $k_{VS,G}$ (ratio between width and length of the leaf blade) was fixed for the model. Afterwards and using the previously fixed $k_{VS,G}$, a parameter p which describes the slope of the curve was calculated for each leaf using Equation 17 and a statistical comparison was carried out between the two cultivars in order to check if they were different with respect to p. Based on this comparison, p was fixed using a linear regression model. The vegetative shoot model (Equation 18) is a descriptive model allowing calculating the individual leaf areas of AR and FU vegetative shoots using only two variables, L_{max} and nl. A regression test was carried out using the linear model between the calculated individual areas and the measured ones.

$$N(A_R) = p.N(R) \quad (17)$$

$$\frac{A_R}{A_{max}} = p.\frac{R}{nl}$$

$$A_R = p.\frac{R}{nl}.A_{max}$$

$$A_R = p.\frac{R}{nl}.\frac{\pi}{4}.k_{j,G}.L_{max}^2 \quad (18)$$

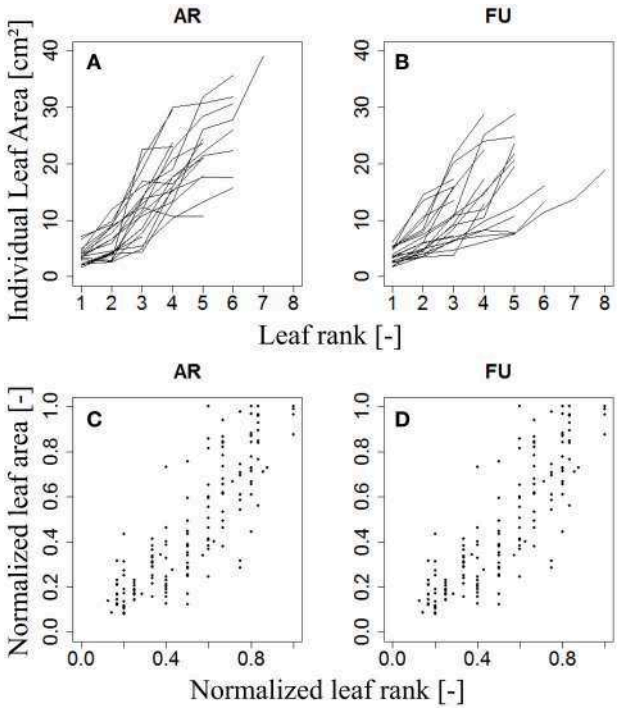

FIGURE 5 | Distribution of individual leaf area as a function of leaf rank (A,B) and distribution of individual normalized leaf area as a function of normalized leaf rank **(C,D)** of AR and FU vegetative shoots ($N = 20$ vegetative shoots for each cultivar).

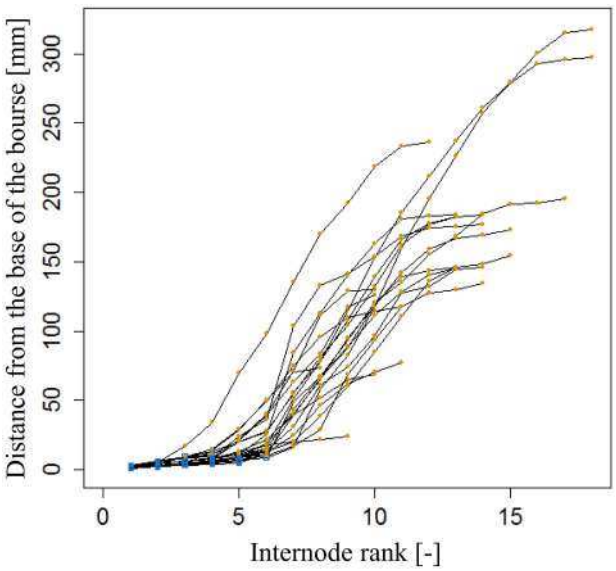

FIGURE 6 | Cumulated length of bourse and bourse shoots, expressed as the distance from the base of the bourse to the point of insertion of a bourse or a bourse shoot leaf of internode rank 1–18 in FU [*N* = 24, continuum: bourse (●) - bourse shoot (●)].

Modeling Length of Spur Internodes

The internode lengths of 20 spurs of "FU" were measured in the orchard in July 2016. As the bourse internodes are very short, we assigned to each one the mean value of the bearing spur calculated as the ratio of "Length of the bourse"/"Number of internodes on the bourse." For each spur, a "cumulative shoot length" D_I between the base of the bourse (rosette) and the node (leaf insertion point) for each bourse and bourse shoot leaf was measured. For bourse shoot nodes, this cumulative shoot length is equal to the sum of the lengths of the rosette internodes from the base of the bourse to the node on which is inserted the bourse shoot (BL) and the sum of the internode lengths from the base of the bourse shoot to the considered node. The rank of each internode, on each spur, was also recorded from the first rosette leaf to the last bourse shoot leaf, assuming that the rank of the first internode of the bourse shoot has the value of the rank of the bourse internode on which it is inserted, plus one. Among the 20 spurs, 16 were bearing only one bourse shoot and the remaining ones were bearing two bourse shoots. Plotting this cumulative shoot length D_I as a function of cumulative (bourse and bourse shoot) rank R_I corresponded to a logistic pattern for each spur (**Figure 6**). However, the pattern seemed to be dependent upon the length of the shoot (bourse plus bourse shoot). Therefore, normalized cumulative internode lengths [$N(D_I)$] between each leaf base and the base of the bourse (Equation 19a) and normalized rank [$N(R_I)$] (Equation 19b) were calculated assuming that the bourse and the bourse shoot are the same shoot unit (and that, therefore, the bourse shoot is a sylleptic extension of the bourse). The normalized cumulative shoot length was calculated as a function of the sum of BL and the bourse shoot length (BSL).

$$N(D_I) = \frac{D_I}{BL + BSL} \tag{19a}$$

$$N(R_I) = \frac{R_I}{nl} \tag{19b}$$

Afterwards, the parameters qi and si of the internode model were fixed by fitting a logistic model (Equation 20) to the distribution of the $N(D_I)$ as a function of $N(R_I)$.

$$N(D_I) = \frac{1}{1 + \exp\left(\frac{qi - N(R_I)}{si}\right)} \tag{20}$$

Once established, this descriptive model would estimate the cumulative shoot length of each leaf insertion point of rank R_I on the bourse or the bourse shoot from the bottom of the bourse providing 3 input variables: nl, $(BL + BSL)$ and R_I (Equation 21).

$$D_I = \frac{1}{1 + \exp\left(\frac{qi - \frac{R_I}{nl}}{si}\right)}.(BL + BSL) \tag{21}$$

Statistical Analyses

Statistical analyses were done using R Studio software version 0.98.1062.0 running R version 3.2.2. and the statistical computing environment of the R-package "agricolae," version 1.2-2. Normality of data used for each analysis was tested on residuals using the Shapiro-Wilk test for data sets with more than 50 samples per group or sample distributions considered to be

normal ($P > 0.05$); ANOVA tests were used to check if there was a significant difference among groups ($P < 0.05$). Otherwise differences between groups were tested with the Kruskal-Wallis test ($P < 0.05$), or both ANOVA and Kruskal-Wallis. Fit of data to selected models was checked using the *lm* function in *R* software for linear distribution models. The logistic model was parameterized using the *SSlogis* function in *R* software and coefficients of determination (R^2) and root mean squared errors (RMSE) were calculated to test the fit of the model.

RESULTS

Modeling the Leaf Area of Bourse Shoots (BS)

ANOVA made on $\beta_{BS,G}$ of bourse shoots showed there was no significant difference between AR (mean $\beta_{BS,AR} = 0.71$) and FU (mean $\beta_{BS,FU} = 0.70$). However, bourse shoots of both AR and FU were significantly different from RB with respect to $\beta_{BS,G}$ (mean $\beta_{BS,RB} = 0.53$). Therefore, the same value of $\beta_{BS,G}$ was used for the training data set of AR and FU bourse shoots, while for RB bourse shoots a separate training data set was used, thus necessitating the parameterization of two linear regression models (**Figures 7A,B**). For both groups, the linear model was significant ($P < 2.10^{-16}$). The coefficients of determination for both the AR|FU model and the RB model were sufficiently high ($R^2 = 0.95$ and $R^2 = 0.89$) to support the assumption that the values of $\beta_{BS,G}$ ($\beta_{BS,AR/FU} = 0.67$ and $\beta_{BS,RB} = 0.50$) were robust.

Using the values of $\beta_{BS,G}$ Equation 8a was solved and $s_{BS,AR|FU}$ and $s_{BS,RB}$ were established as a function of the number of leaves on the bourse shoot. The number of leaves recorded on bourse shoots sampled varied from 1 to 16, 13 and 18, respectively, for AR, FU and RB. Thus 18 values for $s_{BS,G}$ were established for each one of the two groups of genotypes (**Table 2**).

$e_{BS,G}$ was significantly different among genotypes ($p < 2.2.10^{-16}$), with means of $e_{BS,G}$ equal to 0.79, 0.76, and 0.74 for AR, FU and RB, respectively. ANOVA tests showed no significant differences among the shapes of leaves of different ranks on a bourse shoot ($e_{BS,G}$). However, leaves above rank 14 in AR and leaves above rank 15 in RB seemed to indicate a significant difference, but based on the weak frequencies of these leaf ranks (only one bourse shoot of AR and 15 bourse shoots of RB having more than 13 and 15 leaves, respectively), it was decided not to take into account this difference. Furthermore, $e_{BS,FU}$ was not significantly different between 2014 and 2015 ($p = 0.59$). Therefore, it was considered that the impact of the factor year was not significant.

$k_{BS,G}$ was fixed for AR, FU and RB using linear regression models on the training set of each genotype (**Figures 8A–C**) and the leaf length of each genotype was significantly correlated with its width ($P < 2.10^{-16}$ for all the genotypes' models), with coefficients of determination of 0.68, 0.73, and 0.72 for AR, FU

TABLE 2 | Parameterization of $s_{BS,G}$.

NL	AR & FU	RB
1	2.13	1.48
2	0.70	0.43
3	0.38	0.23
4	0.35	0.22
5	0.36	0.22
6	0.38	0.23
7	0.40	0.24
8	0.42	0.25
9	0.44	0.25
10	0.46	0.26
11	0.48	0.27
12	0.49	0.28
13	0.51	0.29
14	0.52	0.30
15	0.53	0.31
16	0.54	0.31
17	0.55	0.32
18	0.55	0.32

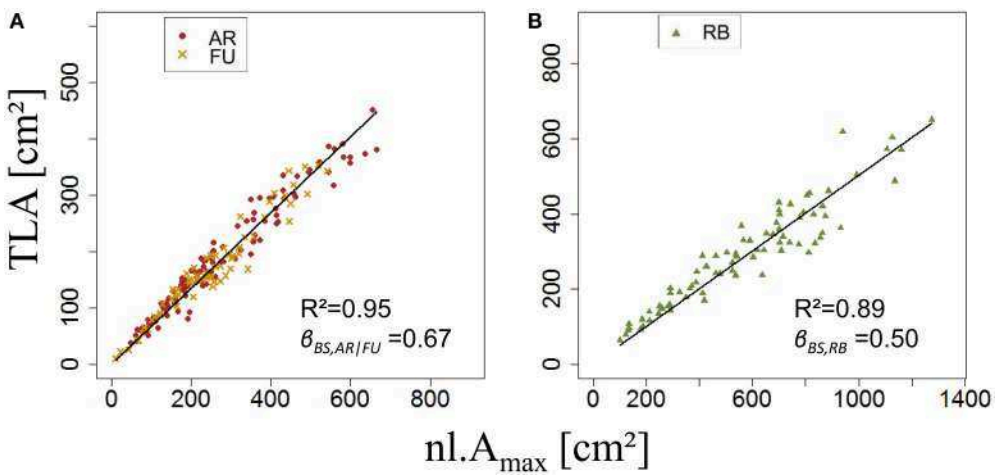

FIGURE 7 | Parameterization of $\beta_{BS,G}$ (N = 180 and 80 bourse shoots, respectively; A,B).

and RB, respectively. $k_{BS,G}$ values were fixed to 0.60, 0.64, 0.66 for AR, FU and RB, respectively.

Once $s_{BS,G}$ and $k_{BS,G}$ were fixed, all leaf areas of the bourse shoot training set were calculated using Equation 15, with the rank of the leaf and the variables L_{max} and nl of each bourse shoot as input. Total leaf area on each shoot was calculated as the sum of individual leaves. Calculated and measured total leaf areas ($CTLA_{BS,G}$ and $TLA_{BS,G}$) of the bourse shoots were compared for each genotype using a linear regression where the slope $\alpha_{BS,G}$ of each regression model of $TLA_{BS,G}$ as a function of $CTLA_{BS,G}$ was expected to be equal to 1 if the calculated and the measured area were identical. The slope parameter was equal to 1.2, 0.99 and 1.87 for AR, FU and RB, respectively (**Figures 9A–C**), which led us to assume that the parameter $\alpha_{BS,G}$ was genotype dependent. Therefore, values of $\alpha_{BS,G}$ fixed using the training set were retained for calibrating the model. The model defined in Equation 15 and built for bourse shoots including the three parameters ($s_{BS,G}$, $k_{BS,G}$ and $\alpha_{BS,G}$) and using the variables L_{max} and nl for the prediction of individual leaf areas was used to calculate individual areas for each leaf of the testing set and the comparison with measured individual data was conducted using a linear model. In the testing set, though linear models of calculated individual leaf area as a function of measured individual leaf area were significant for all genotypes ($P < 2.10^{-12}$), the coefficients of determination were very small ($R^2 = 0.17$, 0.20, 0.30 for AR, FU and RB, respectively). In contrast to this, linear regression modeling of $TLA_{BS,G}$ as a function of $CTLA_{BS,G}$ yielded significant results for all genotypes ($R^2 = 0.84$, 0.67 and 0.64; slope = 1.02, 1.05 and 0.95 for AR, FU and RB, respectively; **Figures 10A–C**).

Modeling the Leaf Area of Rosettes (RO)

Both ANOVA and Kruskal-Wallis test showed there was no significant difference between the three genotypes with respect to $\beta_{RO,G}$. Thus $\beta_{RO,G}$ was fixed to 0.69 using a linear regression model on the training set of rosette data of bourses sampled before harvest of the three genotypes (**Figure 11A**). The model was significant ($P < 2.10^{-16}$) and the coefficient of determination was high ($R^2 = 0.97$). Afterwards, the values of parameters $s_{RO,G}$ and $N_{RO,G}(R_{Amax})$ were fixed to 0.38 and 0.63, respectively.

$e_{RO,G}$ was significantly different among genotypes ($P = 3.46.10^{-8} < 0.05$), with means of $e_{RO,G}$ equal to 0.65, 0.66 and 0.68 for AR, FU and RB, respectively. When comparing e_{BS} of different ranks on rosettes of FU sampled in 2015, both ANOVA and Kruskal –Wallis test showed there were no significant differences among the shapes of leaves of different ranks on the bourse. $e_{RO,FU}$ did in fact significantly vary between the 2 years ($P = 2.162.10^{-7}$).

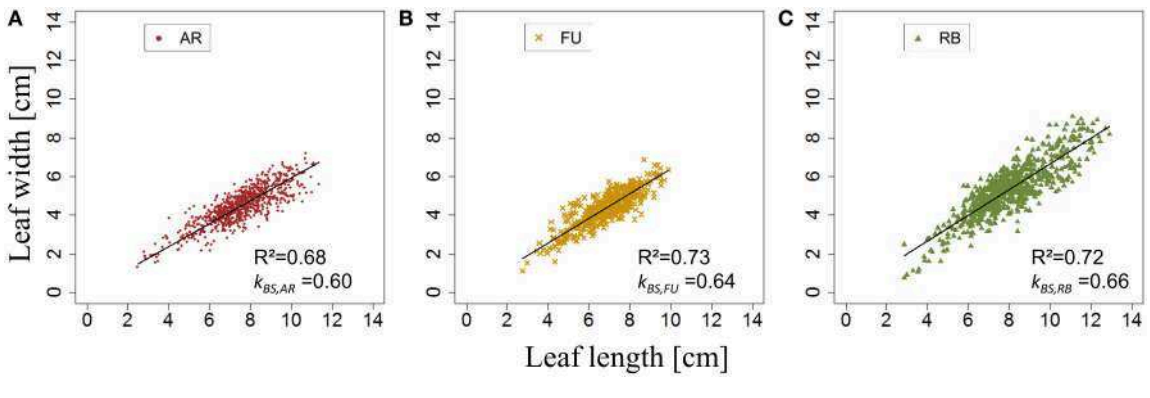

FIGURE 8 | Parameterization of $k_{BS,G}$ (N = 763, 465, and 655 bourse shoot leaves, respectively; A–C).

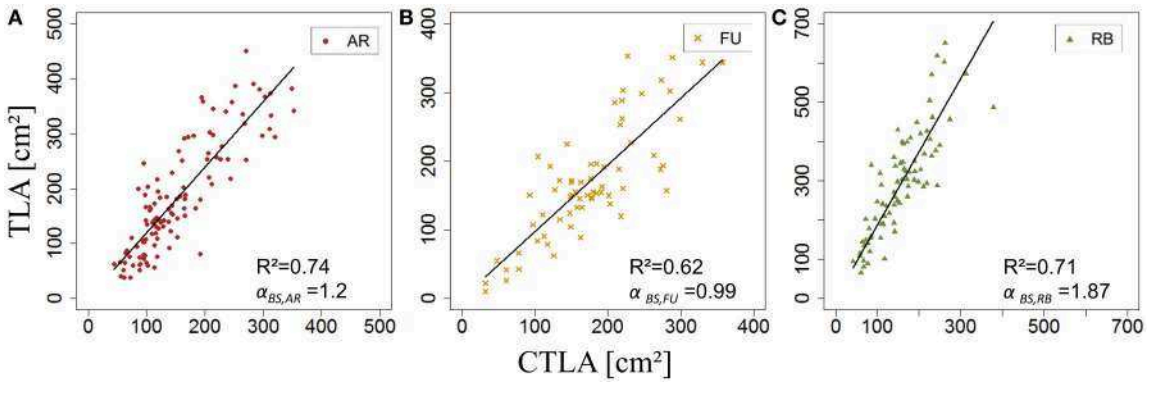

FIGURE 9 | Calibration of the bourse shoot leaf area model: parameterization of $\alpha_{BS,G}$ (N = 114, 66, and 80 bourse shoots, respectively; A–C).

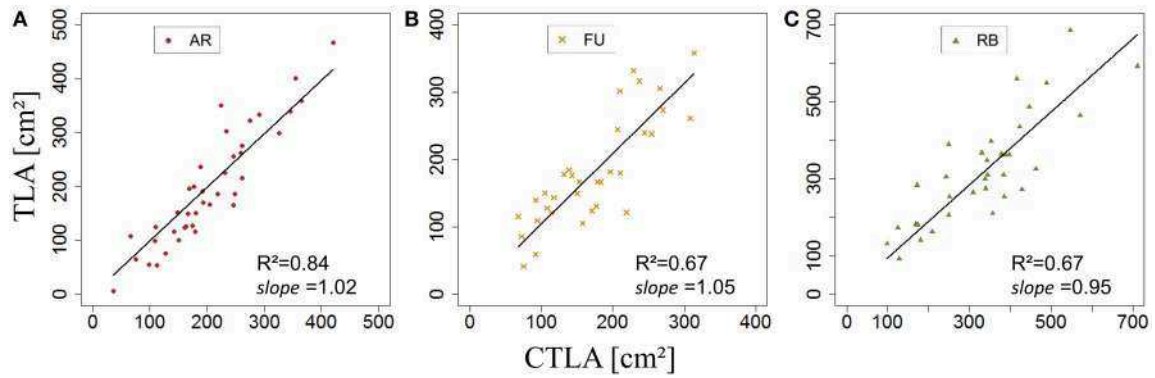

FIGURE 10 | Testing of the bourse shoot leaf area model (*N* = 40, 33, and 34, bourse shoots respectively; A–C).

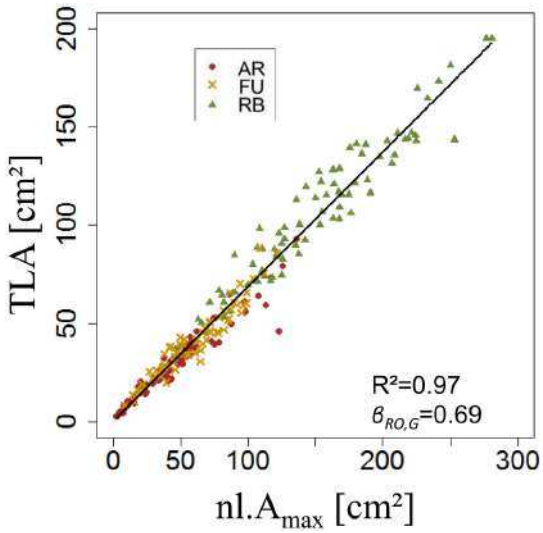

FIGURE 11 | Parameterization of $\beta_{RO,G}$ (*N* = 232 rosettes).

$k_{RO,G}$ was established for AR, FU, and RB using linear regression models on the training set of each genotype (**Figures 12A–C**) and the leaf lengths of each genotype were significantly correlated with leaf width ($P < 2.10^{-16}$ for all the genotypes' models) with $R^2 = 0.86$, 0.85 and 0.85 for AR, FU and RB, respectively. $k_{RO,G}$ values were fixed to 0.75, 0.74 and 0.71 for AR, FU and RB, respectively. Regression models of $TLA_{RO,G}$ as a function of $CTLA_{RO,G}$ conducted on the training data set showed a significant relationship ($P < 2.10^{-16}$) for the three genotypes with R^2 of 0.83, 0.88 and 0.91 for AR, FU and RB, respectively. However, the $CTLA_{RO,G}$ were bigger than the $TLA_{RO,G}$ as can be seen from the slopes. Therefore, their values were assigned to $\alpha_{RO,G}$ (0.86, 0.92, 0.92, respectively) to calibrate the rosette model (**Figure 13**). After that, individual and total leaf areas for each rosette were established for the testing set. The linear regression model of measured individual leaf area as a function of calculated individual leaf area showed a significant relationship ($P < 2.10^{-16}$) for FU samples of 2015 ($R^2 = 0.52$). The slope of the regression model (ratio between measured and calculated leaf area) was equal to 0.92. Linear models simulating $TLA_{RO,G}$ as a function of $CTLA_{RO,G}$ were all significant ($P < 2.10^{-16}$). The predictive models (**Figure 14**) had high coefficients of determination (0.88, 0.85 and 0.70 for AR, FU and RB, respectively) and the slopes were equal to 1 for the three genotypes (1.06, 1 and 1, respectively).

Modeling the Leaf Area of Vegetative Shoots (VS)

Neither ANOVA nor Kruskall-Wallis tests showed any significant difference in $e_{VS,G}$ between AR and FU ($P = 0.54$ and 0.49, for each test, respectively). Thus, $k_{VS,G}$ was fixed ($k_{VS,G} = 0.56$) using a linear regression model using data of both genotypes. The regression model showed a significant relationship between leaf length and width ($P <$ 2.10-16) and R^2 was equal to 0.79. Besides, neither ANOVA nor Kruskal-Wallis test showed any significant difference in the variable p between genotypes AR and FU. The linear model used to fix $p_{VS,G}$ ($p_{VS,G} = 0.95$) was significant ($P < 2.10^{-16}$) with $R^2 = 0.83$.

Modeling Internode Lengths of Spurs

Parameterization of the internode model fixed the value of *qi* to 0.62 and that of *si* to 0.12 (**Figure 15**). Both the coefficient of determination and the RMSE indicated a very good fit of the model to the distribution of measured data ($R^2 = 0.96$; RMSE = 0.08). Indeed, the model exhibited a common pattern involving bourse and bourse shoot internodes. Moreover, the model showed that rosette internodes correspond to the first part of the logistic equation (exponential phase), while bourse shoot internodes belong to the second part (linear phase).

DISCUSSION

Several studies show the determinism of plant architecture traits (Lauri and Trottier, 2004; Kahlen and Stützel, 2007; Massonnet et al., 2008). In this study we assumed that the distribution of normalized individual leaf area as a function of normalized rank is described by a similar pattern regardless of shoot size and, therefore, that the total leaf area of a shoot is proportional to the product of the leaf number times the area of the biggest leaf. Spann and Heerema (2010) also showed relationships between shoot leaf area and the product of the number of leaves and

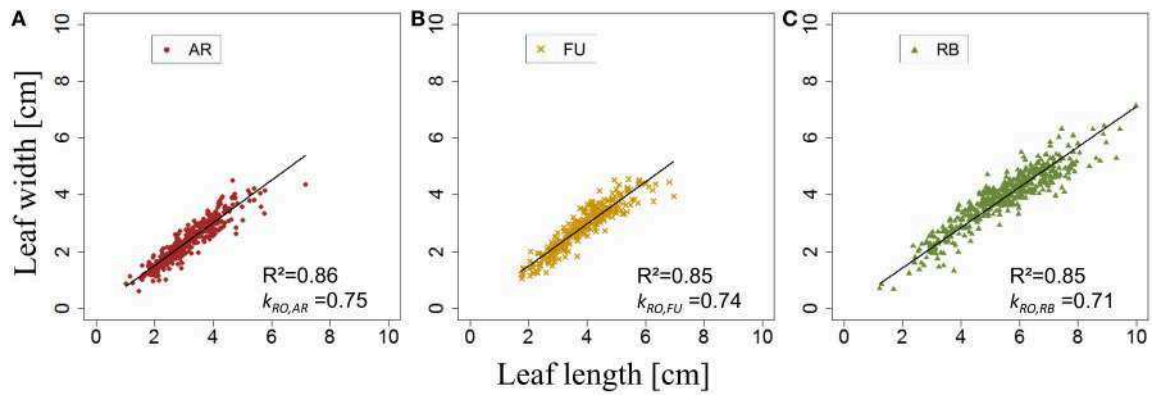

FIGURE 12 | Parameterization of $k_{RO,G}$ (N = 375, 303, and 475 rosette leaves, respectively; A–C).

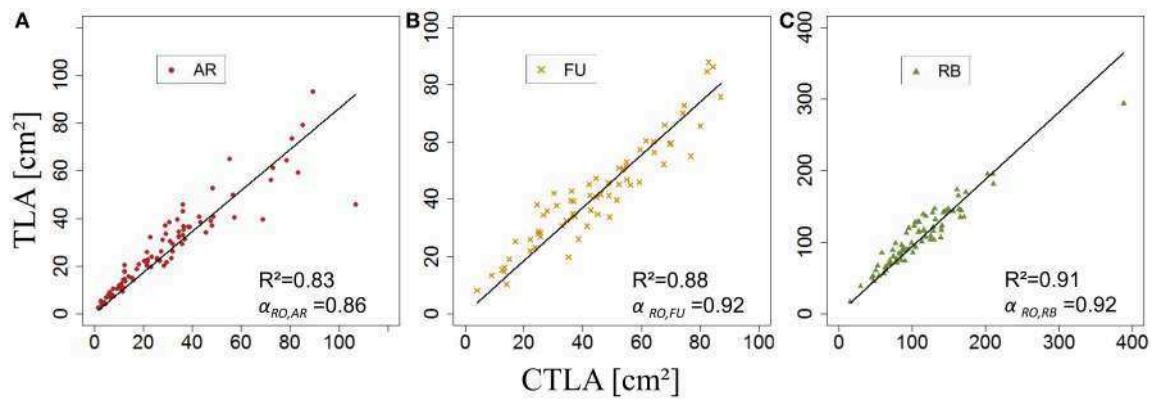

FIGURE 13 | Calibration of the rosette leaf area model: parameterization of $\alpha_{RO,G}$ (N = 87, 67, and 78 rosettes, respectively; A–C).

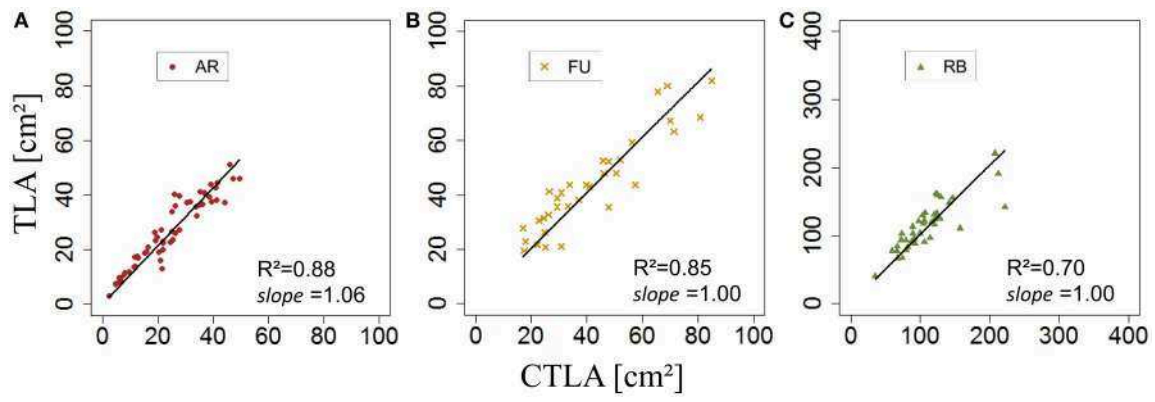

FIGURE 14 | Testing of the rosette leaf area model (N = 57, 33, and 40 rosettes, respectively; A–C).

length of longest leaf, for different species. However, the models presented here were conceived with the aim to link parameters that have the same unit (i.e., cm^2), both being expressions of surface. This is also the reason why in our final model, which only takes into account leaf lengths and numbers, leaf length is expressed as the square of itself. What is more, the linear model linking measured shoot total leaf area (TLA) with the product of leaf number (nl) and area of the biggest leaf (A_{max}), exhibits a larger coefficient of determination than the regression between TLA and the product of nl and the length of the longest leaf (L_{max}) (data not shown). Although the predictive capacity of our models with respect to individual leaf area was not optimal, the model was nevertheless based on a very good prediction of the total shoot leaf area. Indeed, in the case of the rosette and the bourse

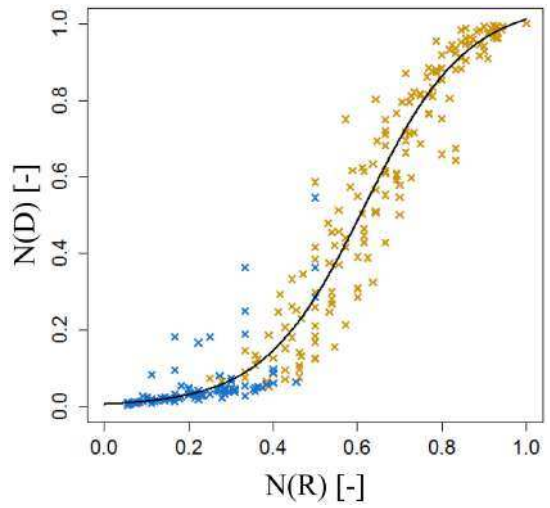

FIGURE 15 | Parameterization of the cumulative shoot length model on FU spurs. $N(R_l)$, normalized rank; $N(D_l)$, normalized cumulative shoot length from the base of the bourse [$N = 24$, continuum: bourse (x) – bourse shoot (x)].

shoot, we have chosen to construct our model as a function of the parameter β which is described by the slope of *TLA* versus $nl.A_{max}$, and not by parameterizing a Lorentz function, on the distribution of the point cloud which describes the normalized individual leaf surface as a function of the normalized rank. This choice was made on the one hand because of the absence of a particular pattern and therefore, the scatter of data points was considered to be too big; on the other hand, because of the proven robustness of β which we wanted to conserve for the development of the model. Besides, it is not unlikely that the fact that we had to use a calibration parameter (α) for each genotype and each shoot type (rosette and bourse shoot) is due to the way the point cloud deviates from the chosen Lorentz equation according to the genotype. Furthermore, even if the prediction of individual leaf area is not ideal, it is still faithful to an existing pattern of distribution of individual leaf area as a function of rank. Similar patterns were described for wheat (Pararajasingham and Hunt, 1996; Bos and Neuteboom, 1998; Hotsonyame and Hunt, 1998) and for rice (Tivet et al., 2001; Zhu et al., 2009). As an alternative to the Lorentz equation, we tested a bilinear equation with five parameters. However, apart from the higher number of parameters compared to Lorentz, this equation also yielded a higher RMSE.

Furthermore, the models developed were thought to go beyond predicting only shoot total leaf area. Indeed, the prediction of individual leaf area is more relevant if we aim to use this in an FSPM because in this approach parameterization takes place at the organ scale. Moreover, unlike the rosette which can be considered a compact functional unit in terms of leaf area, the bourse shoot usually exhibits a more open structure conveying more importance to the individual leaf with respect to light interception or exposure to liquids or dusts (in the case of chemical treatments: Dekeyser et al., 2013; Duga et al., 2015). However, even in a rosette, individual leaf area and its distribution along the shoot will determine the mutual shading of leaves and, therefore, light interception. Furthermore, in an FSPM, the position, shape and orientation of each organ are required as an input. The model proposed in this study is an attempt to optimize and simplify the reconstruction of branch architecture which is needed as an input for many FSPMs. As pointed out by Fisher (1984), the leaf surface of the crown is determined by phyllotaxis of the shoot, leaf orientation, clustering of new leaves on short shoots, internode lengths, and distribution of leaves along a branch (Fisher, 1984). Therefore, besides predicting leaf area (and its distribution along the shoot) our model also integrated internode lengths distribution and phyllotactic leaf angles (data not shown).

The data set used for the establishment of the leaf length model for bourse shoots was based on leaves sampled from shoots from a wide range of dates. This was justified as we determined the time (in GDD) from which onwards shoot leaf areas did no longer differ significantly from final leaf areas in the three different genotypes. This time roughly coincides with the date found by Da Silva et al. (2014), who indicated the 30th of June of each year as the end of annual primary shoot extension for most shoot types.

We found that the shape of rosette leaves, independent of genotype, was always more circular than that of bourse shoots which is not surprising as rosette leaves are preformed (Lauri, 2007). In this study, AR exhibited extreme values for the parameter that describes leaf shape (k), with bourse shoot leaves being much more elongated ($k_{BS,AR} = 0.60$) than rosette leaves ($k_{RO,AR} = 0.75$). This was in sharp contrast to RB where bourse shoot leaves ($k_{BS,RB} = 0.66$) and rosette leaves ($k_{RO,RB} = 0.71$) were much more similar in shape. FU was intermediary between AR and RB. An interesting observation made in this study was that the descriptive model of internode lengths could be optimized if we considered the bourse rosette and the bourse shoot as one single continuous morphogenetic unit. The bourse shoot being a sylleptic extension of the bourse, it in fact represents the continuation of the rosette. We can thus state that the base of the rosette up to the insertion point of the bourse shoot, plus the bourse shoot itself, is forming a unit that is characterized by a basal zone with short internodes, followed by a median zone with longer internodes (base of the bourse shoot), and a subapical zone with short internodes (Buck-Sorlin and Bell, 2000). This tentative conclusion gives rise to the idea that leaf length prediction could be further improved by considering leaf length distribution of the continuum of rosette plus bourse shoot instead of treating the two shoots separately. It would furthermore be interesting to see if there are allometric relations between the length of an internode and the area of the leaf that is inserted on it, given the fact that both have been produced by the vegetative meristem during the same developmental event. According to Da Silva et al. (2014) it is unlikely that leaf area changes independently from internode length, as metamers exhibit a strong allometry (Fisher, 1986).

In the present study we chose to split our data into training and testing sets: the first one was used to calibrate our model while the latter was employed to test it. Admittedly, some aspects of this procedure are arguable: first of all, it could be claimed that the splitting (two thirds training to one third testing) was arbitrary. However, enough data was available to have sufficiently large training and testing sets and more data was needed for calibration than for testing. Secondly, we confounded the FU data

sets of the two experimental years (2014 and 2015)—whereas for AR and RB only data of 2014 was available—and randomly distributed the data into the two sets, instead of using 1 year's data set for calibration and the other one for testing. However, the data sets revealed no significant inter-annual variation, except for the shape of rosettes in FU. As the 2015 data set was smaller than the one from 2014 and contained data only for FU, future testing with independent data sets has to be conducted to further prove the robustness of our models. Thirdly, as an alternative we could have neglected model testing and just have included a description of the variance (as was in fact done for the leaf area of vegetative shoots in this study). However, this would have meant neglecting the clearly robust and stable patterns that emerged among some of the meristic (leaf number) and continuous (length of the biggest leaf, total and individual leaf area) traits. In this study, the use of a test data set was necessary to check the fit of the final model. Indeed, the final model cumulates all the errors of the intermediate steps of parameterization and calibration, and the testing allowed us to quantify this cumulated error.

An accurate prediction of total shoot leaf area for each shoot type, and of the distribution of single leaf area as a function of leaf rank, in connection with individual internode length, are the first steps toward the faithful reconstruction of architecture, to be used in an FSPM to compute light interception or even to estimate the percentage of hidden surfaces in simulations of the efficiency of pesticide spray applications (Dekeyser et al., 2013; Duga et al., 2015). With respect to light interception, leaf area and internode length are in fact the two most important traits contributing to plant architecture whereas branching angle seems to have only little impact on this functional trait (Han et al., 2012; Da Silva et al., 2014). It also appears that in order to explain leaf distribution within the tree the shoot scale is the most appropriate one (Da Silva et al., 2014). This justifies the choice we have made in this study, namely to concentrate on the modeling of leaf area distribution along different shoot types and to neglect divergence angles. As the spatial distribution of leaves in apple trees is not random (Da Silva et al., 2014) but rather characterized by a certain clumpiness (also reported for other tree species by Cohen et al., 1995; Chen et al., 1997; Da Silva et al., 2008), the next step in the reconstruction of branch architecture has to be to position and orient the different shoot types. In doing so, it has to be considered that the proportion of long and short shoots differs among genotypes (Lauri et al., 1995). The genotypes used in this study exhibited such a numerical variability at the scale of the first-order branch, with bourse shoots in AR being much more important than in RB (data not shown). The analysis of the distribution of shoots within the branch will be the subject of a follow-up study (Bairam et al., unpubl.). In any case, it is thus necessary to count the number of shoots of the different types or better still, create a topological map of the branch and its different organs (see Buck-Sorlin and Bell, 2000, for an example) in order to finalize the reconstruction of branch architecture.

CONCLUSIONS AND PERSPECTIVES

In the present study, we provided a new model allowing the reconstruction of the initial branch architecture as an input for a Functional Structural Plant Model of apple, with an emphasis on the prediction of leaf area at the shoot and leaf scale, using allometric relations among shoot architecture variables. The model was calibrated and tested using sufficiently large training and testing data sets, proving that it is robust enough for the prediction of leaf area of the three apple cultivars used in this study, which exhibit a contrasting leaf and shoot morphology. Combined with light response curves measured in 2015 (Bairam et al., unpubl.), the initial architecture thus modeled will help to create a mapping of photosynthetic potential for each leaf. Furthermore, the combination of this information with the developmental kinetics of each fruit on such a branch (Bairam et al., unpubl.) will then allow finding coefficients for daily sugar transport rates from source leaves to fruits.

This study has shown that the distribution of leaves along a shoot of the same type follows certain clear endogenous regularities that seem to be genotype dependent (cf. Lauri, 2007), with rather little phenotypic plasticity. Further experimental and modeling studies will be conducted to try to decipher and quantify the physiological mechanisms behind these regularities, in order to improve the modeling of apple fruit quality in the context of the first-order branch as an experimental system.

AUTHOR CONTRIBUTIONS

EB, MD, and GBS conceived and designed the work; EB, MD, and CLM collected the experimental data; EB developed the mathematical models, and did the programming in R; EB and GBS analyzed and interpreted the data; EB and GBS wrote the paper; MD revised it critically; all authors approved the final version.

FUNDING

The doctoral thesis of EB was funded by a strategic bourse of the Région Pays de la Loire, France, convention no. 2011-12596. All financial help is duly acknowledged.

ACKNOWLEDGMENTS

Sylvain Hanteville and Julienne Fanwoua helped with measurements in the field and the laboratory, and Gilles Hunault gave valuable statistical advice. Michael Henke developed the initial ImageJ script for the automatic measurement of leaf surfaces from scanned images. Antoine Roche helped with scanning leaves and saving images for leaf area analysis. Julienne Fanwoua helped to improve the readability of the manuscript. The staff of the experimental unit at Beaucouzé provided day-to-day maintenance of the orchard. All help is gratefully acknowledged.

SUPPLEMENTARY MATERIAL

The leaf data can be accessed here: https://zenodo.org/record/215977. The R scripts used can be found here: https://github.com/EmnaBairam/Apple_leaf_surface

REFERENCES

Anderson, J. L., and Richardson, E. A. (1982). "Utilizing meteorological data for modeling crop and weed growth," in *Biometeorology in integrated pest management,* eds J. L. Hatfield and I. J. Thomason (New York, NY: Academic), 449–461.

Barthélémy, D. (1991). Levels of organization and repetition phenomena in seed plants. *Acta Biotheor.* 39, 309–323. doi: 10.1007/BF00114184

Björkman, O., and Demmig-Adams, B. (1995). "Regulation of photosynthetic light energy capture, conversion, and dissipation in leaves of higher plants," in *Ecophysiology of Photosynthesis* (Berlin Heidelberg, NY: Springer), 17–47.

Bos, H. J., and Neuteboom, J. H. (1998). Growth of individual leaves of spring wheat (*Triticum aestivum* L.) as influenced by temperature and light intensity. *Ann. Bot.* 81, 141–149. doi: 10.1006/anbo.1997.0532

Buck-Sorlin, G. H. (2002). "L-system model of the vegetative growth of winter barley," in Fifth *German Workshop on Artificial Life*, eds D. Polani, J. Kim, and T. Martinetz (Lübeck: Akademische Verlagsgesellschaft Aka GmbH), 53–64.

Buck-Sorlin, G. H. (2013). "Functional-structural plant modeling," in *Encyclopedia of Systems Biology,* eds W. Dubitzky, O. Wolkenhauer, K. Cho, and H. Yokota (New York, NY: Springer), 778–781. doi: 10.1007/978-1-4419-9863-7

Buck-Sorlin, G. H., and Bell, A. D. (2000). Models of crown architecture in quercus petraea and q.robur: shoot lengths and bud numbers. *Forestry* 73, 1–19. doi: 10.1093/forestry/73.1.1

Casella, E., and Sinoquet, H. (2003). A method for describing the canopy architecture of coppice poplar with allometric relationships. *Tree Physiol.* 23, 1153–1170. doi: 10.1093/treephys/23.17.1153

Chen, K., Hu, G. Q., and Lenz, F. (1997). Training and shading effects on vegetative and reproductive growth and fruit quality of apple. *Gartenbauwiss* 5, 207–213.

Cohen, S., Mosoni, P., and Meron, M. (1995). Canopy clumpiness and radiation penetration in a young hedgerow apple orchard. *Agric. For. Meteorol.* 76, 185–200. doi: 10.1016/0168-1923(95)02226-N

Costes, E., Crespel, L., Denoyes, B., Morel, P., Demene, M. N., Lauri, P. E., et al. (2014). Bud structure, position and fate generate various branching patterns along shoots of closely related Rosaceae species: a review. *Front. Plant Sci.* 5:666. doi: 10.3389/fpls.2014.00666

Da Silva, D., Boudon, F., Godin, C., and Sinoquet, H. (2008). Multiscale framework for modeling and analyzing light interception by trees. *Multiscale Model. Sim.* 7, 910–933. doi: 10.1137/08071394X

Da Silva, D., Han, L., Faivre, R., and Costes, E. (2014). Influence of the variation of geometrical and topological traits on light interception efficiency of apple trees: sensitivity analysis and metamodelling for ideotype definition. *Ann. Bot.* 114, 739–752. doi: 10.1093/aob/mcu034

Dekeyser, D., Duga, A. T., Verboven, P., Hendrickx, N., and Nuyttens, D. (2013). Assessment of orchard sprayers using laboratory experiments and CFD modelling. *Biosyst. Eng.* 114, 157–169. doi: 10.1016/j.biosystemseng.2012.11.013

Duga, A. T., Ruysen, K., Dekeyser, D., Nuyttens, D., Bylemans, D., Nicolai, B. M., et al. (2015). Spray deposition profiles in pome fruit trees: effects of sprayer design, training system and tree canopy characteristics. *Crop Protec.* 67, 200–213. doi: 10.1016/j.cropro.2014.10.016

Evers, J. B., Vos, J., Fournier, C., Andrieu, B., Chelle, M., and Struik, P. C. (2005). Towards a generic architectural model of tillering in Gramineae, as exemplified by spring wheat (*Triticum aestivum*). *New Phytol.* 166, 801–812. doi: 10.1111/j.1469-8137.2005.01337.x

Evers, J. B., Vos, J., Fournier, C., Andrieu, B., Chelle, M., and Struik, P. C. (2007). An architectural model of spring wheat: evaluation of the effects of population density and shading on model parameterization and performance. *Ecol. Model.* 200, 308–320. doi: 10.1016/j.ecolmodel.2006.07.042

Falster, D. S., and Westoby, M. (2003). Leaf size and angle vary widely across species: what consequences for light interception? *New Phytol.* 158, 509–525. doi: 10.1046/j.1469-8137.2003.00765.x

Fanwoua, J., Bairam, E., Delaire, M., and Buck-Sorlin, G. (2014). The role of branch architecture in assimilate production and partitioning: the example of apple (*Malus domestica*). *Front. Plant Sci.* 5:338. doi: 10.3389/fpls.2014.00338

Fisher, J. B. (1984). "Tree architecture: relationships between structure and function," in *Contemporary Problems in Plant Anatomy,* eds R. A. White, and W. C. Dickson (New York, NY: Academic Press), 541–589.

Fisher, J. B. (1986). "Branching patterns and angles in trees," in *The Economy of Plant Form and Function*, ed T. J. Givnish (Cambridge: Cambridge University Press), 493–523.

Freeman, Freeman, G. M., and Bolas, B. D. (1956). A method for the rapid determination of leaf area in the field. *Rep. East Malling Res. Stn.* 1955, 104–107.

Gu, S., Evers, J. B., Zhang, L., Mao, L., Zhang, S., Zhao, X., et al. (2014). Modelling the structural response of cotton plants to mepiquat chloride and population density. *Ann. Bot.* 114, 877–887. doi: 10.1093/aob/mct309

Han, L., Costes, E., Boudon, F., Cokelaer, T., Pradal, C., Da Silva, D., et al. (2012). "Investigating the influence of geometrical traits on light interception efficiency of apple trees: a modelling study with MAppleT," in *2012 IEEE Fourth International Symposium on Plant Growth Modeling, Simulation, Visualization and Applications (PMA),* eds M. Z. Kang, Y. Dumont, and Y. Guo (Shanghai: IEEE Press), 152–159.

Hemmerling, R., Kniemeyer, O., Lanwert, D., Kurth, W., and Buck-Sorlin, G. (2008). The rule-based language XL and the modelling environment GroIMP illustrated with simulated tree competition. *Funct. Plant Biol.* 35, 739–750. doi: 10.1071/FP08052

Hotsonyame, G. K., and Hunt, L. A. (1998). Effects of sowing date, photoperiod and nitrogen on variation in main culm leaf dimensions in field-grown wheat. *Can. J. Plant Sci.* 78, 35–49. doi: 10.4141/P97-027

Kahlen, K., and Stützel, H. (2007). Estimation of geometric attributes and masses of individual cucumber organs using three-dimensional digitizing and allometric relationships. *J. Am. Soc. Hortic. Sci.* 132, 439–446.

Lauri, P. E. (2007). Differentiation and growth traits associated with acrotony in the apple tree (*Malus domestica*, Rosaceae). *Am. J. Bot.* 94, 1273–1281. doi: 10.3732/ajb.94.8.1273

Lauri, P. E., Térouanne, E., Lespinasse, J. M., Regnard, J. L., and Kelner, J. J. (1995). Genotypic differences in the axillary bud growth and fruiting pattern of apple fruiting branches over several years—an approach to regulation of fruit bearing. *Sci. Hortic.* 64, 265–281. doi: 10.1016/0304-4238(95)00836-5

Lauri, P. É., and Trottier, C. (2004). Patterns of size and fate relationships of contiguous organs in the apple (*Malus domestica*) crown. *New Phytol.* 163, 533–546. doi: 10.1111/j.1469-8137.2004.01136.x

Lindenmayer, A. (1968a). Mathematical models for cellular interactions in development. I. Filaments with one-sided inputs. *J. Theor. Biol.* 18, 280–299. doi: 10.1016/0022-5193(68)90079-9

Lindenmayer, A. (1968b). Mathematical models for cellular interactions in development II. *Simple and branching filaments with two-sided inputs. J. Theor. Biol.* 18, 300–315. doi: 10.1016/0022-5193(68)90080-5

Massonnet, C., Regnard, J. L., Lauri, P. E., Costes, E., and Sinoquet, H. (2008). Contributions of foliage distribution and leaf functions to light interception, transpiration and photosynthetic capacities in two apple cultivars at branch and tree scales. *Tree Physiol.* 28, 665–678. doi: 10.1093/treephys/28.5.665

Montgomery, D. C., Peck, E. A., and Vining, G. G. (2015). *Introduction to Linear Regression Analysis*. New Jersey, NJ: J. Wiley and Sons.

Pararajasingham, S., and Hunt, L. A. (1996). Effects of photoperiod on leaf appearance rate and leaf dimensions in winter and spring wheats. *Can. J. Plant Sci.* 76, 43–50. doi: 10.4141/cjps96-008

Prusinkiewicz, P. (1998). Modeling of spatial structure and development of plants: a review. *Sci. Hortic.* 74, 113–149.

Snee, R. D. (1977). Validation of regression models: methods and examples. *Technometrics* 19, 415–428. doi: 10.1016/S0304-4238(98)00084-3

Spann, T. M., and Heerema, R. J. (2010). A simple method for non-destructive estimation of total shoot leaf area in tree fruit crops. *Sci. Hortic.* 125, 528–533. doi: 10.1016/j.scienta.2010.04.033

Štampar, F., Hudina, M., Usenik, V., Šturm, K., Marn, V., and Batič, F. (1999). Influence of leaf area on net photosynthesis, yield and flower-bud formation in apple (*Malus domestica* Borkh.). *PlantPhysiol.* 39, 101–106.

Sussex, I. M., and Kerk, N. M. (2001). The evolution of plant architecture. *Curr. Opin. Plant Biol.* 4, 33–37. doi: 10.1016/S1369-5266(00)00132-1

Tivet, F., Pinheiro, B. D. S., Raïssac, M. D., and Dingkuhn, M. (2001). Leaf blade dimensions of rice (*Oryza sativa* L. and *Oryza glaberrima* Steud.). Relationships between tillers and the main stem. *Ann. Bot.* 88, 507–511. doi: 10.1006/anbo.2001.1447

Tsukaya, H. (2004). Leaf shape: genetic controls and environmental factors. *Int. J. Dev. Biol.* 49, 547–555. doi: 10.1387/ijdb.041921ht

Vos, J., Evers, J. B., Buck-Sorlin, G. H., Andrieu, B., Chelle, M., and de Visser, P. H. B. (2010). Functional-structural plant modelling: a new versatile tool in crop science. *J. Exp. Bot.* 61, 2102–2115. doi: 10.1093/jxb/erp345

Zhu, Y., Chang, L., Tang, L., Jiang, H., Zhang, W., and Cao, W. (2009). Modelling leaf shape dynamics in rice. *NJAS* 57, 73–81. doi: 10.1016/j.njas.2009.11.001

Conflict of Interest Statement: The authors declare that the research was conducted in the absence of any commercial or financial relationships that could be construed as a potential conflict of interest.

Chapitre 3

Fruit and Leaf Response to Different Source-Sink Ratios in Apple, At the Scale of the Fruit-Bearing Branch

Ce chapitre a été rédigé en Anglais afin d'être envoyé à une revue internationale à comité de lecture

Abstract Dans la continuité du chapitre 1 qui visait à mieux comprendre les relations sources-puits à l'échelle du spur, ce chapitre aborde l'analyse de ces relations mais à un niveau d'échelle plus important, celui de la branche fruitière. L'étude a été réalisée chez 2 cultivars de pommier : 'Fuji' et 'Ariane' grâce à une série d'expérimentations visant à étudier l'effet de différents ratios sources/puits (suppression de pousses et/ou de fruits à l'échelle de la branche) sur la croissance des fruits et l'activité photosynthétique des feuilles. Pour mieux contrôler les sources et les puits et éviter qu'il n'y ait un apport de carbone du reste de l'arbre, les différentes branches utilisées ont été isolées des arbres porteurs grâce une incision annulaire (« girdling ») et les expérimentations ont débuté une fois que l'ensemble des pousses aient achevé leurs développements afin d'éviter les compétitions entre les jeunes pousses et les fruits pour le carbone. La cinétique de croissance des fruits a été suivie au cours de leur développement ainsi que, de manière ponctuelle, la réponse à la lumière de l'activité photosynthétique nette de feuilles de trois types différents de pousses. Ce dispositif expérimental nous a permis de quantifier un certain nombre de processus tels que la surface foliaire nécessaire pour permettre la croissance du fruit. Il a également permis de mettre en évidence de manière indirecte que la diminution de la surface foliaire (suite à une défoliation) pouvait être compensée par une régulation du taux d'assimilation du carbone. Par ailleurs, nous avons utilisé un modèle structuro-fonctionnel (Functional-Structural Plant Model, FSPM) statique de la charpentière afin de montrer, sur l'exemple d'une seule branche, l'avantage de conduire des simulations de l'interception de lumière à une très fine résolution temporaire et spatiale. Le FSPM utilisé simule la production de carbone à l'échelle de chaque feuille grâce à l'interception lumineuse (en fonction du microclimat) et la photosynthèse. Les sorties du modèle ont été très pertinentes pour la structure simplifiée (branche expérimentale) utilisée dans cette simulation. En effet, la prédiction de la production de carbone produit au niveau des feuilles de la charpentière correspond avec beaucoup de justesse aux besoins calculés des fruits.

Fruit and Leaf response to different source-sink ratios in apple, at the scale of the fruit-bearing branch

Emna Baïram[1], Julienne Fanwoua[1,2], Michael Henke[3], Magalie Poirier-Pocovi[1], Christian leMorvan[1], Mickaël Delaire[1], and Gerhard Buck-Sorlin[1]

[1]UMR 1345 Institut de Recherche en Horticulture et Semences (IRHS), Agrocampus Ouest, Angers, France

[2]UR 1115 Plantes et Systèmes de Culture Horticoles, Institut National de la Recherche Agronomique, Avignon, France

[2]Department Ecoinformatics, Biometrics and Forest Growth, University of Göttingen, Germany

Keywords: Malus x domestica Borkh., apple, branch, carbon transport, photosynthesis, defoliation, FSPM, fruit growth.

Abstract

In the present study, we designed an experimental system in which parts of fruit-bearing branches of two apple cultivars (‘Fuji’ and ‘Ariane’) were isolated from the rest of the tree by girdling and then subjected to specific pruning and fruit removal treatments in order to create a wide range of global (branch-level) source-sink ratios. We monitored fruit kinetics but also the light response to photosynthesis of leaves of the three different shoot types. This experimental setup allowed us to investigate and quantify a number of processes, such as the leaf area necessary for potential (sink-driven) growth, or else the minimal leaf area sustainable for fruit growth. It also gave some indirect evidence to what extent defoliation is compensated by an upregulation of the carbon net assimilation rate. We furthermore used a simplified static Functional-Structural Plant Model (FSPM) of the fruit-bearing branch to demonstrate, at the example of a single branch, the advantage of conducting light interception simulations at a very fine temporal and spatial solution. Model results showed that for a small and simplified structure like our experimental branches, predictions of source capacity based on simulations of light simulations were very accurate and matched the computed demands of the sinks.

1. Introduction

One of the most important parameters for fruit quality is its size at harvest. From the sites of its production or remobilisation (source organs such as leaves or reserve tissues), carbon is transported to the sink organs (more specifically the fruits) where it accumulates and is involved in the growth process. A qualitative appreciation and ultimately, quantification of carbon transport and distribution in the frame of variable source-sink relations during fruit development, should help to better understand or even predict fruit size and even quality at harvest. Carbon transport within the fruit tree is thus a complex process the study of which is requiring a consideration of both structural components linked to tree architecture, and functional ones linked to source-sink relations and assimilate production and transport. In apple, this complexity is exacerbated by the diversity of the vegetative shoot types (long, short, proleptic and sylleptic: Costes 2003), the age structure of the branch wood carrying the sink organs, and the composition of the fruit-bearing units. In any case, the appreciation of these phenomena constitutes a major problem to be resolved, ultimately in order to have a better grip on fruit growth and quality.

Dedicated ecophysiological experiments provide some evidence that the position of an apple on the fruit-bearing branch has repercussions on its growth and quality, e.g. fruit weight (Reyes et al., 2016), fruit colour (Robinson and Lakso, 1988), soluble solids content (Campbell and Marini, 1992) or general fruit quality traits (Wagenmakers and Callesen, 1988, 1995). Effectively, depending on its position, the fruit is surrounded by a specific microclimate (Chelle, 2005), but also exhibits a unique topological and geometrical distance to the nearest leaf (source) as well as to competing sinks that could be very decisive for fruit growth and quality. Fruit growth is determined by the availability of assimilates (source) and its ability to attract assimilates which in turn depends on its sink strength. It is well known that apple fruit sink strength is determined during early fruit development (i.e. cell division) and depends in part on sink competition at the spur level (Wünsche and Lakso, 2000; Goffinet et al., 1995, see also chapter 1 of this thesis). In later development (i.e. during cell expansion), fruit growth could depend on the ratio between sources and sinks (i.e. source availability for each sink) and distance between sources and sinks, as observed in several fruit species such as in peach (Bruchou and Génard, 1999). However, in apple, there is some evidence that distance between source and sink is not very decisive for carbon distribution (Hansen, 1969). Furthermore, under conditions of a high source-sink ratio, leaf photosynthetic activity in apple leaves could possibly be reduced due to lower carbon demand, which in turn could lead to a carbon budget comparable to one obtained under a moderate source-sink ratio (Palmer et al. 1997). This result points out the necessity

to take into account the real carbon production in apple, to determine the amount of carbon available for fruit growth and quality or at least to know the impact a given source/sink ratio has on photosynthetic activity in order to obtain an approximate idea of carbon availability. However, as stated before, microclimate must also be taken into account to improve the accuracy of prediction of photosynthesis, as each individual leaf, due to its position, size and orientation in space, might experience a different light regime and therefore, photosynthetic rate dynamics, during the day and during an entire season. The reconstruction of branch architecture plus microclimate necessitates a 3D modelling approach: Functional-Structural Plant Modelling (FSPM, Vos et al., 2010; Buck-Sorlin 2013) is a suitable modelling method that considers plant architecture in 3D, as well as basic physiological and biophysical processes (light interception, photosynthesis, growth, respiration…) at the organ scale. In such models certain predefined organs act as interfaces to the environment, the latter represented either by spatial data, simple descriptive models (e.g., vertical temperature gradients) or powerful simulators (e.g., Monte-Carlo light models: Hemmerling et al., 2008). The use of such models can be challenging with respect to the rather tedious data acquisition, which is a real bottleneck. Recently published work by Baïram et al. (2017) proved that accurately modelling leaf area could be a very valuable first step for the reconstruction of branch architecture and leaf area as input to a static FSPM.

Given this global context, the objectives of this work, which was conducted at the scale of the fruit-bearing branch were threefold: (1) to study the impact of source-sink distance on carbon partitioning in order to confirm or not the results obtained by Hansen (1969); (2) to investigate the impact of source/sink ratio on fruit growth and leaf photosynthetic activity and (3) to develop a first FSPM to simulate light interception and carbon production by a single isolated branch, in order to derive a carbon balance from it for comparison with measured fruit growth.

2. Materials and Methods

2.1. Plant material

The experiments were performed in 2015 on apple trees planted in 2008 in an experimental orchard at the INRA experimental unit in Beaucouzé, France. Two cultivars were selected for this experiment: ‘Fuji’ and ‘Ariane’ (in the following labelled as FU and AR, respectively). 'Ariane' is a modern cultivar that was developed by INRA Angers, by crossing a hybrid of 'Florina' x 'Prima' with pollen from 'Golden Delicious', and released in the year 2000, as a scab resistant variety. The ‘Fuji’ cultivar is a hybrid developed by growers at Tohoku Research Station in Fujisaki, Aomori, Japan, in the late 1930s, and has been commercialized since 1962. The origin of this cultivar is two American

apple varieties: ‘Red Delicious’ and ‘old Virginia Ralls Genet’. Trees of these two cultivars, plus four other varieties (‘Rome Beauty’, ‘Elstar’, ‘Florina’, and ‘Reine de Reinette’) make up the experimental orchard (with three rows of 96 trees each, or 72 blocks of four trees, arranged regularly). The main aim of these experiments was to study the effect of source/sink balance on sub-branches of apple trees. Therefore, 48 sub-branches of FU and 30 of AR were selected. However, one of the sub-branches of FU was accidentally lost during the experiment and therefore only 47 will be considered in this work. In this study, is defined as a sub-branch a part of a first-order branch comprising three annual extensions. Each sub-branch is composed of a single-order axis composed of one two-year-old shoot (Y2), one one-year-old shoot (Y1) and one current Y0 unit corresponding to a spur (composed of rosette leaves, a bourse, a bourse shoot and fruits) in terminal position and several ramifications in axillary position on Y2 and Y1 corresponding to spurs or vegetative shoots. One week before the onset of the experiment, all sub-branches were thinned to one fruit – the king fruit – per spur. Afterwards, several defoliation and/or fruit-thinning treatments were applied in order to test the impact of source/sink ratio on fruit growth and photosynthetic activity.

2.2. Experimental design

Considering that apple leaves are photoassimilate sinks at the beginning of their development as shown by Grappadelli et al. (1994), experiments were conducted once all the leaves were fully developed in order to be sure that leaves exclusively exerted the function of a source.Treatments were applied on June 22, 2015, after all vegetative or bourse shoots were completely developed. A girdling was applied at the base of Y2, and all fruits from Y0, all fruiting spurs born on Y1 and all vegetative or bourse shoots and non-fruiting spurs born on Y2 were removed. Therefore, the experimental design was such that all fruits (sinks) were located on Y2 and vegetative shoots and bourse shoots on Y1 and Y0. The girdling treatment was applied in order to have a closed system with respect to the carbon budget, which could subsequently be reconstructed in the model and for which we could compute the carbon balance, knowing that no carbon can be exported to the rest of the tree (see section 3.6).

Afterwards, four different leaf/fruit ratio treatments were applied on both FU and AR with between 6 and 9 replicates for each treatment (Figure 1). For each treatment, two spurs bearing one fruit on Y2 were kept, and leaf/fruit ratios were modulated by shoot pruning applied to Y1 and Y0 in order to have (i) high, (ii) medium, (iii) low and (iv) very low source availability: (i) no shoot pruning (treatment ‘2F_H’); (ii) removal of half of the bourse shoot on Y0 (treatment ‘2F_M’); (iii) removal

of half of the bourse shoot on Y0 and of all shoots on Y1 (treatment '2F_L'); (iv) removal of all shoots and non-fruiting spurs on Y1 and Y0 (treatment '2F_Z').

Two supplementary treatments were applied on FU in order to test extreme leaf/fruit ratios by (v) keeping only one fruit-bearing spur on Y2 while applying no shoot pruning (treatment '1F_H') and (vi) keeping three fruit-bearing spurs on Y2 while pruning half of the bourse shoot on Y0 and all shoots on Y1 (treatment '3F_L').

For all treatments, rosette leaves were kept on fruiting-spurs (on Y2) in order to limit fruit drop between the beginning of the experiment and harvest.

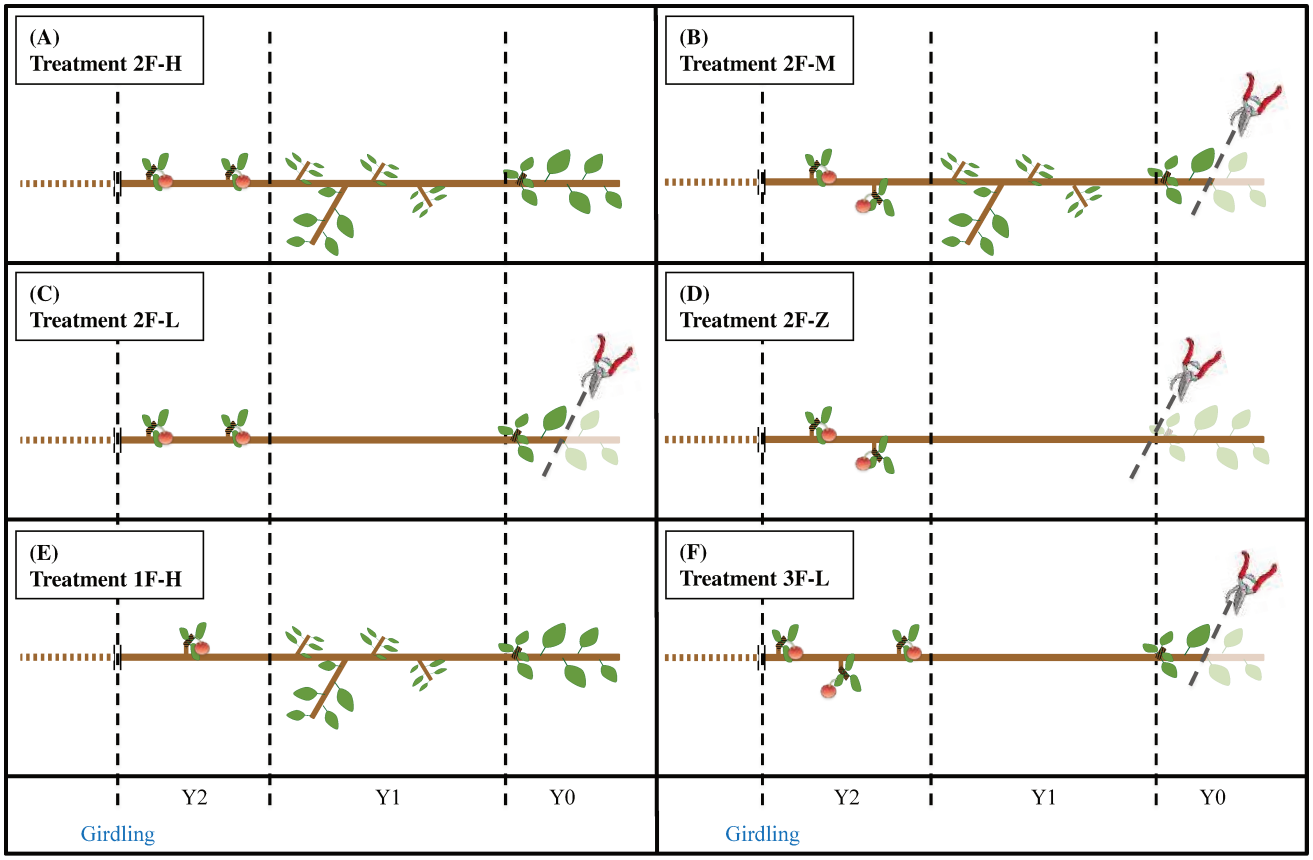

Figure 1. Schematic representation of the leaf/fruit-ratio treatments applied to 'Ariane' (A to D) and 'Fuji' (A to F): two one-fruit-bearing spurs without bourse shoot on Y2 with (A) 'high' ('2F_H'), (B) 'medium' ('2F_M'), (C) 'low' ('2F_L') and (D) 'very low' ('2F_Z') source availability; (E) one and (F) three one-fruit-bearing spurs without bourse shoot on Y2 with 'high' ('1F_H') and 'low' ('3F_L') source availability, respectively (see text for explanation). Number of replicates for each treatment was 9, 7, 8, 7, 9, 8 for treatments A to F in 'Fuji' and 8, 8, 8 and 6 for treatments A to D in 'Ariane'.

Experiments carried out at the sub-branch scale were completed by an experiment conducted at the spur scale using twenty intact one-fruit-bearing-spurs in terminal position (Y0) and isolated from the rest of the branch by girdling (treatment '1F-T'). This experiment, which was started on June 30,

2015, was designed to check if structures comprising a fruit with nearby sources on the same spur would behave differently from the structures considered above, and to compare the characteristics of terminal fruit to axillary fruits on the branch.

2.3. Developmental time

Developmental time was first measured using growing degree hours [GDH, with a base temperature T_b=7°C (Anderson and Richardson, 1982)] calculated using hourly air temperatures (°C) obtained from the weather station of Beaucouzé (47° 28' N, 0° 37' W, 50 m a.s.l.) and accessed from the INRA Climatik platform, https://intranet.inra.fr/climatik_v2 :

$$GDH_i = \sum_{h=1}^{24}(HT_h - T_b) \quad (1)$$

where HT_h is replaced by T_b if $HT_h < T_b$; HT_h is the hourly air temperature at hour h; and GDH_i are the growing degree hours on day i. In this study, the thermal time variable expressed in GDD was normalized to cumulated thermal time (GDD_{cum}) after full bloom (equation 2).

$$GDD_{cum} = \sum_{i=FB}^{D} \frac{GDH_i}{24} \quad (2)$$

where FB is the day of full bloom and D is the number of days since FB. Full bloom occurred on April 16th, 2015 in AR and on April 20th, 2015 in FU.

2.4. Characterization of the sources

2.4.1. Leaf area estimation

For each treatment, total leaf area (TLA) of vegetative shoots (VS), bourse shoots (BS) and rosettes (RO) was estimated using the models established by Baïram et al. (2017) (see chapter 2): these models consider the type of shoot (j=RO, BS, VS) and the genotype (G) and use two variables as input: the length of the biggest leaf (L_{max}) and the number of leaves (nl). Except for bourse shoots on Y0 which were half pruned (i.e. '2F-M', '2F-L', '3F-L' treatments), TLA was calculated using Equation 3 with parameters β and k depending on shoot type and genotype (Table 1). For non-fruiting spurs kept on Y1 and Y0, TLA was calculated as the sum of TLA obtained for RO and BS.

$$TLA = \beta_{j,G}.nl.\frac{\pi}{4}.k_{j,G}.L_{max}^2 \quad (3)$$

Table 1. β and k parameters used in computing total leaf area for each shoot based on shoot type and genotype.

		G			
		FU		AR	
		β	k	β	k
j	RO	0.69	0.74	0.69	0.75
	BS	0.67	0.64	0.67	0.6
	VS	0.48	0.56	0.48	0.56

Estimation of TLA of the bourse shoots half pruned in terminal position (i.e. Y0) was computed using Equation 4 where $\alpha_{BS,G}$ was equal to 0.99 and 1.20 in FU and AR, respectively, and values for parameter $s_{BS,G}$ were as described by Baïram et al., 2017 according to the number of leaves.

$$\int_{\frac{-2}{n}}^{\frac{\frac{nl}{2}-2}{nl}} \alpha_{BS,G} \frac{\frac{\pi}{4}.k_{BS,G}.\boldsymbol{L_{max}^2}}{1+\frac{(R-2)^2}{\boldsymbol{nl^2}.s_{BS,G}^2}}.dR \qquad (4)$$

Comparisons of estimated total leaf area among treatments were made for FU and AR, respectively, in order to establish if treatments actually were different among different types of pruning.

2.4.2. Measurement of instantaneous net photosynthesis rate

Between July 15 and July 31, 2015, CO_2 exchange measurements were made on: (i) three leaves per shoot of three bourse shoots subjected to treatments '1F_H' (noted 'BS_1F_H'), (ii) two or three leaves per shoot of three bourse shoots subjected to treatments '3F_L' (noted 'BS_3F_L'), (iii) two or three leaves per shoot of two bourse shoots for terminal spurs with basal girdling (noted 'BS_T_WG'), (iv) three or four leaves per shoot of two bourse shoots for terminal spurs without basal girdling (noted 'BS_T_NG'), (v) one rosette leaf of a fruit-bearing spur for treatment '2F_Z' (noted'RO_2F_Z'), (vi) one or three rosette leaves of three terminal spurs with basal girdling (noted 'RO_T_WG'), (vii) three rosette leaves of two terminal spurs without basal girdling (noted 'RO_T_NG') and (viii) one leaf per shoot of nine vegetative shoots for treatments '1F_H' (noted 'VS_1F_H'), yielding a total of 51 light-response curves. Net CO_2 assimilation rate was measured as a response to a range of 11 to 13 levels of irradiance from 0 to 2000 $\mu mol.m^{-2}.s^{-}1$ of photosynthetically active radiation (PAR) using a portable LI-6400XT infrared gas analyzer photosynthesis system (Li-Cor, Lincoln, NE, USA) using a standard chamber that allowed the clamping of a 9 cm² leaf surface. Measurements were made only on FU, between 8 a.m. and 12 a.m. During measurements, leaf temperature was kept constant at 20°C. Measurement data were logged

continuously using the monitoring software of the device. Photosynthetic light response curves were then parameterized for each leaf using the model described in section 2.5.1.

2.5. Characterization of sinks

At the beginning of the experiments and until harvest, all fruit diameters were surveyed once every one to two weeks (Figure 2). At harvest, all fruits were collected together with their bearing bourse and both organ diameters, heights, volumes, fresh and dry weights measured. Fruit circumferences were also measured. All harvested fruits were cut, and then dried during 6 days at 60°C in a ventilated oven (type HORO 900 V/RS, Dr. Hofmann GmbH, Stuttgart, Germany).

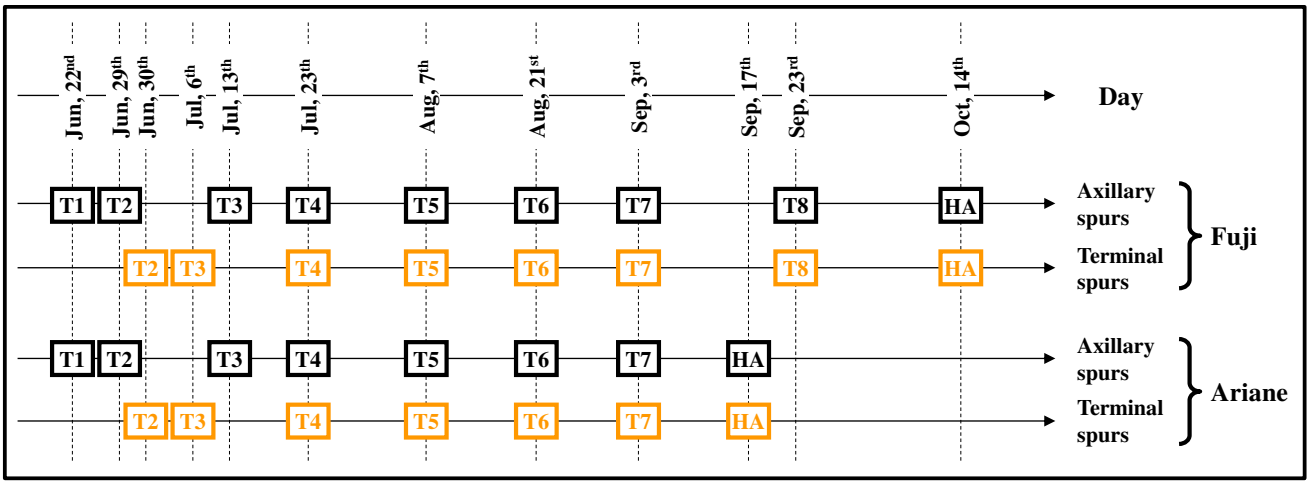

Figure 2. Schedule of the sampling dates for 'Ariane' and 'Fuji' in 2015. T1 refers to the sampling made on the day the treatments were started in 2015. Ti refers to the ith sampling per genotype and type of spur after T1. HA refers to harvest date.

As a control, the diameters of each fruit born on Y2 for each sub-branch were compared at the beginning of experiments in order to be sure that fruits were equivalent in size to exclude that a difference in fruit size at harvest could be caused by an initial difference.

2.6. Data analysis

2.6.1. Modelling of photosynthesis

We modelled the instantaneous net photosynthesis rate [µmol CO_2 m^{-2} leaf surface s^{-1}] for each simulated leaf using the model proposed by Marshall and Biscoe (1980), which is a non-rectangular hyperbola (equation 5).

$$P_n = \frac{(P_{max}+\alpha I-\theta R_d)\pm\sqrt{(P_{max}+\alpha I-\theta R_d)^2-4\theta(\alpha I(P_{max}-(1-\theta)R_d)-R_d P_{max})}}{2\theta} \qquad (5)$$

where P_n is the photosynthesis rate [µmol CO_2 m^{-2} leaf surface s^{-1}]; P_{max} is the PAR saturated maximum photosynthesis rate; α is the photosynthetic efficiency at low PAR intensities, ϑ is a

parameter describing the overall resistance of the system (leaf – stomata – chloroplasts) to diffusion of CO_2; and R_d is the dark respiration rate [µmol CO_2 m^{-2} leaf surface s^{-1}]. Normally, the maximum photosynthesis rate P_{max} is a function of leaf age and air temperature. However, as we measured photosynthesis rates only at one temperature and on recently mature leaves (aged about 20-30 days) we assumed, for simplicity's sake, that P_{max} did not vary over most of the temperature and leaf age range observed in the field.

The nls function in R was used to compute three of the four model parameters to make the model fit the data. Initial parameters for the nls function were fixed to P_{max}=12, α=0.04 and θ=0.8 with ranges of (5, 25), (0.01, 0.1) and (0.2, 1) for each parameter, respectively. R_d was set as the absolute value of the measured response to light in the leaf at PAR equal to zero. Impact of treatments on photosynthetic light response was studied by testing the impact of treatments on the four parameters fixed for each leaf light response by using ANOVA or Kruskal-Wallis, depending on whether the distribution of residuals was following a normal distribution or not, respectively.

2.6.2. Modelling of fruit growth kinetics

A growth curve for each fruit that did not drop before harvest was fitted using the negative exponential model (equation 6). This equation was first described by Von Bertalanffy (1938) and used by Zadravec et al. (2014):

$$D(t) = D_{max}(1 - e^{(-e^{s}(t-x0))}) \qquad (6)$$

where D(t) is fruit diameter at time t [days after full bloom]; D_{max} is the asymptote of the curve (potential final fruit size, mm); s describes the slope of the curve and is related to growth rate; and x0 is the intercept of the curve with the x-axis. The nls function in R was used to compute two of the three model parameters to make the model fit the data. Initial parameters for the nls function were fixed to s=-7 and x_0=-700. D_{max} was set as the highest measured value of fruit diameter. As fruit increases in size, D_{max} was generally measured at harvest; however, some fruits lost in diameter as they went on senescence, for those, D_{max} corresponded to their diameter before they started decreasing in size. Impact of treatments on fruit growth was evaluated using tests on the impact of treatments on parameters D_{max} and s for their biological meanings. These tests were conducted using ANOVA or Kruskal-Wallis, depending on whether the distribution of residuals was following a normal distribution or not, respectively.

2.6.3. Competition between sinks for sources

Competition between fruits was analyzed by testing the impact of vicinity of the fruit to sources on five parameters: parameters (i) D_{max} and (ii) s established above, measured (iii) total fresh (FW) and

(iv) total dry (DW) weights of the fruit at harvest and (v) dry matter content (DMC) of the fruit as the ratio of its dry weight by fresh weight at harvest. As, we assume that differences in the former parameters may also result from the amount of leaf area available per fruit, the tests were conducted using a two-way ANOVA with both vicinity and total available leaf area per fruit (ALA, calculated as total leaf area on the branch divided by the number of fruits) as factors.

2.6.4. Studying the interaction between sources and sinks

The five parameters describing fruit response to treatments were selected and their distribution as a function of the leaf area available per fruit (ALA) was graphically represented. Then, tests were made on axillary fruits in order to check if ALA had an impact on the five parameters cited above for each group of (i) 'Fuji', 1 axillary fruit/branch, (ii) 'Fuji', 2 axillary fruits per branch, (iii) 'Fuji', 3 axillary fruits per branch and (iv) 'Ariane', 2 axillary fruits per branch.

2.7. Branch model

2.7.1. Overall concept and workflow of model development

Generally, the model presented here is part of a larger model that foresees the modelling of processes linked to active and passive sugar transport as well as water transport between sources and sinks in the fruit-bearing branch of apple, with a resolution of one hour. The modelling strategy pursued was to provide as many simplifications as possible to the experimental system whose architecture is then faithfully reconstructed and input to the model, the latter only simulating fruit growth, while other organs (leaves, internodes) are assumed to have reached their final size. This restricts the time domain to the period at which vegetative growth has ceased until fruit harvest (June 20 to October 14). Source and sink behaviour is also input to the model, providing, on the source side, leaf dimensions and representative net assimilation rates (measured in July and August 2015, see section 2.3), and on the sink side the kinetics of the experimental fruits in terms of diameter development (see section 2.4). Thus, with the majority of sink and source parameters plus the branch architecture used as input, during a first modelling cycle, transport coefficients for sugar and water can be quantified and then fixed for a second modelling cycle in which the model is validated by predicting fruit size of another experimental branch.

2.7.2. Basic structure of the branch model

In the current version of the model, a branch is explicitly represented at the organ scale with the topology and geometry of each organ reconstructed, using allometric relations for leaf area (Baïram et al., 2017: chapter 2 of this thesis), and measurements of organ divergence and azimuth angles, the

latter estimated in the field to the nearest 10 degrees. In this way, an experimental branch consisting of two to three bourses plus infructescence and bourse shoot on 2013 wood, a number of lateral vegetative shoots on 2014 wood and the terminal bourse shoot (2015) were faithfully reconstructed as geometric objects (cylinder, parallelogram, and sphere, for internode/peduncle/petiole, leaf, and fruit, respectively). We programmed organs as modules in an object-oriented way, allowing the representation of variables and processes specific for an organ class. For instance, a module called Leaf harbours processes for leaf photosynthesis rate and maintenance respiration, while the Fruit module contains process descriptions for maintenance respiration and growth in diameter and dry weight. As the model is strictly modular, addition of further process descriptions (for sugar and water transport, transpiration, etc..) is very straightforward and has indeed already been tackled (Buck-Sorlin et a1., unpublished).

2.7.3. Simulation of light microclimate

The light microclimate of a leaf, shoot or primary branch is all but stable in time and space: it undergoes more or less rapid changes (daily, hourly or minutely), depending on its exposition (azimuth, insertion height on the stem, inclination or divergence angle); tree characteristics (height and canopy diameter), orchard characteristics (azimuthal orientation of the rows, tree and row spacing); and climatic and geographic characteristics [the distribution of direct and diffuse light on a given day, as well as the time of the day, the Julian day (of the year) and the latitude of the place, the latter two determining the solar height and its position]. As it was our objective to simulate in 3D the light microclimate with a temporal resolution of at least one hour and a spatial resolution of the single organ, and this for a number of experimental branches that were located on different trees within the orchard, it was necessary to implement the geometry of a virtual orchard and then try to faithfully reposition the experimental branches into this geometric model. In this way a purely structural model, which just consisted of geometric objects (parallelograms for leaves, cylinders for internodes, spheres for fruits) without internal functionality, provided the light (or more precisely shade) context for the virtual branch, which latter was explicit in terms of geometry and functionality (see description in previous section). The virtual orchard (Figure 3) consisted of twelve trees (three rows times four trees in a row), with stochastic functions for height, principal branch number, branch length, branch orientation (mostly spiral), branch basal divergence angle, and in which all other orchard characteristics (row orientation, inter-tree spacing, row spacing) were chosen to reconstruct the situation at our experimental orchard (neglecting, though, a very slight slope running in parallel to the rows, from east to west).

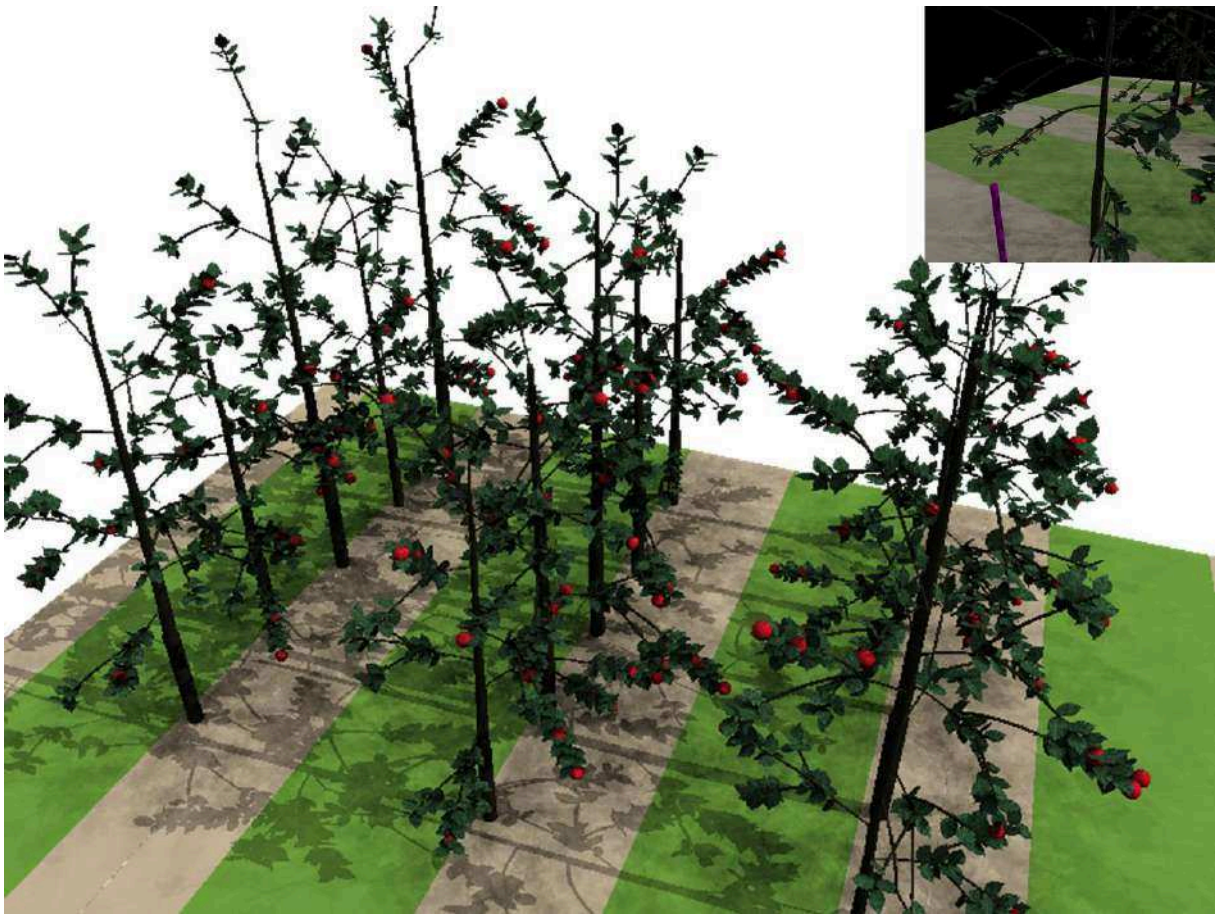

Figure 3. Simulated virtual orchard consisting of twelve apple trees, and a ground floor, to provide the light context for the virtual branch model. The inset shows the experimental branch that is inserted on one of the trees, thereby reproducing the position, insertion height, and azimuth of the measured experimental branch. The picture shows the light climate for the 20th of June 2015, at 16:00h, as seen from a southwestern direction (the inset shows the branch from a southeastern direction). Soft and hard shadows on the ground and leaves were created by a diffuse sky and a direct sun light object that were parameterized with climate data from the Beaucouzé weather station (sky transmissivity, daily global radiation).

We implemented the models as modular XL-systems using the GroIMP simulation platform version 1.5 (Kniemeyer 2008, Hemmerling et al. 2008). To simulate light dynamics in 3D and over time we used the GroIMP radiation model (class `lightmodel`). This is an inversed path tracer with Monte Carlo integration, which computes, from a so-called scene (consisting of one to n light sources, visible objects, and light sensors) the absorption of radiation from light sources by scene objects, as well as the detection by sensors. The amount of radiation locally absorbed by an object or detected by a sensor may be queried at any point of the simulation, for information or for further use in the model (e.g. photosynthesis). In order to faithfully model daily dynamics of daylight, two light sources were

implemented in the scene (a hemisphere at the centre of which is located the virtual orchard), a moving light source emitting direct light (the sun) consisting of a single directional light pointing always to the centre of the scene, and a stationary hemispheric light source (the sky) consisting of 72 directional light sources that were equidistant to the centre of the scene and otherwise randomly positioned on the surface of the hemisphere, thereby recreating a diffuse light environment. The light source simulating the sun is moving as a function of the time of the day, the day of the year and the latitude of the place [for details of this model see Buck-Sorlin et al. (2009)].

3. Results

3.1. Characterization of sources as a response to treatments

3.1.1. Characterization of leaf area

Total leaf area of both FU and AR was very variable among branches (Figure 4). In FU, leaf area was equally distributed among the lateral vegetative shoots (Y1) and the terminal spur (Y0), whereas, in AR, leaf area was unevenly distributed, with most leaf area on Y0. However, standard deviations of both total leaf area on Y1 and Y0 indicated that the variation among branches was high in both genotypes in Y1 and Y0, respectively. Therefore, the same type of branch pruning would not alter leaf area to the same extent for the two genotypes; however, the removal of vegetative shoots did indeed strongly reduce total leaf area in FU compared to AR. In addition, the standard deviation in leaf area of FU vegetative shoots was very large.

Globally, total leaf area (TLA) of the branch differed significantly among some treatments in both FU and AR (Figure 5). Indeed, in FU, TLA under ‘low’ treatments (‘2F_L’ and ‘3F_L’) was significantly lower than TLA obtained under ‘high’ (‘1F_H’ and ‘2F_H’) and ‘medium’ (‘2F_M’) treatments, which in turn were not otherwise significantly different amongst each other. Moreover, TLA of ‘high’ and ‘medium’ treatments did not differ significantly from TLA of terminal spurs on Y0 under the ‘1F_T’ treatment. In AR, no significant difference in TLA was observed among treatments excepted for ‘1F_T’ which exhibited a higher value compared to ‘medium’ and ‘low’ treatments with 2 fruits per branch.

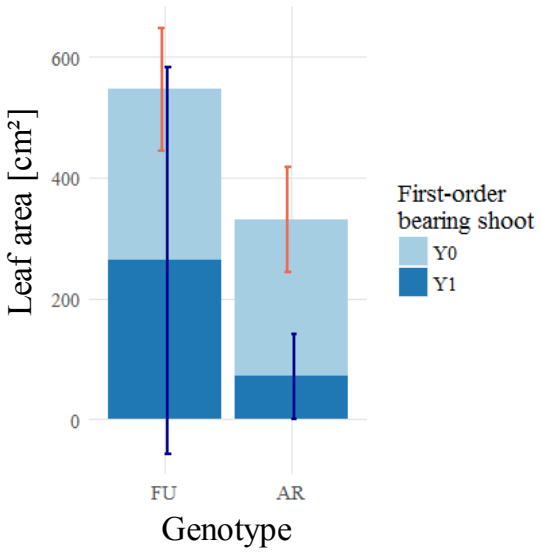

Figure 4. Bar plots of mean leaf area of unpruned branches (treatments with 'high' leaf area), expressed as the sum of mean leaf area shoots born on Y1 and Y0 (see text for further explanation) in 'Ariane' (AR) and 'Fuji' (FU). Bars indicate standard deviation of Y1 (–) and Y0 (–).

In conclusion, these results seemed to show that pruning did not induce clear differences in TLA among treatments and therefore that analysis of the effect of TLA on fruit growth could be done on the basis of computed TLA rather than using the treatment labels 'high', 'medium' and 'low', as these were in fact more or less arbitrary labels employed before the accurate computation of TLA (see below).

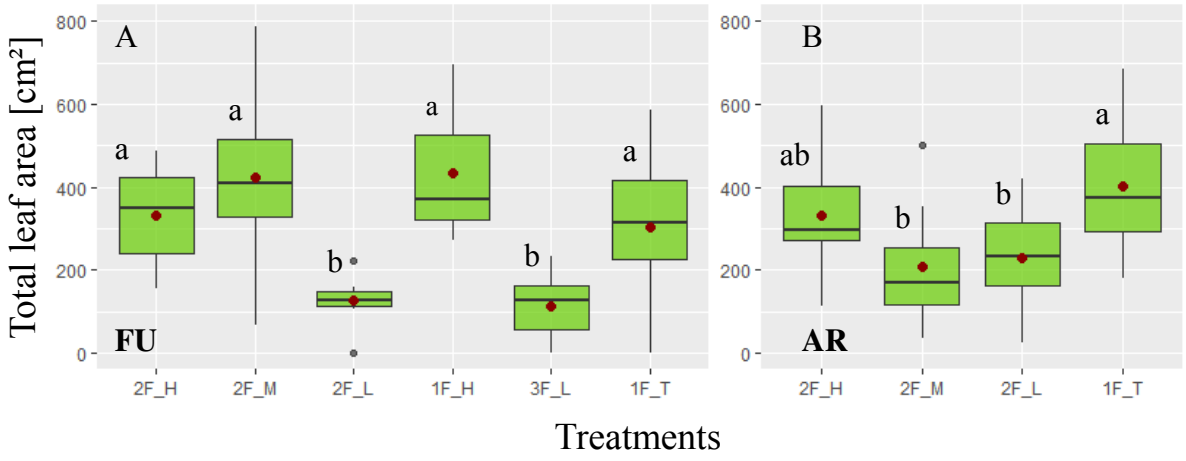

Figure 5. Boxplots of total leaf area (TLA, cm^{-2}) as a function of different pruning and defruiting treatments on 'Fuji' branches : one and two axillary fruits and high TLA ('1F_H' and '2F_H'), two axillary fruits with medium ('2F_M') and low TLA ('2F_L'), three axillary fruits with low TLA ('3F_L'), one fruit on the terminal spur ('1F_T'). (•) mean value of TLA for each treatment. Treatments with the same letter were considered to be non-significantly different according to one-way ANOVA and/or Kruskal-Wallis results ($P<0.05$).

3.1.2. Impact of treatments on light response of leaves

Modelled photosynthetic light response curves show a reasonably good fit to the measured data, with the exceptions of those curves, which had a very low P_{max} [Figure 6 (A-B)]. Moreover, curves of both measured and modelled data differed in shape among the different groups of branch treatments. ANOVA and/or Kruskal-Wallis showed that the parameters α and ϑ of the Marshall and Biscoe model were not significantly different among groups of leaves, in contrast to P_{max} and R_d. For P_{max}, three significantly different groups were distinguished; a significantly highest P_{max} in terminal bourse shoot leaves ('BS_T_NG'), an intermediate P_{max} in leaves of 'BS_T_WG' and 'BS_3F_L', and finally a low P_{max} in all other leaves (Figure 7). As for the dark respiration rate R_d the highest values were found in rosette leaves on totally defoliated branches with two fruits ('RO_2F_Z'), terminal rosette leaves ('RO_T_WG'), and terminal bourse shoot leaves ('BS_T_WG') (Figure 8); while the significantly lowest R_d was found in only one treatment (3 fruits and 'low' leaf area ,'BS_3F_L'), with the remaining treatments showing intermediate values that were not significantly different from the two other groups (Figure 8).

3.2. Impact of treatments on fruits

Logistic regression applied to fruit drop between the onset of the experiments and harvest showed no significant difference, neither among genotypes nor among treatments. However, it was noted that fruit drop was not more important on branches on which we applied a lighter pruning (Table 2).

In FU, initial fruit diameter measured at the onset of the experiments showed no significant difference with respect to their "rank" (topological distance of fruit to the sources: first, second, or third fruit) in branches with two and three axillary fruits, respectively (data not shown). This was also the case in branches with 2 axillary fruits in AR (ANOVA, P-value>0.05). Moreover, initial fruit diameter did not show any difference among treatments in FU and AR, respectively. Therefore, it was considered that, at the onset of the experiment, axillary fruits were equivalent among their ranks on the branch and among treatments set in FU and AR, respectively (data not shown). However, initial fruit diameter was significantly different among genotypes (Kruskal-Wallis test, P-value$<2.2*10^{-16}$); therefore, in the following, fruit growth and response of fruits to treatments will be treated separately for each genotype.

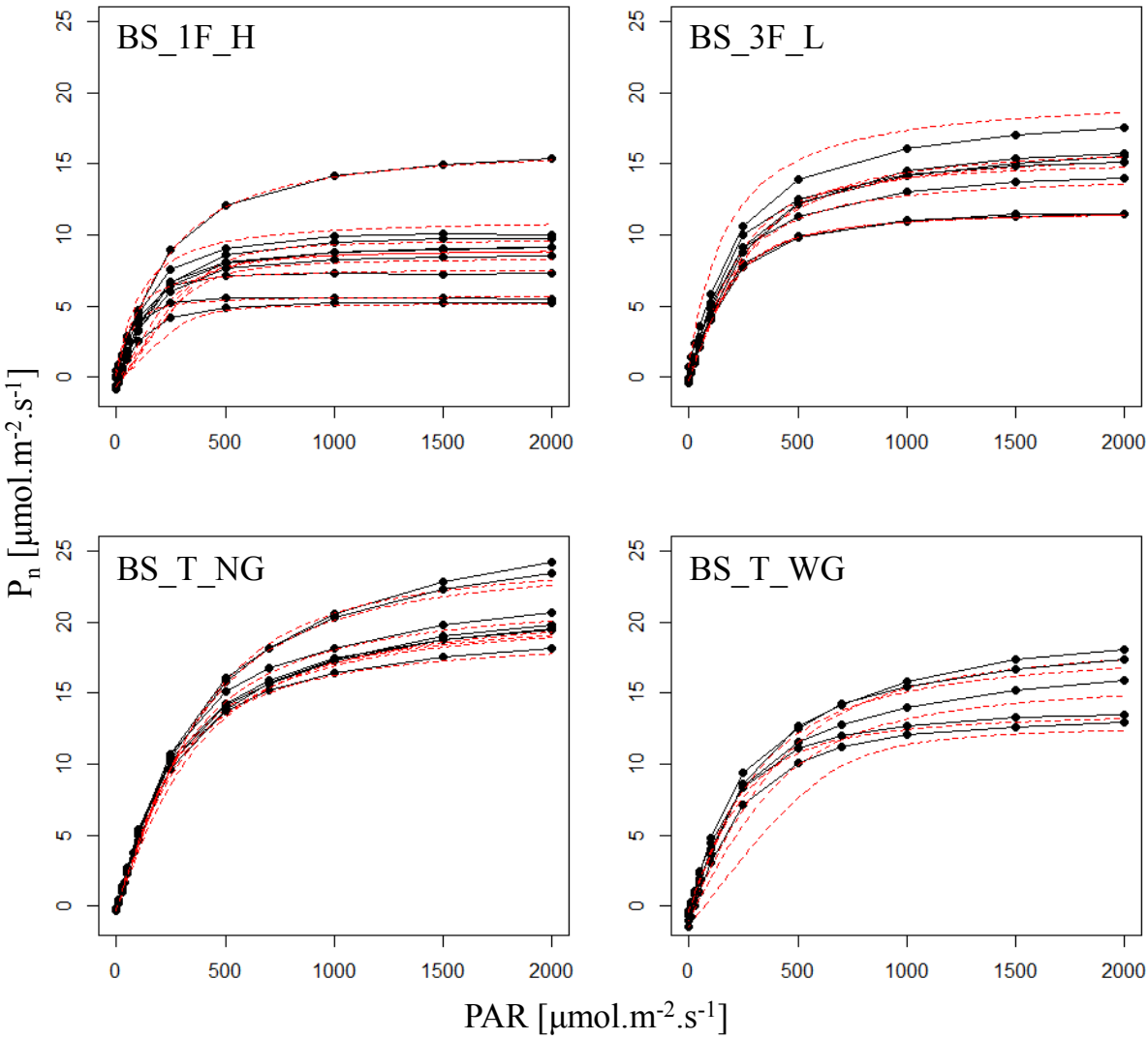

Figure 6A. Photosynthetic light response curves obtained from bourse shoot leaves of 'Fuji'. Treatments were as follows (TLA = total leaf area): 1 fruit and 'high' TLA (1F_H), 3 fruits and 'low' TLA ('3F_L'), 1 fruit on terminal spur with ('T_WG') or without girdling ('T_NG') at the base of the spur. Groups of leaves were labelled 'BS_1F_H', 'BS_3F_L', 'BS_T_NG' and 'BS_T_WG', respectively. (•) Measured data, (–) curves linking measured data for the same leaf, (--) modelled curves for individual leaf light response curves using the model proposed by Marshall and Biscoe (1980).

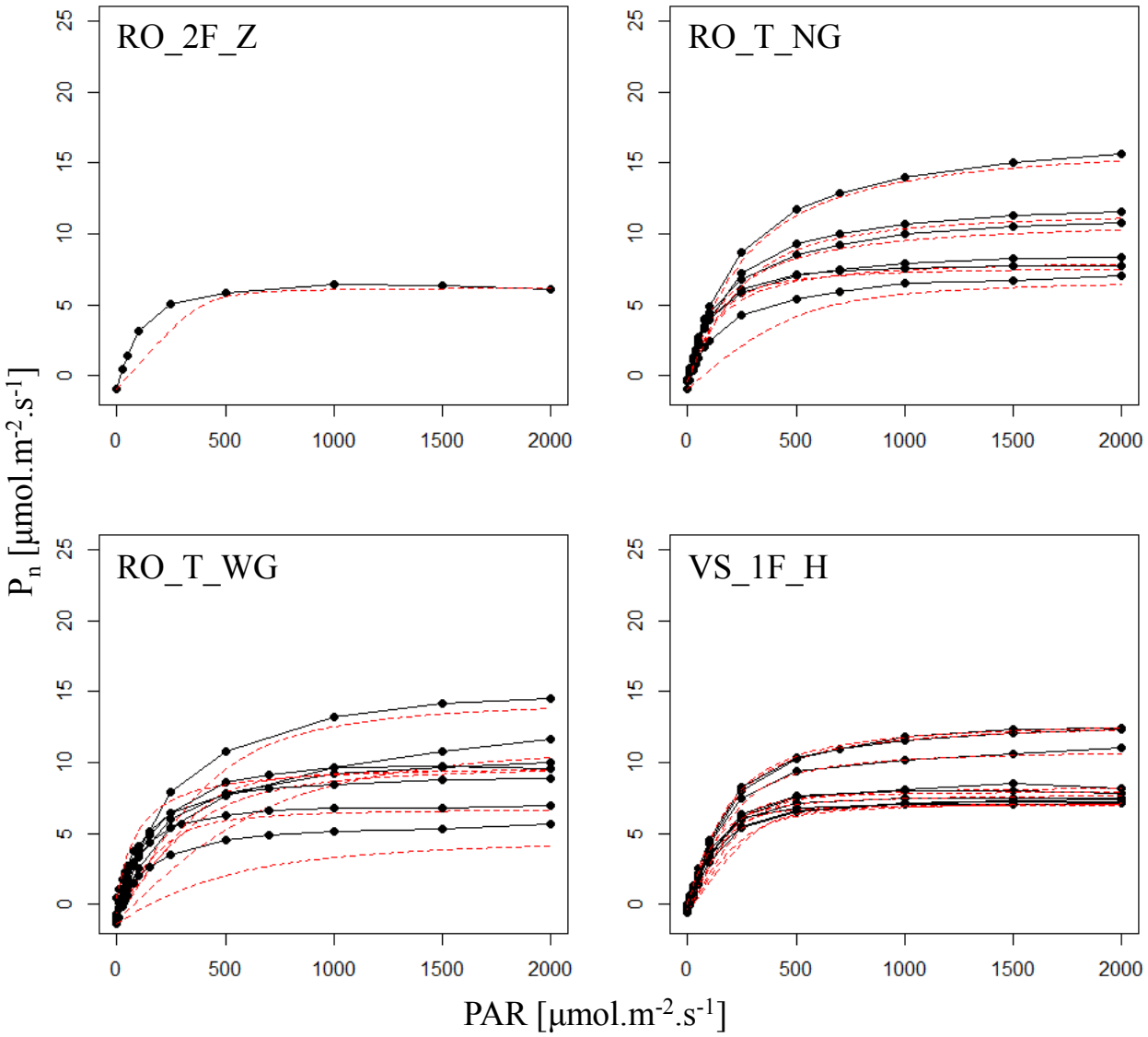

Figure 6B. Photosynthetic light response curves obtained from rosette and vegetative shoot leaves on 'Fuji'. Treatments were as follows: 2 fruits and no shoot leaves ('2F_Z'), 1 fruit on terminal spur with ('T_WG') or without girdling ('T_NG') at the base of the spur; 1 fruit and 'high' TLA ('1F_H', vegetative shoot). Groups of rosette (RO) and vegetative shoot (VS) leaves were labelled 'RO_2F_Z', 'RO_T_NG', 'RO_T_WG' and 'VS_1F_H', respectively. (•) Measured data, (–) curves linking measured data for a same leaf, (--) modelled curves for individual leaf light response curve using the model proposed by Marshall and Biscoe (1980).

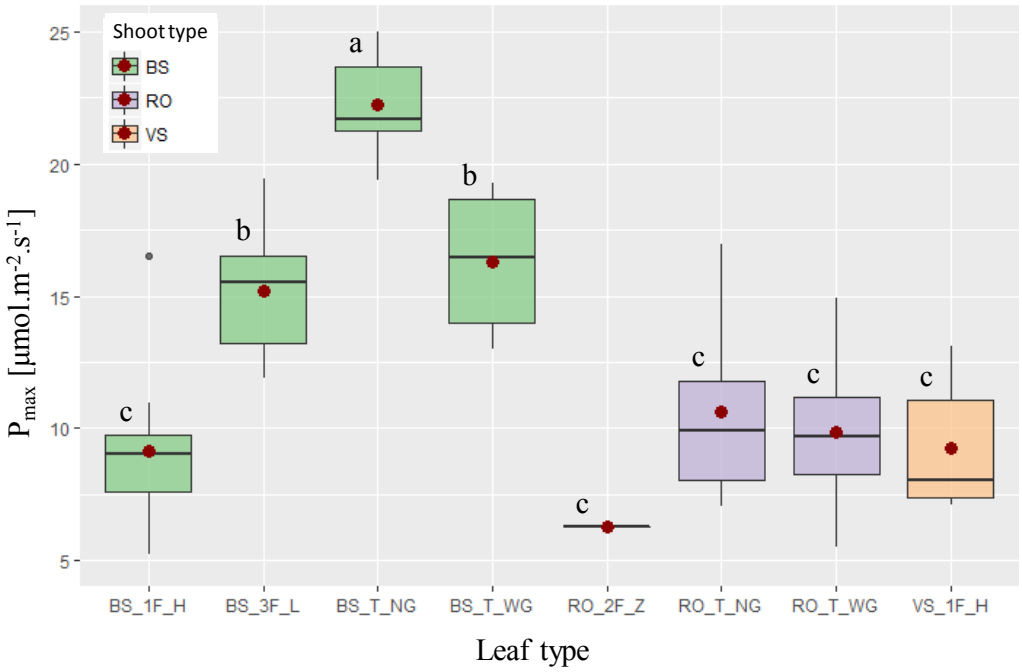

Figure 7. Boxplots of PAR saturated maximum photosynthesis rate [P_{max} (µmol.m^{-2}.s^{-1})] as a function of different pruning and defruiting treatments on 'Fuji' branches: bourse shoot (BS) leaves on branches with one axillary fruit and high leaf area ('1_F_H'), with three axillary fruits and low leaf area ('3F_L'), with one fruit on the terminal spur without girdling ('T_NG') and with one fruit on the terminal spur with a girdling at the base of the spur ('T_WG'). Vegetative shoot (VS) leaves on branches with one axillary fruit and high leaf area ('1F_H'); and rosette (RO) leaves on spurs in terminal position without girdling ('T_NG') and with girdling ('T_WG'), as well as with two axillary fruits and almost zero leaf area ('2F_Z'). Mean values for each group of leaves (•). Groups of leaves with the same letter are considered to be non-significantly different according to one-way ANOVA results ($P<0.05$).

Growth in fruit diameter, from the start of the experiment to harvest, showed distinct patterns among treatments for both 'Fuji' and 'Ariane' [Figures 9(A-B) and 10]. It was also observed that, for the same treatment, fruits that went on growing when their neighboring fruit (or fruits) on the same branch dropped showed quite different patterns compared to those fruits that grew with a competing sink on the same branch. This change in growth behavior compared to other fruits occurred in most cases when the competing fruit on the branch dropped early in the season (Figure 9A, treatment 2F_Z; Figure 9B, treatment 3F_L; Figure 10, treatments 2F_H, 2F_L and 2F_Z). However, some cases showed that the fruit that had lost its competitor sink attained a rather very low diameter at harvest compared to other fruits having experienced the same treatment, which in most cases indicated a tendency of the fruit itself to senesce even if it did not drop (Figure 10, treatment 2F_M). Furthermore, the highest heterogeneity for a same treatment was observed in terminal fruits (1F_T) and those of treatment '2F_M'; this could be due to the large differences in leaf area among branches of these treatments.

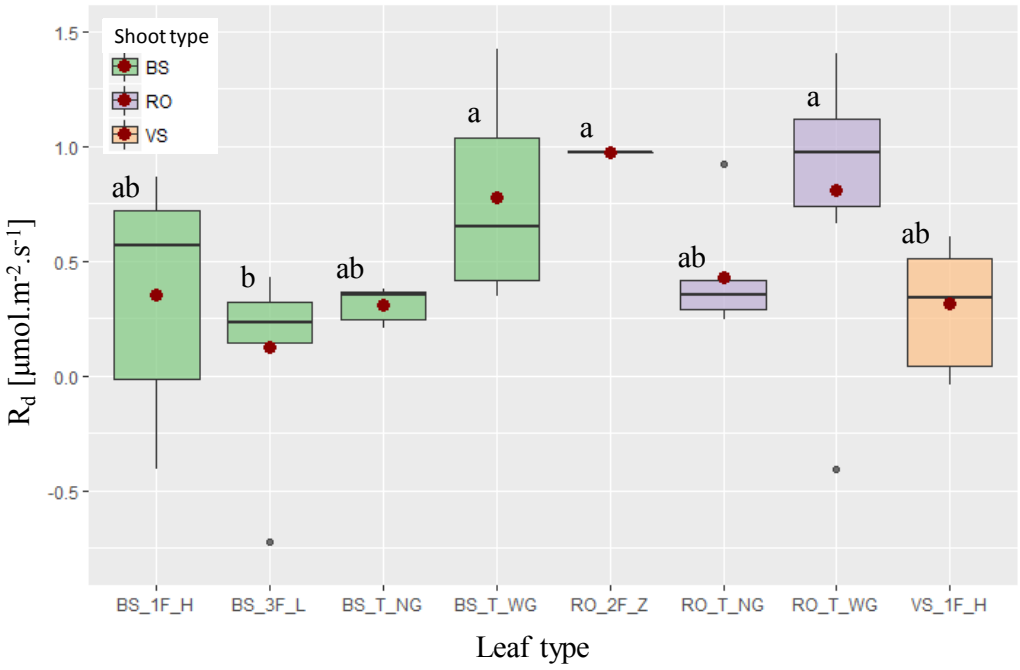

Figure 8. Boxplots of R_d (dark respiration rate, µmol CO_2.m^{-2}.s^{-1})] as a function of different pruning and defruiting treatments on 'Fuji' branches: For treatment labels see Figure 7. Mean values for each group of leaves (•). Groups of leaves with the same letter are considered to be non-significantly different according to Kruskal-Wallis results ($P<0.05$).

Table 2. Number of fruits that dropped before harvest (DF) and were retained until harvest (HF); number of branches on which at least one fruit (B_DF) or no fruit dropped until harvest (B_HF) among treatments in 'Fuji' and 'Ariane'. Total F and Total B: total number of fruits and total number of branches selected at the beginning of the experiment. For treatment labels see Materials and Methods and legend of Figure 5.

		Fruits				Branches		
Genotype	Treatments	DF	HF	Total F		B_DF	B_HF	Total B
'Fuji'	2F_H	8	10	18		5	4	9
	2F_M	1	13	14		1	6	7
	2F_L	1	15	16		1	7	8
	2F_Z	3	11	14		3	4	7
	1F_H	3	6	9		3	6	9
	3F_L	4	20	24		3	5	8
	1F_T	4	16	20		4	16	20
'Ariane'		DF	HF	Total F		B_DF	B_HF	Total B
	2F_H	5	11	16		3	5	8
	2F_M	4	12	16		4	4	8
	2F_L	6	10	16		5	3	8
	2F_Z	3	9	12		3	3	6
	1F_T	4	16	20		4	16	20

Difference in distance to the source did not have any impact on either the asymptote (D_{max}) or the slope (s) of the Von Bertalanffy model used to describe fruit growth in diameter. Moreover, the difference in source distance had no effect on fruit fresh and dry weight at harvest, nor on fruit dry matter content at harvest (Table 3).

Table 3. Results ANOVA tests of the impact of the rank of the sink and leaf area available per fruit, on model parameters D_{max} and s, fruit fresh weight at harvest, fruit dry weight at harvest and fruit dry matter content at harvest. D_{max} and s were parametrized for each fruit using the model by Von Bertalanffy (equation 6). Two fruits, 3 fruits: branches bearing two and three fruits, respectively, with no fruit drop until harvest (N=21 and 15 on branches with 2 fruits, of Fuji and Ariane, respectively and N=5 on branches with three fruits, of Fuji). *, ** and *** for P-values < 0.05, 0.01 and 0.005.

		Sink ranking		Leaf area		Sink Ranking x Leaf area	
Genotype	Variable	2 fruits	3 fruits	2 fruits	3 fruits	2 fruits	3 fruits
Fuji	parameter Dmax	ns	ns	***	ns	ns	ns
	parameter s	ns	ns	ns	ns	ns	ns
	Fresh weight	ns	ns	***	ns	ns	ns
	Dry weight	ns	ns	***	ns	ns	ns
	Dry matter content	ns	ns	***	ns	ns	ns
Ariane	parameter Dmax	ns	-	***	-	*	-
	parameter s	ns	-	ns	-	**	-
	Fresh weight	ns	-	***	-	*	-
	Dry weight	ns	-	***	-	*	-
	Dry matter content	ns	-	***	-	ns	-

The parameters D_{max} and s that were fitted on data of individual fruit growth in diameter and the model of Von Bertalanffy (1938) showed significant differences among treatments in both FU and AR genotypes (Figure 11). In FU, highest values of D_{max} were observed in axillary fruits of treatments with 'high' and 'medium' leaf area ('1F_H', '2F_H' and '2F_M') and in terminal fruits ('1F_T'), while the lowest values were observed in axillary fruits on branches with no leaves ('2F_Z'). Treatments with axillary fruits with 'high' leaf area showed the significantly highest means in D_{max} (Figure 11A). In AR, terminal fruits showed the significantly highest mean of D_{max}, and axillary fruits on branches with no leaves exhibited the significantly lowest D_{max} (Figure 11B). These results indicate that in axillary fruits, D_{max} was increasing with available leaf area. Moreover, terminal fruits had a high D_{max}. Parameter s is linked to the slope of the curve, which means that fruit growth rate increased with increasing s. In both FU and AR, s was significantly the highest in terminal fruits. However, s was not significantly different among treatments for axillary fruits in FU (Figure 11C).

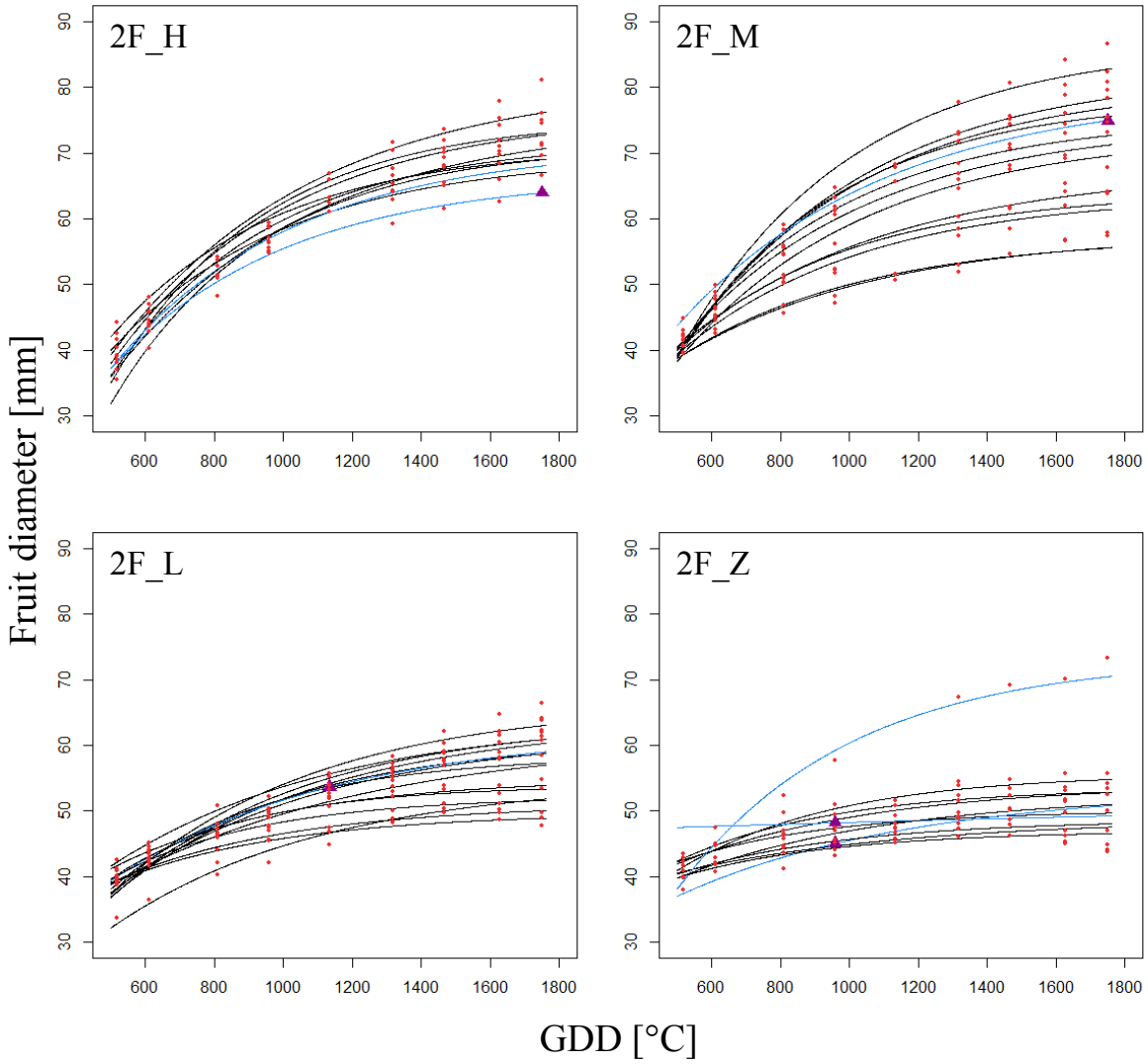

Figure 9A. Diameter growth kinetics of fruits growing on differently treated branches of 'Fuji' cultivar: Two axillary fruits on 'high' ('2F_H'), 'medium' ('2F_M'), 'low' ('2F_L') and almost 'zero' ('2F_Z') leaf area branches. Data modelled using equation of Von Bertalanffy (1938).

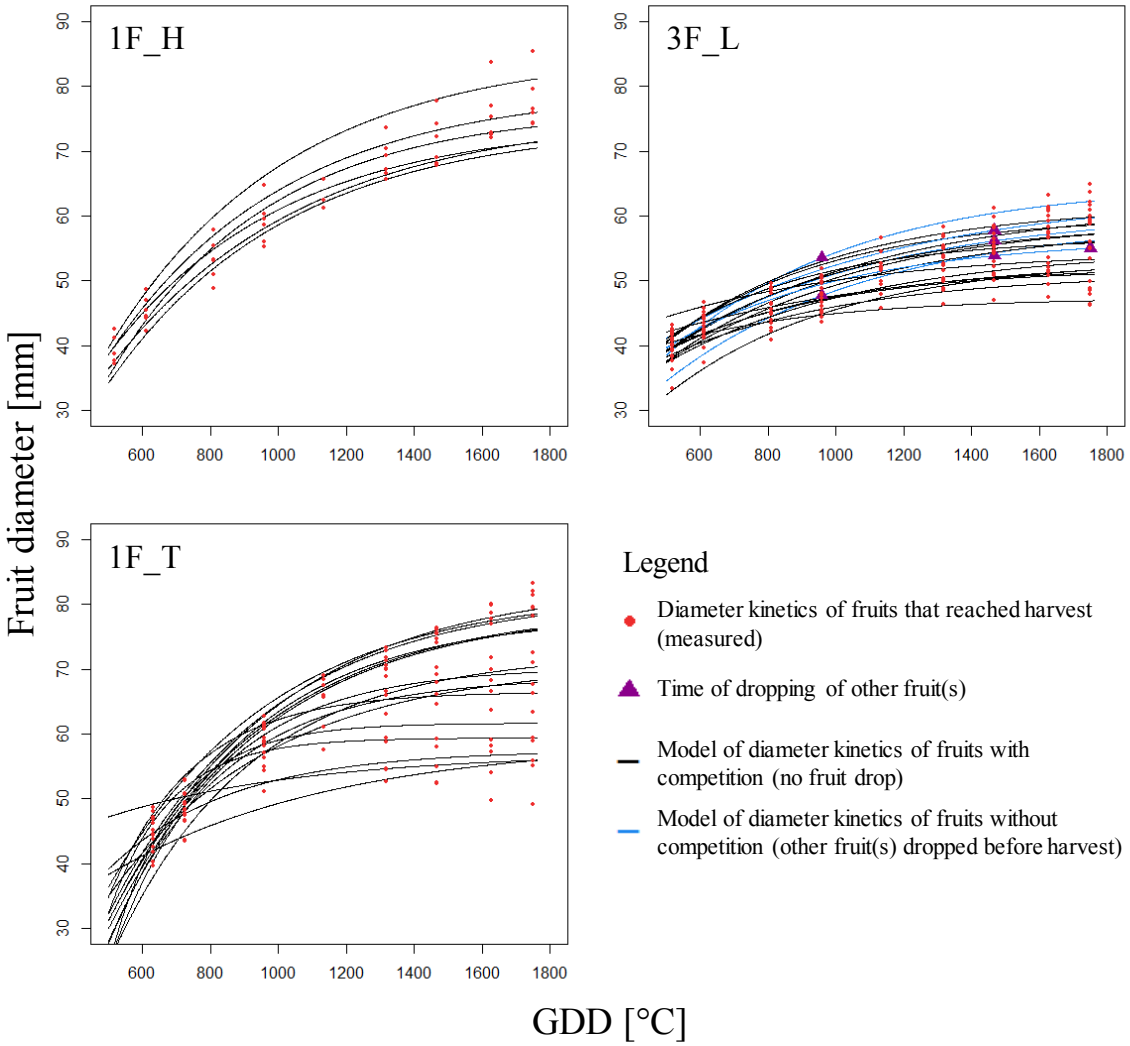

Figure 9B. Diameter growth kinetics of fruits growing on differently treated branches of 'Fuji' cultivar: 1 axillary fruit with 'high' ('1F_H'), 3 axillary fruits with 'low' ('3F_L') leaf area; and 1 fruit in terminal spurs with girdling at the base of the spur ('1F_T'). Data modelled using equation of Von Bertalanffy (1938).

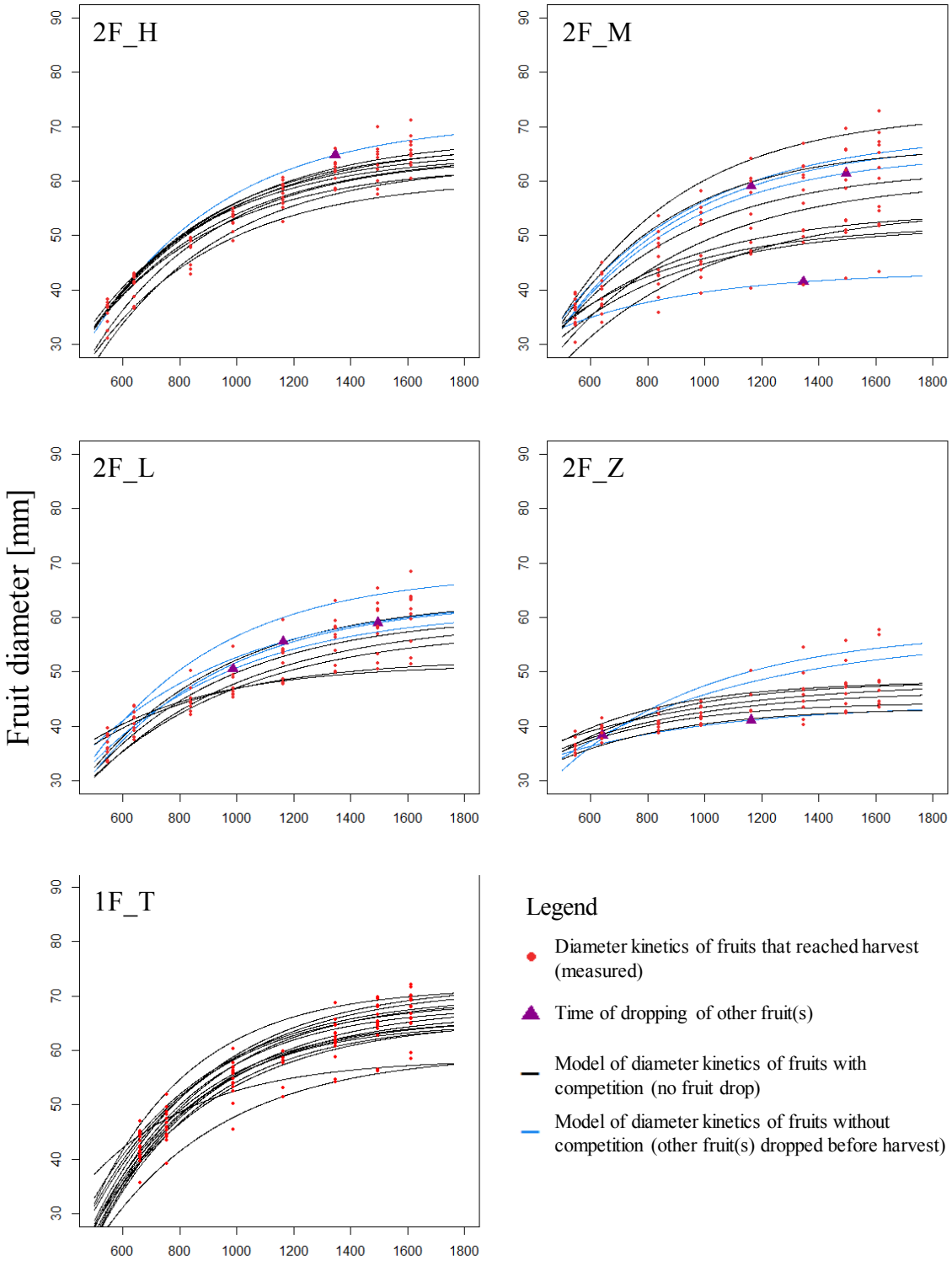

Figure 10. Fruit growth in diameter for fruits growing on differently treated branches of 'Ariane' cultivar. Two axillary fruits on 'high' ('2F_H'), 'medium' ('2F_M'), 'low' ('2F_L') and almost 'zero' ('2F_Z') leaf area branches; and 1 fruit in terminal spurs with girdling at the base of the spur ('1F_T'). Data modelled using equation of Von Bertalanffy (1938).

In addition, in AR, s was significantly higher in axillary fruits with 'high' and 'zero' treatments compared to those on 'medium' and 'low' treatments (Figure 11D). However, these results could depend on the variability of leaf area available per fruit in each treatment and the fact that branches did not always exhibit differences in leaf area as a function of treatments (see Figures 4 and 5). Figure 12 shows the distribution of five parameters describing fruit response to treatments as a function of the leaf area available per fruit (ALA). These parameters were: Dmax and s established for fruit growth curves, fresh weight of the fruit at harvest (FW, g), dry weight of the fruit at harvest (DW, g) and dry matter content of the fruit at harvest (DMC, -). The figure shows equivalent patterns for axillary fruits, which seem unrelated to treatments and genotypes. However, fruits on terminal spurs of both FU and AR showed quite different patterns. Moreover, treatments with 3 axillary fruits and 'low' leaf area ('3F_L') were very similar in terms of leaf area available per fruit and in fact the points were too close to each other to show a coherent pattern. Tests made on axillary fruits in order to check if ALA had an impact on the aforementioned five parameters for each group of axillary fruits [Fuji, 1 axillary fruit/branch, (ii) Fuji, 2 axillary fruits per branch, (iii) Fuji, 3 axillary fruits per branch and (iv) Ariane, 2 axillary fruits per branch] consistently showed a significant impact of ALA on Dmax, FW, DW and DMC except in Fuji, 3 axillary fruits per branch ('3F_L' treatment) (data not shown). However, as indicated above, leaf area in this treatment was too low to be correctly analyzed. However, ALA did not have a significant impact on s in all groups of axillary fruits.

Moreover, treatments on axillary fruits indicated a logistic pattern for maximum fruit diameter D_{max} as a response to ALA (Figure 12A). When considering each group of axillary fruits separately, all FW, DW and DMC as a function of ALA seemed to follow a linear pattern. In particular, if we assume that (i) sugars provided by reserve remobilization were negligible, (ii) rosette leaves near the fruit were equal in their sugar supply and (iii) the girdling provided isolation of the branch from the rest of the tree, dry weight of the fruit should indicate the amount of sugars supplied by leaves from the beginning of the experiment until harvest. As the pattern was linear for each group of axillary fruits (i.e. Fuji, 1 axillary fruit/branch, (ii) Fuji, 2 axillary fruits per branch, (iii) Fuji, 3 axillary fruits per branch and (iv) Ariane, 2 axillary fruits per branch), it is assumed that for each group, the increase in leaf area per fruit was proportional to fruit increase in diameter (Figure 12D); however, the figure suggested that the slope varied with the number of fruits per branch but not with genotype when considering the same fruit load (2 axillary fruits per branch). Therefore, a linear regression model was used to describe fruit dry weight at harvest (equation 7).

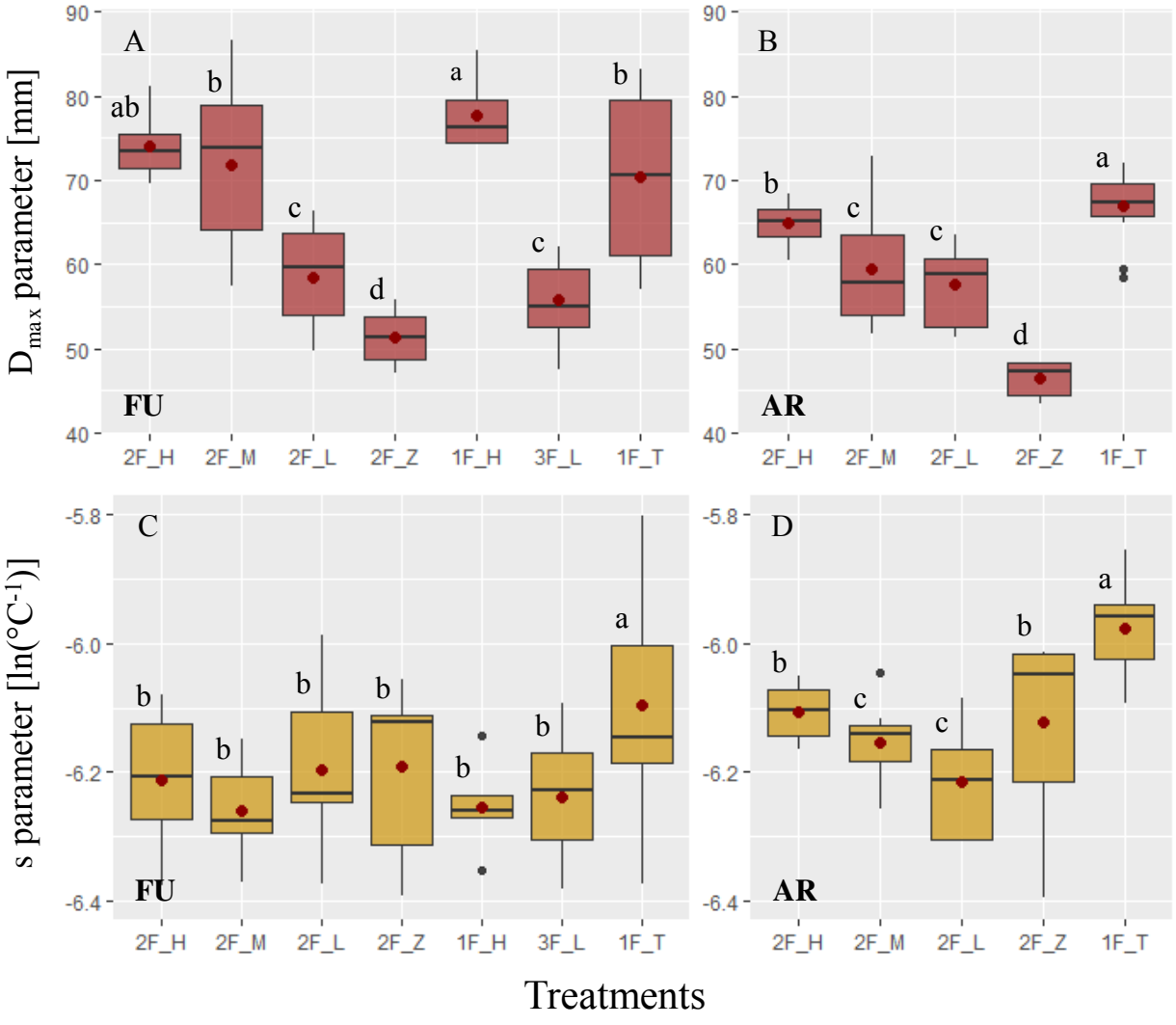

Figure 11. Boxplots of (A, B) maximum fruit diameter D_{max}(mm) and (C, D) parameter s [ln(°C^{-1})] parameterized for each fruit using the Von Bertalanffy model (equation 6) as a function of different pruning and defruiting treatments on 'Fuji' (FU) and 'Ariane' (AR) branches, respectively: For treatment labels see Materials and Methods. Mean values for each treatment (●). Treatments with the same letter are considered to be non-significantly different according to one-way ANOVA and/or Kruskal-Wallis results (P<0.05).

$$DW_H(ALA) = DW0_{G,n} + p_{G,n}.ALA \qquad (7)$$

DW_H is fruit dry weight at harvest; ALA is the leaf area available per fruit; $DW0_{G,n}$ is 'minimal' fruit dry weight at harvest when all leaves were removed except the rosette leaves of the fruit itself and $p_{G,n}$ is the slope of the curve for branches bearing n axillary fruits of a genotype G.

Table 4. Output of regression models $M_{FU,1}$, $M_{FU,2}$ and $M_{AR,2}$ for dry weight at harvest (DW_H) in 'Fuji', 1 axillary fruit/branch; 'Fuji', 2 axillary fruits per branch; and 'Ariane', 2 axillary fruits per branch, respectively, as a function of leaf area available per fruit (ALA) (see Equation 7). *, ** and *** for P-value < 0.05, 0.01 and 0.005. ns: non-significant.

	$DW0_{G,n}$				$p_{G,n}$					
Model	value	P-value			value	P-value			R^2	adj_R^2
$M_{FU,1}$	13.38	0.06018	ns		0.049	0.00957	**		0.84	0.81
$M_{FU,2}$	7.51	0.000529	***		0.083	7.93e-10	***		0.72	0.71
$M_{AR,2}$	6.39	0.000317	***		0.074	2.74e-07	***		0.71	0.69

Regression models $M_{FU,1}$, $M_{FU,2}$ and $M_{AR,2}$ established for dry weight at harvest DW_H in Fuji (1 and 2 axillary fruit/branch), and Ariane (2 axillary fruits per branch) as a function of leaf area available per fruit (ALA) showed coefficients of determination which indicates that in all three cases the increase in fruit dry weight at harvest was proportional to the increase in leaf area available per fruit. Moreover, the slopes of $M_{FU,2}$ and $M_{AR,2}$ were quite similar, whereas $M_{FU,}1$ exhibited a smaller slope coefficient. This indicates that treatments with two axillary fruits per branch exhibited the same rate of increase in DW_H as a function of ALA, while in the treatment with one axillary fruit this rate was lower. Moreover, the ratio between $p_{FU,2}$ and $p_{FU,1}$ of the models $M_{FU,2}$, $M_{FU,1}$, respectively, was equal to 1.71 which indicates that in 'Fuji', the same leaf area per fruit in branches bearing two fruits provided 71% more dry matter to the fruit than in branches bearing only a single fruit, and this for a large range of leaf areas per branch.

Therefore, in order to take into account the upregulation of the assimilation rate of a given leaf area compared to the one obtained when only a single sink was present on the branch, we introduced a coefficient $\lambda_{FU,n}$ as well as a variable 'adapted available leaf area'(AdALA) (Equation 8):

$$AdALA = \lambda_{FU,n}.ALA \qquad (8a)$$

$$\lambda_{FU,1} = \begin{cases} 1 & if \quad N_{fr} = 1 \\ \frac{p_{FU,2}}{p_{FU,1}} & if \quad N_{fr} = 2 \end{cases} \qquad (8b)$$

where N_{fr} is the number of fruits per branch. Afterwards, we modelled fruit dry weight at harvest, dry matter content at harvest and parameter D_{max} as a function of ALA [Figure 13 (A, C, E)] and as a function of AdALA [Figure 13 (B, D, F)], respectively for axillary fruits of 'Fuji'.

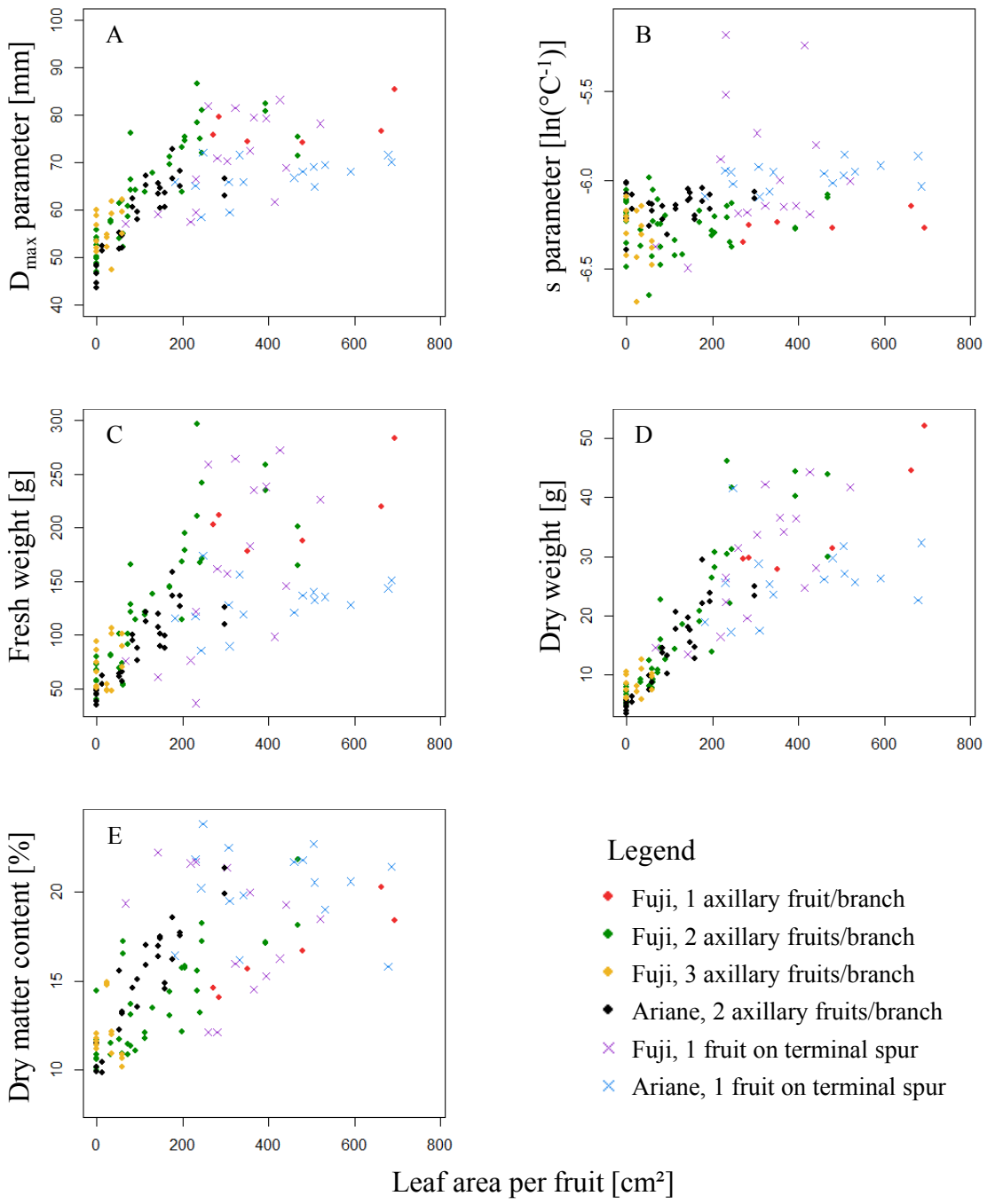

Figure 12. Distribution of (A) maximum fruit diameter D_{max}(mm), (B) the parameter s [ln(°C^{-1})] parametrized for each fruit using Von Bertalanffy model (equation 6), (C) fruit fresh weight at harvest (g) , (D) fruit dry weight at harvest (g) and (E) fruit dry matter content at harvest (%) as a function of leaf area available per fruit (cm²). In the legend, "1 axillary fruit/branch" refers to one axillary fruit with 'high' leaf area; "2 axillary fruits/branch" refers to two axillary fruit with 'high', 'medium', 'low' and almost 'zero' leaf area ('2F_H', '2F_M', '2F_L', '2F_Z'); "3 axillary fruits/branch" refers to three axillary fruits with 'low' leaf area treatment ('3F_L'); and "1 fruit on terminal spur" refers to treatment with one fruit on girdled terminal spur.

A regression model using AdALA as input allowed a better adjustment of simulating dry matter content when combining treatments of branches bearing both one and two-fruits (R^2=70, Figure 13D) compared to a regression model using ALA as input (R^2=0.66, Figure 13C). Fits of D_{max} to a negative exponential model using both AdALA and ALA showed a good fit. Models also showed that DW at harvest was different according to the number of fruits per branch; however, this result cannot be confirmed, as we did not test the case of having one fruit with no or 'low' leaf area on the branch. Models showed that dry matter content was almost the same for one or two fruits per branch even if the branch did not bear any leaves, which indicates that this variable is constant among treatments in 'Fuji'.

3.3. Branch model

3.3.1. Simulation of light interception of the experimental orchard

Figure 14 shows the simulated hourly rate of light output of direct (sun) and diffuse (sky) light, as well as of the amount of light being absorbed by the ground, for the period June 20 to October 31, 2015, corresponding to the time the experimental branches were monitored. This simulation output served to test the light model of GroIMP, which is sensitive to the number of rays chosen. Finally, for all simulations a light model with 20 million rays was used as this represented a compromise between faithfulness of output and computation time. Simulations were run with 168 to 744 steps (corresponding to one week or one month of development, respectively) each on three different computers. The average simulation time per step was 15 seconds (results not shown). As can be seen in figure 14, the radiation climate in the summer and autumn of 2015 in the experimental orchard was rather mixed, with cloudy and sunny days frequently alternating with each other. The simulated light absorption by the unexposed soil corresponded very well with the theoretical value (results not shown).

3.3.2. Simulation of light interception at the level of the branch

For reasons of time and model economy, only one experimental branch ('Fuji', first-order branch 3, tree number 1, rank 1, exposition southwest) was modelled, i.e. its architecture reconstructed and then inserted in the correct position and orientation within the virtual orchard. This simplified branch had served as a control treatment in the experiments; having relatively high leaf area and bearing two fruits (see Figure 15 for a simulated view of the branch).

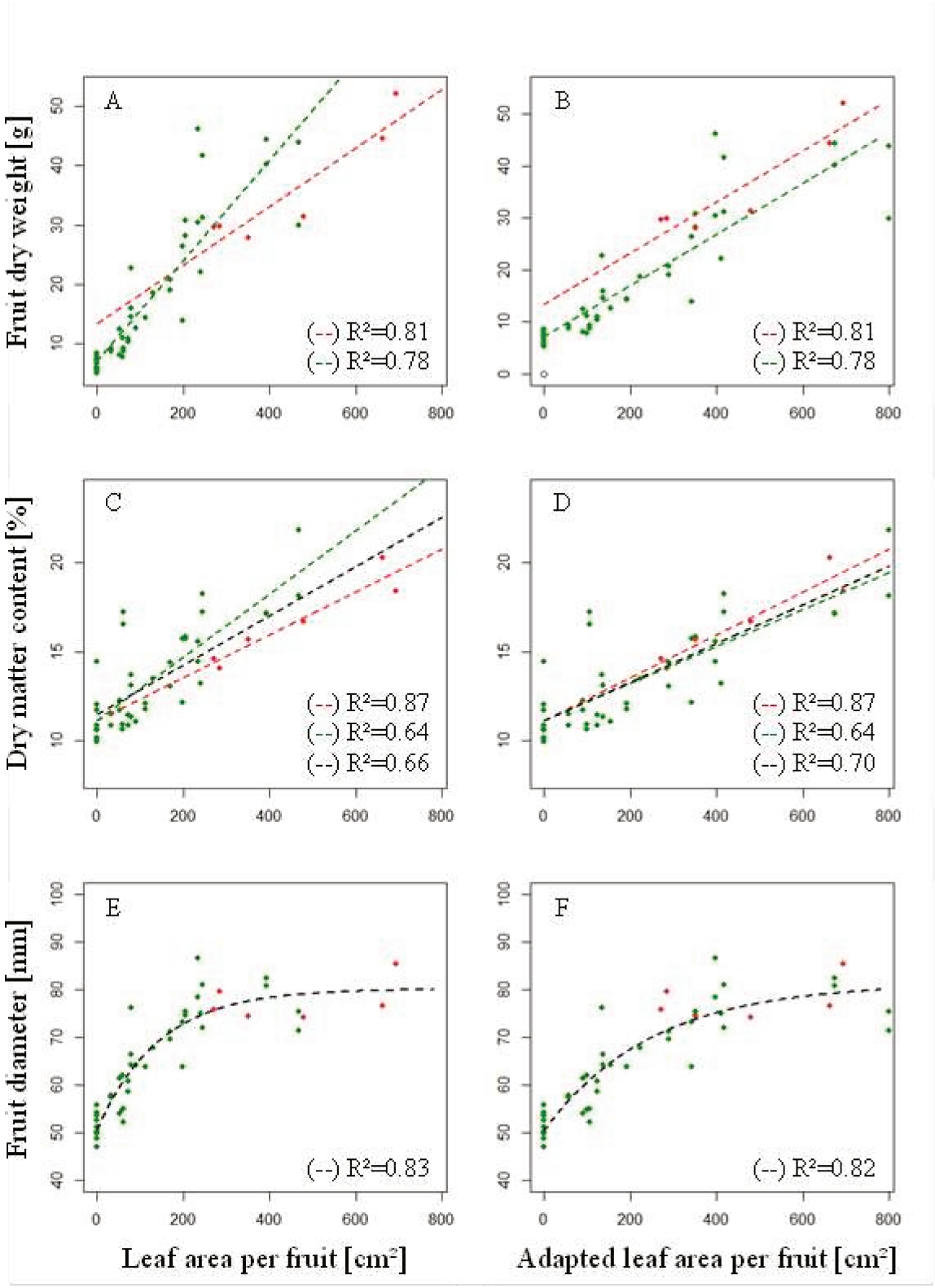

Figure 13. Distribution of (A, B) fruit dry weight at harvest (g), (C, D) dry matter content of the fruit at harvest (%) and (E, F) the highest diameter of the fruit observed during its development D_{max} (mm as a function of leaf area available per fruit (A, C, E; cm²) and adapted leaf area available per fruit (B, D, F; cm²). Experimental data (●): One fruit/branch; (●): Two fruits/branch. Linear (A-D) and negative exponential (Von Bertalanffy (1938); (E-F)) models (--): One fruit/branch; (--): Two fruits/branch (--): Models for both one and two fruit/branch

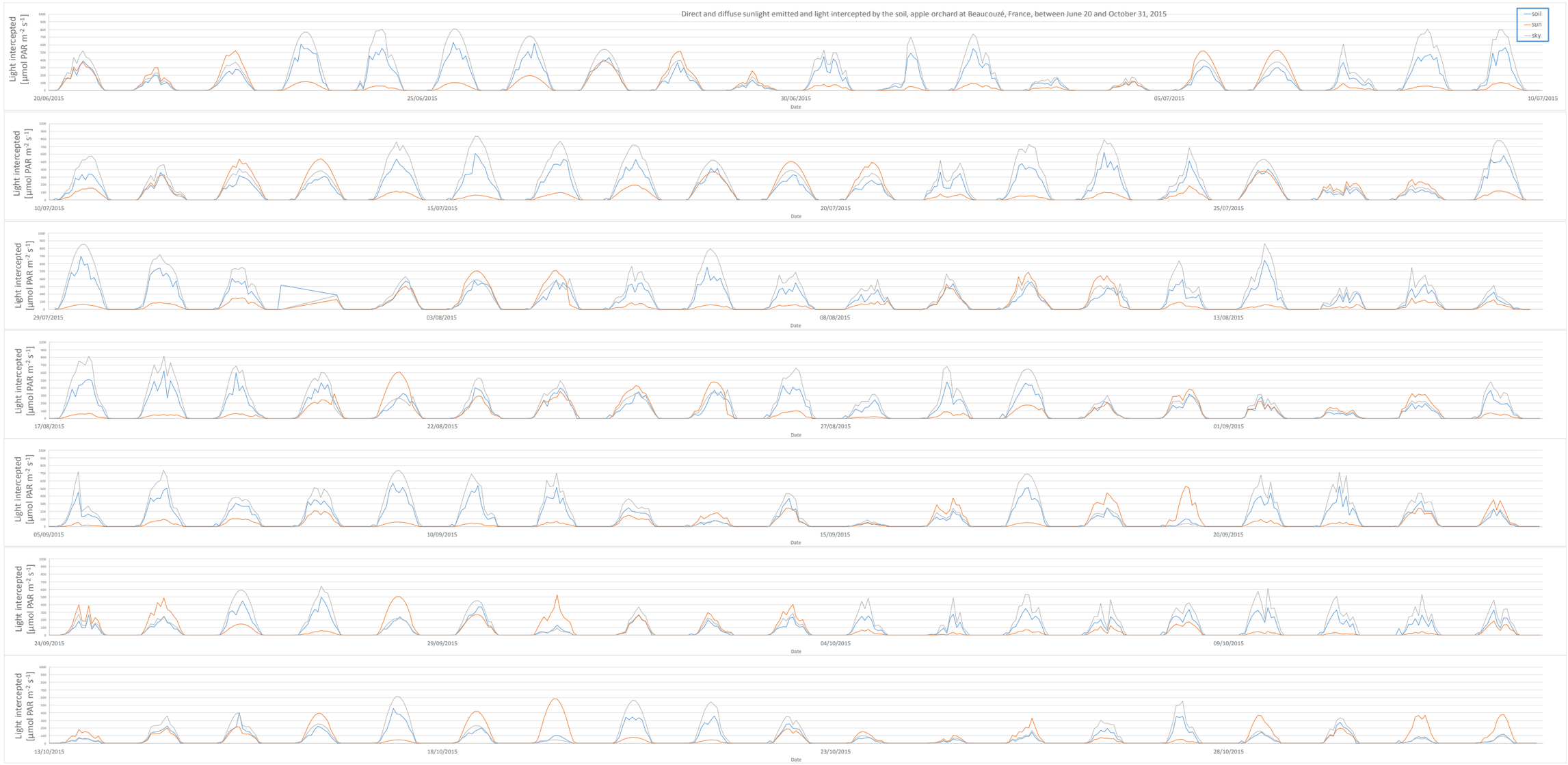

Figure 14. Simulated hourly light emission by the sun (direct —) and sky (diffuse —) and light absorbed by the soil (—), 20th of June to 31st of October, 2015, for a virtual orchard of 3 x 4 trees, with radiation data from Beaucouzé weather station (for further information see text).

Using the model of Baïram et al. (2017), we computed for this branch, the individual leaf areas of the bourse shoot, the vegetative shoot, and the rosette leaves (121, 339, and 28 cm^3, respectively). Other architectural parameters (orientation and divergence angle of the mother branch; amphitonous or epitonous orientation of each shoot on the mother branch; divergence angles of stems and leaves) had been determined once in July 2015 (see section 2.3) and were used to reconstruct the branch in GroIMP. Figure 16 shows the simulated daily integral of absorbed light for the three different leaf types. Vegetative shoots absorbed up to four times more PAR than the bourse shoot, and the bourse shoot up to seven times more PAR than the rosette. Large differences in absorption existed between bright and cloudy days (Figure 16), with the latter exacerbating the differences and the latter diminishing them. Generally, the trends in absorption in bourse shoot and vegetative shoot leaves were similar until the end of August after which the matching patterns seemed to be out of phase by one day. We also differentiated light interception for each leaf rank. Figure 17 shows the daily average light interception rate per acropetal leaf rank of all leaves of the bourse shoot. Apart from the fact that we observed the same strong fluctuation in light interception rate (between 5 and 16 µmol PAR m^{-2} s^{-1}) as in the daily integral (Figure 16), there was also a clear rank-specific gradient, with high leaf ranks (11, 12) showing the tendency to intercepting more light than lower ones (1, 3). However, this trend was not consistent as relatively high ranks (7, 9…) intercepted rather little light. This trend was particularly visible on bright days when the highest interception rates were above 120 µmols.

Figure 15. Rendered view of simulated branch (‘Fuji’, tree 3), treatment with two fruit and high leaf area.

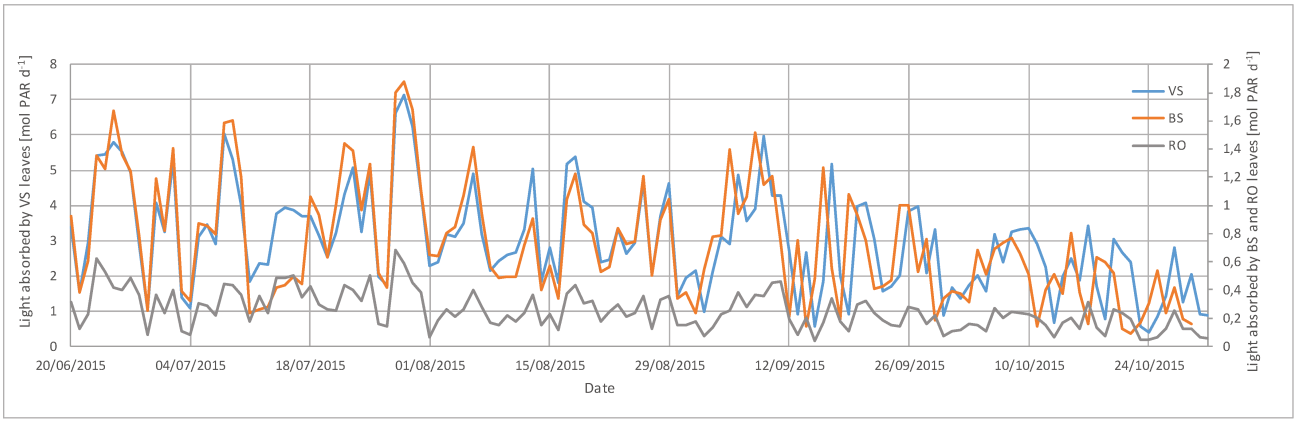

Figure 16. Simulated daily light interception of all rosette, bourse shoot and vegetative shoot leaves of a reconstructed experimental branch (‘Fuji’, tree number 3, fruit-bearing branch number 4 from below, exposition south-west), 20 June – 31 October 2015. Note different scale for vegetative shoots, which absorbed up to four times more than bourse shoot and rosette leaves.

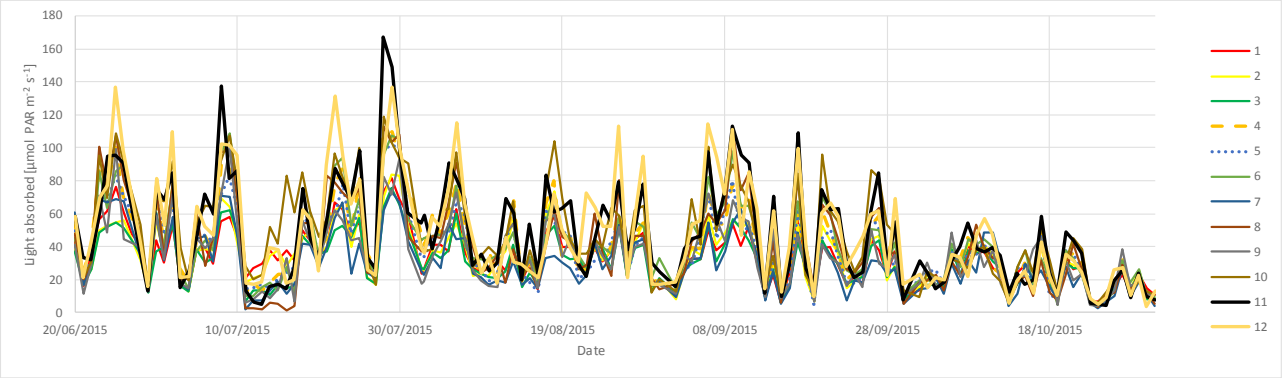

Figure 17. Simulated daily light interception of bourse shoot leaves of different acropetal leaf ranks (1 – 12) of a reconstructed experimental branch ('Fuji', tree number 3, fruit-bearing branch number 4 from below, exposition south-west), 20 June – 31 October 2015.

3.3.3. Simulation of carbon balance of the branch

Figure 18 shows the simulated development of the two fruits that grew on the experimental branch in terms of dry weight kinetics, as well as the kinetics of daily maintenance and growth respiration of the fruits and the wood.

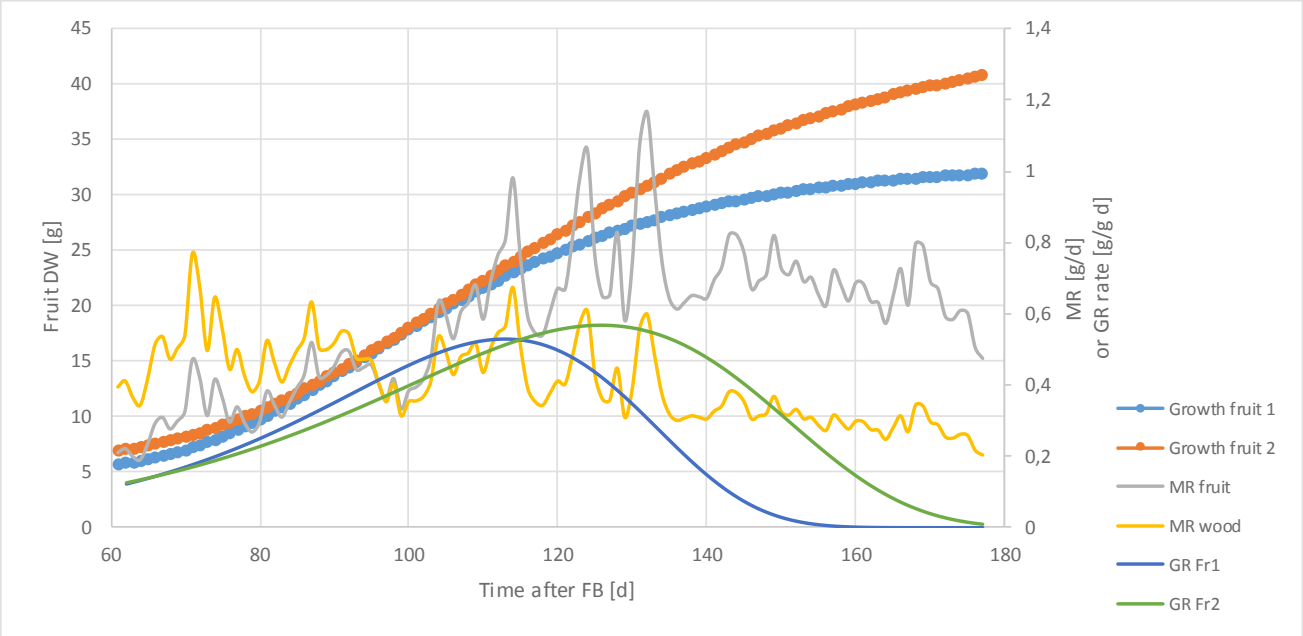

Figure 18. Simulated developmental dynamics of the two fruits growing on an experimental branch ('Fuji', tree number 3, fruit-bearing branch number 4 from below), from 20 June – 14 October 2015. Variables simulated were growth (fruit dry weight); maintenance respiration (MR fruit) of the two fruits [g d^{-1}]; maintenance respiration (MR wood) of the internodes and leaf petioles [g d^{-1}]; growth respiration of each fruit (GR Fr1, 2; g g^{-1} d^{-1}).

We modelled dry matter kinetics from the measured kinetics in fruit diameter, assuming a constant relationship between dry matter and diameter (0.32 g/cm), using a Gompertz function (equation 9) with four parameters:

$$dw(t) = y_0 + ae^{-be^{ct}} \qquad (9)$$

where dw(t) is the dry matter of the fruit at time t, t is the number of days after full bloom, y_0 is initial fruit dry weight, and a, b, and c are model parameters (Table 5). We initially tried the Von Bertalanffy equation which had been used to model diameters (section 3.2) but applied to dry matter kinetics it gave a worse fit (results not shown).

We assumed that there was no secondary growth of branch wood during the period in which we carried out the experiments (based on branch diameter measurements conducted, results not shown). This is a reasonable assumption, as secondary growth seems to be neglected by the tree in favour of fruit growth (Heim et al., 1979). Table 5 shows the model parameters used for the simulation. For growth respiration, we assumed a coefficient of 1.2; i.e. for each gram of new dry mass 1.2 g of sugar (glucose equivalent) needs to be invested (Lakso et al. 1999). We further assumed that daily maintenance respiration was a function of daily average temperature (equation 10):

$$mr(t) = dw_{fr,wo} * MR_{fr,wo} e^{0.0693(T_m - 25)} \qquad (10)$$

where $dw_{fr,wo}$ is the dry weight of fruit or wood [g], $MR_{fr,wo}$ is the coefficient of maintenance respiration of fruits or wood [g g^{-1}], respectively (Table 5), and T_m is the daily mean temperature [°C].

Using the average values of the parameters (Table 6) found for the photosynthesis rate model by Marshall and Biscoe (1980), we simulated the hourly average photosynthesis rate for each leaf type and from there the daily and total assimilate production (in glucose equivalents). A summary of the model output can be found in Table 7. Overall, assuming that the girdling of the branch isolated it from the rest of the tree we were able to do a complete carbon balance (Table 7). The comparison between predicted total source production and sink demand yielded a prediction error of 0.3 %.

4. Discussion

This work aimed at the understanding of the dynamic interactions between sources and sinks in apple at the scale of the (first-order) fruit-bearing branch. Furthermore, the present study provided parameters and initial architectures for an FSPM of apple set up to integrate the knowledge gathered during this study and to help explain or put into context, the findings. It was therefore an essential prerequisite to have an accurate characterization of sources and sinks, more specifically of leaf area

and fruit growth dynamics, in order to describe the initial branch architecture and the sink behaviour as accurately as possible, with the ultimate aim to derive hidden parameters such as transport coefficients.

Table 5. Model parameters used for the simulation of fruit dry matter kinetics, growth respiration, and maintenance respiration of fruits and wood (see Fig. 13).

Parameter	**Name**	**Value**	**Reference**
MR_{fr}	Coefficient of maintenance respiration of fruits	0.02112	Lakso et al. 1999
MR_{wo}	Coefficient of maintenance respiration of wood	0.015	Lakso et al. 1999
GR_{fr}	Coefficient of growth respiration of fruits	1.2	Lakso et al. 1999
$DW_{fr,ini}$	Initial fruit dry weight for fruit 1 and 2	5.1, 6.0	Own data
a	Parameter of Gompertz model for fruit dry matter growth (fruits 1 and 2)	27.676, 39.034	fitted using MS Excel
b	Parameter of Gompertz model for fruit dry matter growth (fruits 1 and 2)	48.365, 23.772	fitted using MS Excel
c	Parameter of Gompertz model for fruit dry matter growth (fruits 1 and 2)	-0.041, -0.030	fitted using MS Excel

Table 6. Model parameters used for the simulation of leaf photosynthesis in three different shoot types (BS bourse shoot, VS vegetative shoot, and RO rosette).

	Parameter of Marshall and Biscoe (1980) model			
Shoot type	P_{max}	R_d	α	ϑ
RO	9.919	-0.6600	0.0348	0.649
VS	8.474	-0.4573	0.0322	0.871
BS	7.615	-0.6241	0.0231	0.912

In the present study, total leaf area per shoot and per leaf was not measured but predicted using the new allometric model we created (Baïram et al., 2017, chapter 2). Using this model we computed the leaf areas both to recreate the initial architecture of the branch used in the FSPM to predict light interception, and to quantify a posteriori the actual total leaf area of the experimental branches that prior to this, had just been labelled as 'High', 'Medium', or 'Low'. Having done the latter, we found that these treatment labels were not indicative of the leaf area (see fig. 5), leading to wrong conclusions, i.e. sometimes an 'M' branch had a higher leaf area than a branch labelled as 'H'.

Concerning fruit growth dynamics, the Von Bertalanffy equation (VBE, cited in Zedrovec 2014) instead of the expolinear equation proposed by Lakso et al. (1995) was used.

Table 7. Summary of model output. Simulated period was June 20 to October 14, 2015.

Variable	**Name**	**Simulated value**
TLA_{BS}	Total leaf area of bourse shoot	120.9 cm^2
TLA_{RO}	Total leaf area of rosettes	28.2 cm^2
TLA_{VS}	Total leaf area of vegetative shoots	338.5 cm^2
DW_{wood}	Dry weight of wood	43.2 g
DWG_{fr}	Dry weight gain of the two fruits	60.1 g
TMR_{fruit}	Total maintenance respiration of the two fruits	66.9 g
TGR_{fruit}	Total growth respiration of the two fruits	72.1 g
TMR_{wood}	Total maintenance respiration of the wood (incl. leaf petioles)	47.9 g
TResp	Total respiration	186.9 g
AS_{BS}	Integral of assimilation by bourse shoot leaves	21.9 g
AS_{RO}	Integral of assimilation by rosette leaves	17.2 g
AS_{VS}	Integral of assimilation by vegetative shoot leaves	208.7 g
AS_{tot}	Total amount of assimilates produced	247.8 g
SK_{tot}	Total sink demand (respiration plus dry mass produced)	247.1 g
Δ_{SoSk}	Difference between source offer and sink demand	0.3 %

Effectively, VBE describes the later stages of fruit growth better than the expolinear equation, which is more suitable for the early stages of fruit growth where cell division is still ongoing, and during the transition from exponential to linear growth. Although experiments were done after natural 'June drop', we observed some late fruit drop, which could be related to the wounding effect caused by girdling as fruits in lateral positions (i.e. on Y2 wood) were very close to the girdling zone. However, no significant effect of pruning treatments on fruit drop was noted.

The first aim of this study was to investigate the effect of source sink distance on fruit growth. Our results indicate no significant difference among fruits belonging to different ranks, and this independent from source availability. These results, therefore, seem to confirm those obtained by

Hansen (1969), who showed that the distribution of carbon between sources and sinks could not be explained exclusively by source-sink distance. What is more, these results suggest that carbon allocation takes place in a similar and homogeneous manner among all fruits on the same branch. Indeed, such a result is in contradiction with those obtained by Hansen (1969), who, though not demonstrating a distance effect for carbon allocation, nevertheless provided some evidence for an unequal distribution of carbon among the different fruits, which he attributed to the preferred vascular connections between certain leaves and fruits at the scale of the fruiting branch. Still, this hypothesis, which was taken up by other authors (Watson and Casper, 1984; Dengler, 2006) and attributed to the phyllotaxy of the plant (Barlow, 1979; Orians et al., 2005; Dengler, 2006) remains controversial since the differences might also be explained by differences in initial sink strength among fruits of the branch, contrary to our study in which the initial size of fruits, and thus a priori their sink strengths, were statistically tested to be equal. It would therefore be interesting, in the frame of a follow-up study, to simultaneously test the effect of initial fruit size and of source-sink distance in order to know which one of these two factors is the most determinate for carbon allocation at the level of the fruit-bearing branch in apple. Although in the present study we did not notice an effect of source-sink distance on fruit growth, we nevertheless identified an effect of the position of the fruit on the branch: Indeed, we observed a clear effect of apical dominance when comparing terminal with lateral spurs. This effect was visible for all fruit growth-related traits.

Our second objective was the investigation of the effect of the source/sink ratio on fruit growth and leaf photosynthetic rate. We found evidence that it is in fact the number of growing fruits (sinks) and not the leaf area available per fruit (as usually assumed), which determines dry matter accumulation. This was surprising as it contradicted the literature and common orchard practice. Effectively, our results show that a modification of the source/sink ratio seems to be compensated by an alteration of the photosynthetic rate of leaves, with stronger and weaker values obtained for weaker and stronger ratios, respectively. These observations, which were already made by other authors (Palmer 1992; Blanke 1997, or Wünsche et al., 2005), could be explained by a modulation of the foliar concentration of starch, which latter is known to have an inhibitory effect on stomatal conductance (Roden and Ball, 1996), as a function of carbon demand. Although this result was only quantified for branches with one and two fruits, it is an interesting finding and puts into a wholly different light the definition of potential growth or rather, the method to obtain it, which is usually by reducing the number of sinks, thereby obtaining a high (saturating) source-sink ratio. Moreover, our results seem to suggest that two growing sinks together will upregulate the photosynthetic rate more strongly than one growing sink on its own, and this with the same leaf area per fruit. As for the likely mechanisms

involved in this upregulation, we can only speculate: firstly, perhaps two sinks achieve a more rapid depletion of stored starch from intermediate stores (leaves), thereby lifting product inhibition of photosynthesis (Roden and Ball, 1996); secondly, as suggested by Sané et al (2012) two fruits could induce an increase in xylem area that could facilitate carbon transport by reducing flow resistance; or thirdly, competition between the two fruits could induce an increase in their sink activity, which in turn could induce an increase in their sink strength and thus their ability to attract carbon. On the other hand, we cannot generalize our findings to normal conditions. In our experiments, we worked with rather small, girdled branches, which represent closed systems with respect to carbon as well as slightly suboptimal systems with respect to water flow and transpiration because of the xylem that is exposed to the air at the girdling zone. What is more, at the base of a girdled branch, upstream of the girdling zone, assimilates destined for export to the tree trunk and roots will accumulate, which usually leads to a downregulation of photosynthesis rate (Poirier-Pocovi, unpubl. research). Our results nevertheless suggest that in order to obtain a satisfactory source sink-ratio (i.e. one that guarantees near-potential fruit growth) at the scale of the fruit-bearing branch, one should take into consideration the number of fruits available for a given leaf area. One should then evaluate the source-sink ratio using an “effective” leaf area rather than the apparent leaf area, where the former includes both a quantification of photosynthetic efficiency and area available for photosynthesis. In the present study, we subjected a single static reconstructed branch to a detailed light regime with an hourly resolution, in a virtual orchard, and this from the start of the experiments (June 2) to the harvest date (October 14): we did this for one branch only, for reasons of model economy and time. In fact, we could have inserted several measured branches into the scene but this would have meant to restructure the model code, thereby allowing the testing of several different organs of the same type (leaf and fruit) and their data written into separate files during the same run. We will in fact do this in a follow-up study where the performance of the model will be validated on several other branches.

The predicted source and sink behaviour of the simulated branch matched very well, exhibiting a very low error. This could be interpreted as proof that the processes considered (light absorption, photosynthesis, growth, respiration) were already well calibrated and sufficient in number, i.e. that no major process was neglected. However, it should be cautioned that even in a "simple" system like the present one, which was isolated from the rest of the tree and in which, therefore, only a limited number of sources and sinks were present, we surely have neglected certain state variables and the processes they represent, e.g., soluble sugars transported and therefore present in the branch, or starch in the leaves (in the present model, all assimilates are actually used up for growth and respiration). In

addition, the fact that only a single branch was simulated prohibits any generalizing conclusions about model validity.

5. Conflict of Interest

The authors declare that the research was conducted in the absence of any commercial or financial relationships that could be construed as a potential conflict of interest.

6. Author Contributions

EB, MD and GBS conceived and designed the work; EB, GBS and CLM collected the experimental data; EB and GBS analyzed and interpreted the data; EB conducted the programming in R; EB and MH programmed the ImageJ script for automatic leaf scanning; GBS, JF and MH developed the models; MH and GBS carried out the majority of the model runs; EB, GBS and MD wrote the paper; all authors approved the final version.

7. Funding

The doctoral thesis of EB was funded by a strategic bourse of the Région Pays de la Loire, France, convention no. 2011-12596. All financial help is duly acknowledged.

8. Acknowledgments

Sylvain Hanteville helped with measurements in the laboratory, and Gilles Hunault gave valuable statistical advice. Lifeng Xu helped running the simulations. The staff of the experimental unit at Beaucouzé provided day-to-day maintenance of the orchard. All help is gratefully acknowledged.

DISCUSSION GÉNÉRALE

"Comment établir une vérité unique sur quoi que ce soit, quand un simple changement de distance, une modification de la lumière altèrent le monde que nous croyions le mieux connaître ? Je me souviens d'un vol en hélicoptère au-dessus de la vallée de Gstaad : ce que nous avions tenu, au cours de nos promenades, pour un grand désordre de détails, les uns charmants, les autres déplaisants, il suffisait d'un envol de quelques centaines de mètres pour l'ordonner, pour former sous nos yeux un merveilleux dessin de chemins, de barrières, de ruisseaux sur la neige."

Philippe Jaccottet

Ce travail de thèse s'inscrit dans un projet global de l'équipe consistant à la caractérisation des relations sources-puits chez le pommier ainsi que les facteurs régulant le transport des sucres dans la charpentière du pommier. Pour la réalisation de ces objectifs, les travaux intègrent une approche expérimentale en écophysiologie du pommier ainsi que l'élaboration d'un FSPM qui permet de simuler le transport des sucres et de l'eau dans la charpentière du pommier, allant de l'assimilation photosynthétique du carbone inorganique dans l'air jusqu'à à l'accumulation des sucres dans les différents organes portés par la branche.

Le comportement de toute la plante est la résultante d'un ensemble de processus physiologiques complexes et connectés qui émanent d'un déterminisme génétique mais aussi de l'influence de l'environnement. Ce comportement englobe, entre autres, les séries de mécanismes entraînant la croissance et le développement des organes, les défenses immunitaires de la plante mais aussi sa plasticité afin d'assurer la meilleure adaptation de la plante au milieu et aux conditions environnantes. Vu la sophistication des processus mis en jeu au sein de la plante, les manières classiques les plus communément utilisées durant des siècles afin de comprendre les processus de développement, de croissance et de fonctionnement des plantes et les caractériser ont été soit de décrire ce qu'on observait, soit d'intervenir sur les conditions environnementales afin d'étudier leur impact sur le comportement de la plante. Ce type d'approche a permis d'enrichir la base de connaissance à l'égard du fonctionnement des plantes à plusieurs niveaux. Toutefois, depuis la fin du 20ème siècle, l'avancée des moyens informatiques a propulsé la modélisation mathématique qui a connu un essor encore plus important au cours des dernières années par l'incorporation de moyens infographiques permettant de simuler de façon combinée la structure et la fonction de la plante (DeJong et al., 2011). Il s'agit donc, dans cette approche, d'acquérir les connaissances par une synthèse, et non plus par une analyse, du système investigué. Cette reconstruction – forcément très incomplète à cause de sa complexité – du système plante dans un cadre mathématique permet l'intégration de différentes sources d'information (littérature, observations botaniques et données mesurées propres ou d'autres équipes…) et est réalisée dans le but de pouvoir simuler une partie de la réalité représentée par le système et ainsi de voir si les processus, paramètres et variables d'état sont essentiels pour la compréhension du fonctionnement du système. De façon globale, les modèles fonction-structure de plantes (FSPM, 'functional-structural plant models') permettent, en effet, l'étude et la modélisation du développement, la croissance et la fonction de cellules, tissus, organes ou plantes dans leur contexte spatial et temporel (Godin and Sinoquet, 2005). L'intégration du modèle FSPM dans les travaux entrepris par l'équipe a modulé d'une certaine façon la réflexion faite

autour du questionnement scientifique. En effet, l'utilisation d'un FSPM suggère de partir de la base même de la structure de la plante afin de simuler le transport des sucres et de l'eau. L'utilisation de la structure est plutôt novatrice puisqu'elle permet de tenir compte aussi bien du microclimat dans le voisinage de la branche mais aussi de la vascularisation de la branche et de la connexion entre les organes sources et puits via le réseau constitué par les entre-nœuds des pousses. Bien que cette approche nécessite, dans un premier temps, un ajustement spécifique supplémentaire par rapport à une approche classique, elle permet, dans un deuxième temps, un gain de temps dans les simulations ainsi qu'une intégration d'un nombre considérable de facteurs supplémentaires dans l'étude des relations sources-puits et le transport des sucres. Il faut souligner, de ce fait, que le modèle ne constitue pas la finalité des travaux mais un outil d'étude complémentaire et/ou alternatif aux expérimentations écophysiologiques.

Dans une première étape, l'idée était de partir d'un modèle assez simple et de l'enrichir au fil du temps. Cette procédure a consisté à définir les données bibliographiques requises pour la simulation de la photosynthèse en réponse à l'interception lumineuse par les feuilles, du transport des sucres des sources vers les puits et l'accumulation des sucres dans les fruits. Ainsi un premier prototype a été construit sur une base de données bibliographiques comprenant les lois d'assimilation photosynthétique du carbone et les lois de transport de l'eau et des sucres dans le phloème. Après quoi, ce prototype a dû être testé afin de cerner son degré de justesse par rapport à la réalité. Les travaux entrepris au cours de cette thèse se positionnent de part et d'autre de la construction de ce premier prototype. En effet, outre les données bibliographiques utilisées pour l'élaboration du modèle, la collecte de données sous forme des jeux de données corrélées a été nécessaire afin de paramétrer le modèle. Cette collecte de données concerne principalement une meilleure caractérisation de la structure du pommier, des aspects de fonctionnement de la source, ainsi qu'une caractérisation des relations entre les sources et les puits. Une deuxième partie des travaux a été dédiée à apporter des éléments de comparaison aux sorties du prototype ; ces travaux ont consisté à effectuer des expérimentations sur la branche du pommier afin de vérifier la justesse de prédiction du modèle quant au transport des sucres depuis les feuilles jusqu'aux fruits.

Caractérisation de la structure

La représentation de l'architecture se base sur (i) la décomposition des différents composants de la plante, potentiellement de différents types, (ii) la géométrie décrivant les formes et leurs positions dans l'espace et (iii) la topologie qui définit la hiérarchie de branchement, i.e. de quelle

façon les composants sont interconnectés (Godin, 2000). Dans le cas des travaux faits au cours de cette thèse la représentation de l'architecture s'avère être un élément clé puisqu'elle rend compte, d'une part, de l'exposition spatiale des différents organes de la charpentière du pommier et, d'autre part, des connections permettant le cheminement des sucres et de l'eau entre les sources et les puits. Par ailleurs, le modèle FSPM élaboré par l'équipe intègre l'architecture de la branche comme entrée ; et sur la base de cette architecture, est simulée la synthèse du carbone au niveau des feuilles et son transport jusqu'aux fruits. Bien que l'architecture du pommier, comme la plupart des espèces végétales, répond à une réitération de ses structures, le devenir des bourgeons et la vigueur des pousses qui en proviennent n'en demeure pas moins difficile à prédire. Plusieurs travaux, ont permis de cerner certains de ces aspects (Costes et Guédon, 2002). Néanmoins, la caractérisation dépend grandement de la variété, des conditions environnementales ainsi que de la pousse porteuse. Dans les travaux accomplis au cours de cette thèse, l'impact de l'environnement sur la plasticité de la plante et le devenir des bourgeons n'ont pas été abordés ; par ailleurs, le modèle utilise comme entrée la structure de la branche. De ce fait, nos travaux se positionnent sur la compréhension du transport des sucres et de l'eau à un stade survenant bien après le débourrement des bourgeons et le modèle FSPM en particulier se positionne au stade ou la croissance végétative primaire est achevée. Pour cette raison la caractérisation de la structure post-débourrement a constitué un élément primordial, d'une part, pour l'étude des processus de transport des sucres entre les sources et les puits et, d'autre part, afin de fournir au modèle la structure la plus fidèle à celle étudiée pour d'éventuelles comparaisons entre les résultats des simulations et le devenir réel des organes. Ainsi, une partie des objectifs de cette thèse s'est orientée vers la détermination de modèles permettant de reconstruire les pousses en fonction de leur nature. L'utilisation de trois variétés a permis de recenser certains points communs mais aussi certaines différences auxquelles nous pouvons faire face pour la modélisation des pousses du pommier. Toutefois, les résultats novateurs proposés dans l'utilisation de ces modèles résident dans la possibilité de reconstruire, à partir de deux variables très facilement mesurables, une représentation des trois types de pousses du pommier qui est très fiable en ce qui concerne la surface foliaire totale de la pousse, mais qui tient aussi compte de la surface et de la forme de chaque feuille. L'établissement de ces modèles peut constituer un moyen de prédiction et une alternative non destructive à la digitalisation, d'autant plus que cette dernière s'avère être très chronophage et difficilement réalisable au niveau d'un verger. Ces modèles ont ainsi été intégrés dans le FSPM afin de reconstruire de l'architecture de la branche, architecture qui constitue l'entrée du modèle.

Par ailleurs, outre la reconstruction des pousses en utilisant les modèles établis, l'architecture de la charpentière dans le FSPM intègre d'autres données topologiques et géométriques, à savoir le rang de la charpentière et des sous-charpentières, l'orientation de la charpentière porteuse, l'emplacement de l'arbre portant la structure étudiée dans le verger par rapports aux autres pommiers. L'utilisation de ces données avait pour but de recréer le contexte de la sous-charpentières afin de mieux cerner l'ombrage et dans l'optique de simuler l'interception lumineuse d'un modèle en 3 dimensions. Les simulations du premier prototype FSPM ont abouti à des résultats très satisfaisants, ce qui valide de manière indirecte l'idée que les modèles de prédiction de l'architecture des pousses sont satisfaisants. Cependant, il faut admettre que ce seul résultat ne peut pas être extrapolé au-delà de l'échelle de la branche puisqu'elle est isolée du reste de l'arbre par une incision annulaire.

Relations sources-puits

Au cours de ce travail, une base de données caractérisant les relations sources-puits et le transport a aussi été utilisée dans l'élaboration du FSPM. Ces données ont été utilisées dans la paramétrisation des lois régissant un ensemble de mécanismes intervenant depuis la photosynthèse en réponse à l'interception lumineuse jusqu'au transport des assimilats carbonés vers les puits.

Dans un premier temps, les données de réponse photosynthétique à la lumière suggèrent que l'accroissement du ratio sources/puits régule négativement la photosynthèse et inversement. De même que les feuilles les plus sénescentes (feuilles de rosette) avaient une photosynthèse plus réduite. Toutefois, les mesures de la réponse de la feuille à la lumière n'ont été faites qu'au cours d'un laps réduit de temps (2 semaines au cours du mois de juillet). Ceci suggère que ces mesures ne peuvent pas rendre compte du comportement saisonnier global des feuilles, surtout en ce qui concerne l'étude de la photosynthèse et la respiration nette. En effet, la photosynthèse nette augmente jusqu'à une valeur maximale puis chute de nouveau au cours du cycle de vie des feuilles tandis que la respiration nette décroit au cours de ce même cycle (Lieth et Pasian, 1990). Les mesures ayant été faites au cours de deux semaines consécutives, elles ne peuvent que représenter l'étude de ces variables au cours d'un moment donné de ce cycle. Par ailleurs, la comparaison de ces variables pour des feuilles n'ayant pas le même "âge" ne tient pas compte de leur comportement passé et futur et peut de ce fait inclure une erreur due au décalage dans leur réponse par rapport à leur stade de développement. Dans cette optique, une étude plus étalée sur la saison de la réponse photosynthétique pourrait apporter des éléments de réponse plus affinés à cette caractérisation. Ce type d'étude a ainsi été conduit récemment au sein de l'équipe.

Dans un deuxième temps, la caractérisation des puits en réponse à la disponibilité des sources s'est faite à deux échelles : celle du spur et celle de la branche. En effet, en se basant sur des données bibliographiques, il est stipulé que plus le fruit est jeune, plus il s'alimente à partir de sources proches, et plus il grossit, plus il s'alimente à partir de sources éloignées sur la charpentière voire l'arbre (Hansen, 1969). De ce fait, l'étude des relations sources-puits et leur impact sur le développement et la croissance du fruit a été décomposée au cours du travail de thèse en deux étapes. Ainsi, une première expérimentation a visé la caractérisation des relations sources-puits à l'échelle du spur (Chapitre 1) et une deuxième la caractérisation des sources-puits à l'échelle de la branche (Chapitre 3). Dans les deux cas, les expérimentations ont consisté à créer des déséquilibres dans les relations entre les sources et les puits afin de comprendre le rôle et le comportement des organes définis comme sources dans le développement du fruit. Pour induire ces déséquilibres, nous avons testé l'effet de défoliations, de tailles et d'éclaircissages. Par ailleurs, pour mieux comprendre les mécanismes mis en jeu, nous avons créé des situations extrêmes de déséquilibre. En supposant que le fruit puise le carbone à partir de sources très proches au début de sa croissance, les défoliations ont été effectuées à la floraison et deux semaines après la floraison, au niveau du spur, afin de vérifier si la division cellulaire en est perturbée. Toutefois dans cette première expérimentation, le spur n'a pas été isolé par "girdling" du reste de la branche afin d'éviter que la blessure n'engendre une chute massive des fruits. Mais si tel avait été le cas, en nous basant sur notre hypothèse, le fruit auraitt été impacté à plus ou moins long terme dans la mesure où il aurait été alors dans l'impossibilité de capter du carbone en provenance de sources lointaines. Dans l'expérimentation à l'échelle de la charpentière, les sources et les puits ont été choisis intentionnellement éloignés et positionnés sur des pousses d'âges différents.

L'expérimentation menée à l'échelle du spur a permis de montrer la possibilité que le fruit puisse s'alimenter à partir de sources en dehors du spur. Toutefois, dans la situation d'une suppression totale des feuilles du spur, le fruit est fortement pénalisé et cela conduit alors à une chute massive des fruits sur de tels spurs. Ceci pourrait à la fois s'expliquer par la trop faible disponibilité en carbone au début du développement du fruit impactant la phase de division cellulaire mais aussi – et surtout – une alimentation hydrique fortement réduite en l'absence de feuilles à proximité.
Par ailleurs, le réseau de corrélations entre variables met la lumière sur les organes les plus connectés au sein du spur. Il en ressort que les caractères morphométriques du fruit sont très peu corrélés à ceux des feuilles de la rosette et de la pousse de bourse même à des stades précoces du fruit. Ceci confirme que le fruit parvient à s'alimenter à partir de sources plus éloignées que les feuilles s'étant

développées sur le même spur. Par ailleurs, une étude plus poussée – notamment histologique ou utilisant du carbone marqué – et intégrant l'impact de ces défoliations précoces sur la division cellulaire pourrait apporter des réponses plus précises sur la dépendance des fruits des feuilles voisines à ce stade de leur croissance. Le réseau de corrélations met, néanmoins les variables caractérisant la bourse au centre des connexions entre les autres organes. Schématiquement, la bourse est le carrefour entre tous les autres organes du spur et donc entre les sources et les puits. A partir des résultats obtenus à l'échelle du spur, différentes hypothèses ont été formulées quant aux rôles joués par la bourse (organe de réserve, zone de forte vascularisation) et qui mériteraient d'être confirmées. Des travaux ont d'ores et déjà débuté au sein de l'équipe avec une analyse de la composition en sucres et amidon de la bourse au cours de son développement et en fonction de la présence/absence de feuilles au sein du spur.

Les expériences réalisées à l'échelle de la branche viennent appuyer la conclusion que les fruits ont la capacité de s'alimenter en carbone à partir de feuilles situées plus loin sur la charpentière. En effet, seule l'isolation de la branche par girdling couplée à une réduction des feuilles (sources) a permis de réduire le développement des fruits de façon évidente. De plus, dans cette expérimentation, les branches disposant d'une surface foliaire suffisante ont permis un développement normal du fruit bien que ces feuilles soient localisées sur des parties éloignées sur la branche. Par ailleurs, dans le cas où plusieurs fruits étaient présents sur la branche et peu de sources étaient disponibles, la photosynthèse a été régulée de sorte que les feuilles produisent plus de carbone ; toutefois les feuilles les plus éloignées (pousse de bourse terminale) et les feuilles les plus proches (pousses végétatives axillaires) ne montraient aucune différence significative pour leurs activités photosynthétiques. Ceci suppose que les feuilles les plus éloignées sont sollicitées autant que les feuilles les plus proches pour la production de sucres et confirme le fait que les fruits s'alimentent à partir de sucres produits assez loin sur la charpentière.

L'autre résultat intéressant qui a été pointé au cours de ces travaux réside dans le fait que la compétition entre fruits semble augmenter leurs forces de puits. En effet, pour une surface foliaire par fruit équivalente, les fruits accumulent plus de matière sèche quand ils sont deux que lorsqu'il n'y en a qu'un seul par branche. Ce résultat semble aussi indiquer un effet bénéfique de la compétition entre fruits sur leur capacité à capter le carbone, avec l'hypothèse que cette compétition pourrait augmenter leurs forces de puits individuelles. De plus, cela semble aussi indiquer, contrairement à ce que nous pensions, que la croissance potentielle d'un fruit peut difficilement être évaluée par la limitation de la compétition trophique entre fruits même en augmentant la disponibilité en carbone. Les résultats de cette partie de la thèse ont permis de montrer que le coefficient de régulation de la photosynthèse

était autour de 1,7 lorsqu'on passe de 1 à 2 fruits par charpentière ; en d'autres termes, lorsque deux fruits sont en compétition sur une même branche, chacun d'entre eux est capable de s'approvisionner de 70% de plus de carbone qu'un fruit seul sur une branche, et ce pour une même surface foliaire relative disponible. En effet, nous supposons que cette régulation se fait au niveau de la photosynthèse des feuilles puisque, d'une part, nous avons pu prouver que la demande des fruits peut réguler la photosynthèse et, d'autre part, parce qu'il n'existait pas d'autres réelles sources de carbone que les feuilles sur la branche. Ce coefficient pourrait donc s'appliquer à la régulation de la photosynthèse dans le cadre du modèle FSPM en cours de développement. Pour cela, davantage d'investigations seraient toutefois nécessaires afin, d'une part, confirmer ces résultats et, d'autre part, cerner si ce coefficient continue à augmenter en fonction de l'augmentation du nombre de fruits par branche ou s'il est le même dès le moment où une concurrence existe et aussi s'il est le même pour tous les cultivars.

Les travaux de cette thèse permettent, de ce fait, aussi bien de répondre à certains questionnements écophysiologiques sur le transport et l'accumulation du carbone chez le pommier que d'apporter des éléments de paramétrisation du modèle FSPM.

Perspectives pour la modélisation

"All models are wrong but some are useful "

George Box

Il est important de noter que le but ultime n'est pas le modèle lui-même mais la rigueur scientifique et la réflexion interdisciplinaire qu'il impose ou induit à son développeur ou à son utilisateur et qui, ensuite, peut conduire à l'émergence d'une nouvelle compréhension du système en question –même si cela implique l'acte de devoir exclure un modèle qui après les tests de validation s'avère être inapproprié.

Dans le cadre de ces travaux, nous nous sommes focalisés sur une structure statique d'une branche reconstituée soumise à un régime lumineux horaire au sein d'un verger virtuel, et ce depuis le 2 juin 2015 à la date de récolte, i.e. le 14 octobre 2016. Nous avons dû nous restreindre à une seule branche en raison de la contrainte chronophage des premiers tests de simulation. Evidemment, ce type de test aurait pu être appliqué à toute autre structure mais pour chaque nouvelle structure, le code d'entrée de la structure aurait dû être paramétré de nouveau afin d'y inclure toutes les données enrichissant la caractérisation de la structure de la branche. Ce type d'études est prévu dans la

poursuite du développement et la paramétrisation du FSPM dans le but de valider la robustesse du modèle par l'utilisation d'un échantillon composé de plusieurs branches.

Toutefois, en nous basant sur les résultats préliminaires obtenus, la prédiction du comportement sources-puits concorde très bien avec les données mesurées et l'erreur obtenue était minime. On pourrait en déduire que les processus utilisés dans le modèle (absorption lumineuse, photosynthèse, croissance des fruits, respiration) étaient déjà suffisamment calibrés et qu'aucun processus supplémentaire n'a été négligé. Toutefois, il va de soi que même dans un système plutôt « simple » et isolé du reste de l'arbre et dans lequel un nombre bien défini de sources et de puits étaient présents, nous avons certainement négligé certaines variables d'état et les processus qu'elles représentent. A titre d'exemple, il est possible de citer les sucres solubles demeurant dans la branche ou encore l'amidon dans les feuilles (dans le modèle actuel, tous les assimilats sont effectivement dédiés à la croissance et la respiration). De plus, le fait que les simulations ont été faites sur une seule structure rend impossible une généralisation et surtout une validation du modèle. Ainsi, les futurs tests de validation pourraient outre le fait de valider le modèle renseigner quelle part des assimilats aurait été dédiée aux organes autres que les fruits.

Références bibliographiques

Abbott, D.L. (1960). The bourse shoot as a factor in the growth of apple fruits. Ann. Appl. Biol. 48(2), 434-438.

Allen, M.T., Prusinkiewicz, P., deJong, T.M. (2005). Using L-systems for modeling source-sink interactions, architecture and physiology of growing trees: the L-PEACH model. New Phytol. 166, 869-880.

Aloni, R. (1987). Differentiation of vascular tissues. Annu. Rev. Plant Physiol. 38, 179-204.

Anderson, J.L., and Richardson, E.A. (1982). "Utilizing meteorological data for modeling crop and weed growth" in Biometeorology in integrated pest management, ed. J.L. Hatfield and I.J. Thomason (New York: Academic), 449–461.

Antognozzi, E., Tombesi, A., Ferranti, F., and Frenguelli, G. (1991). Influence of sink competition on peduncle histogenesis in kiwifruit. N. Z. J. Crop Hortic. Sci.19, 433-439.

Archbold, D.D. (1992). Cultivar-specific apple fruit growth rates in vivo and sink activities in vitro. J. Am. Soc. Hortic. Sci. 117, 459-462.

Archbold, D.D. (1999). Carbohydrate availability modifies sorbitol dehydrogenase activity of apple fruit. Physiol. Plant. 105, 391-395.

Atkinson, C., Taylor, L., and Taylor, J. (1995). The influence of temperature and water supply on apple fruit-growth and the development of orchard-grown trees. J. Horticult. Sci. 70, 691–703.

Baïram, E., Delaire, M., Le Morvan, C. and Buck-Sorlin, G. (2017). Models for Predicting the Architecture of Different Shoot Types in Apple. Front. Plant Sci. 8, 65.

Bangerth, F., Li, C.J., and Gruber, J. (2000). Mutual interaction of auxin and cytokinins in regulating correlative dominance. Plant Growth Regul. 32, 205-217.

Barlow, H.W.B. (1979). Sectorial patterns in leaves on fruit tree shoots produced by radioactive assimilates and solutions. Ann. Bot. 43, 593-602.

Barthélémy, D. (1991). Levels of organization and repetition phenomena in seed plants. Acta Biotheor. 39, 309-323.

BenMimoun, M., Génard, M., Habib, R., and Besset, J. (2000). Effect of sink-source distance on peach fruit growth, in XXV International Horticultural Congress, Proceedings - Pt 6: Culture Techniques with Special Emphasis on Environmental Implications Physiological Processes in Plants, M. DeProft, ed. (Leuven 1: International Society Horticultural Science). 83–87.

Bergh, O. (1985). Effect of the previous crop on cortical cell number of Malus domestica cv. Starking Delicious apple flower primordia, flowers and fruit. S Afr J Plant Soil 2(4), 191-196.

Bergh, O. (1990). Effect of time of hand thinning on apple fruit size. S Afr J Plant Soil. 7, 1-10.

Bertin, N. (2005). Analysis of the tomato fruit growth response to temperature and plant fruit load in relation to cell division, cell expansion and DNA endoreduplication. Ann. Bot. 95, 439–447.

Berüter, J. (2004). Carbohydrate metabolism in two apple genotypes that differ in malate accumulation. J. Plant Physiol. 161, 1011-1029.

Björkman, O., and Demmig-Adams, B. (1995). "Regulation of photosynthetic light energy capture, conversion, and dissipation in leaves of higher plants". In: Ecophysiology of photosynthesis. Springer Berlin Heidelberg. 17-47.

Black, B.L., Bukovac, M.J., Stopar, M. (2000). Intraspur fruit competition and position influence fruit size at harvest and response to chemical thinning agents in spurtype 'Delicious' apple, Acta Hort. 527, 119-125.

Blanke, M.M., and Lenz, F. (1989). Fruit photosynthesis. Plant Cell Environ. 12, 31–46.

Blanke, M.M. (1997). Effects of fruit load on whole tree carbon assimilation, dark respiration, and water relations in apple. Acta Hort. 451, 313-317.

Bos, H.J., and Neuteboom, J.H. (1998). Growth of individual leaves of spring wheat (Triticum aestivum L.) as influenced by temperature and light intensity. Ann. Bot. 81, 141-149.

Botton, A., Eccher, G., Forcato, C., Ferrarini, A., Begheldo, M., Zermiani, M., Moscatello, S., Battistelli, A., Velasco, R., Ruperti, B., et al. (2011). Signaling Pathways Mediating the Induction of Apple Fruitlet Abscission. Plant Physiol.155, 185–208.

Bruchou, C., and Génard, M. (1999) A space–time model of carbon translocation along a shoot bearing fruits. Ann Bot. 84:565–576.

Buck-Sorlin, G.H., and Bell, A.D. (2000). Models of crown architecture in Quercus petraea and Q.robur: shoot lengths and bud numbers. Forestry 73, 1-19.

Buck-Sorlin, G.H. (2002). "L-system model of the vegetative growth of winter barley", in Fifth German workshop on artificial life, eds. D. Polani, J. Kim, T. Martinetz (Lübeck: Akademische Verlagsgesellschaft Aka GmbH), 53-64.

Buck-Sorlin, G.H., Hemmerling, R., Kniemeyer, O., Burema, B., and Kurth, W. (2008). A rule-based model of barley morphogenesis, with special respect to shading and gibberellic acid signal transduction. Ann Bot. 101, 1109-1123.

Buck-Sorlin, G.H., Hemmerling, R., Vos, J., and de Visser, P.H. (2009, November). Modelling of spatial light distribution in the greenhouse: description of the model. In Plant Growth Modeling, Simulation, Visualization and Applications (PMA), Third International Symposium on (pp. 79-86). IEEE.

Buck-Sorlin, G.H., de Visser, P.H.B., Henke, M., Sarlikioti, V., van der Heijden, G.W.A.M., Marcelis, L.F.M., and Vos, J. (2011). Towards a functional-structural plant model of cut-rose – simulation of light environment, light absorption, photosynthesis and interferences with the plant structure, Ann Bot. 108, 1121-1134.

Buck-Sorlin, G.H. (2013). “Functional-structural plant modelling”. In Encyclopedia of Systems Biology (pp. 778-781). Springer New York.

Bustan, A., Erner, Y., and Goldschmidt, E.E. (1995). Interactions between developing Citrus fruits and their supportive vascular system. Ann Bot. 76, 657-666.

Buwalda, J.G. and Noga, G. (1994). Intra-plant differences in leaf chlorophyll fluorescence parameters in perennial fruiting plants. N.Z. J. Crop Hortic. Sci. 22, 373– 380.

Campbell, R.J., and Marini, R.P. (1992). Light Environment and Time of Harvest Affect Delicious' Apple Fruit Quality Characteristics. J. Am. Soc. Hortic. Sci. 117, 551-557.

Casella, E., and Sinoquet, H. (2003). A method for describing the canopy architecture of coppice poplar with allometric relationships. Tree Physiol. 23, 1153-1170.

Chelle, M. (2005). Phylloclimate or the climate perceived by individual plant organs: what is it? How to model it? What for? New Phytol. 166, 781–790.

Chen, K., Hu, G.Q., and Lenz, F. (1997). Training and shading effects on vegetative and reproductive growth and fruit quality of apple. Gartenbauwiss. 5, 207-213.

Cheng, Y.H., Arakawa, O., Kasai, M., and Sawada, S. (2008). Analysis of reduced photosynthesis in the apple leaf under sink-limited conditions due to girdling. J. Japan. Soc. Hortic. Sci. 77, 115-121.

Cieslak, M., Seleznoyva, A.N., and Hanan, J. (2011). A functional-structural kiwifruit vine model integrating architecture, carbon dynamics and effects of the environment. Ann Bot. 107, 747-764.

Clijsters, H. (1969). On the photosynthetic activity of developing apple fruits. Qual. Plant. Mater. Veg. 19, 129-140.

Costes, E., and Guédon, Y. (2002). Modelling Branching Patterns on 1-year-old Trunks of Six Apple Cultivars. Ann. Bot. 89, 513-524.

Costes, E. (2003). Winter bud content according to position in 3-year-old branching systems of ‘granny smith’ apple. Ann. Bot. 92, 581-588.

Costes, E., Lauri, P.E., and Regnard, J.L. (2006). Analyzing Fruit Tree Architecture: Implications for Tree Management and Fruit Production. Horticultural Reviews. 32, 1–61.

Costes, E., Smith, C., Renton, M., Guédon, Y., Prusinkiewicz, P., and Godin, C. (2008). MAppleT: Simulation of Apple Tree Development Using Mixed Statistical and Biomechanical Models. Funct. Plant Biol. 35, 936-950.

Costes, E., Crespel, L., Denoyes, B., Morel, P., Demene, M.N., Lauri, P.E., and Wenden, B. (2014). Bud structure, position and fate generate various branching patterns along shoots of closely related Rosaceae species: a review. Front. Plant Sci. 5, 666-676.

Cournède, P.H., Mathieu, A., Houllier, F., Barthélémy, D., and De Reffye, P. (2008). Computing competition for light in the GREENLAB model of plant growth: a contribution to the study of the effects of density on resource acquisition and architectural development. Ann. Bot. 101, 1207-1219.

Da Silva, D., Boudon, F., Godin, C., and Sinoquet, H. (2008). Multiscale framework for modeling and analyzing light interception by trees. Multiscale Model. Sim. 7, 910-933.

Da Silva, D., Han, L., and Costes, E. (2014). Light interception efficiency of apple trees: a multiscale computational study based on MAppleT. Ecol. Mod. 290, 45-53.

Da Silva, D., Han, L., Faivre, R., and Costes, E. (2014). Influence of the variation of geometrical and topological traits on light interception efficiency of apple trees: sensitivity analysis and metamodelling for ideotype definition. Ann. Bot. 114, 739–752.

Dai, Z.W., Vivin, P., Robert, T., Milin, S., Li, S.H., and Génard, M. (2009). Model-based analysis of sugar accumulation in response to source-sink ratio and water supply in grape (Vitis vinifera) berries. Funct. Plant Biol. 36, 527–540.

Davie, S.J., Stassen, P.J.C., and van der Walt, M. (1995). Girdling for increased 'Hass' fruit 283 size and its effect on carbohydrate production and storage. In Proceedings of the World 284 Avocado Congress, III, 25-28.

De Reffye, P., Heuvelink, E., Guo, Y., Hu, B.G., and Zhang, B.G. (2009). Coupling process-based models and plant architectural models: a key issue for simulating crop production. In : Crop Modeling and Decision Support. Springer Berlin Heidelberg, 2009. p. 130-147.

DeJong, T.M., Da Silva, D., Vos, J., and Escobar-Gutiérrez, A.J. (2011). Using functional–structural plant models to study, understand and integrate plant development and ecophysiology. Ann. Bot. 108, 987-989.

Dekeyser, D., Duga, A.T., Verboven, P., Hendrickx, N., and Nuyttens, D. (2013). Assessment of orchard sprayers using laboratory experiments and CFD modelling. Biosyst. Eng. 114, 157–169.

Dengler, N.G. (2006). The shoot apical meristem and development of vascular architecture Can. J. Bot. 84, 1660-1671.

Denne, M.P. (1960). The growth of apple fruitlets, and the effect of early thinning on fruit development. Ann. Bot. 24, 397-406.

Denne, M.P. (1963). Fruit development and some tree factors affecting it. N.Z. J. Bot. 1, 265-294.

Diao, J., De Reffye, P., Lei, X.D., Hong Guo, H., and Letort, V. (2012). Simulation of the topological development of young eucalyptus using a stochastic model and sampling measurement strategy. In: Computers and Electronics in Agriculture, 80, 2012, pp. 105-114

Dražeta, L., Lang, S., Hall, A., Volz, R., Jameson, P.E., and Pollock, K.M. (1999). Seed set and the development of fruit shape in apple. In Proceedings of a Seed Symposium. Massey University, Palmerston North, New Zealand (Vol. 12, pp. 99-101).

Dražeta, L., Lang, A., Cappellini, C., Hall, A.J., Volz, R.K., and Jameson, P.E. (2004). Vessel differentiation in the pedicel of apple and the effects of auxin transport inhibition. Physiol. Plant 120, 162-170.

Duga, A.T., Ruysen, K., Dekeyser, D., Nuyttens, D., Bylemans, D., Nicolai, B.M., and Verboven, P. (2015). Spray deposition profiles in pome fruit trees: Effects of sprayer design, training system and tree canopy characteristics. Crop Prot. 67, 200-213.

Einset, O. (1939). Correlation of number of seed to weight of fruit in the apple. Gartenbauwissenschaft. 13, 351-353.

Etienne, A., Génard, M., Bancel, D., Benoit, S., and Bugaud, C. (2013). A model approach revealed the relationship between banana pulp acidity and composition during growth and post-harvest ripening. Sci. Hortic. 162, 125-134.

Evers, J.B., Vos, J., Fournier, C., Andrieu, B., Chelle, M., and Struik, P. C. (2005). Towards a generic architectural model of tillering in Gramineae, as exemplified by spring wheat (Triticum aestivum). New Phytol. 166, 801-812.

Evers, J.B., Vos, J., Fournier, C., Andrieu, B., Chelle, M., and Struik, P.C. (2007). An architectural model of spring wheat: evaluation of the effects of population density and shading on model parameterization and performance. Ecol. Model. 200, 308-320.

Falster, D.S., and Westoby M. (2003). Leaf size and angle vary widely across species: what consequences for light interception? New Phytol. 158, 509–525.

FAO. http://faostat3.fao.org/

Fan, P.G., Li, L.S., Duan, W., Li, W.D., and Li, S.H. (2010). Photosynthesis of young apple trees in response to low sink demand under different air temperatures. Tree Physiol. 30, 313–325.

Fanwoua, J., Baïram, E., Delaire, M., and Buck-Sorlin, G. (2014). The role of branch architecture in assimilate production and partitioning: the example of apple (Malus domestica). Front Plant Sci. 5: 338. doi:10.3389/fpls.2014.00338.

Feir-Walsh, B.J., and Toothaker, L.E. (1974). An empirical comparison of the ANOVA F-test, normal scores test and Kruskal-Wallis test under violation of assumptions. Educ. Psychol. Meas. 34, 789-799.

Ferree, D.C., Bishop, B.L., Schupp, J.R., Tustin, D.S., and Cashmore, W.M. (2001). Influence of flower type, position in the cluster and spur characteristics on fruit set and growth of apple cultivars. J. Horticult. Sci. Biotechnol. 76, 1–8.

Fisher, J.B. (1984). “Tree architecture: relationships between structure and function”, in Contemporary problems in plant anatomy, ed. R.A. White, and W.C. Dickson (New York: Academic Press), 541-589.

Fisher, J.B. (1986). “Branching patterns and angles in trees”, in On the economy of plant form and function, ed. T.J. Givnish (Cambridge: Cambridge University Press), 493-523.

Fishman, S., and Génard, M. (1998). A biophysical model of fruit growth: simulation of seasonal and diurnal dynamics of mass. Plant Cell Environ. 21, 739–752.

Fourcaud, T., Zhang, X., Stokes, A., Lambers, H., and Körner, C. (2008). Plant growth modelling and applications: the increasing importance of plant architecture in growth models. Ann Bot. 101, 1053-1063.

Fournier, C., Andrieu, B. (1999). ADEL-maize: an L-system based model for the integration of growth processes from the organ to the canopy. Application to regulation of morphogenesis by light availability. Agronomie. 19, 313-327.

Fournier, C., Andrieu, B., Ljutovac, S., Saint-Jean, S. (2003). Adel-wheat: A 3D architectural model of wheat development In B-G Hu, M Jaeger, eds, Plant growth modeling and applications. Tsinghua University Press and Springer, Beijing, China, pp 54-66.

Freeman, G.M., Bolas, B.D. (1956). A Method for the rapid Determination of Leaf Area in the Field. In: Report of the East Malling Research Station. 1955, 104-107.

Génard, M., Bertin, N., Borel, C., Bussières, P., Gautier, H., Habib, R., Lechaudel, M., Lecomte, A., Lescourret, F., Lobit, P., and Quilot, B. (2007). Towards a virtual fruit focusing on quality: modelling features and potential uses. J. Exp. Bot. 58, 917-928.

Génard, M., Bertin, N., Gautier, H., Lescourret, F., and Quilot, B. (2010). Virtual profiling: a new way to analyse phenotypes. Plant J. 62, 344-355.

Godin, C. (2000). Representing and encoding plant architecture: a review. Ann. For. Sci. 57, 413-438.

Godin, C., and Sinoquet, H. (2005). Functional-structural plant modelling. New Phytol. 166, 705–708.

Goffinet, M.C., Robinson, T.L., and Lakso, A.N. (1995). A Comparison of 'Empire' Apple Fruit Size and Anatomy in Unthinned and Hand-Thinned Trees. J. Hortic. Sci. 70, 375–387.

Goldschmidt, E.E., and Lakso, A.N. (2005). Fruit tree models: scope and limitations. Information and Communication Technology (ICT) Development and Adoption: Perspectives of Technological Innovation,(E. Gelb, A. Offer, eds.), European Federation for Information Technologies in Agriculture, Food and the Environment. URL. http://departments. agri. huji. ac. il/economics/gelb-fruit-8.pdf.

Grappadelli, L.C., Lakso, A.N., and Flore, J.A. (1994). Early-Season Patterns of Carbohydrate Partitioning in Exposed and Shaded Apple Branches. J. Am. Soc. Hortic. Sci. 119, 596–603.

Grossman, Y.L., and DeJong, T.M. (1995a). Maximum Fruit Growth Potential and Seasonal Patterns of Resource Dynamics During Peach Growth. Ann. Bot. 75, 553–560.

Grossman, Y.L., and DeJong, T.M. (1995b). Maximum Fruit Growth Potential Following Resource Limitation During Peach Growth. Ann. Bot. 75, 561–567.

Gu, S., Evers, J.B., Zhang, L., Mao, L., Zhang, S., Zhao, X., Liu, S., van der Werf, W., and Li, Z. (2014). Modelling the structural response of cotton plants to mepiquat chloride and population density. Ann. Bot. 114, 877-887.

Gucci, R., Grappadelli, L.C., Tustin, S., and Ravaglia, G. (1995). The effect of defruiting at different stages of fruit development on leaf photosynthesis of 'Golden Delicious' apple. Tree Physiol. 15, 35-40.

Guo, Y.A.N., Ma, Y., Zhan, Z., Li, B., Dingkuhn, M., Luquet, D., and De Reffye, P. (2006). Parameter optimization and field validation of the functional–structural model GREENLAB for maize. Ann. Bot. 97, 217-230.

Hallé, F., and Oldeman, R. (1970). Essai sur l'architecture et la dynamique de croissance des arbres tropicaux.

Han, H.H., Coutand, C., Cochard, H., Trottier, C., and Lauri, P.E. (2007). Effects of shoot bending on lateral fate and hydraulics – invariant and changing traits across five apple genotypes. J. Exp. Bot. 58, 3537–3547.

Han, L., Costes, E., Boudon, F., Cokelaer, T., Pradal, C., Da Silva, D., and Faivre, R. (2012). "Investigating the influence of geometrical traits on light interception efficiency of apple trees: a modelling study with MAppleT", in 2012 IEEE Fourth International Symposium on Plant Growth Modeling, Simulation, Visualization and Applications (PMA), 152-159.

Hansen, P. (1967a). ^{14}C-studies on apple trees. I. The effect of the fruit on the translocation and the distribution of photosynthates. Physiol. Plant. 20, 382–91.

Hansen, P. (1967b). ^{14}C-studies on apple trees. II. Distribution of photosynthates from top and base leaves from extension shoots. Physiol. Plant. 20, 720–725.

Hansen, P. (1967c). ^{14}C- Studies on Apple Trees III. The Influence of Season on Storage and Mobilization of Labelled Compounds. Physiol. Plant. 20, 1103-1111.

Hansen, P. (1969). ^{14}C-studies on apple trees. IV. Photosynthate consumption in fruits in relation to the leaf–fruit ratio and to the leaf-fruit position. Physiol. Plant. 22, 186–198.

Hansen, P. (1971). ^{14}C-Studies on Apple Trees. VII. The Early Seasonal Growth in Leaves, Flowers and Shoots as Dependent upon Current Photosynthates and Existing Reserves. Physiol Plant 25, 469–473.

Hansen, P., and Grauslund, J. (1973). ^{14}C studies on apple trees. VIII. The seasonal variation and nature of reserves. Plant Physiol. 28, 24-32.

Heim, G., Landsberg, J.J., Watson, R.L., and Brain, P. (1979). Eco-physiology of apple trees: dry matter production and partitioning by young Golden Delicious trees in France and England. J Appl Ecol. 16, 179-194.

Hemmerling, R., Kniemeyer, O., Lanwert, D., Kurth, W., and Buck-Sorlin, G. (2008). The rule-based language XL and the modelling environment GroIMP illustrated with simulated tree competition. Funct. Plant Biol. 35, 739-750.

Hemmerling, R., Evers, J.B., Smolenŏvá, K., Buck-Sorlin, G.H., and Kurth, W. (2013). Extension of the GroIMP modelling platform to allow easy specification of differential equations describing biological processes within plant models. Computers and Electronics in Agriculture. 92, 1-8.

Herremans, E., Verboven, P., Verlinden, B.E., Cantre, D., Abera, M., Wevers, M., and Nicolaï, B.M. (2015). Automatic analysis of the 3-D microstructure of fruit parenchyma tissue using X-ray micro-CT explains differences in aeration. BMC Plant Biol. 15, 264.

Hirota, O., Oka, M., and Takeda, T. (1990). Sink Activity Estimation by Sink Size and Dry Matter Increase During the Ripening Stage of Barley (Hordeum vulgare) and Rice (Oryza sativa). Ann. Bot. 65, 349–353.

Ho, L. (1988). Metabolism and Compartmentation of Imported Sugars in Sink Organs in Relation to Sink Strength. Annu. Rev. Plant Physiol. Plant Molec. Biol. 39, 355–378.

Horvath, D.P., Anderson, J.V, Chao, W.S., and Foley, M.E. (2003). Knowing when to grow: signals regulating bud dormancy. Trends Plant Sci. 8, 534–540.

Hosmer, D., and Lemeshow, S. (1989). Applied Logistic Regression. New York: J. Wiley and Sons.

Hotsonyame, G.K., and Hunt, L.A. (1998). Effects of sowing date, photoperiod and nitrogen on variation in main culm leaf dimensions in field-grown wheat. Can. J. Plant Sci. 78, 35-49.

Johnson, R.S., and Lakso, A.N. (1986a). Carbon balance model of a growing apple shoot. I: development of the model. J. Am. Soc. Hortic. Sci. 111, 160-164.

Johnson, R.S., and Lakso, A.N. (1986b). Carbon balance model of a growing apple shoot. II. Simulated effects of light and temperature on long and short shoots. J. Am. Soc. Hortic. Sci.. 111, 164-169.

Jones, H.G., and Higgs, K.H. (1982). Surface conductance and water balance of developing apple (Malus pumila Mill.) fruits. J. Exp. Bot. 33, 67-77.

Jullien, A., Malezieux, E., Michaux-Ferriere, N., Chillet, M., and Ney, B. (2001a). Within-bunch variability in banana fruit weight: Importance of developmental lag between fruits. Ann. Bot. 87, 101–108.

Jullien, A., Munier-Jolain, N.G., Malezieux, E., Chillet, M., and Ney, B. (2001b). Effect of pulp cell number and assimilate availability on dry matter accumulation rate in a banana fruit Musa sp AAA group “Grande Naine” (Cavendish subgroup). Ann. Bot. 88, 321–330.

Kahlen, K., and Stützel, H. (2007). Estimation of geometric attributes and masses of individual cucumber organs using three-dimensional digitizing and allometric relationships. J. Am. Soc. Hortic. Sci. 132, 439-446.

Kang, M.Z., Cournède, P.H., De Reffye, P., Auclair, D., and Hu, B.G. (2008a). Analytical study of a stochastic plant growth model: Application to the GreenLab model. Math. Comput. Simul. 78, 57-75.

Kang, M., Evers, J.B., Vos, J., and De Reffye, P. (2008b). The derivation of sink functions of wheat organs using the GREENLAB model. Ann. Bot. 101 1099-1108.

Kniemeyer, O. (2008). Design and Implementation of a Graph Grammar Based Language for Functional-Structural Plant Modelling. Doctoral dissertation, University of Technology at Cottbus.

Kniemeyer, O., Buck-Sorlin, G.H., and Kurth, W. (2007). "GroIMP as a Platform for Functional-Structural Modelling of Plants" (Chapter 4). In: Vos J, Marcelis LFM, De Visser PHB., Struik PC, Evers JB (eds.): Functional-Structural Plant Modelling in Crop Production. Springer, Dordrecht, pp. 43-52.

Knight, J.N. (1980). Fruit Thinning of the Apple Cultivar Cox Orange Pippin. J. Hortic. Sci. 55, 267–273.

Koutinas, N., Pepelyankov, G., and Lichev, V. (2010). Flower Induction and Flower Bud Development in Apple and Sweet Cherry. Biotechnol. Biotechnol. Equip. 24, 1549–1558.

Kurth, W. (1994). Morphological models of plant growth: Possibilities and ecological relevance. Ecol. Mod. 75/76, 299-308.

Kurth, W. (1998). Some new formalisms for modelling the interactions between plant architecture, competition and carbon allocation. In Bayreuther Forum Ökologie (Vol. 52, pp. 53-98).

Lai, R., Woolley, D., and Lawes, G. (1989). Effect of leaf to fruit ratio on fruit growth of kiwifruit (Actinidia deliciosa) Rid F-2171-2011. Sci. Hortic. 39, 247–255.

Lakso, A.N. (1984). Leaf area development patterns in young pruned and unpruned apple-trees. J. Am. Soc. Hortic. Sci. 109, 861–865.

Lakso, A.N., and Johnson, R.S. (1989, September). A simplified dry matter production model for apple using automatic programming simulation software. In II International Symposium on Computer Modelling in Fruit Research and Orchard Management 276 (pp. 141-148).

Lakso, A.N., and Grappadelli, C.L. (1992). Implications of pruning and training practices to carbon partitioning and fruit development in apple. Acta Hort. 322, 231-240.

Lakso, A.N., Grappadelli, C.L., Barnard, J., and Goffinet, M.C. (1995). An expolinear model of the growth pattern of the apple fruit. J. Hortic. Sci. 70, 389-394.

Lakso, A.N., Bepete, M., Goffinet, M.C., and Corelli Grappadelli, L. (1996, November). Aspects of carbon supply and demand in apple fruits. In II Workshop on Pome Fruit 466 (pp. 13-18).

Lakso, A.N., Wünsche, J.N., Palmer, J.W., and Corelli Grappadelli, L. (1999). Measurement and modeling of carbon balance of the apple tree. HortScience. 34, 1040-1047.

Lakso, A.N., White, M.D., and Tustin, D.S. (2000, January). Simulation modeling of the effects of short and long-term climatic variations on carbon balance of apple trees. In VII International Symposium on Orchard and Plantation Systems 557, pp. 473-480.

Lalonde, S., Tegeder, M., Throne-Holst, M., Frommer, W.B., and Patrick, J.W. (2003). Phloem loading and unloading of sugars and amino acids. Plant, Cell Environ. 26, 37-56.

Lang, A. (1990). Xylem, phloem and transpiration flows in developing apple fruits. J. Exp. Bot. 41, 645-651.

Lang, A., and Ryan, K.G. (1994). Vascular development and sap flow in apple pedicels. Ann Bot. 74. 381-388.

Lang, A., and Volz, R.K. (1998). Spur leaves increase calcium in young apples by promoting xylem inflow and outflow. J. Am. Soc. Hortic. Sci., 123, 956-960.

Lauri, P.E., Térouanne, E., Lespinasse, J.M., Regnard, J.L., and Kelner, J.J. (1995). Genotypic differences in the axillary bud growth and fruiting pattern of apple fruiting branches over several years—an approach to regulation of fruit bearing. Sci. Hortic. 64, 265-281.

Lauri, P.E., Térouanne, E., Lespinasse, J.M. (1996). Quantitative analysis of relationships between inflorescence size, bearing-axis size and fruit-set —an apple tree case study. Ann. Bot. 77, 277-286.

Lauri, P.E., and Lespinasse, J.M. (2001). Genotype of apple trees affects growth and fruiting responses to shoot bending at various times of year. J. Am. Soc. Hortic. Sci. 126, 169-174.

Lauri, P.E., and Kelner, J.J. (2001). Shoot type demography and dry matter matter partitioning: a morphometric approach in apple (Malus × domestica). Can. J. Bot. 79, 1270–1273.

Lauri, P.E., and Trottier, C. (2004). Patterns of size and fate relationships of contiguous organs in the apple (Malus domestica) crown. New Phytol. 163, 533-546.

Lauri, P.E. (2007). Differentiation and growth traits associated with acrotony in the apple tree (Malus domestica, Rosaceae). Am. J. Bot. 94, 1273–1281.

Lauri, P.E., Kelner, J.J., Trottier, C., and Costes, E. (2010). Insights into secondary growth in perennial plants: its unequal spatial and temporal dynamics in the apple (Malus domestica) is driven by architectural position and fruit load. Ann. Bot. 105, 607–616.

Léchaudel, M., Génard, M., Lescourret, F., Urban, L., and Jannoyer, M. (2005). Modeling effects of weather and source–sink relationships on mango fruit growth. Tree Physiol. 25, 583-597.

Lechaudel, M., Vercambre, G., Lescourret, F., Normand, F., and Genard, M. (2007). An analysis of elastic and plastic fruit growth of mango in response to various assimilate supplies. Tree Physiol. 27, 219–230.

Lescourret, F., Mimoun, M.B., and Génard,M. (1998). A simulation model of growth at the shoot-bearing fruit level: I. Description and parameterization for peach. European Journal of Agronomy. 9, 173-188.

Lescourret, F., Moitrier, N., Valsesia, P., and Génard, M. (2011). QualiTree, a virtual fruit tree to study the management of fruit quality. I. Model development. Trees 25, 519-530.

Lespinasse, J.M. (1980). La conduite du pommier. II – L'axe vertical. La renovation des vergers. I.N.V.U.F.L.E.C. Paris. 120pp.

Lespinasse, J.M., and Delort, F. (1986). Apple tree management in vertical axis: appraisal after ten years of experiments. Acta Hort. 160, 120-155.

Lespinasse, Y. (1992). "Breeding apple tree: aims and methods". In: Rousselle-Bourgeois F, Rousselle P, eds. In Proceedings of the joint conference of the E.A.P.R. breeding and varietal assessment section and the E.U.C.A.R.P.I.A potato section. Janvier 1992, Landerneau, France. Ploudaniel, France: INRA., 103-110

Lespinasse, J.M., and Delort, J.F. (1993). Regulation of fruiting in apple role of the bourse and crowned brindles. In V International Symposium on Orchard and Plantation Systems 349 (pp. 239-246).

Li, K.T. and Lakso, A.N. (2004). Photosynthetic characteristics of apple spur leaves after summer pruning to improve exposure to light. HortSci. 39, 969–972.

Lieth, J.H., and Pasian, C.C. (1990). A model for net photosynthesis of rose leaves as a function of photosynthetically active radiation, leaf temperature, and leaf age. J. Am. Soc. Hortic. Sci., 115, 486-491.

Lindenmayer, A. (1968a). Mathematical models for cellular interactions in development. I. Filaments with one-sided inputs. J. Theor. Biol. 18, 280-299.

Lindenmayer, A. (1968b). Mathematical models for cellular interactions in development II. Simple and branching filaments with two-sided inputs. J. Theor. Biol. 18, 300-315.

Link, H. (2000). Significance of flower and fruit thinning on fruit quality. Plant Growth Regul. 31, 17–26.

Liu, H.F., Genard, M., Guichard, S., and Bertin, N. (2007). Model-assisted analysis of tomato fruit growth in relation to carbon and water fluxes. J. Exp. Bot. 58, 3567–3580.

Lopez, G., Favreau, R.R., Smith, C., Costes, E., Prusinkiewicz, P., DeJong, T.M. (2008). Integrating simulation of architectural development and source-sink behaviour of peach trees by incorporating Markov chains and physiological organ function sub-models into L-PEACH. Funct. Plant Biol. 35, 761-771.

Lucas, W.J., Groover, A., Lichtenberger, R., Furuta, K., Yadav, S.R., Helariutta, Y., He, X.Q., Fukuda, H., Kang, J., Brady, S.M., Patrick, J.W., Sperry, J., Yoshida, A., Lopez-Millan, A.F., Grusak, M.A., and Kachroo, P. (2013). The plant vascular system: evolution, development and functions. Journal of integrative plant biology 55, 294-388.

Luckwill, L.C. (1970). The control of growth and fruitfulness of apple trees. Proc. Symp. Long Ashton Res. Sta., 237-254.

Luquet, D., Dingkuhn, M., Kim, H., Tambour, L., and Clement-Vidal, A. (2006). EcoMeristem, a model of morphogenesis and competition among sinks in rice. 1. Concept, validation and sensitivity analysis. Funct. Plant Biol. 33, 309-323.

Ma, Y.T., Guo, Y., Zhan, Z.G., Li, B.G., and De Reffye, P. (2006). Evaluation of the plant growth model GREENLAB-maize. Acta Agronomica Sinica 32, 956-963.

Marcelis, L. (1993). Effect of assimilate supply on the growth of individual cucumber fruit. Physiol. Plant. 87, 313–320.

Marcelis, L.F.M. (1996). Sink strength as a determinant of dry matter partitioning in the whole plant. J. Exp. Bot. 47, 1281–1291.

Marshall, B., and Biscoe, P.V. (1980). A model for C3 leaves describing the dependence of net photosynthesis on irradiance. J. Exp. Bot. 31, 29-39.

Massonnet, C., Regnard, J.L., Lauri, P.E., Costes, E., and Sinoquet, H. (2008). Contributions of foliage distribution and leaf functions to light interception, transpiration and photosynthetic capacities in two apple cultivars at branch and tree scales. Tree Physiol. 28, 665–678.

Mathieu, A. (2006). Essai sur la modélisation des interactions entre la croissance et le développement d'une plante-Cas du modèle GreenLab. Doctoral dissertation. Ecole Centrale Paris.

Mathieu, A., Zhang, B.G., Heuvelink, E., Liu, S.J., Cournède, P.H., and De Reffye, P. (2007). Calibration of fruit cyclic patterns in cucumber plants as a function of source-sink ratio with the greenlab model. In Proceedings of the 5th International Workshop om Functional-Structural Plant Models, Napier, New Zealand, 4-9 November, 2007, pp. 5-1.

McArtney, S., Palmer, J.W., and Adams, H.M. (1996). Crop loading studies with “Royal Gala” and “Braeburn” apples: Effect of time and level of hand thinning. N. Z. J. Crop Hortic. Sci. 24, 401–407.

Mehri, H., and Crabbé, J. (2002). Growth and organogenesis processes in apple tree cv. Golden Delicious. BASE. 6, 51-60.

Mierowska, A., Keutgen, N., Huysamer, M., Smith, V. (2002). Photosynthetic acclimation of apple spur leaves to summer-pruning. Sci. Hort. 92, 9–27.

Miller, R.H. (1982). Apple fruit cuticles and the occurrence of pores and transcuticular canals. Ann. Bot. 50, 355-371.

Minchin, P.E.H., Thorpe, M.R., Wünsche, J.N., Palmer, J.W., and Picton, R.F. (1997). Carbon partitioning between apple fruits: short-and long-term response to availability of photosynthate. J. Exp. Bot. 48, 1401-1406.

Ming-yu, H., Yong-wu, L., Chong-hui, F., and Cai-ping, Z. (2008). Effects of branch bending angle on physiological characteristics and fruit quality of Fuji apple. Acta Hort. Sinica, 35, 1345-1350.

Mirás-Avalos, J.M., Egea, G., Nicolás, E., Génard, M., Vercambre, G., Moitrier, N., Valsesia P, Gonzalez-Real MM, Bussi C, and Lescourret, F. (2011). QualiTree, a virtual fruit tree to study the management of fruit quality. II. Parameterisation for peach, analysis of growth-related processes and agronomic scenarios. Trees 25, 785-799.

Mirás-Avalos, J.M., Alcobendas, R., Alarcón, J.J., Valsesia, P., Génard, M., and Nicolás, E. (2013a). Assessment of the water stress effects on peach fruit quality and size using a fruit tree model, QualiTree. Agric Water Manag. 128, 1-12.

Mirás-Avalos, J.M., Alcobendas, R., Alarcón, J.J., Pedrero, F., Valsesia, P., Lescourret, F., and Nicolás, E. (2013b). Combined effects of water stress and fruit thinning on fruit and vegetative growth of a very early-maturing peach cultivar: assessment by means of a fruit tree model, QualiTree. Irrigation Science. 31, 1039-1051.

Montgomery, D.C., Peck, E.A., and Vining, G.G. (2015). Introduction to linear regression analysis. New Jersey: J. Wiley and Sons.

Murneek, A.E., and Schowengerdt, G.C. (1935). A study of the relation of size of apples to number of seeds and weight of spur leaves. Proc. Amer. Soc. Hort. Sci. 33, 6.

Naschitz, S., Naor, A., Genish, S., Wolf, S., and Goldschmidt, E.E. (2010). Internal management of non-structural carbohydrate resources in apple leaves and branch wood under a broad range of sink and source manipulations. Tree Physiol. 30, 715–727.

Niu, C., Smith, N., Garteiser, P., Towner, R., and Verchot, J. (2011). Comparative analysis of protein transport in the N. benthamiana vasculature reveals different destinations. Plant Signal Behav. 6, 1793.

Nordey, T., Léchaudel, M., Génard, M., and Joas, J. (2014). Spatial and temporal variations in mango colour, acidity, and sweetness in relation to temperature and ethylene gradients within the fruit. Plant Physiol. 171, 1555-1563.

Oliveira, C.M., and Priestley, C.A. (1988). Carbohydrate reserves in deciduous fruit trees. Hortic Rev. 10, 403-430.

Orians, C.M., Smith, S.D., and Sack,L. (2005). How are leaves plumbed inside a branch? Differences in leaf-to-leaf hydraulic sectoriality among six temperate tree species. J. Exp. Bot. 56, 2267-2273.

Pallas, B., Loi, C., Christophe, A., Cournède, P.H., and Lecoeur, J. (2011). Comparison of three approaches to model grapevine organogenesis in conditions of fluctuating temperature, solar radiation and soil water content. Ann Bot. 107, 729-745.

Pallas, B., Soulié, J.C., Aguilar, G., Rouan, L., and Luquet, D. (2013). X-Palm, a functional structural plant model for analysing temporal, genotypic and inter-tree variability of oil palm growth and yield. In Proceedings of the 7th international conference on Functional Structural Plant Model, eds. Sievänen R, Nikinmaa E, Godin C, Lintunen A, Nygren P. (Vantaa, Finland: Finnish Society of Forest Science). pp 319-321.

Pallas, B., Da Silva, D., Valsesia, P., Yang, W., Guillaume, O., Lauri, P.E., Vercambre, G., Génard, M., and Costes, E. (2016). Simulation of carbon allocation and organ growth variability in apple tree by connecting architectural and source–sink models. Ann. Bot. 118, 317-330.

Palmer, J.W. (1986). “Light interception and dry matter production by apple orchards”. In: Lakso, A.N., and Lenz, F. (Eds.), The regulation of photosynthesis in fruit trees. New York State Agricultural Experiment Station, Cornell University, pp. 24-27.

Palmer, J.W. (1992). Effects of varying crop load on photosynthesis, dry matter production and partitioning of Crispin/M.27 apple trees. Tree Physiol. 11, 19-33.

Palmer, J.W., Cai, Y.L., and Edjamo, Y. (1991). Effect of Part-Tree Flower Thinning on Fruiting, Vegetative Growth and Leaf Photosynthesis in Cox Orange Pippin Apple. J. Horticult. Sci. 66, 319–325.

Palmer, J.W., Giuliani, R. and Adams, H.M. (1997). Effect of crop load on fruiting and leaf photosynthesis of ‘Braeburn’/M.26 apple trees. Tree Physiol. 17, 741–746.

Pararajasingham, S., and Hunt, L. A. (1996). Effects of photoperiod on leaf appearance rate and leaf dimensions in winter and spring wheats. Can. J. Plant Sci. 76, 43-50.

Pavel, E.W., and DeJong, T.M. (1993a). Relative growth rate and its relationship to compositional changes of nonstructural carbohydrates in the mesocarp of developing peach fruits. J. Am. Soc. Hortic. Sci. 118, 503-508.

Pavel, E.W., and DeJong, T.M. (1993b). Estimating the photosynthetic contribution of developing peach (Prunus persica) fruits to their growth and maintenance carbohydrate requirements. Physiol Plant 88, 331–338.

Pavel, E.W., and DeJong, T.M. (1995). Seasonal patterns of nonstructural carbohydrates of apple (Malus pumila Mill.) fruits: relationship with relative growth rates and contribution to solute potential. J. Hortic. Sci. 70, 127-134.

Pearson, J.A., and Robertson, R.N. (1953). The Physiology of Growth in Apple Fruits IV. Seasonal Variation in Cell Size, Nitrogen Metabolism, and Respiration in Developing Granny Smith Apple Fruits. Australian Journal of Biological Sciences, 6, 1-20.

Perttunen, J., Sievänen, R., Nikinmaa, E., Salminen, H., Saarenmaa, H., and Väkevä, J. (1996). LIGNUM: a tree model based on simple structural units. Ann Bot. 77, 87-98.

Peterson, C. and Currier, H.B. (1969). An Investigation of Bidirectional Translocation in the Phloem. Physiol Plant 22: 1238–1250.

Prusinkiewicz, P. (1998). Modeling of spatial structure and development of plants: a review. Sci. Hortic. 74, 113-149.

Prusinkiewicz, P. (2004). Modeling plant growth and development. Current Opinion in Plant Biology 7, 79–83.

Quilot, B., and Génard, M. (2008). Is competition between mesocarp cells of peach fruits affected by the percentage of wild species genome? Journal of Plant Research, 121, 55-63.

Quinlan, J.D., and Preston, A.P. (1971). The Influence of Shoot Competition on Fruit Retention and Cropping of Apple Trees. J. Hortic. Sci. Biotechnol. 46, 525–534.

Reyes, F., DeJong, T., Franceschi, P., Tagliavini, M., and Gianelle, D. (2016). Maximum growth potential and periods of resource limitation in apple tree. Front Plant Sci. 7.

Robinson, T.L., and Lakso, A.N. (1988, August). Light interception, yield and fruit quality of 'Empire' and 'Delicious' apple trees grown in four orchard systems. In IV International Symposium on Research and Development on Orchard and Plantation Systems 243 (pp. 175-184).

Roden, J.S., and Ball, M.C. (1996). The effect of elevated [CO2] on growth and photosynthesis of two eucalyptus species exposed to high temperatures and water deficits. Plant Physiol. 111, 909-919.

Room, P.M., Maillette, L., and Hanan, J.S. (1994). Module and metamer dynamics and virtual plants. Adv. Ecol. Res. 25, 105–157.

Sané, F., Guillermin, P., Mauget, J.C., and Delaire, M. (2012). Effects of fruit load and intra-inflorescence competition of fruits on apple growth during fruit development. Acta Hort. 932, 179-186.

Sattelmacher, B., and Laidig, R. (1991). Interrelation between growth-rate of individual potato (Solanum tuberosum L.) tubers and their cell number. Ann. Bot. 68, 41–45.

Schechter, I., Proctor, J.T.A., and Elfving, D.C. (1992). Morphological differences among apple leaf types. HortScience 27, 101-103.

Schechter, I., Proctor, J.T.A., and Elfving, D.C. (1993a). Characterization of seasonal fruit growth of "Idared" apple. Sci. Hortic. 54, 203–210.

Schechter, I., Proctor, J.T.A., and Elfving, D.C. (1993b). Reappraisal of seasonal apple fruit growth. Can. J. Plant Sci. 73, 549–556.

Schmider, E., Ziegler, M., Danay, E., Beyer, L., and Bühner, M. (2010). Is it really robust? Methodology 6,147–151.

Seleznyova, A.N., Thorp, T.G., Tustin, S., and Costes, E. (2003) Application of architectural analysis and AMAPmod methodology to study dwarfing phenomenon: the branch structure of 'Royal Gala' apple grafted on dwarfing and non- dwarfing rootstock/interstock combinations. Ann. Bot. 91, 665-672.

Sievänen, R., Nikinmaa, E., Nygren, P., Ozier-Lafontaine, H., Perttunen, J., and Hakula, H. (2000). Components of functional-structural tree models. Ann. For. Sci. 57, 399-412.

Skene, D.S. (1966). The Distribution of Growth and Cell Division in the Fruit of Cox's Orange Pippin. Ann. Bot. 30, 493–512.

Smith, W.H. (1950). Cell-multiplication and cell-enlargement in the development of the flesh of the apple fruit. Ann. Bot. 14, 23-38.

Smith, C., Costes, E., Favreau, R.R., Lopez, G., and DeJong, T.M.. (2008). Improving the architecture of simulated trees in L-PEACH by Integrating Markov chains and pruning. Acta Hort. 803, 201-208.

Snee, R.D. (1977). Validation of regression models: methods and examples. Technometrics. 19, 415-428.

Spann, T.M., and Heerema, R.J. (2010). A simple method for non-destructive estimation of total shoot leaf area in tree fruit crops. Sci. Hortic. 125, 528-533.

Štampar, F., Hudina, M., Usenik, V., Šturm, K., Marn, V., and Batič F. (1999). Influence of Leaf Area on Net Photosynthesis, Yield and Flower-Bud Formation in Apple (Malus domestica Borkh.). Plant Physiol. 39, 101-106.

Stéphan, J., Lauri, P.E., Donès, N., Haddad, N., Talhouk, S. and Sinoquet, H. (2007). Architecture of the pruned tree - Impact of contrasted pruning procedures over two years on shoot demography and spatial distribution of leaf area in apple (Malus domestica Borkh.). Ann. Bot. 99, 1055-1065.

Stopar, M. (1998). Apple fruitlet thinning and photosynthate supply. J. Hortic. Sci. Biotechnol. 73, 461–466.

Sussex, I.M., and Kerk, N.M. (2001). The evolution of plant architecture. Curr. Opin. Plant Biol. 4, 33-37.

Teo, G., Suzuki, Y., Uratsu, S.L., Lampinen, B., Ormonde, N., Hu, W.K., Dejong, T.M., and Dandekar, A.M. (2006). Silencing leaf sorbitol synthesis alters long-distance partitioning and apple fruit quality. PNAS 103, 18842–18847.

Tarter, M.E., and Keuter, S.E. (2005). Effect of Rachis Position on Size and Maturity of Cabernet Sauvignon Berries. Am. J. Enol. Vitic. 56, 86–89.

Titus, J. S., and Kang, S. M. (1982). Nitrogen metabolism, translocation, and recycling in apple trees. Hortic Rev. 4, 204-246.

Tivet, F., Pinheiro, B.D.S., Raïssac, M.D., and Dingkuhn, M. (2001). Leaf blade dimensions of rice (Oryza sativa L. and Oryza glaberrima Steud.). Relationships between tillers and the main stem. Ann. Bot. 88, 507-511.

Tsukaya, H. (2004). Leaf shape: genetic controls and environmental factors. Int. J. Dev. Biol. 49, 547-555.

Turgeon, R. (1989). The sink-source transition in leaves. Annu. Rev. Plant Physiol. Plant Mol. Biol. 40, 119–138.

Tustin, S., Corelli-Grappadelli, L., and Ravaglia, G. (1992). Effect of previous-season and current light environments on early-season spur development and assimilate translocation in 'Golden Delicious' apple. J. Hortic. Sci. 67, 351-360.

Vaillant-Gaveau, N., Maillard, P., Wojnarowiez, G., Gross, P., Clément, C., and Fontaine, F. (2011). Inflorescence of Grapevine (Vitis vinifera L.): A High Ability to Distribute Its Own Assimilates. J. Exp. Bot. 62, 4183–4190.

Volz, R.K., Ferguson, I.B., Hewett, E.W., and Woolley, D.J. (1994). Wood Age and Leaf-Area Influence Fruit Size and Mineral-Composition of Apple Fruit. J. Hortic. Sci. 69, 385–395.

Von Bertalanffy, L. (1938). A quantitative theory of organic growth (inquiries on growth laws. II). Human biology 10, 181-213.

Vos, J., Evers, J.B., Buck-Sorlin, G.H., Andrieu, B., Chelle, M., and de Visser, P.H.B. (2010). Functional–structural plant modelling: a new versatile tool in crop science. J Exp Bot 61, 2101-2115. doi:10.1093/jxb/erp345

Wagenmakers, P.S., and Callesen, O. (1988). Influence of light interception on apple yield and fruit quality related to arrangement and tree height. In IV International Symposium on Research and Development on Orchard and Plantation Systems 243 (pp. 149-158).

Wagenmakers, P.S., and Callesen, O. (1995). Light distribution in apple orchard systems in relation to production and fruit quality. J. Hortic. Sci. 70, 935-948.

Wang, F., Sanz, A., Brenner, M.L., and Smith, A. (1993). Sucrose Synthase, Starch Accumulation, and Tomato Fruit Sink Strength. Plant Physiol. 101, 321–327.

Wardlaw, I.F. (1990). Tansley Review No 27 - the Control of Carbon Partitioning in Plants. New Phytol. 116, 341–381.

Wareing, P., and Patrick, J. (1975). "Source-sink relations and the partition of assimilates in the plant". In Photosynthesis and Productivity in Different Environments, (Cambridge University Press), pp. 481– 499.

Warren Wilson, J. (1972). "Control of crop processes". In Crop Processes in Controlled Environments: Proceedings of an International Symposium Held at the Glasshouse Crops Research Institute, Littlehampton, Sussex, England, July 1971, (London: Academic Press), pp. 7–30.

Warrington, I.J., Fulton, T.A., Halligan, E.A., and De Silva, H.N. (1999). Apple fruit growth and maturity are affected by early season temperatures. J. Am. Soc. Hortic. Sci., 468-477.

Watson, M.A., and Casper, B.B. (1984). Morphogenetic constraints on patterns of ion in plants. Annual Review of Ecology and Systematics 15, 233-258.

Westwood, M.N., and Bjornstad, H.O. (1974). Fruit set as related to girdling, early cluster thinning and pruning of 'Anjou' and 'Cornice' pear. HortScience, 9, 342-344.

Westwood, M.N. (1978). Temperate Zone Pomology (Postharvest, storage and Nutritional value). New York: WN Freeman and Company, 428 p.

Wünsche, J.N. and Lakso, A.N. (2000a). Apple tree physiology-implications for orchard and tree management. Compact Fruit Tree 33, 82–88.

Wünsche, J., and Lakso, A. (2000b). The relationship between leaf area and light interception by spur and extension shoot leaves and apple orchard productivity. HortScience 35, 1202–1206.

Wünsche, J.N., Greer, D.H., Laing, W.A., and Palmer, J.W. (2005). Physiological and biochemical leaf and tree responses to crop load in apple. Tree Physiol. 25, 1253-1263.

Xu, L., Henke, M., Zhu, J., Kurth, W., and Buck-Sorlin, G.H. (2011). A functional-structural model of rice linking quantitative genetic information with morphological development and physiological processes. Ann Bot. 107, 817-828.

Yamaki, S. (2010). Metabolism and Accumulation of Sugars Translocated to Fruit and Their Regulation. J. Jpn. Soc. Hortic. Sci. 79, 1–15.

Zadravec, P., Veberic, R., Stampar, F., Schmitzer, V., and Eler, K. (2014). Fruit growth patterns of four apple cultivars using nonlinear growth models. Eur. J. Hortic. Sci. 79, 52-59.

Zaïdi, L., Crabbé, J., and Barnola, P. (1993). Preliminary study of pear fruit bourse: anatomical structure and histological evolution of starch storage. Acta Bot. Gall. 140, 413-419.

Zanne, A.E., Sweeney, K., Sharma, M., and Orians, C.M. (2006). Patterns and consequences of differential vascular sectoriality in 18 temperate tree and shrub species. Funct Ecol. 20, 200-206.

Zhang, C., Tanabe, K., Tamura, F., Matsumoto, K., and Yoshida, A. (2005). ^{13}C-photosynthate accumulation in Japanese pear fruit during the period of rapid fruit growth is limited by the sink strength of fruit rather than by the transport capacity of the pedicel. J. Exp. Bot. 56, 2713-2719.

Zhang, C., and Tanabe, K. (2008). Partitioning of 13C-photosynthates from different current shoots neighboring with fruiting spur in later-maturing Japanese pear during the period of rapid fruit growth. Sci. Hortic. 117, 142–150.

Zhang, C., Tanabe, K., Tamura, F., and Itai, A. (2005). Spur characteristics, fruit growth, and carbon partitioning in two late-maturing Japanese pear (Pyrus pyrifolia Nakai) cultivars with contrasting fruit size. J. Am. Soc. Hortic. Sci. 130, 252–260.

Zhu, Y., Chang, L., Tang, L., Jiang, H., Zhang, W., and Cao, W. (2009). Modelling leaf shape dynamics in rice. NJAS 57, 73-81.

RÉSUMÉ *ABSTRACT*

Étude des processus écophysiologiques caractérisant la distribution du carbone entre les sources et les puits au sein de la charpentière du pommier. Éléments pour un modèle fonction-structure

La synthèse et le transport du carbone chez le pommier repose sur un ensemble de mécanismes complexes et imbriqués dépendants de facteurs endogènes et exogènes. Une approche combinant une caractérisation écophysiologique et l'utilisation d'un modèle structure-fonction de la plante (Functional-Structural Plant Model, FSPM) présente un moyen intéressant pour ce champ de recherche dans la mesure où un modèle structure-fonction permet d'intégrer la topologie et la géométrie de la plante et de ses différents organes à l'ensemble des facteurs impliqués dans l'assimilation et le transport du carbone et de l'eau. Le travail présenté ici a contribué à la compréhension des relations sources-puits mais également à l'élaboration d'un modèle FSPM à plusieurs niveaux. Premièrement, le développement de modèles de prédiction de l'architecture des différentes pousses du pommier à partir de variables simples apporte un moyen novateur pour simplifier la simulation de l'architecture des branches mais également pour quantifier de façon robuste la surface foliaire. Deuxièmement, l'établissement d'un réseau de corrélations entre variables morphométriques des différents organes issus du bourgeon mixte met en évidence les organes les plus connectés à l'échelle du spur. Enfin, une étude des relations sources-puits à l'échelle de la branche a permis, d'une part, une caractérisation de la régulation de la photosynthèse nette des feuilles en réponse à des changements dans le ratio sources/puits mais aussi en fonction des types de feuilles et, d'autre part, à mettre la lumière sur l'influence de la compétition entre fruits à augmenter la force de puits et de ce fait à réguler l'assimilation du carbone par les feuilles afin de répondre à la demande des fruits. Les premiers tests sur les simulations apportées par le FSPM apportent une validation supplémentaire quant à la pertinence des résultats et modèles développés.

Mots clés : Pommier, transport, carbone, sources, puits, FSPM, modélisation

Ecophysiological Processes characterizing the Carbon Partitioning between Sources and Sinks in the Fruit-bearing Branch of Apple: Elements for a Functional-Structural Plant Model

The synthesis and the transport of carbon in apple are based on a whole host of complex and interlaced mechanisms that depend on endogenous and exogenous factors. An approach that combines the ecophysiological characterisation with the use of a Functional-Structural Plant Model (FSPM) represents an interesting method in this field of research, inasmuch as such an FSPM allows integrating the topology and the geometry of the plant and its constituting organs with the entirety of factors involved in assimilation as well as water and carbon transport. The present study has contributed to the better understanding of the source-sink relations characterizing this system but also to the elaboration of a multi-scaled FSPM. First, the development of models for the prediction of the architecture of different shoot types in apple from simple variables provides a novel way to simplify the simulation of the initial structure of branches but also to quantify leaf area in a robust manner. Second, the creation of a network of correlations among morphometric variables of the different organs formed by the mixed bud of apple clearly shows the functional relations among the spur organs. In the end, the study of source-sink relations at the branch scale has allowed, on the one hand, to characterize the regulation of net photosynthesis as a function of a changed source/sink ratio but also as a function of leaf type and, on the other hand, to shed some light on the influence that the competition among fruits has on increasing sink strength and thus regulating the leaf net photosynthesis in order to meet the demand of the fruits. First tests conducted using the FSPM provided an additional validation with respect to the importance of the model results developed here.

Keywords: *Apple, transport, carbon, source, sink, FSPM, modelling*

AGROCAMPUS OUEST • Institut supérieur des sciences agronomiques, agroalimentaires, horticoles et du paysage
65 rue de Saint-Brieuc – CS84215 – F-35042 Rennes Cedex
Tél. : 02 23 48 50 00
www.agrocampus-ouest.fr